NASA CR-159520

UNCONVENTIONAL NOZZLE TRADEOFF STUDY

(NASA-CR-159520) UNCONVENTIONAL NOZZLE TRADEOFF STUDY (Aerojet Liquid Rocket Co.) 311 p CSCL 21H
N79-28224
Unclas
G3/20 29408

AEROJET LIQUID ROCKET COMPANY

Sacramento, California

prepared for

NATIONAL AERONAUTICS AND SPACE ADMINISTRATION

July 1979

CONTRACT NAS 3-20109

NASA Lewis Research Center
Cleveland, Ohio
C. A. Aukerman, Project Manager

1. Report No. NASA CR-159520	2. Government Accession No.	3. Recipient's Catalog No.
4. Title and Subtitle Unconventional Nozzle Tradeoff Study, Final Report		5. Report Date July 1979
		6. Performing Organization Code
7. Author(s) C. J. O'Brien		8. Performing Organization Report No.
		10. Work Unit No.
9. Performing Organization Name and Address Aerojet Liquid Rocket Company, Post Office Box 13222, Sacramento, California 95813		11. Contract or Grant No. NAS3-20109
		13. Type of Report and Period Covered Contractor Report, Final
12. Sponsoring Agency Name and Address National Aeronautics and Space Administration, Washington, D. C. 20546		14. Sponsoring Agency Code

15. Supplementary Notes

Project Manager, C. A. Aukerman, Space Propulsion and Power Division, NASA-Lewis Research Center, Cleveland, Ohio

16. Abstract

Plug cluster engine design, performance, weight, envelope, operational characteristics, development cost, and payload capability, were evaluated and comparisons were made with other Space Tug engine candidates using oxygen/hydrogen propellants.

Parametric performance data were generated for existing developed or high technology thrust chambers clustered around a plug nozzle of very large diameter. The uncertainties in the performance prediction of plug cluster engines with large gaps between the modules (thrust chambers) were evaluated.

The major uncertainty involves the aerodynamics of the flow from discrete nozzles, and the lack of this flow to achieve the pressure ratio corresponding to the defined area ratio for a plug cluster. This uncertainty was reduced through a cluster design that consists of a plug contour that is formed from the cluster of high area ratio bell nozzles that have been scarfed. Light-weight, high area ratio, bell nozzles were achieved through the use of AGCarb (carbon-carbon cloth) nozzle extensions.

The plug cluster engine proved to be competitive with the uprated RL10 engines, the Aerospike, and the Advanced Space Engine. High vacuum performance is achieved with the low pressure Plug Cluster Engine because of the large area ratio available with the baseline Space Tug.

17. Key Words (Suggested by Author(s)) Plug Cluster Engine; Space Tug Propulsion; Liquid Rocket Engine; Oxygen/Hydrogen Cryogenic Engine	18. Distribution Statement Unclassified - Unlimited

19. Security Classif. (of this report) Unclassified	20. Security Classif. (of this page) Unclassified	21. No. of Pages 296	22. Price*

*For sale by the National Technical Information Service, Springfield, Va. 22151

FOREWORD

The work described herein was performed at the Aerojet Liquid Rocket Company under NASA Contract NAS3-20109 with Mr. Carl A. Aukerman, NASA-Lewis Research Center, as Project Manager. The ALRC Program Manager was Mr. Larry B. Bassham, the Operations Project Manager was Dr. R. J. LaBotz, and the Project Engineer was Mr. Charles J. O'Brien.

The technical period of performance for the study was from 1 July 1976 to 28 April 1978.

The author wishes to acknowledge the efforts of the following ALRC engineering personnel who contributed significantly to this report:

L. L. Bickford
P. E. Brown
K. L. Christensen
H. O. Davis (ASPC)
J. A. Heney
R. A. Hewitt
M. C. Huppert
G. R. Janser
L. L. Lang
S. Leone
S. A. Lorenc
E. Lueders
G. M. Meagher
R. W. Michel
G. H. Peirson
J. L. Pieper
N. M. Richardson
D. C. Rousar
J. V. Smith

I also wish to thank Mr. Rudi Beichel, ALRC Senior Scientist, for his comments and assistance throughout the study effort.

TABLE OF CONTENTS

TABLE OF CONTENTS (cont.)

TABLE OF CONTENTS (cont.)

TABLE OF CONTENTS (cont.)

LIST OF TABLES

LIST OF TABLES (cont.)

LIST OF TABLES (cont.)

LIST OF TABLES (cont.)

LIST OF FIGURES

LIST OF FIGURES (cont.)

LIST OF FIGURES (cont.)

LIST OF FIGURES (cont.)

LIST OF FIGURES (cont.)

LIST OF FIGURES (cont.)

SECTION I

SUMMARY

A. STUDY OBJECTIVES AND SCOPE

The major objectives of this study program were to: (1) conduct a propulsion system analysis to assess the potential of the plug cluster engine concept for the Space Tug baseline vehicle and nominal missions, (2) assess the potential of utilizing an existing or high technology thrust chamber as a module for such a plug cluster application, and (3) identify the technology requirements for the development of a plug cluster engine.

To accomplish the objectives, the eleven task study program, summarized on Figure 1, was conducted.

Design criteria were obtained from the literature on Space Tug systems, on plug and plug cluster nozzles, on H/O thrust chambers and on H/O turbopump assemblies.

Engine performance and envelope parametric data were established over a wide range of mixture ratios and engine geometry, using a plug cluster performance model.

Subsystems of the engine were evaluated to determine their impact on the design, and any limitations resulting from the utilization of the various cycles were established.

Based upon the results of Tasks I through III and the study guidelines, three configurations and two cycles were selected to be carried into conceptual preliminary designs. The three configurations involved use of: (1) ITA modules, (2) minimum change ITA modules, and (3) regeneratively cooled modules. The two cycles were the expander and the gas generator cycle. In addition to the cooled plug design, an uncooled carbon-carbon cloth plug design was evaluated.

Plug cluster engine design, performance, weight, envelope and operational characteristics were evaluated for a variety of candidate cluster configurations (Figures 2, 3 and 4). The selected plug cluster engines were compared with the engine candidates that were evaluated for the baseline Space Tug. The comparison was based on mission performance, cost, life, and engine geometry.

Upon completion of the first six tasks, an amendment was made to the contract to address the "real world" problems of an actual engine. Lightweight engine structures were examined, with the AGCarb (carbon-carbon cloth) nozzle extension providing a significant configuration improvement.

Techniques for providing thrust vector control for the plug cluster engine were evaluated, and module hinging appeared to offer the best potential.

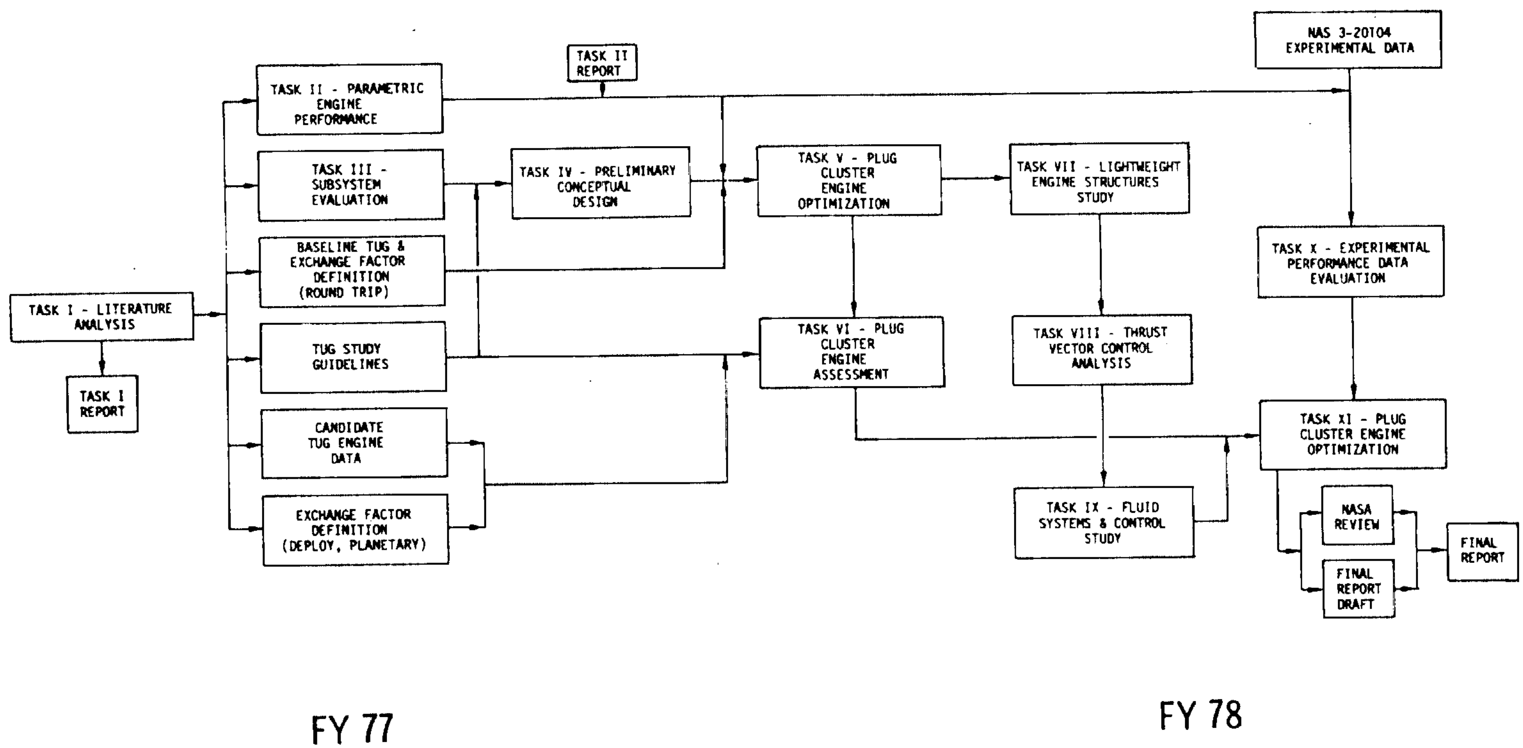

Figure 1. Unconventional Nozzle Tradeoff Study Program Summary

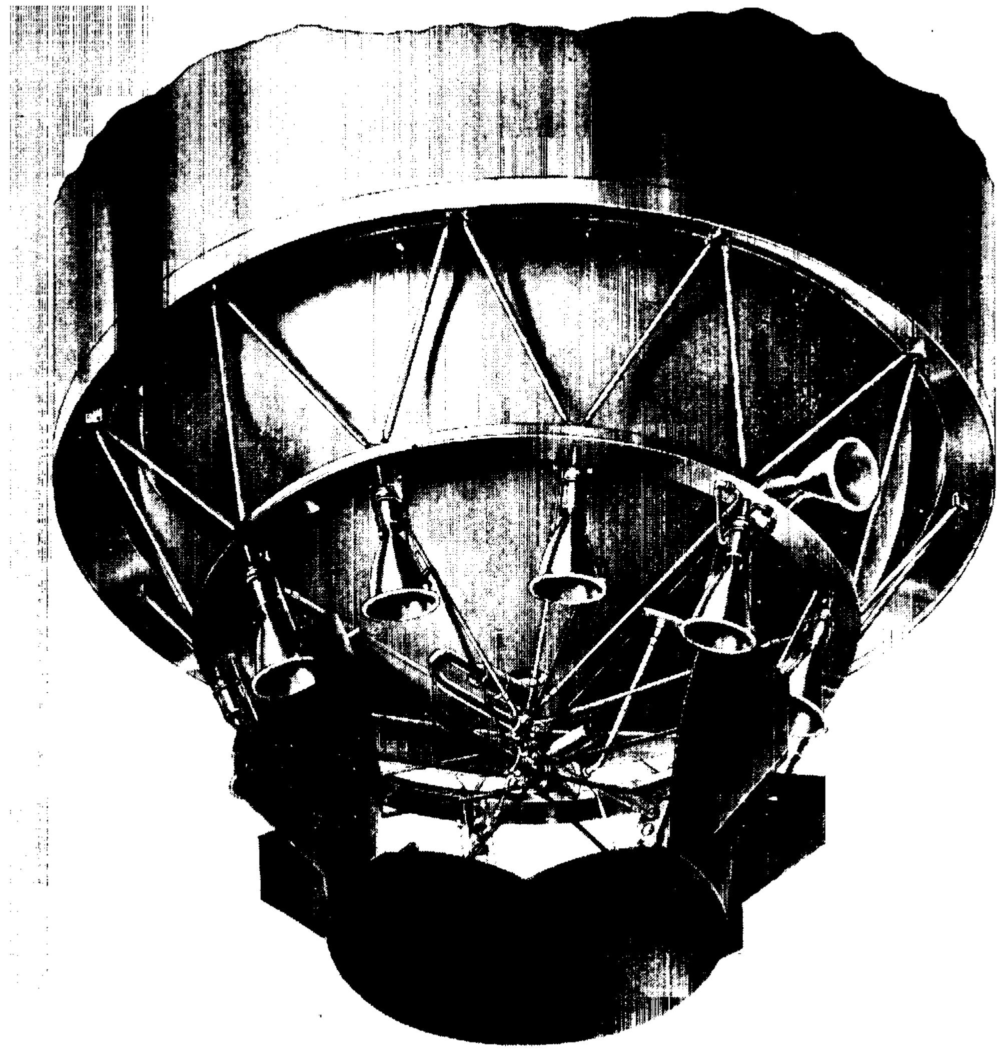

Figure 2. Plug Cluster Engine

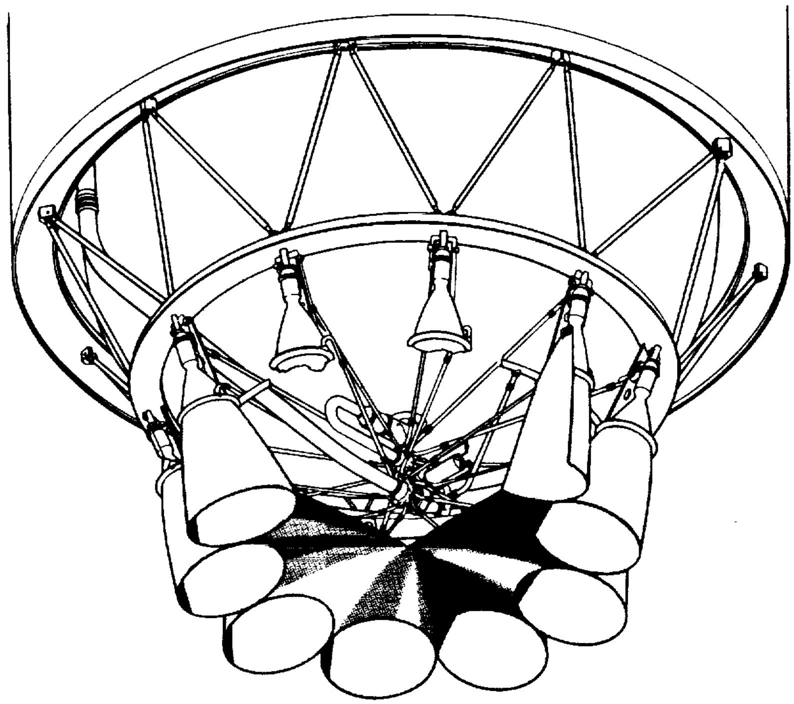

Figure 3. Clustered Bell Nozzle Concept

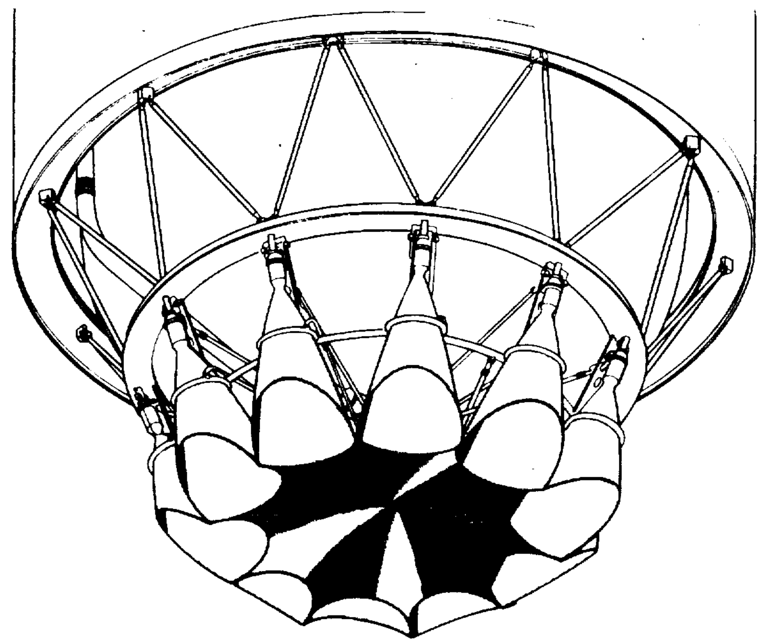

Figure 4. Scarfed Bell/Plug Cluster Engine Concept

The lightest weight configuration for the fluid systems, their components, and controls for a plug cluster was determined.

Analysis of the experimental cold flow data recently obtained on Contract NAS 3-20104 (NASA CR-135229 "Plug Cluster Nozzle Flow Evaluation") was made, and discrepancies in the data noted. The plug cluster engine performance methodology was modified to reflect the cold flow data. Engine performance calculated by this methodology rules out the large gap cluster configuration on a standard plug nozzle due to the poor aerodynamic flow conditions. Optimum performance is achieved, however, through the use of a fluted plug formed from a cluster of large area ratio scarfed bell nozzles.

Throughout the entire study effort, basic data gaps and areas requiring technology work were identified.

B. RESULTS AND CONCLUSIONS

High vacuum performance is achieved with the low pressure plug cluster engine which makes maximum use of the large area available with the baseline Space Tug. Low development and production costs for the engine are achieved through the utilization of existing developed technology. The combination of high performance and low cost makes the plug cluster engine competitive with the baseline Space Tug RL10 IIB engine and the higher pressure Advanced Space Engine, as shown in Figure 5.

The objectives of the program have been successfully accomplished. The fact that existing developed, long cycle life thrusters can be clustered in various manners and numbers, allows the designer the flexibility to configure a large number of Orbital Transfer Vehicles (OTV) that operate at almost any thrust level desired.

S.I. UNITS

	RL10 IIB	PCE 300	PCE 500	ASE
MR	6	6	6	6
P_c (atm)	27.2	20.4	34.0	136
ϵ_E	205	895	894	400
W_E (Kg)	201	219	194	183**
D_E (m)	1.80	4.32	3.35	1.07
L_E (m)	1.40***	0.81	0.94	1.28***
*I_s (s)	460.6	464.4	466.6	469.3
η_E (I_s/I_s ODE)	0.965	0.945	0.949	0.966
<u>PAYLOAD (Kg)</u>				
Deploy	3740	3827	3964	4084
Retrieve	1649	1721	1820	1911
Round Trip	1001	1041	1098	1150
Planetary	4945	5019	5129	5224

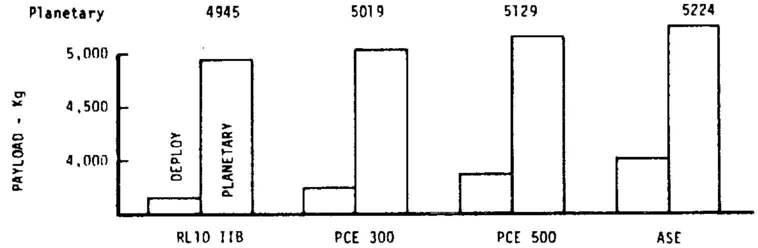

* Performance based on JANNAF simplified methodology

** Thrust/Weight ratio assumed same as for 66,723 N engine (Ref. 27)

***Stowed length of deployable nozzle

ENGLISH UNITS

	RL10 IIB	PCE 300	PCE 500	ASE
MR	6	6	6	6
P_c (psia)	400	300	500	2000
ϵ_E	205	895	894	400
W_E (lbm)	443	482	428	404**
D_E (in.)	71	170	132	42
L_E (in.)	55***	32	37	44***
*I_s (s)	460.6	464.4	466.6	469.3
η_E (I_s/I_s ODE)	0.965	0.945	0.949	0.966
<u>PAYLOAD (lbm)</u>				
Deploy	8245	8436	8740	9003
Retrieve	3135	3794	4013	4212
Round Trip	2207	2294	2421	2535
Planetary	10901	11065	11307	11518

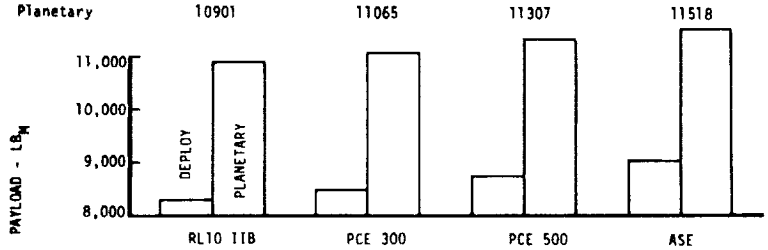

* Performance based on JANNAF simplified methodology

** Thrust/Weight ratio assumed same as for 20,000 lb_f engine (Ref. 27)

***Stowed length of deployable nozzle

Figure 5. Space Tug Engine Evaluation

SECTION II

INTRODUCTION

A. BACKGROUND

Several analyses of the propulsion systems required for the Space Tug vehicle have been conducted in the past, but in each case, the studies were conceived and conducted in a traditional fashion with primary consideration given to engines having conventional bell nozzles. The use of unconventional nozzles offers a great deal of potential for high performance, long life, and flexibility in design, that had never been exploited nor even studied in these vehicle applications. In cases where unconventional nozzles were considered, restrictive assumptions that were applicable only to the bell nozzles were arbitrarily imposed on the unconventional nozzles. As a result, many options that an engine designer might have had in developing advanced thrust chambers were ground ruled out of the studies. This restrictive situation becomes particularly troublesome when low cost and reusability are required of the propulsion system in addition to high performance.

Space Tug vehicle application studies for the purpose of evaluating candidate propulsion systems have been based on fixed input conditions, such as propellant combination, narrow mixture ratio range, and engine envelope, i.e., engine length and diameter. It is well known that the area ratio for conic section (bell shaped) nozzles varies in a direct relationship with nozzle length and inversely with throat radius ($\varepsilon \propto L_n/R_t$). It is also well known that an increase in propulsion system vacuum performance occurs primarily by an increase in nozzle area ratio and is essentially independent of chamber pressure ($Is \ \alpha \ \varepsilon$). Early candidate engines were limited in performance for a fixed length application. There were four approaches available to achieve a higher area ratio in this length: (1) high chamber pressure, (2) extendible nozzle, (3) multiple engines, and (4) conventional nozzle.

The approach ultimately selected to attain high area ratio was to increase the chamber pressure to make the throat area smaller for the same nozzle length. This high chamber pressure then led to a specific set of problems (high unit heat flux, high wall temperatures, and small, high speed, high pressure turbomachinery) that must be solved to meet the high cycle life required.

What is overlooked in this approach is that the true diameter limit for the engine installation, i.e., the vehicle diameter, has not been utilized by the conventional bell nozzle to arrive at a solution to the basic problem. Unconventional nozzles, i.e., clusters of small thrusters around a contoured plug, can utilize this dimension to arrive at engine designs which feature lower chamber pressures, with attendant lower heat flux, lower wall temperatures, longer fatigue life, and less critical turbomachinery.

From 1969 to 1974, the NASA sponsored a number of efforts to establish an adequate technology base for a cryogenic Attitude Control Propulsion System for the Space Transportation System. The final design life goal for the thruster was 50,000 cycles (pulses) and 5,000 deep thermal cycles. The Integrated Thruster Assembly (ITA) accumulated the best of the component designs available and was life cycle tested 51,005 cycles. Designs for higher performing, regeneratively cooled thrusters were also established with high cycle life capability, but not tested as extensively as the ITA.

One of the intriguing variations, therefore, in the application of plug nozzles to a Space Tug type vehicle and mission, is the possibility that existing developed or high technology thrust chambers could be clustered around a plug nozzle of very large diameter. Thus, the primary problems of a high pressure engine are completely avoided in exchange for a different set of problems such as clustered performance, base pressurization, and installed weight. The engine designer then has a choice of problems to solve to best meet the needs of the given application, with cost comparisons involving the two types of propulsion systems also being an important factor.

B. PURPOSE AND SCOPE

The feasibility of the clustered plug Space Tug is heavily dependent on the delivered performance and weight of the engine system, with the trade-off in performance versus the gap between module nozzle exits being a significant factor. It is the purpose of this study to conduct a propulsion system analysis to assess the potential of the plug cluster engine concept for the Space Tug baseline vehicle and nominal mission.

Plug cluster engine design, performance, weight, envelope, and operational characteristics were evaluated for a variety of candidate cluster configurations. The selected plug cluster engines were compared with the engine candidates that were evaluated for the baseline Space Tug. The comparison was based on mission performance, cost, life, and engine geometry.

C. GENERAL REQUIREMENTS

For purposes of this study, the engine design point for plug cluster engine evaluation was assumed to be that given in Table I, commensurate with the baseline Space Tug requirements.

TABLE I. - PLUG CLUSTER ENGINE DESIGN POINT

Propellant Combination	Hydrogen and Oxygen
Mixture Ratio (nominal)	O/F = 6.0
Maximum Engine Diameter	447 cm (176 in.)
Maximum Engine Length (at engine gimbal, beyond base of LOX tank)	139.7 cm (55 in.)
Engine Cyclic Life (no factor of safety)	1200 firings
Engine Thrust (nominal)	66,723 N (15,000 lbf)

D. APPROACH

To accomplish the program objectives, a study involving eleven technical tasks was conducted. The results of the first three tasks were utilized to select the configurations to be conceptually designed and analyzed to optimize the plug cluster engine. Tasks conducted were:

1. TASK I: Literature Analysis

Significant publications pertinent to the conduction of this study were reviewed and evaluated, including:

a. Space Tug system studies.

b. Plug cluster nozzle and plug nozzle experimental and analytical studies.

c. H/O thrust chambers of existing and high technology status.

d. H/O turbopump assemblies of existing and high technology status.

2. TASK II: Parametric Engine Performance

A simplified plug cluster engine performance methodology was established and performance maps were prepared to display the delivered specific impulse in terms of the engine variables.

3. TASK III: Subsystem Evaluation

Base pressurization, engine cooling, and turbomachinery and power subsystems analyses were conducted to determine any limitations inherent in the various engine cycles proposed for the plug cluster engine.

4. TASK IV: Preliminary Design

Preliminary conceptual designs of plug cluster engines were prepared for selected configurations and engine cycles.

5. TASK V: Plug Cluster Engine Optimization

Parametric system analyses of the plug cluster engine were conducted and tradeoffs were made in performance and engine weight to arrive at an optimum set of engine designs. The technology requirements for such an engine were defined.

6. TASK VI: Plug Cluster Engine Assessment

The plug cluster engine was compared with candidate Space Tug engines for several baseline geosynchronous and interplanetary missions.

7. TASK VII: Lightweight Engine Structures

Structural techniques, designs, and materials were selected to provide the lightest weight plug cluster engine concept for typical space applications.

8. TASK VIII: Thrust Vector Control Analysis

Techniques for providing thrust vector control (TVC) for a plug cluster engine were evaluated and the best method selected.

9. TASK IX: Fluid Systems and Control Study

The lightest weight configuration for the fluid systems, their components, and controls for a plug cluster engine were selected from an evaluation of several candidate systems.

10. TASK X: Experimental Performance Data Evaluation

An analysis was conducted and an appraisal was made of the experimental cold flow data reported in NASA CR-135229 "Plug Cluster Nozzle Flow Evaluation". These results were compared with the performance predictions in Tasks II, III and V. The methodology employed in Tasks II through V was updated and revised in order to reflect the experimentally measured effects of gaps, fairings, tilt angle, and base pressurization.

11. TASK XI: Plug Cluster Engine Optimization

The engine optimization obtained in Task V was revised to include the results of the Tasks VII through IX analyses. The plug cluster assessment conducted in Task VI was revised accordingly.

SECTION III

LITERATURE ANALYSIS

A. OBJECTIVES AND GUIDELINES

A literature analysis was conducted to provide background data on the Space Tug system, plug cluster nozzles, H/O thrust chambers, and H/O turbopumps to be considered in the study. Pertinent information from the literature was included in detail in the Task I Report (Unconventional Nozzle Tradeoff Study - Monthly Technical Progress Report 20109-M-2, Task I - Literature Analysis, Aerojet Liquid Rocket Co., Contract NAS 3-20109, September 1976). The Task I Report provided narratives on the reports containing data that served to allow evaluation of the plug cluster concept. The narratives included a summary, the scope of work, results attained (pertinent figures and supporting data), an assessment of the state-of-the-art, and the strong and weak points of the work. The bibliography is repeated in Appendixes B through E of this report.

Specific information from the Task I Report that became the background data for the study is summarized in this section.

B. SPACE TUG SYSTEM STUDIES

Assessment of the plug cluster engine concept as a Space Tug propulsion system involves a multitude of factors, many of which have been previously studied in depth for other Tug candidates. The system studies involving the main engine propulsion have considered both storable and cryogenic propellants, interim upper stages, and full capability Space Tugs. The literature search conducted in this study was concentrated on the cryogenic, full capability Tug.

The envelope of the cryogenic Tug is constrained by the dimensions of the Space Shuttle payload bay. The baseline Tug vehicle utilizes a Category II RL10 engine with a two-position nozzle in order to conserve length. Typical engine data resulting from the study efforts indicate a thrust requirement between 66,723 and 88,964 Newtons (15,000 and 20,000 pounds force), and an engine mixture ratio between 5 and 6. Payload optimizes at the lower mixture ratio for engines with lower chamber pressure.

The selection of the RL10 engine over more advanced engines was primarily based upon DDT&E cost rather than the amount of payload delivered. The engine Isp increase was originally evaluated using a sensitivity of +41 kg (+90 lb) of payload per second of Isp, and the engine weight increase was evaluated using a sensitivity of -2.5 kg (lb) of payload per kilogram (pound) of inert weight for the deploy mission.

1. Baseline Space Tug

The current (October 1974) NASA definition (Ref. 1) of the baseline Space Tug is given in Tables II and III and in Figures 6 and 7.

TABLE II - BASELINE SPACE TUG CHARACTERISTICS SUMMARY (Ref. 1)

VEHICLE DESCRIPTION

ENGINE Pratt & Whitney RL-10-IIB (Retractable Nozzle)

ACTUATOR Hydraulic

APS SYSTEM 24 Hydrazine thrusters (25#)

STRUCTURE

- Skirts - Graphite Epoxy/Aluminum Composite
- Tanks - Aluminum Alloy/Elliptical Bulkheads
- Tank Supports - Fiber Glass Struts
- Thrust Structure - Fiber Glass Strut Truss

THERMAL CONTROL SYSTEM

- Tank Insulation - Goldized Super floc
- Active System for Fuel Cell
- Heat Pipes for Other Avionics

PAYLOAD CAPABILITY TO GEOSYNCHRONOUS ORBIT

Deploy	7926 lbs
Retrieve	3396 lbs
Round trip	2070 lbs

AVIONICS SYSTEM

- Antenna - Electronically steerable phased array
- Platform - Strapdown
- Power - Fuel Cell (2) plus Battery
- Data Management - Data Bus
- SC Retrieval - Laser Radar
- SC Deployment Inspect - TV

MAIN ENGINE PERFORMANCE

	THRUST(LBS)	I_{SP} (SEC)
Full	15000	456.5
Pumped Idle	3750	434.7
Tank Head Idle	157	377

VEHICLE CHARACTERISTICS

Length	30 ft
Diameter	14.67 ft
Dry Weight	5140 lbs
Burnout Weight	5755 lbs
First Ignition Weight	56,779 lbs
Deployment Adapter & Shuttle Systems	1900 lbs
Ground Liftoff Weight	58,679 lbs

PAYLOAD SENSITIVITIES

	DEPLOY ONLY	RETRIEVAL ONLY
$\frac{\partial PL}{\partial w_s}$	-2.62	-1.38
$\frac{\partial PL}{\partial UP}$	0	0.23
$\frac{\partial PL}{\partial w_o}$	-0.38	0
$\frac{\partial PL}{\partial I_{SP}}$	83 lb/sec.	59 lb/sec.

TABLE III - BASELINE SPACE TUG WEIGHT BREAKDOWN

	Weight kg (lb)		
STRUCTURE	895 (1,974)		
PROPULSION AND MECHANICAL	611 (1,346)		
THERMAL CONTROL	200 (441)		
AVIONICS	418 (921)		
10% GROWTH CONTINGENCY INCLUDING FASTENERS	212 (468)		
TOTAL DRY WEIGHT		2,336 (5,150)	
UNUSUABLE RESIDUALS	274 (605)		
BURN-OUT WEIGHT		2,610 (5,755)	
EXPENDABLES		248 (547)	
PROPELLANT RESERVES		136 (300)	
USABLE PROPELLANTS		22,760 (50,177)*	
FIRST IGNITION WEIGHT		25,755 (56,779)	
ORBITER ACCOMMODATIONS (including 10% contingency)		862 (1,900)	
GROUND LIFT-OFF			26,616 (58,679)

*Maximum propellant weight, propellant may be off-loaded to accommodate additional payload weight.

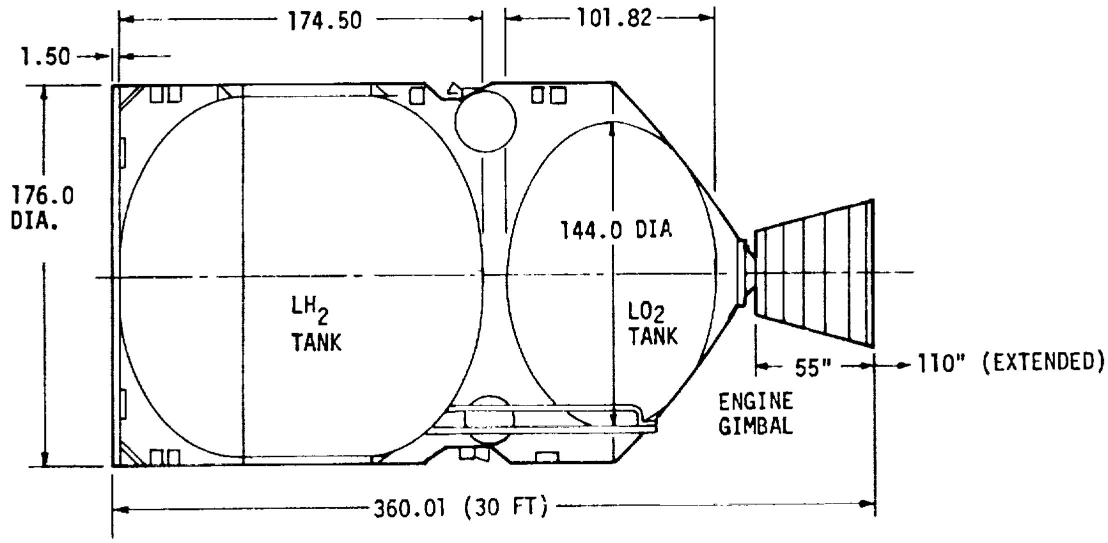

Figure 6. Baseline Space Tug General Arrangement and Size

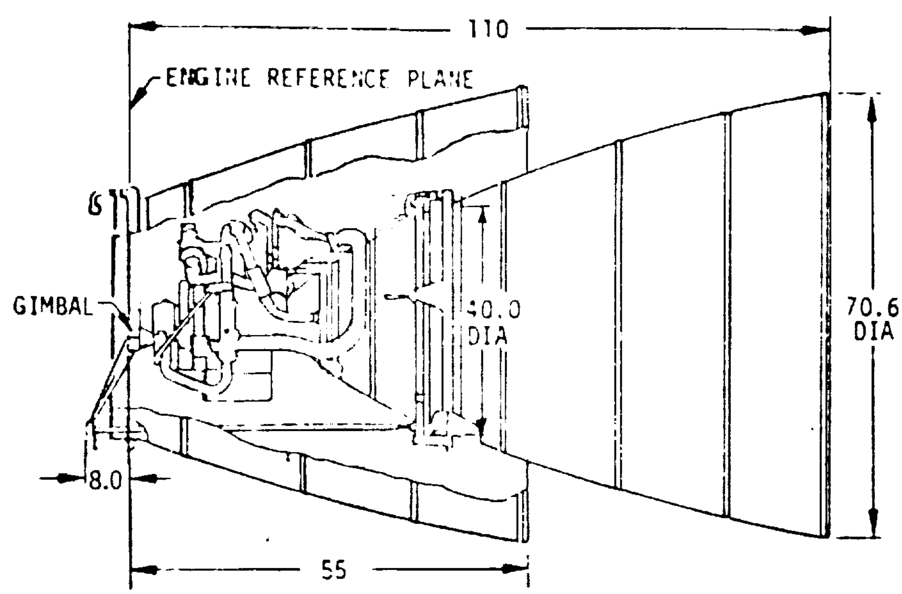

Figure 7. Baseline Tug Engine

Geosynchronous performance capability of the Space Tug is a function of various vehicle characteristics. The partials for the deploy only and the retrieval only geosynchronous missions listed in Table II are explained as follows:

$\frac{\partial PL}{\partial W_S}$ An increase of Tug stage weight (dry weight plus unusable propellants) by one kg (one lb) reduces the payload that can be deployed to geosynchronous orbit by 1.19 kg (2.62 lb), and that which can be retrieved by 0.63 kg (1.38 lb).

$\frac{\partial PL}{\partial UP}$ An increase of Tug usable propellant capacity by one kg (one lb) increases the payload that can be retrieved from geosynchronous orbit by 0.10 kg (0.23 lb). In the case of deployment of a maximum weight payload $\partial PL/\partial UP = 0$ since the Tug already has more propellant capacity than can be utilized (i.e., propellants must be off-loaded to meet the Orbiter constraint of 29,484 kg [65,000 lb] at liftoff for the Tug plus its payloads).

$\frac{\partial PL}{\partial W_0}$ A one kilogram (one lb) increase in weight of the equipment chargeable to the Tug but remaining in the Orbiter (such as adapter structure and propellant fill and vent equipment) decreases the weight of payload that can be deployed to geosynchronous orbit by 0.17 kg (0.38 lb). This decrease comes about because of the Orbiter constraint for Tug plus its payload at liftoff (when the interface weight is increased, propellant must be off-loaded to satisfy the constraint).

$\frac{\partial PL}{\partial I_{SP}}$ Increasing the main engine specific impulse by one second increases the payload that can be delivered to geosynchronous orbit by 38 kg (83 lb) and that which can be retrieved by 27 kg (59 lb).

The baseline Space Tug is composed of structures, propulsion and mechanical, avionics, and thermal control systems. The general arrangement and size of the Tug systems are shown in Figure 3, and the weight breakdown is given in Table III. The thrust structure is an open fiberglass conic frustrum truss with an aluminum gimbal block to interface with the engine. It is attached directly to the LO_2 tank with eight fiberglass epoxy struts as shown in Figure 6.

The engine (RL10 Cat. IIB) shown in Figure 7, is a derivative of the flight proven Pratt and Whitney RL10 engine. It provides a vacuum thrust of 66,723 N (15,000 lb) and a specific impulse of 456.5 sec at a mixture ratio of 6.0, ϵ = 205:1. The life expectancy is 5 hours with 190 starts. The overall stowed engine length is seen to be 140 cm (55 in.), where the gimbal point is 44 cm (17 in.) aft of the LO_2 tank.

2. Engine Evaluation

A sensitivity study was conducted in Reference 2 to determine the overall program impact when the Option 2 Category IIA RL10 main engine is replaced with an advanced engine candidate, i.e., Category IV RL10, Advanced

Space Engine (ASE), or the Aerospike (Figure 8). With the exception of the Aerospike, the engine change effects are primarily engine related, i.e., engine DDT&E cost, weight and specific impulse. The Aerospike engine provides maximum Tug performance at an engine mixture ratio of 5.0, while the other engines maximize tug performance at an engine mixture ratio of 6.0. Therefore, a Tug using an Aerospike engine would have different tank sizes than a Tug using the other engine candidates.

Results of this study (Figure 9) show that the Tug performance increases by 10 to 20 percent with the use of advanced engines. For the mission model used, the number of flights does not change significantly and the fleet size does not change at all. The figure also shows that the total program cost decreases with the advanced engines and the cost impact is due primarily to DDT&E cost (mostly due to the main engine).

C. PLUG AND PLUG CLUSTER ROCKET NOZZLE STUDIES

During the past twenty years, many investigations have been conducted in the field of unconventional rocket nozzles, and in the process, a large volume of literature was generated. The most pertinent references on the subject of plug and plug-cluster nozzles are listed in Appendix C.

The literature, reviewed in the Task I Report, describes experimental and theoretical investigations of several types of plug nozzles generally referred to as annular-throat, discrete-throat, Aerospike, and plug cluster nozzles. Inverse-plug or expansion-deflection nozzles were also discussed in the review.

In addition to plug nozzle performance in terms of thrust efficiency, specific impulse or velocity coefficient, plug wall and base pressure and heat transfer data were presented. The experimental data on thrust vector control methods applicable to plug nozzles were also reviewed. In general, a good agreement was found between the model cold-flow data and hot-flow H_2/O_2 propellant test results.

The analytical methods discussed in the literature, are generally adequate for the design and performance prediction of annular-throat isentropic plug nozzles, but inadequate for the analysis of nozzles which deviate considerably from the annular-throat configuration, such as plug-cluster nozzles utilizing bell modules. In such cases, authors of various reports generally resort to empirical correction factors to account for shock wave interaction occurring at the module exit. These factors were developed from testing of specific plug-cluster configurations and must be applied with caution to new plug concepts.

Most of the analytical and experimental studies were stimulated by the altitude compensation aspect of plug nozzles, which is a desirable characteristic of nozzles for booster application. For this reason, the range of many plug variables was limited to the booster phase of rocket propulsion. The space tug vehicle operates in a vacuum at infinite pressure ratio and the altitude compensation, which occurs at pressure ratios less than design

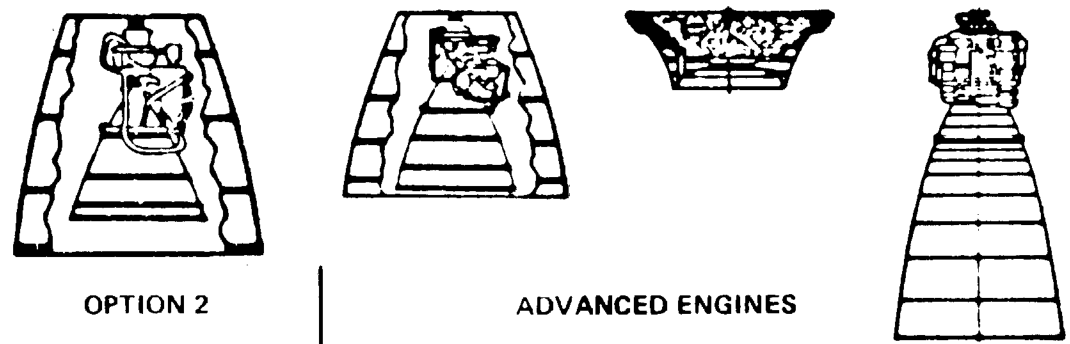

	OPTION 2	ADVANCED ENGINES		
	CAT. IIA RL 10	CAT. IV RL10	AEROSPIKE	ADVANCE SPACE ENGINE (ASE)
THRUST (LB)	15 K	15K	15K	15K
I_{SP} (SEC)	459	470	468	470
MIXTURE RATIO	6	6	5	6
WEIGHT (LB)	476	424	280	270
LENGTH (IN.)	70/127	57/114	20	88
DDT&E COST ($ M)	50*	119	140	154

*106 WITH PUMPED IDLE

Figure 8. Advanced Engine Characteristics

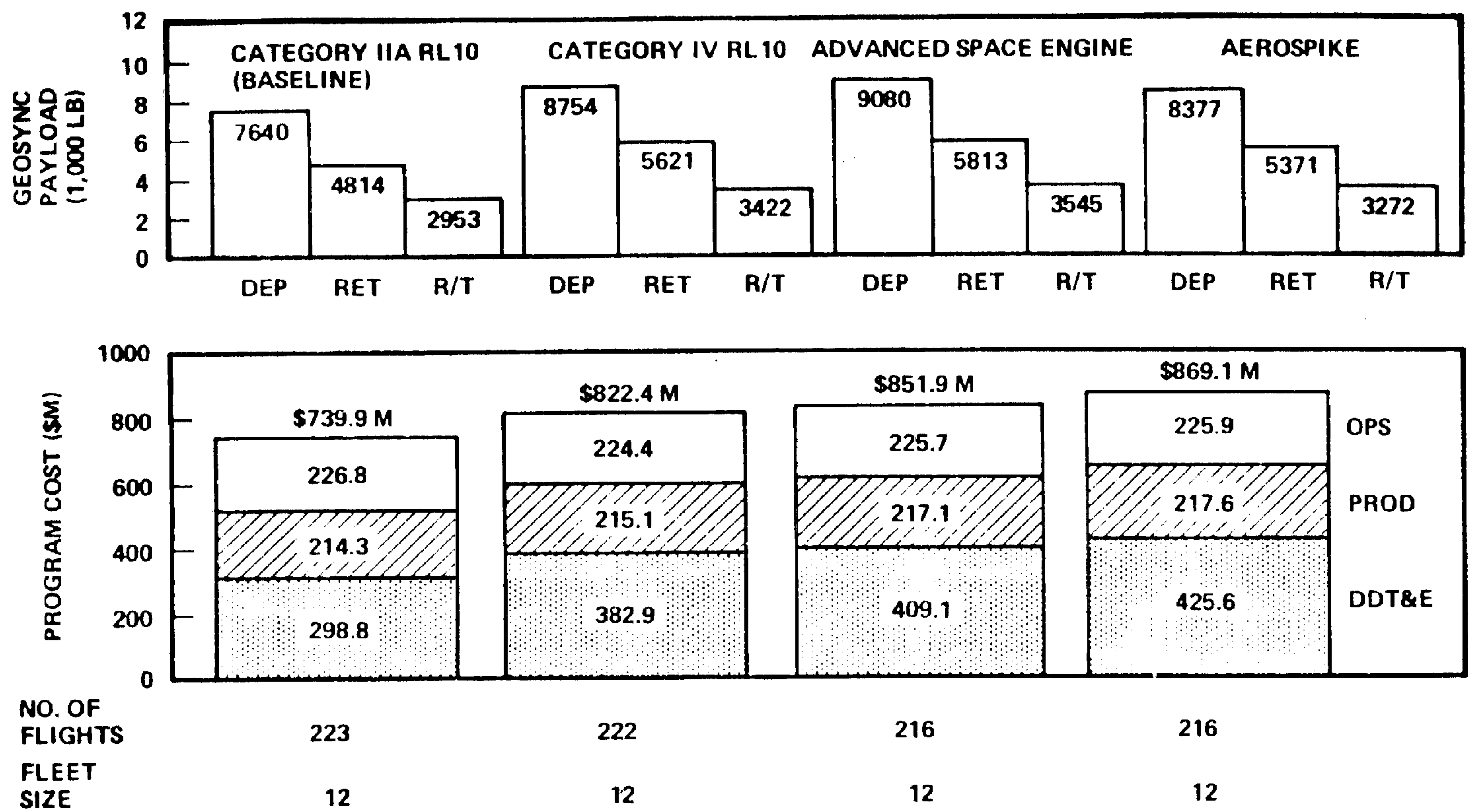

Figure 9. Advanced Engine Evaluation

value, does not apply. Here, the performance objective is to select the plug-cluster configuration that would produce the maximum specific impulse for a specified nozzle length.

Review of the literature on plug and plug-cluster nozzles allows the following general observations to be made concerning the advantages and disadvantages of plug-cluster nozzles for Space Tug application:

ADVANTAGES:

(1) Plug cluster concept lends itself to modular approach, and full utilization of available diameter.

(2) Thrust vector control can be produced by gimbaling or throttling of individual modules or group of modules.

(3) Design techniques for bell module design are well developed.

(4) Plug cluster concept offers fail-operational potential for module-out or turbopump-out fail-safe modes, whereas present Tug propulsion systems are only fail-safe.

(5) Concept allows application of low pressure, long life propulsion system components.

(6) Concept leads to shorter equivalent engine length.

DISADVANTAGES:

(1) Shock wave interaction at the cluster discharge reduces nozzle performance.

(2) Analytical methods are not available at the present time.

(3) Plug cluster engines are slightly heavier than single engines of the same thrust level.

1. Plug Nozzle Performance Criteria

The plug and plug cluster nozzle literature indicates definite trends in the performance of the nozzle as a function of the major design variables. However, these trends can be misleading at the larger area ratios ($\epsilon \geq 80$) and module gaps of this study. For example, plug engine performance appears to decrease significantly with the degree of truncation (i.e., the reduction in the ratio of plug length to isentropic plug length) as shown for the ALRC data curve in Figure 10 (taken from Task I Report, pg. 107).

What is not indicated in the figure is that the tilt angle of the annular throat remains constant at 38 degrees, and that the loss in thrust for a zero length plug is primarily a divergence loss. If it is assumed that a zero length plug does not turn the gas stream axially, the expected thrust efficiency would be $C_{TI}\cos\theta$, or 0.78, which appears to be a valid extrapolation of the ALRC curve in Figure 10.

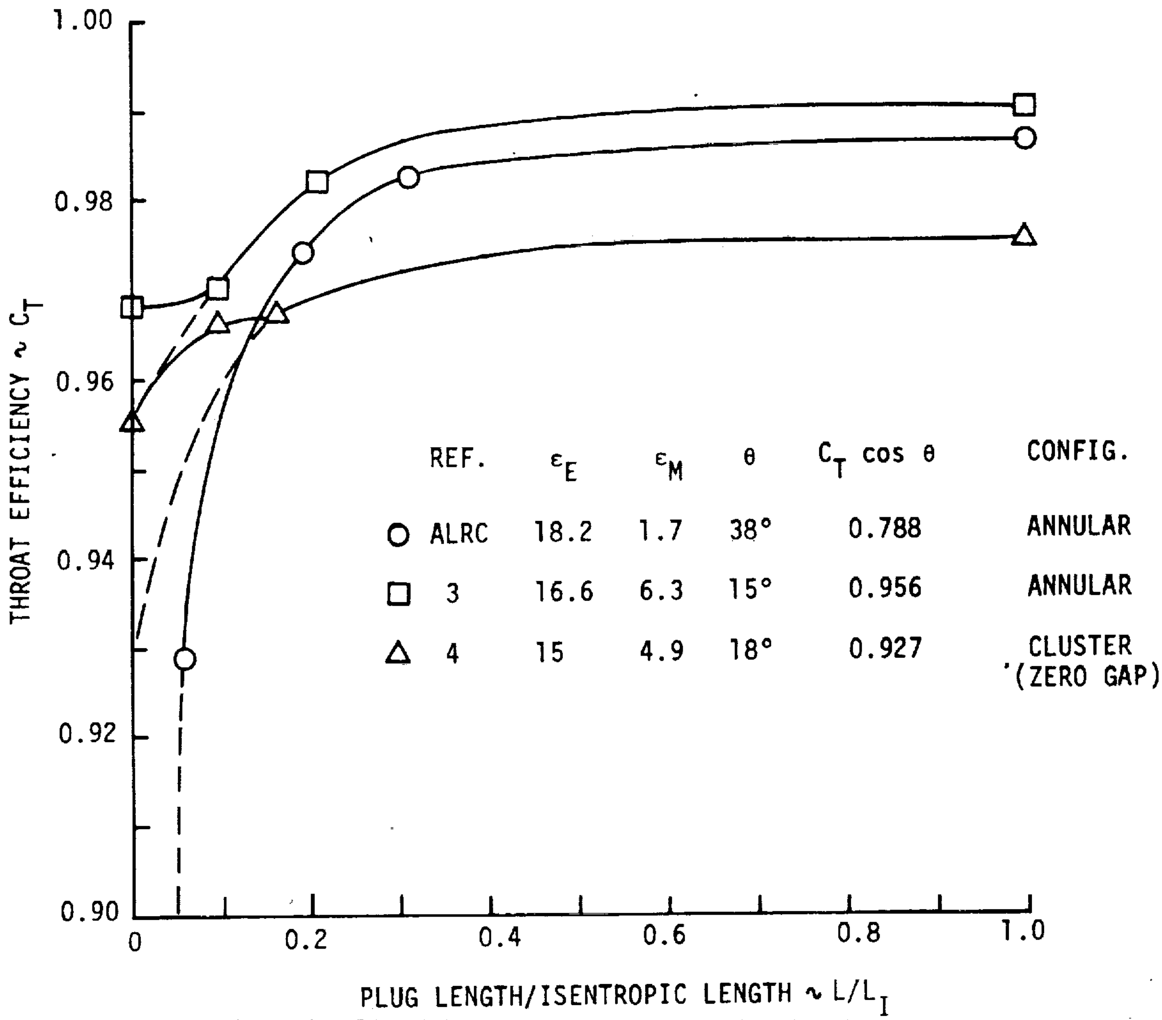

Figure 10. Effect of Truncating the Plug on Thrust Efficiency

The loss in performance for an annular throat plug nozzle with a smaller tilt angle (Ref. 3) is shown in Figure 10 to be much less. The value for $C_{TI}\cos\Theta$ of 0.956 is seen to be a close approximation to the experimental efficiency, when zero flow turning is assumed.

The same trend is evident in the data for clustered modules on a plug (Ref. 4). The value for $C_{TI}\cos\Theta$ is 0.927 for the assumed isentropic C_T in the figure.

Another example of a literature trend involves the performance loss due to gaps between module exits of a plug cluster engine. A typical representation is given in Figure 11 (Ref. 5). Experimental data (Ref. 4, pp. II-53 and II-84) showing the effect of fairings on gap performance are depicted in Figure 12. Addition of the fairing is seen to improve the performance about 50% of the difference between the zero and one gap cases. It is seen that C_T drops significantly when the gap is increased. But this drop may be due to the gap (loss of effective area and/or aerodynamic losses), or due to the increase in tilt angle or change in base pressure. Figure 13 (data from Ref. 4, p. II-39) shows the effect that can be attributed to the tilt angle when the plug length is held constant. Interpretation of the curves in Figure 10 requires superposition of data giving the module C_T contribution ($C_T\cos\Theta$), the base C_T contribution, and the contour C_T contribution all versus the tilt angle. Such data are given in Ref. 4 but only for the baseline tilt angle.

The effect of tilt angle on base pressurization and thus C_T, is depicted on Figure 14 (Ref. 4) for zero plug length.

Base pressurization of the Aerospike annular plug engine amounts to 2.4% of the thrust as shown in Table IV (Ref. 6). Experimental data, giving the relationship between the base pressure and the base flowrate, are shown in Figure 15 (Ref. 7) for an earlier version of the engine. Figure 16 (Ref. 7) depicts the nozzle thrust coefficient efficiency (C_T) variation with amount of base flow for the Aerospike. A maximum is seen to occur at about .004 base flow.

A difference appears in this relationship when data for a plug cluster (Ref. 4) is examined (Fig. 17). The maximum now appears between 1 and 2 percent (but no data points are shown between 0 and 2%). The aerodynamic conditions are entirely different, however. Data for the plug cluster were obtained at (flowrates) pressures such that the wake might not have closed on the plug. In vacuum, the wake will close unless the added base flow becomes excessive, causing flow separation.

2. Plug Nozzle Design Criteria

Reference 4 describes the five geometric parameters that must be determined to completely define a plug cluster configuration: module area ratio (ϵ_E), number of modules (N), engine (cluster) area ratio (ϵ_E), gap distance (δ/D_e), and tilt angle (Θ). The equation relating these parameters is given as

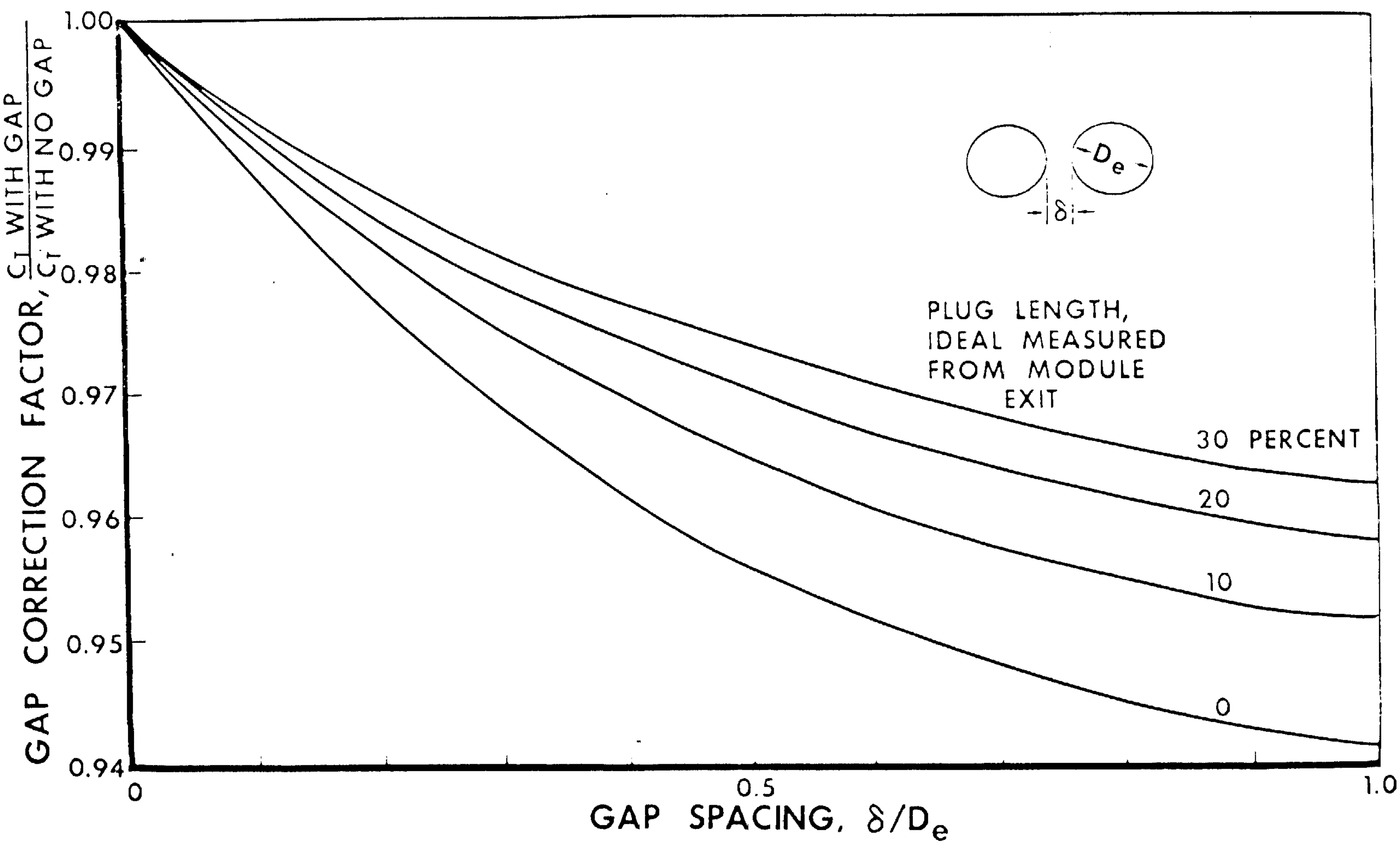

Figure 11. Effect of Module Spacing on Propulsion System Performance

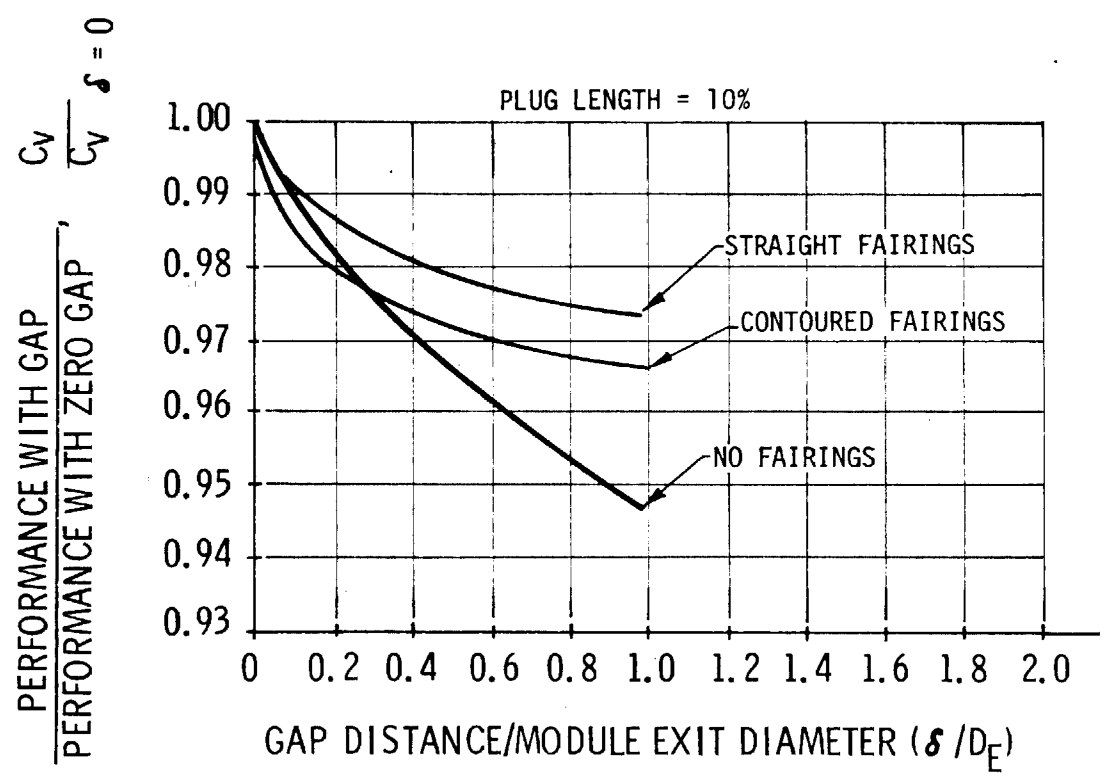

Figure 12. Effect of Fairings and Gap on Performance

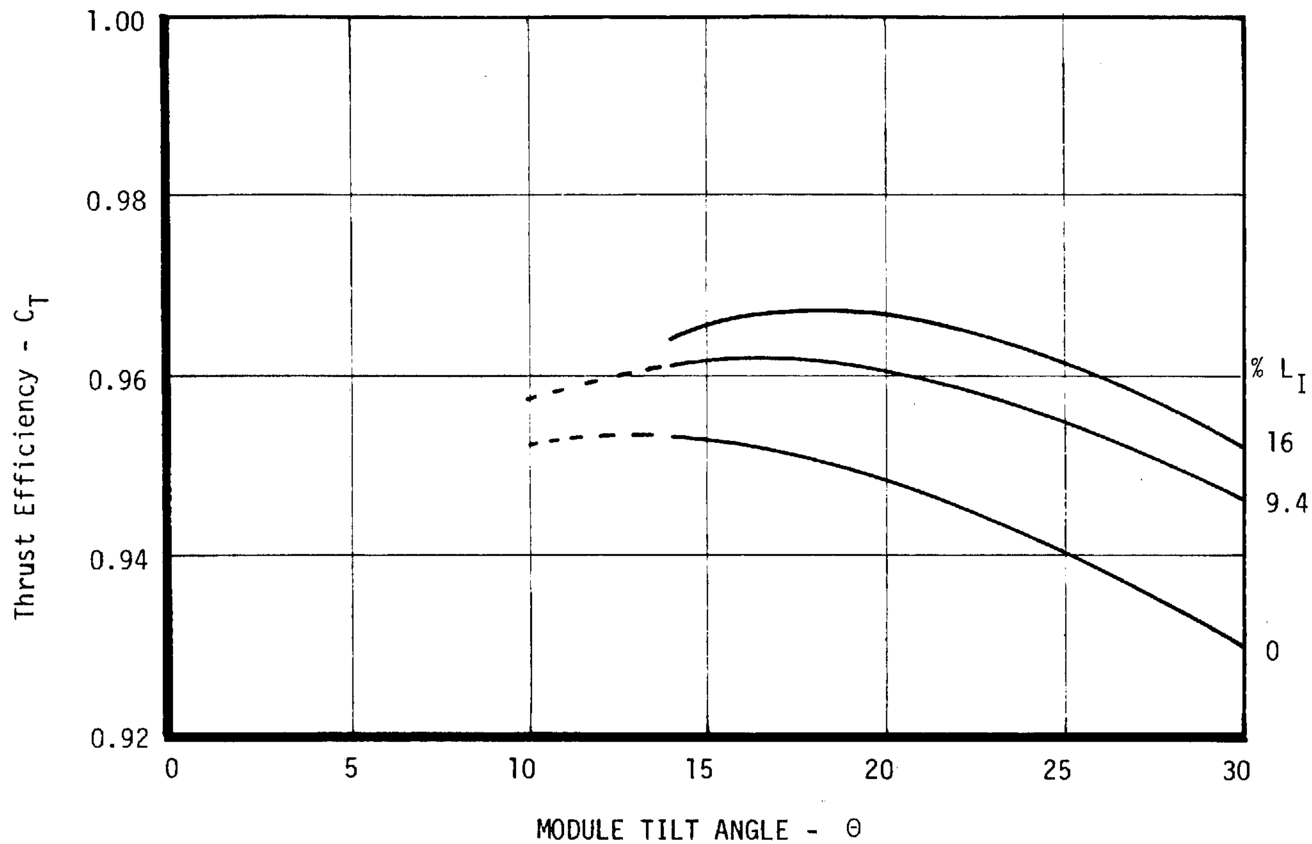

Figure 13. Tilt Angie Model Performance for a Plug Cluster Nozzle

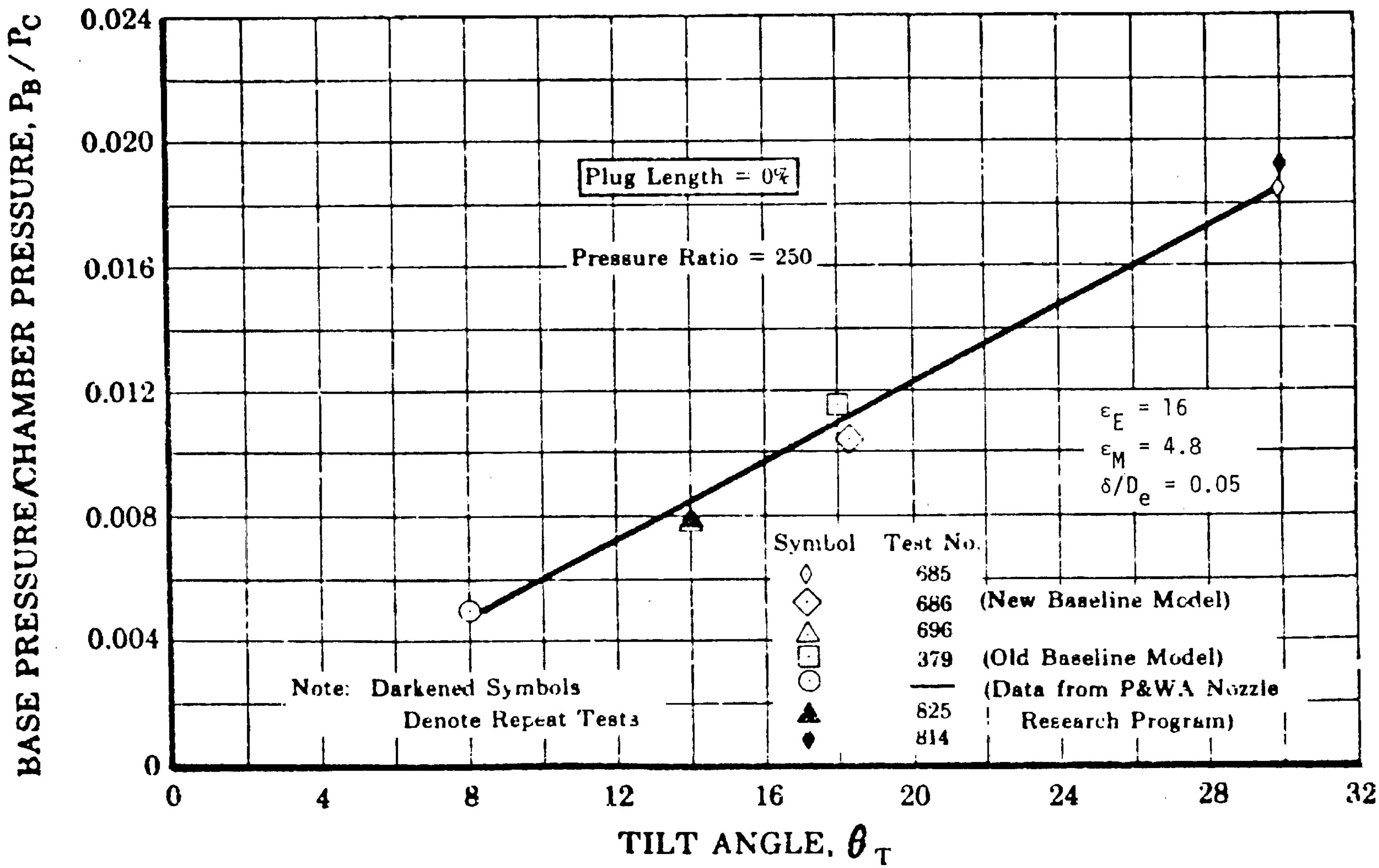

Figure 14. Effect of Tilt Angle on Base Pressure

TABLE IV - NOMINAL PERFORMANCE, DOUBLE-PANEL AEROSPIKE ENGINE SHOWING BASE CONTRIBUTION

Nozzle Type	Aerospike
Engine Thrust, pounds	25,000
Engine Mixture Ratio	5.5:1
Area Ratio	200:1
Stagnation Pressure, psia	1000
Injector Mixture Ratio	5.572
Injector Flowrate, lbm/sec	52.99
Hydrogen Injection Enthalpy, Kcal/mole	2.18
Oxygen Injection Enthalpy, Kcal/mole	-1.005
ODIE Specific Impulse, lbf-sec/lbm	498.5
ODK Specific Impulse, lbf-sec/lbm	497.3
Divergence Efficiency	0.9671
Boundary Layer Loss, lbf-sec/lbm*	-17.93
Energy Release Efficiency	0.995
Base Specific Impulse**, sec.	6056.2
Base Flow Ratio, $\dot{M}_{secondary}/\dot{M}_{primary}$	0.0019
Base Flowrate, lb/sec	0.10
Base Pressure, psia	0.60
Base Thrust, lbf	609.7
Engine Delivered Specific Impulse, sec.	470.4

---

*$\Delta F_{BL}/\dot{M}_{injector}$

** $F_{secondary}/\dot{M}_{secondary}$

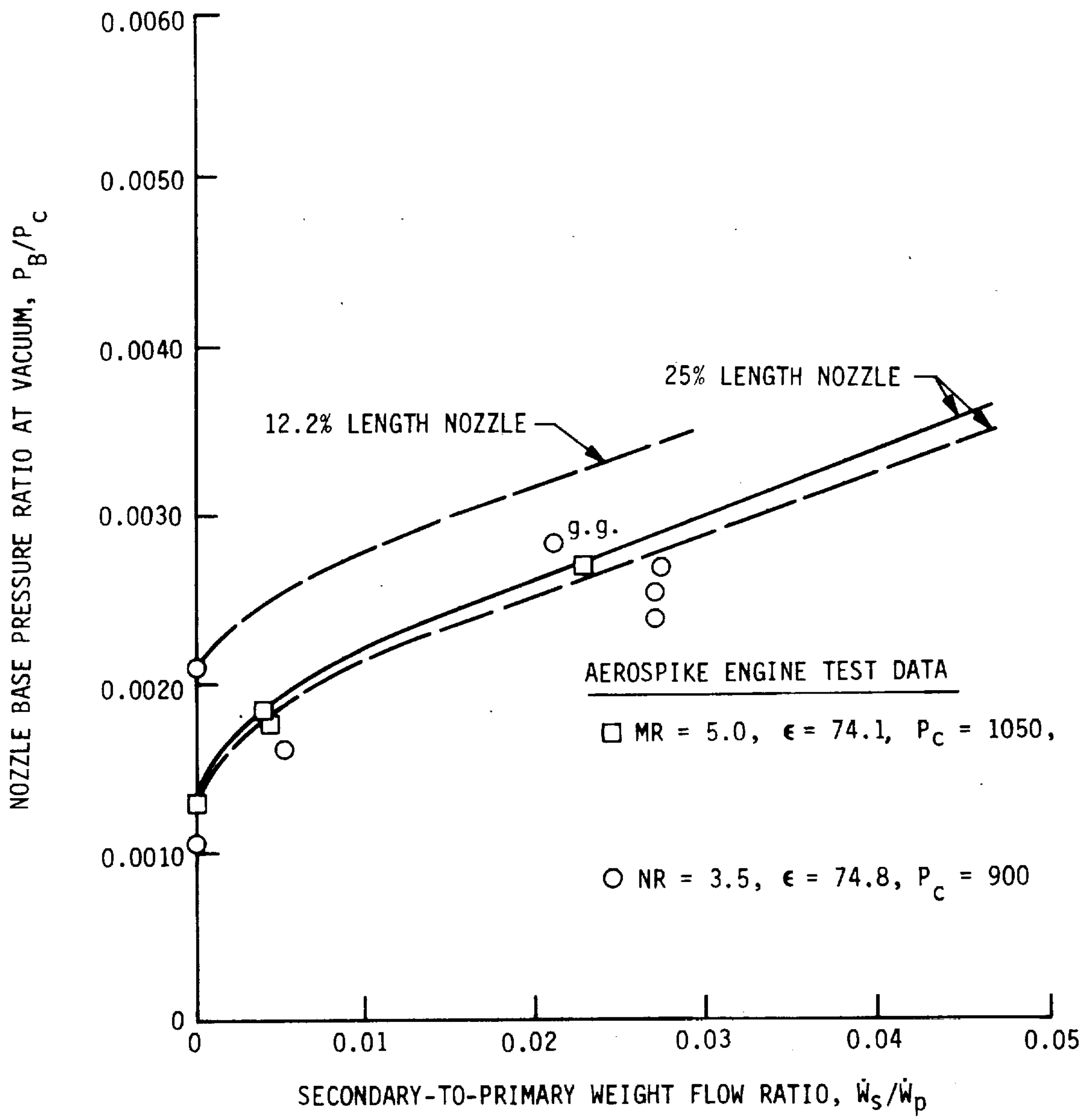

Figure 15. Base Pressure Versus Secondary Flow at Vacuum

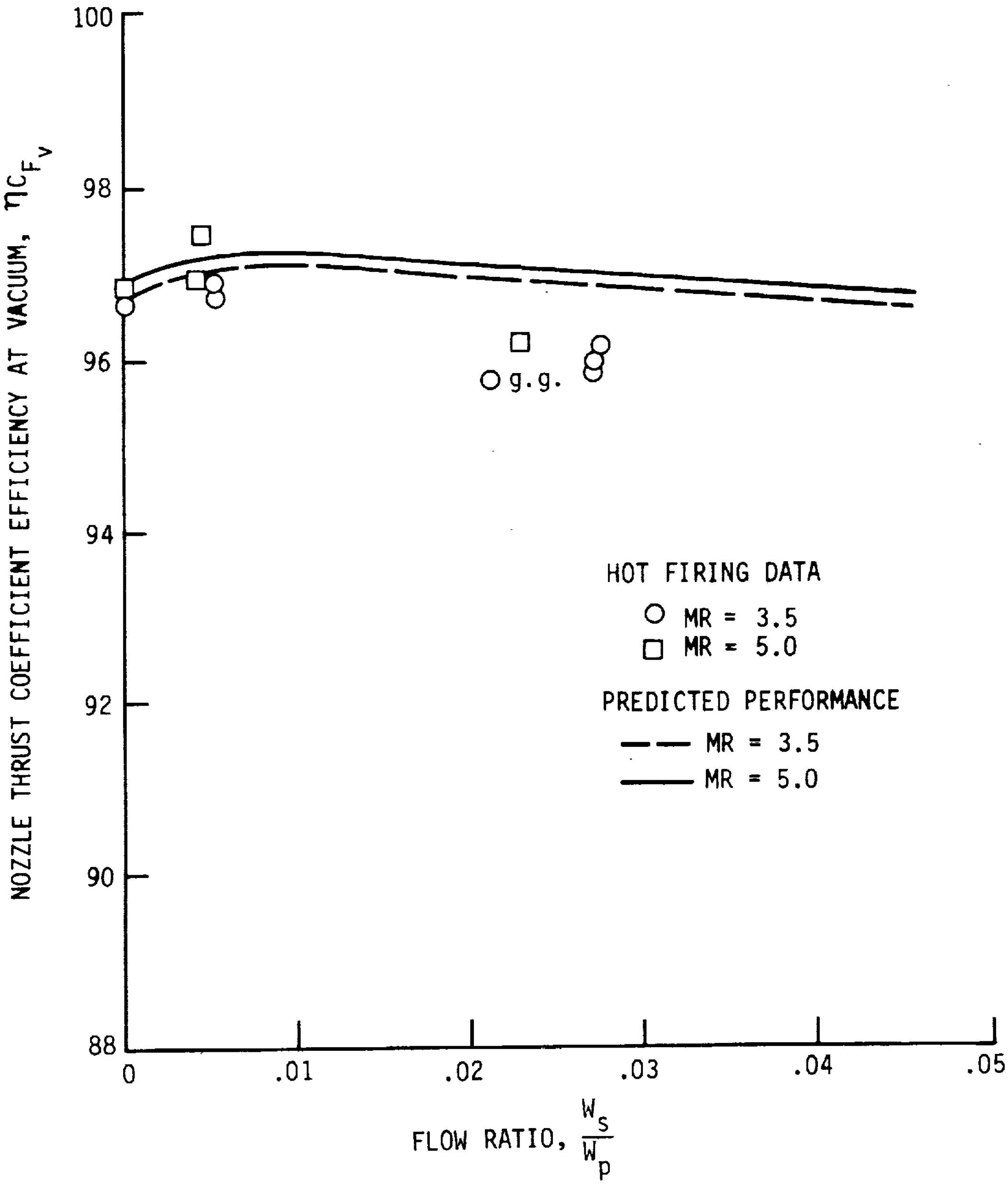

Figure 16. Vacuum Thrust Coefficient Efficiency Versus Secondary Flow

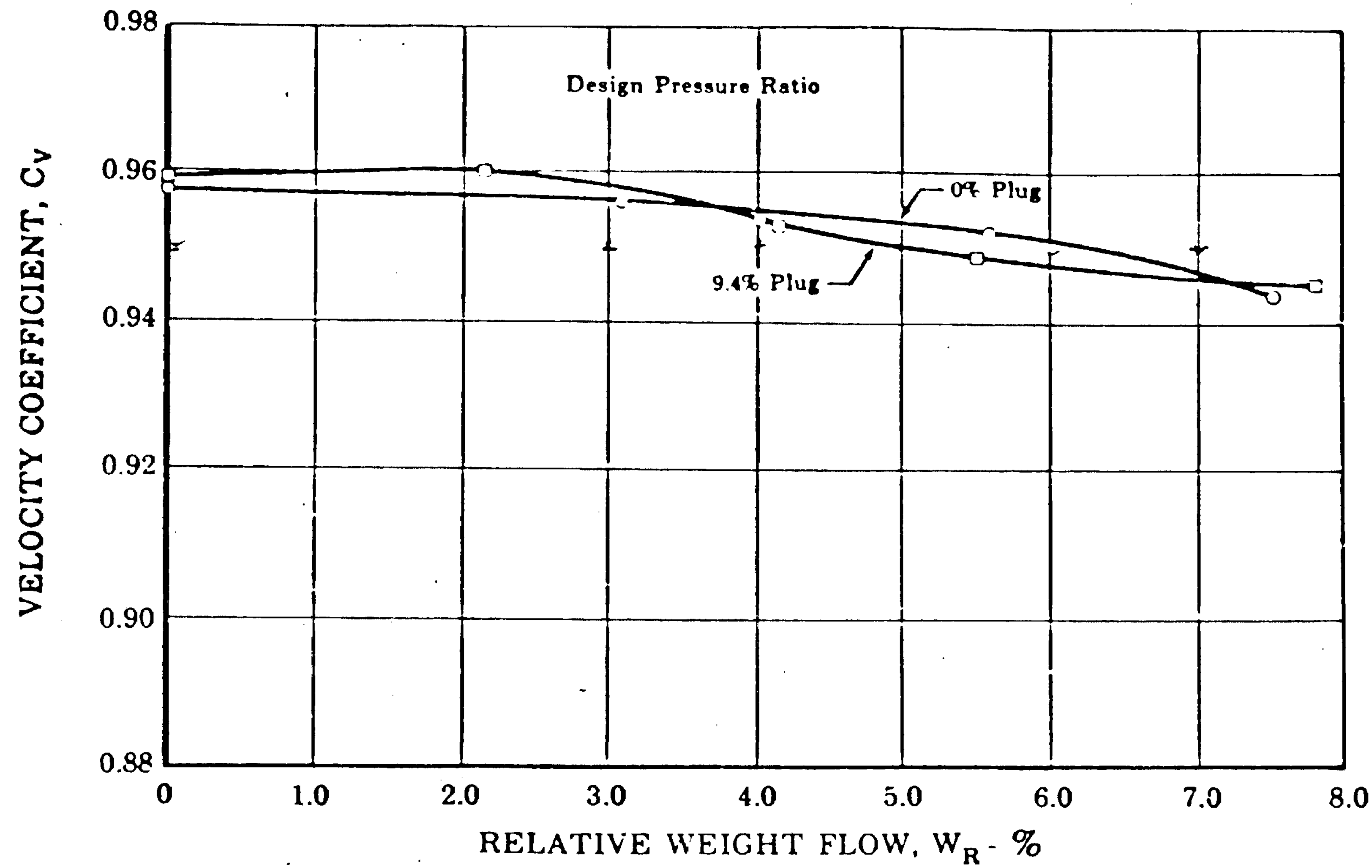

Figure 17. Effect of Radial Inward Base Bleed on Baseline Model Performance

$$\frac{\varepsilon_E}{\varepsilon_M} = \frac{1}{N}\left[\frac{(1 + \delta/D_e)\cos\Theta}{\sin\left[\arctan\left(\cos\Theta\tan\frac{180}{N}\right)\right]}\right]^2 \qquad \text{(Eq. 1)}$$

The choice of any three of the parameters determines the other two.

For a given number of modules, module area ratio, and gap distance, the cluster area ratio and then tilt angle may be calculated. With module and engine area ratios known, the tilt angle is obtained from a figure such as Figure 18 (Ref. 4), as the difference between the Prandtl-Meyer turning angles for the engine and module area ratios. A curve, illustrating the relationship between cluster area ratio, number of modules, and tilt angle, for the case of $\delta/D_e = 0$, is shown in Figure 19 (Ref. 4). With a gap between the modules, the amplification factor ($\varepsilon_e/\varepsilon_M$) will increase; correspondingly, the engine area ratio, as well as the tilt angle, will increase.

There are two regions that must be considered in designing the contour of the plug (Figure 20A): (1) the expansion region of the plug, and (2) the transition region where the flows from the modules merge and mix to form an annular flow field. The method used in Ref. 4 to design the plug contour is as follows: (1) a single-expansion plug nozzle computer program employing the method of characteristics is used to design a plug contour for the desired cluster area ratio. This program provides a full-length plug nozzle with the external expansion starting from a Mach 1 annular throat (Figure 20B). (2) A module is then positioned, as shown in Figure 20C, so that the outer lip of the module coincides with the expansion corner of the single-expansion plug nozzle. Thus, the exit Mach line (corresponding to the cluster area ratio or Mach number) for both the plug cluster nozzle and the single-expansion plug nozzle coincide. (3) A smooth curve from the inside module lip is then faired into the isentropic contour.

D. H/O THRUST CHAMBER TECHNOLOGY

Hydrogen-oxygen thrust chambers that offer potential in a clustered plug configuration for the Space Tug application fall into two categories: (1) existing, or (2) demonstrated (high) technology status. All of the candidate engines for the single-engine Space Tug can be correspondingly categorized except for the existing RL10 that has been carried to operational engine status.

The technology on small thrusters was recently reviewed by Gregory and Herr (Ref. 8). Their paper covered the comprehensive program sponsored by NASA-LeRC to provide the technology groundwork for the use of hydrogen-oxygen propellants in the Space Shuttle Attitude Control Propulsion System (ACPS) thrusters. Final reports on these projects were reviewed in Task I of this study with the objective to independently assess the state-of-the-art of these thrusters and their components with reference to the feasibility of the plug cluster engine concept.

A prime candidate for the plug cluster engine is the NASA LeRC/ALRC Integrated Thruster Assembly (ITA). Another high technology candidate is

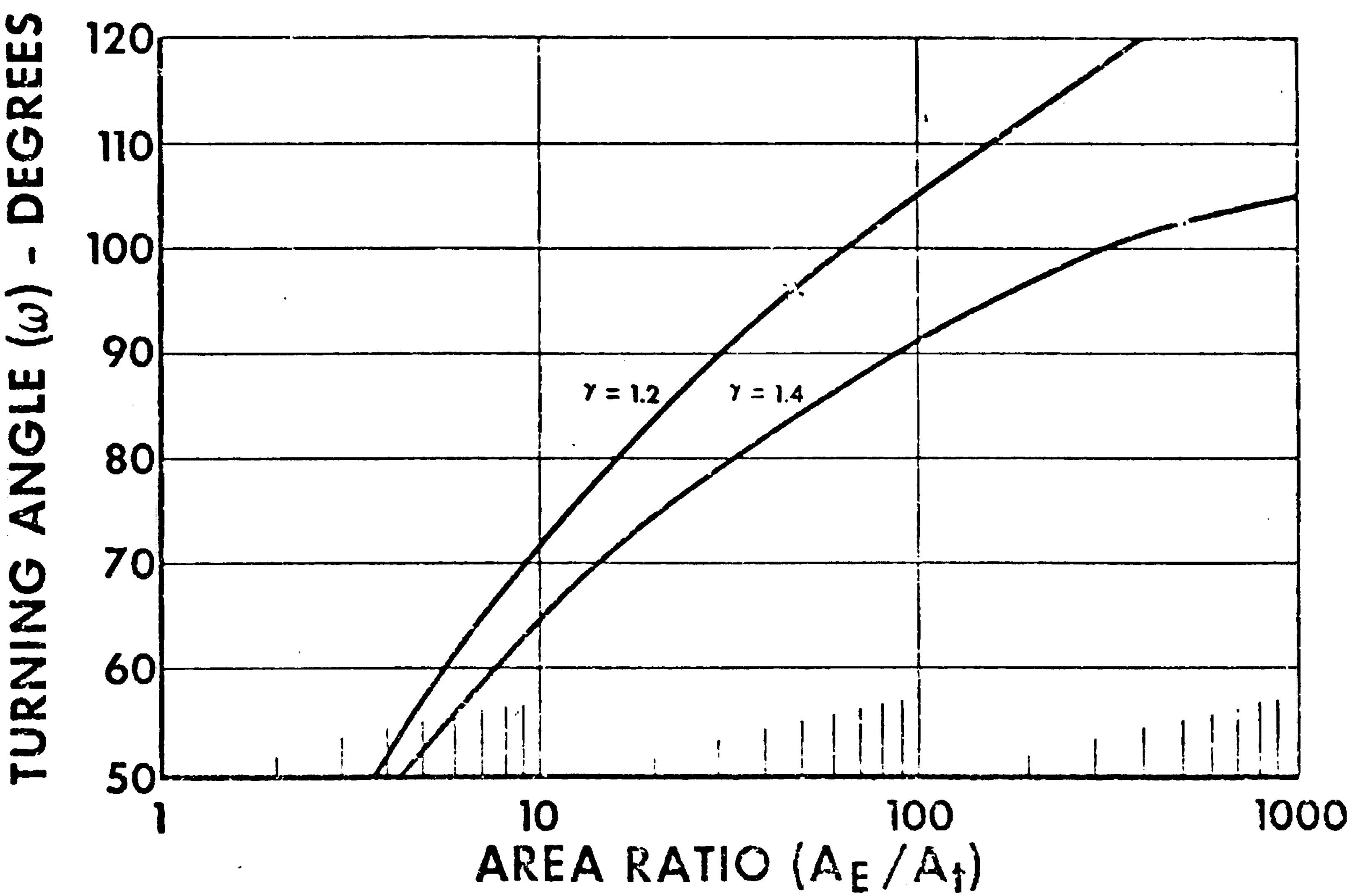

Figure 18. Prandtl-Meyer Turning Angle as a Function of Area Ratio (one-dimensional)

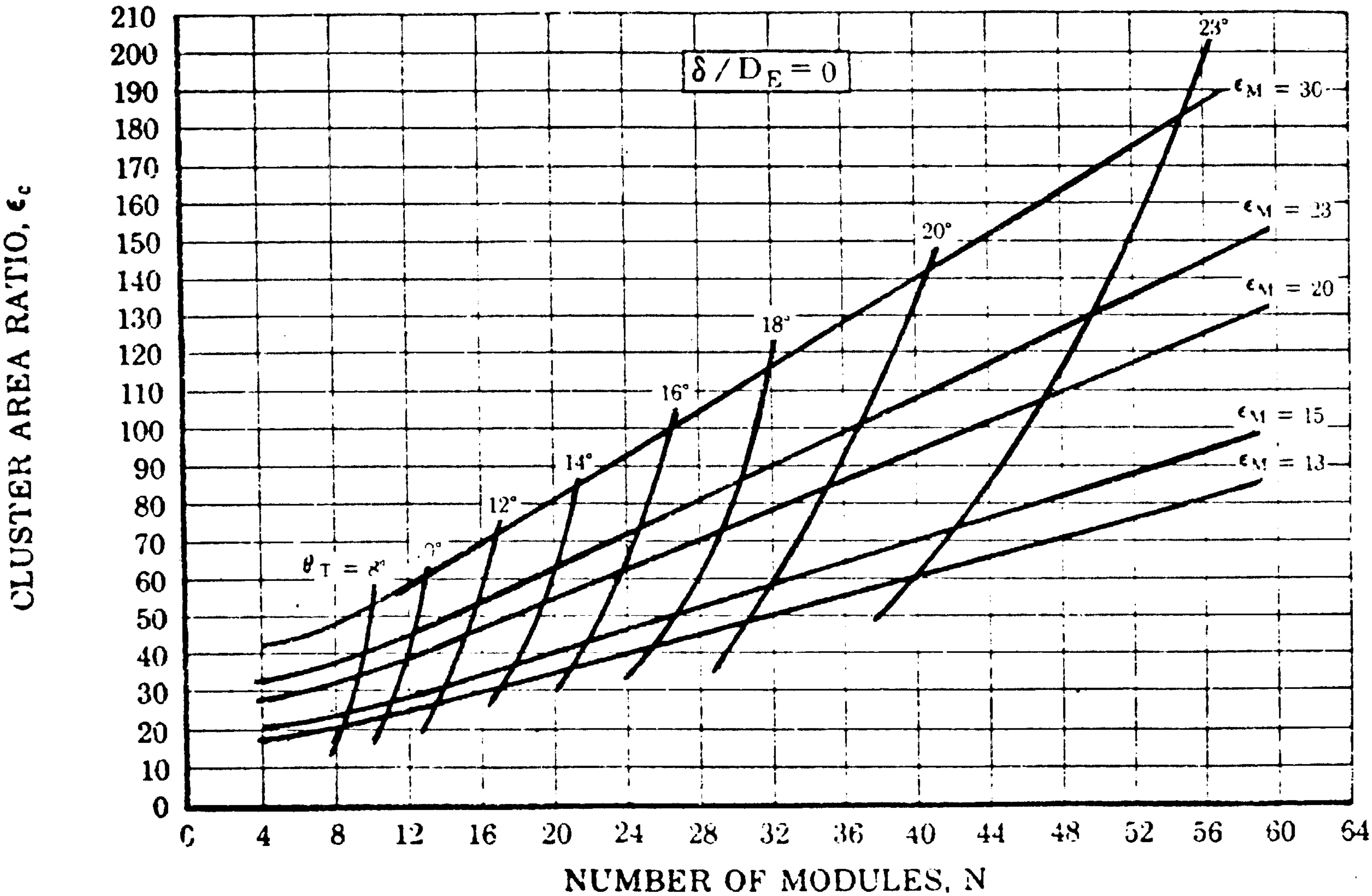

Figure 19. Cluster Area Ratio Versus Number of Modules

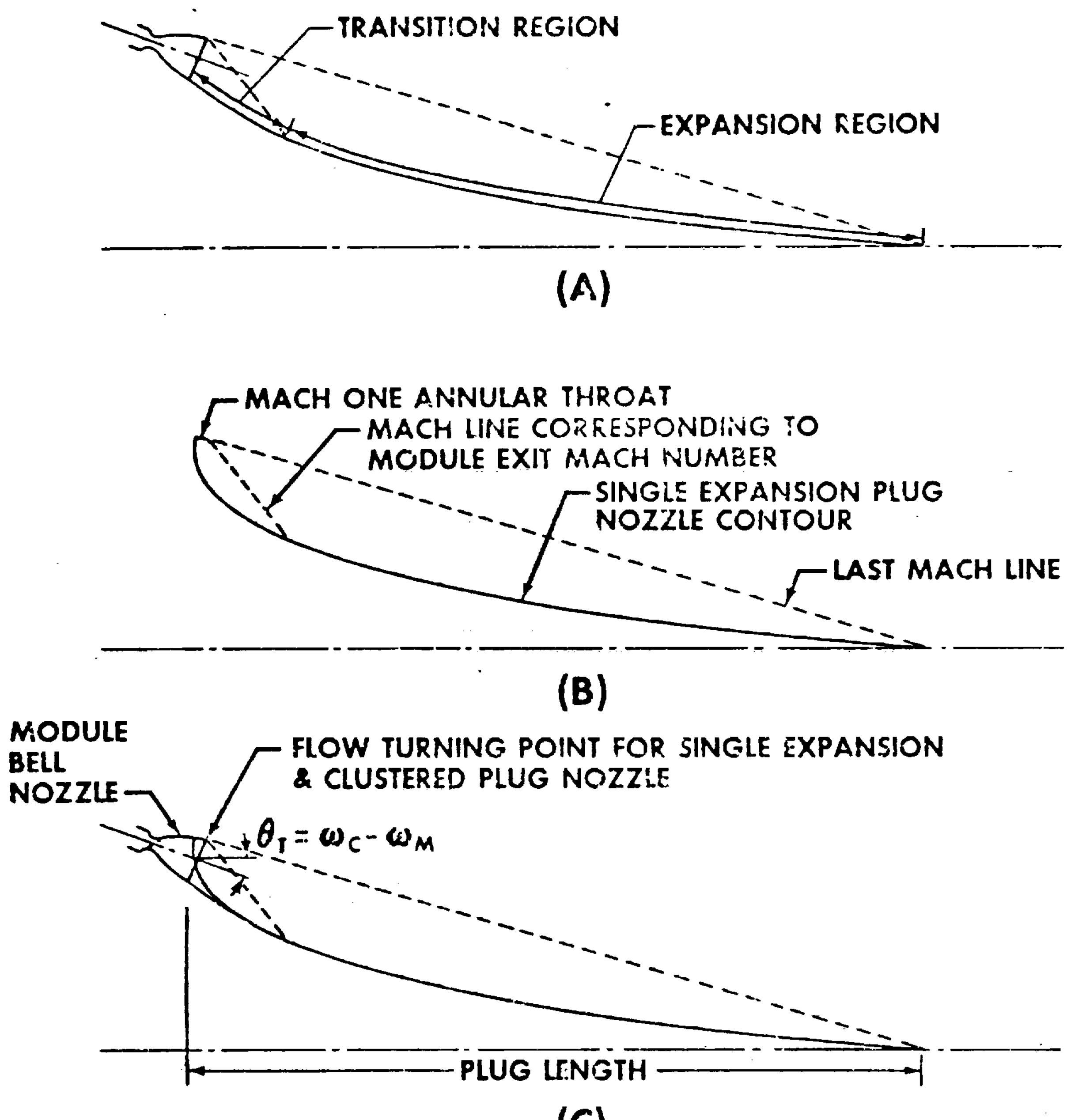

Figure 20. Plug Contour Design

the Extended Temperature Range (ETR) ACPS thruster. Additional candidates include regeneratively cooled thrusters.

A bibliography of pertinent reports that serve in the evaluation of the thrusters for the plug cluster assembly engine is given in Appendix D.

1. Integrated Thruster Assembly

The Integrated Thruster Assembly (ITA), Figures 21 and 22 (Ref. 9), is a flightweight GH_2/GO_2 ACPS engine employing a spark initiated igniter. The nominal operating conditions are: 6672 N (1500 lbf) thrust, 207 N/cm^2 (300 psia) chamber pressure, and a 4.0 mixture ratio, as given in Table V. The thruster has demonstrated a steady state specific impulse of 435 sec at a mixture ratio of 4.0 and 431 seconds at an O/F = 5.5 (Ref. 45). The ITA consists of a premix triplet injector, a regeneratively cooled chamber, and a dump-film cooled throat and skirt; an ox rich torch type igniter and integral exciter/spark plug; two igniter valves, and two main propellant valves. The ITA S/N 002 was fired 42,266 times over 4200 full thermal cycles. A similar unit achieved 51,000 cycles in life testing at NASA/LeRC.

The scope of the ITA program included review of H_2/O_2 ACPS technology, design and fabrication of an optimized flightweight thruster, and test firing to evaluate the thruster operation over a range of conditions such as would be encountered in a Space Shuttle application. The objective of the ITA program was to develop the technology for flightweight ACPS thrusters by investigating areas of unresolved technology such as: (1) chamber/injector life, (2) component interaction and optimization of a design to meet the often conflicting requirements of steady state performance and cooling, (3) pulsing with cold propellants, (4) response time, (5) flightweight, and (6) long cycle life.

The results of the ITA program are as follows: (1) the ITA design is satisfactory, simple to operate, and has adequate life, (2) the igniter is very reliable, (3) chamber coolant part to part hydraulic characteristics have no significant variations, (4) 51,000 pulses were demonstrated on a single unit, (5) the predicted thermal cycle life of 65,000 cycles agrees with measured temperature data, (6) fuel lead starts can result in damage, thus .01 to .02 sec oxidizer leads are used, (7) fuel lag shutdowns are preferred, (8) the longest firing duration made with the ITA was 513 sec, and (9) the ITA weight was 6.895 kg (15.2 lbm) exclusive of valves.

The ITA program demonstrated a lightweight, compact, high performing thruster which meets duty cycle and cycle life requirements. The primary problem area of the ITA thruster was the main propellant valves, which started to leak after 20,690 pulses. The upper limit on operating pressure was 348 N/cm^2 (482 psia) due to the pressure limit of main propellant valves. Neither of these main propellant valve considerations should limit the use of the ITA results.

2. Extended Temperature Range Thruster

The Extended Temperature Range (ETR) Program (Ref. 10) involved the study of five cooling concepts (Figure 23) and the design, fabrication,

Figure 21. Integrated Thruster Assembly is a Prime Candidate for the Plug Cluster Engine

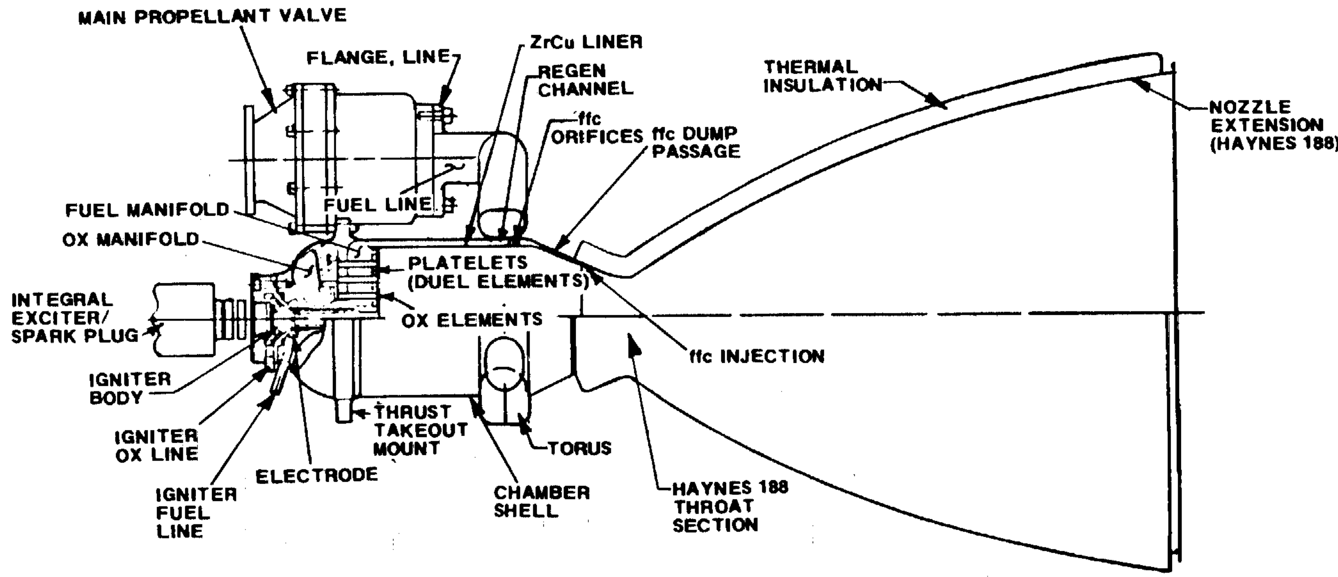

Figure 22. ITA is a Flightweight High Technology Thruster

TABLE V. - ITA DESIGN SUMMARY

Design Characteristics	
Thrust	6672 N (1500 lb_f)
Chamber Pressure	207 N/cm^2 (300 psia)
Mixture Ratio	4.0
Pressure at Inlet to Valves	276 N/cm^2 (400 psia)
Fuel Flow Rate	
Regen and Injector	247 g/sec (.545 lb/sec)
Fuel Film Coolant	65.6 g/sec (.145 lb/sec)
Total	313 g/sec (.69 lb/sec)
Oxidizer Flow Rate	1252 g/sec (2.76 lb/sec)
Fuel Temperature	130°C (250°R)
Oxidizer Temperature	208°C (376°R)
Igniter Fuel Flow Rate	
Core	.726 g/sec (.0016 lb/sec)
Coolant	4.26 g/sec (.0094 lb/sec)
Total	4.99 g/sec (.011 lb/sec)
Igniter Oxidizer Flow Rate	32.66 g/sec (.072 lb/sec)
Igniter Core MR	45
Igniter Overall MR	6.55
Geometry	
Throat Diameter	4.88 cm (1.92 in.)
Exit Diameter	30.73 cm (12.1 in.)
Chamber Contraction Ratio	3.3
Nozzle Exit Area Ratio	40:1
Chamber L*	43.18 cm (17 in.)
Overall Length	74.68 cm (29.4 in.)
Overall Length (less exciter/spark plug)	61.37 cm (24.16 in.)
Fwd End Clearance Diameter	33.78 cm (13.3 in.)
Dimension of Cylinder Enclosing ITA	74.68 x 36.32 cm (29.4 x 14.3 in. Dia)
Weights (Design)	
ITA (incl. Main Propellant Valves)	14.016 kg (30.9 lb)
Main Propellant Valves	7.257 kg (16.0 lb)
ITA (less valves)	6.758 kg (14.9 lb)
Thrust Chamber (Incl. Insulation)	3.933 kg (8.67 lb)
Injector	1.887 kg (4.16 lb)
Igniter	.939 kg (2.07 lb)
Design Performance	
Specific Impulse	
Steady State	4266 N-sec/kg (435 lb_f-sec/lb_m)
Pulsing @ MIB	3923 N-sec/kg (400 lb_f-sec/lb_m)
MIB	222 N-sec (50 lb-sec)
Response (electrical signal to 90% thrust)	.050 sec

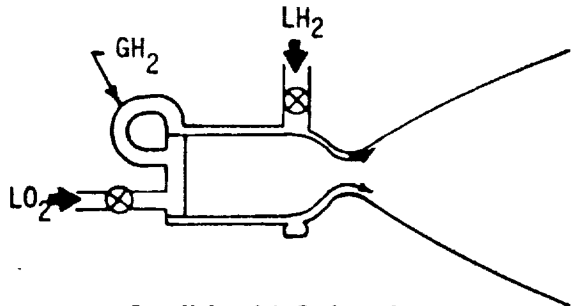

a. Gas/Liquid Injection
Upstream Valve Film
Cooled Throat

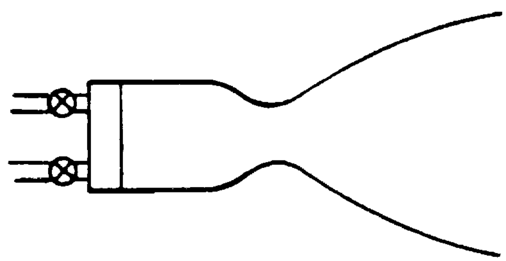

b. Liquid/Liquid
Injection Film Cooled
Chamber

Figure 23. Tested ETR Candidate Propellant Thermal Management Concepts

and testing of two non-flightweight engine designs which are viable candidates for Space Shuttle and Tug engine systems. One ETR design, using a 24-element liquid/liquid injector, was fired 66 times as a full thruster at sea-level conditions, and 10 times with a cooled chamber at altitude conditions, and was damaged after four seconds duration. The second design was a 36-element gas/liquid injector that was fired successfully 48 times at sea-level conditions, and 44 times with a cooled chamber at altitude conditions with five tests of 20 seconds duration each. The operating point of both engines is 5560 N (1250 lbf) thrust, 345 N/cm^2 (500 psia) chamber pressure and 4.5 mixture ratio with cryogenic propellants.

The ETR program successfully demonstrated a non-flightweight 36-element coaxial G/L thruster with a dump cooled regenerative chamber and a Haynes nozzle over a chamber pressure range of 152 to 345 N/cm^2 (220 to 500 psia) and a mixture ratio range of 2.3 to 6.2 with fuel inlet temperature of 36 to 116°K (64 to 208°R). A cumulative firing duration of 273 sec, including five 20 sec tests, was made without damage. The igniter and valve capability, reliability, and durability were demonstrated.

The G/L thruster demonstrated durations of 20 sec without damage, and a steady state performance of 4266 N-sec/kg (436 lbf-sec/lbm) with 18% fuel film cooling. A hydrogen inlet temperature of as low as 35.6°K (64°R) and as high as 111°K (200°R) was demonstrated in the G/L thruster. A wide range of operating conditions were tested. Combustion stability was demonstrated on all testing. Large amounts of thermal data were obtained.

3. Hydrogen-Oxygen Auxiliary Propulsion Engines

Technology for long life, high performing hydrogen-oxygen (H/O) rocket engines suitable for Space Shuttle auxiliary propulsion systems (APS) were obtained in several NASA sponsored programs. Injectors, fast response valves, igniters, and regeneratively and film-cooled thrust chambers were tested over a wide range of operating conditions and durations (Ref. 11 and 12). A typical schematic of a thrust chamber that was tested is shown in Figure 24.

The scope of the H/O APS programs included the screening of candidate cooling methods during analysis and design studies, and the fabrication and testing of the selected designs. Design criteria and performance summaries are indicated for these designs in Table VI.

E. H/O TURBOPUMP ASSEMBLY TECHNOLOGY

The plug cluster engine concept is dependent upon the turbomachinery subsystem design, performance and weight. Since the performance of a conventional space engine is essentially insensitive to the level of thrust chamber pressure, pump discharge pressures can be low, and consequently, the turbopump weight, which is then a small percentage of the total engine weight, is low.

For the plug cluster engine, pump weight optimization will depend upon the number of turbopump assemblies (TPAs) selected to feed the

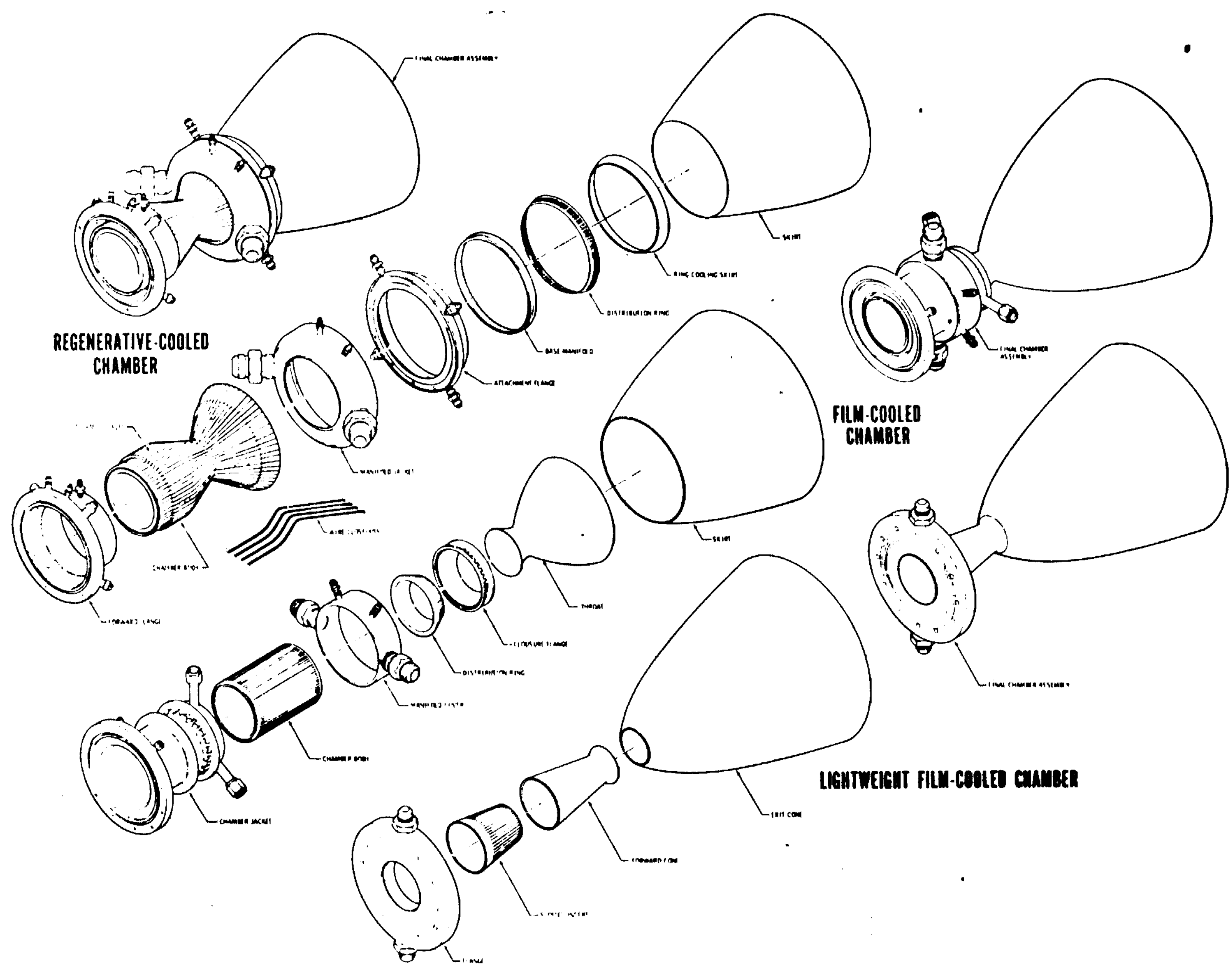

Figure 24. APS Thrust Chamber Assembly Schematics

TABLE VI - APS CYCLE LIFE PERFORMANCE MATRIX (Ref. 11)

PHASE I CHAMBER DESIGNS AND CONDITIONS
AMBIENT TEMPERATURE PROPELLANTS

P_c, psia (N/cm^2)	100 (69)	300 (207)			500 (345)
MR	4	3	4	5	4
Regen Chamber, 10% FFC					
I_s, lbf-sec/lbm	449	455	452	440	455
(N-s/kg)	(4400)	(4459)	(4429)	(43[illegible]2)	(4459)
N_f	3.5×10^4	3×10^4	3×10^4	3×10^4	1.2×10^3
N_{f_T}	3.5×10^4	2×10^3	2×10^3	2×10^3	
Film Cooled Chamber, 20% FFC					
I_s, lbf-sec/lbm		448	443	430	447
(N-s/kg)		(4390)	(4341)	(4214)	(4380)
N_f		--	10^6	--	
N_{f_T}		9×10^3	9×10^3	9×10^3	

PHASE II CHAMBER DESIGNS AND CONDITIONS
COLD PROPELLANTS

P_c, psia (N/cm^2)	100 (69)	300 (207)			500 (345)
MR	4	3	4	5	4
Regen Chamber, 9% FFC					
I_s, lbf-sec/lbm	--	444	442	431	442
(N-s/kg)		(4351)	(4332)	(4224)	(4332)
N_f	10^6	10^6	10^6	10^6	--
N_{f_T}	2×10^5	1.5×10^4	1.5×10^4	1.5×10^4	$7.5\times10^{[illegible]}$
Film Cooled Chamber					
15%FFC					
I_s, lbf-sec/lbm		441	438	428	
(N-s/kg)		(4322)	(4292)	(4194)	
N_f	10^6	10^6	4×10^5	10^5	4×10^4
N_{f_T}	$>10^5$	10^5	10^5	10^5	4×10^4
20% FFC					
I_s, lbf-sec/lbm		438	435	425	
(N-s/kg)		(4292)	(4263)	(4165)	
N_f	10^6	10^6	10^6	8×10^5	2×10^5
N_{f_T}	$>10^5$	10^5	10^5	10^5	--

N_f = Thermal cyclic life for pulses of 200 lbf-sec or less.

N_{f_T} = Thermal cyclic life for full thermal cycles. Firings >[illegible]750 lb-sec total impulse.

All designs provide 10^6 pulse capability for 50 lb-sec bit impulse.

thrusters (modules). Mission reliability, as well as the number of engine restarts per mission, and the effect on chilldown propellant requirements also depend strongly upon the number of TPAs in the feed system.

An important factor in the selection of the number of TPAs is the geometric size of the critical components such as bearings and seals. Miniaturization of these components must be avoided.

The turbopump selection further impacts the system payload capability through the suction pressure requirements, and the classical tradeoff of tank weight versus NPSH and chilldown propellant flow must be made.

A bibliography of reports on turbopump technology pertinent to the plug cluster engine Space Tug application is given in Appendix E. It is apparent that the TPA technology is of sufficient status to allow engine system and design studies to be conducted in a realistic manner.

1. APS Turbopumps

Small, high-performance LO_2 (Table VII) and LH_2 (Table VIII) turbopump assembly configurations were fabricated with each unit consisting of pump, turbine gas generator, and appropriate controls (Ref. 13). Development testing was conducted on each type to demonstrate performance, durability, transient characteristics, and heat transfer under simulated altitude conditions. Following successful completion of the development effort, two LO_2 turbopump units and one LH_2 turbopump unit were acceptance tested. A weld failure in the turbine manifold of one LH_2 turbopump unit prevented its acceptance. The test results on the LO_2 turbopump assembly correlated well with predicted performance, while the LH_2 turbopump test results showed lower than anticipated developed head at the design point and in the high flow range of operation. The lower developed head is attributed to higher than anticipated pump flow passage resistance from effects typical of small multistage pumps. The results of this program have established a sound technology base for future development of small, high performance turbopumps and gas generators.

Assessment of the state-of-the-art of these turbopump configurations shows the breadboard designs are somewhat heavier than desired for use on an engine. Further design refinements would likely be required for adaptation to engine installations.

EDM and casting methods were extensively used in fabrication. Although some difficulties were encountered, the processes were evidently quite successful. The art of fabricating small turbomachinery components will undoubtedly develop further as their use is increased.

2. RL10 Turbopump Assembly

Reference 14 examined selected RL10 derived candidate engines for the cryogenic Space Tug to define detailed engine system performance, mechanical and operational characteristics. A critical element evaluation estab-

TABLE VII - APS OXIDIZER TURBOPUMP PERFORMANCE REQUIREMENTS (Ref. 13)

Pump:	Flow, m^3/sec (gpm)	6.309×10^{-4} (100)
	Inlet Pressure N/m^2 (psia)	137,895 - 344,738 (20-50)
	Developed Pressure, N/m^2 (psid)	1.103×10^7 (1600)
	Inlet Temperature, K (R)	92.8 - 103.9 (167-187)
Turbine:	Energy Source	O_2/H_2
	Exhaust Pressure N/m^2 (psia)	24.317 (35)
Turbopump:	Life, tbo, hrs	10
	Operating Cycles	10,000
	Start Time, sec	1.5
	"ON" Time	2 sec to 600 sec
	"OFF" Time	5 sec to 24 hrs
	Useful Life	10 years
	Seal Leakage	Minimized
	Maximum Surface Temperature	589 K (1060 R)
	Turbine to Pump Heat Flow	<52,752 Joule/hr (50 Btu/hr nonoperative)
		<158,256 Joule/hr (150 Btu/hr operative)

TABLE VIII - APS LH_2 TURBOPUMP PERFORMANCE REQUIREMENTS (Ref. 13)

Pump:	Flow	2.01 kg/s (4.5 lb/sec)
	Flow	0.02902 m^3/sec (460 gpm)
	Developed Pressure	1.103 x 10^7 N/m^2 (1600 psia)
	Inlet Pressure	124,106 - 344,738 N/m^2 (18 - 50 psia)
	Inlet Temperature	20.8 - 25 K (37.5 - 45 R)
Turbine:	Energy Source	O_2/H_2
	Exhaust Pressure	2413.7 N/m^2 (35 psia)
Turbopump:	Life, tbo	10 hrs
	Operating Cycles	10,000
	"ON" Time	2 sec (minimum)
	"OFF" Time	5 sec to 24 hrs
	Start Time	1.5 sec
	Turbine to Pump Heat Flow	158,256 Joule/hr (50 Btu/hr Static)
		52,752 Joule/hr (150 Btu/hr Operating)

lished the feasibility of various engine features such as tank head idle, pumped idle, and autogenous tank pressurization and two-phase pumping. The tank head idle and pumped idle mode are attractive as a means of achieving pump chilldown with minimum loss of total impulse. The two-phase pumping capability relates to minimizing the weight of gas pressurants.

Four engines were investigated with chamber pressures from 400 to 870 psia. The turbopump assembly configured for two-phase pumping required a larger diameter inducer for the LH_2 pump, and a low speed boost pump for the LOX system.

SECTION IV

ENGINE PERFORMANCE METHODOLOGY

A. OBJECTIVES AND GUIDELINES

The program objective was to prepare performance maps for the plug cluster engine concept, displaying the delivered specific impulse in terms of the following variables:

- Combustion chamber pressure
- Engine area ratio
- Engine diameter
- Number of clustered modules (or thrust per module)
- Module area ratio
- Module mixture ratio
- Engine mixture ratio
- Plug nozzle base pressure (or base flow rate)

The program requirement was to utilize simplified engine performance methodology. Test data correlations for base pressurization and fairing corrections were incorporated into the model. Nominal conditions for the plug cluster engine were those of the baseline Space Tug as given in Table I.

A Task Report (Unconventional Nozzle Tradeoff Study - Monthly Technical Progress Report 20109-M-4, Task II - Parametric Engine Performance, Aerojet Liquid Rocket Company, Sacramento, California, Contract NAS 3-20109, November 1976) was issued summarizing the data generated.

Upon receipt of the experimental cold flow data from Contract NAS 3-20104, the engine performance methodology was revised. Performance maps reflecting the experimentally measured effects of gaps, fairings, tilt angle, and base pressurization were generated. Calculations for the baseline case indicated only a small performance improvement over that obtainable from a low area ratio (ε = 40) module. These data led to a reevaluation of the plug cluster design and to the formulation of a design and consistent performance methodology.

B. MODULE PARAMETRIC PERFORMANCE MODEL

The approaches taken to define the performance of the plug cluster engine involve the establishment of the individual thruster (module) performance as well as the performance contribution from the plug nozzle extension. Module performance is discussed in this section.

Module parametric performance analysis was accomplished using a computer model constructed to meet the study's specific requirements. It was built upon the procedures specified by the JANNAF Liquid Rocket Performance Subcommittee (Ref. 15) and was a modification of a computer model formulated for another engine study (Ref. 16). The JANNAF Subcommittee has recommended two performance analysis methods. The standard procedure which utilizes the best available analytical procedure is primarily used for single point performance analysis of existing engine systems. The second method is a simplified procedure which utilizes design chart data and lower cost computer programs. It is designed for the parametric analysis of engine systems and was ideally suited to this study. The simplified method, therefore, was utilized.

The program calculates delivered module performance and the module envelope as a function of engine thrust (F), chamber pressure (P_c), area ratio (EPS), mixture ratio (O/F), film cooling level, nozzle length (% Bell), and injector type. To accomplish this wide-range, parametric analysis with a minimum cost, the JANNAF procedures have been expanded to include: (1) ODE and ODK I_{sp} and C* data tabulations as a function of O/F, P_c, F, and EPS, (2) injector design limits, and (3) envelope design data. Delivered module performance and envelope are determined for any set of design and operating conditions through the evaluation of the one-dimensional equilibrium (ODE) specific impulse and the appropriate performance losses. The module envelope is determined from the calculated performance level and the nozzle design and chamber length requirements and specific operating conditions. A brief description of the methods used to evaluate the above parameters follows.

1. Performance Losses

a. One-Dimensional Equilibrium (ODE) and One-Dimensional Kinetic (ODK) Performance

The ODE and ODK I_{sp} and C* are included in block data form in a subroutine. The data were calculated using the JANNAF approved ODK/ODE computer program. A parametric evaluation of the ODE and ODK I_{sp} and C* over a wide range of nozzle expansion ratios, O/F ratios, and chamber pressures was accomplished and its results are included in the evaluation program. The ODE I_{sp} is included in the computer printout under the heading ISPT.

b. Divergence Loss

The nozzle divergence loss (% DL) is evaluated for Rao (Bell) nozzles using design charts similar to those presented in Appendix A of Ref. 17. Data from these charts are contained in block data format in a subroutine which supplies the nozzle divergence efficiency and nozzle length for a specified nozzle area ratio and % Bell. The divergence efficiency as a function of length and area ratio is determined from a method-of-characteristics computer program using the design technique developed by Rao.

c. Boundary Layer Performance Loss

The boundary layer performance loss (% BLL) is evaluated using the Design Charts presented in Appendix B of Reference 17. The Design Chart data are included in block data format in a boundary layer loss subroutine of the computer program. Inputs to the subroutine include the nozzle area ratio and throat radius, chamber pressure, gamma (1.20), nozzle exit angle, CSTAR, and wall temperature ratio.

d. Fuel Film Cooling Loss

The fuel film cooling loss (% FCL) is calculated using the thermal exchange stream tube model from the ITA program (Ref. 9). This model resulted in fair correlations of the ITA film cooling loss. The film cooling loss was also evaluated as part of the Plug Cluster Module Demonstration Program (Contract NAS 3-20107), and these results were incorporated into the Parametric Analysis Program that was used for engine optimization in Task V.

e. Energy Release Loss

Two options were included in the program. The first option assumes a fixed injector design (i.e., ITA) is utilized at all operating conditions. The energy release loss (% ERL) is based on the empirical energy release performance loss determined from the ITA program and extended using the Gas/Gas mixing model developed under Contract NAS 3-14379 (Ref. 18). This fixed injector design results in a larger energy release loss with increasing mixture ratio and decreasing propellant temperature.

The second option included in the Parametric Computer Program allows for development of a new injector design for each operating condition. In this case, it was assumed that the new injector could be developed to produce an energy release efficiency of 99% which is comparable to the ITA design at nominal operating conditions (O/F = 4, P_c = 207, F = 6672, ambient propellants). The 99% ERE option was utilized in all of the engine optimization studies as it represents the more realistic approach.

2. Module Performance

Performance and module geometric parameters for a fixed ITA type injector and a new injector design (ERE = 99%), fully developed for each operating point over the specified range of design and operating conditions, are shown in the following tabulation:

TABLE IX. - MODULE PERFORMANCE PARAMETRIC RANGES

Propellants:	(1); Hydrogen (T = 139°K), Oxygen (T = 208°K)*
Injector Design:	(2); Fixed (ITA Type) and Variable (ERE Constant)
Thrust Level:	(4); 2224, 6672, 13345, 22241 N (500-5000 lbf)
Chamber Pressure:	(2); 20.41 and 34.02 ATM
Mixture Ratio:	(5); 4, 5, 5.5, 6, 7
Area Ratio:	(4); 40, 100, 150, 200
Film Cooling:	(4); 0, 15, 20, 25%
Nozzle Length:	(1); 75.5% Bell
Total Cases	= 1280

*ITA operating temperatures - the propellants for the Space Tug engine, however, are stored as liquids at their normal boiling point. The performance calculations included in Figures 25-30 show the trends in performance, but are from 6 to 10 seconds higher in ODE specific impulse due to the use of ITA conditions.

The parametric performance analysis results were tabulated in the Task II Report for the fixed injector (ITA) and optimized (ERE = 99%) injector designs respectively. Included in each table are the estimated delivered performance, performance losses, and engine envelope dimensions for 1280 specific design points which cover the range of parametric conditions included in this study. The calculated delivered specific impulse is summarized as a function of mixture ratio and fuel film cooling in Figures 25-27. Figure 25 shows the variation of delivered I_{sp} with mixture ratio for the fixed injector design. Figures 26 and 27 contain similar plots of delivered specific impulse for the optimized injector design at chamber pressures of 20.4 and 34 atm, respectively. In all cases, maximum specific impulse is obtained at the low mixture ratio (4.0) point for a constant value of fuel film cooling. The influence of mixture ratio is less, however, for the optimized injector design since its energy release loss is unaffected by the operating mixture ratio.

The effect of area ratio on module specific impulse at an assumed constant 20% FFC is illustrated in Figures 28 and 29 for the fixed and optimized injector designs, respectively. Module specific impulse increases approximately 10-20 sec over the range of area ratio included in this study (40-200). The effect of module thrust level on specific impulse is shown in Figure 30 for an optimized injector design. With the assumption of a constant energy release efficiency, specific impulse increases slightly (approximately 1%) with increasing thrust level because of reduced kinetic and boundary layer performance losses.

C. PLUG PERFORMANCE ANALYSIS

Plug cluster engine performance has been shown to reach, as a limit, the performance of an annular throat plug nozzle. To a first approximation, then, the performance contribution of the plug nozzle portion can be estimated by comparing plug cluster and annular plug nozzle performance data. Therefore, the performance of the annular throat plug is discussed in this section.

Plug nozzle contour and performance was analyzed by means of a computer program based on theory developed in Reference 19. This well known theory is valid for an annular throat truncated plug nozzle expanding from Mach 1 to a desired Mach number, M_E, at the plug exit. The sketch of the plug nozzle control surface is shown in Figure 31.

In performing parametric calculations, the Mach number M_E and initial flow angle Θ_E are chosen and the base pressure is assumed zero. (Θ_E and M_E are design parameters which determine the plug area ratio and truncated length.) The results are plotted as a function of plug area ratio (ε_E) and non-dimensional plug length (L/R_E) with Mach number as a parameter as shown in Figure 32. It can be seen that the effect of truncation of an ideal plug of length L_I is to reduce the Mach number leaving the plug. At a given plug area ratio, the truncation can be defined as follows:

$$L/L_I \ \% = (L/R_E / L_I/R_E)\ 100 \qquad \text{(Eq. 2)}$$

FIXED INJECTOR DESIGN (ITA)

Pc = 20.4 ATM

Area Ratio = 40:1

F = 6672 N (1500 lbf)

75% Bell Nozzle

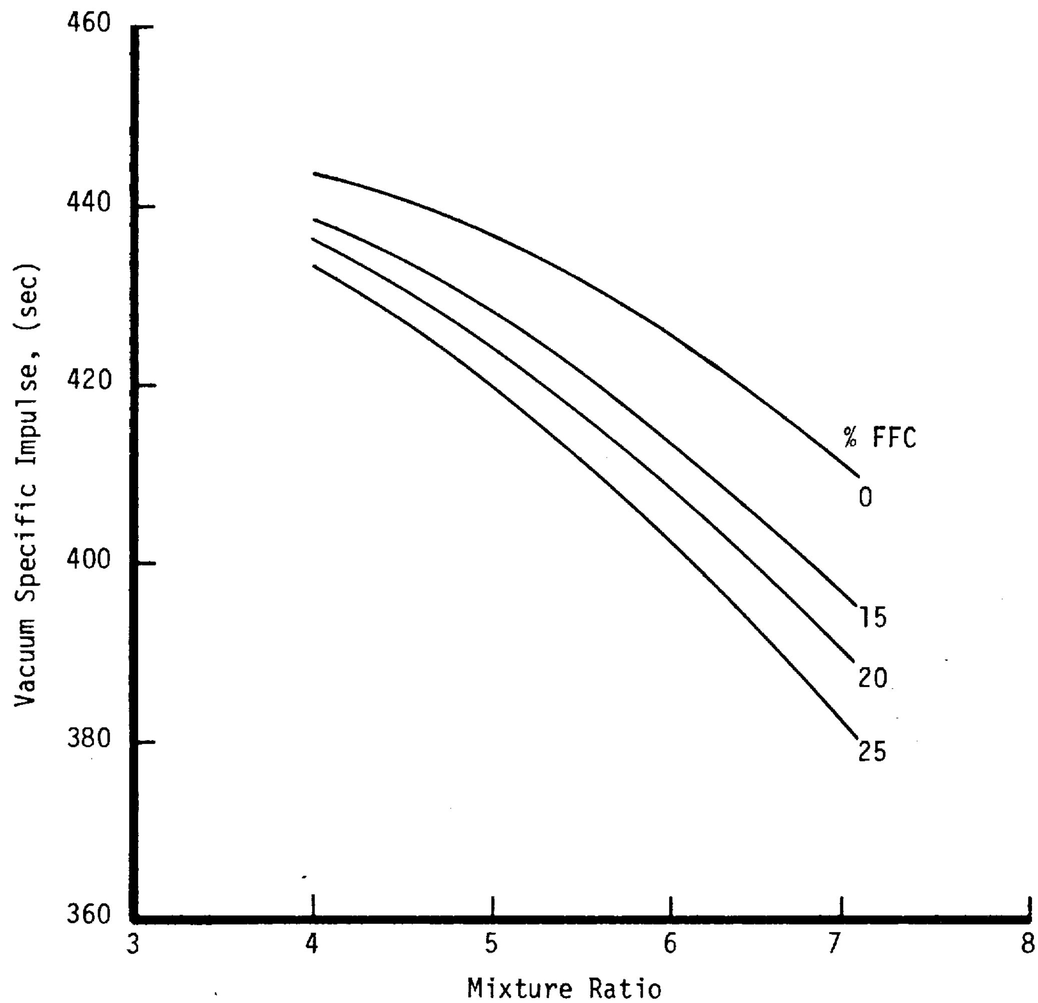

Figure 25. Module Delivered Specific Impulse for a Fixed Injector Design Operating at a Chamber Pressure of 20.4 ATM

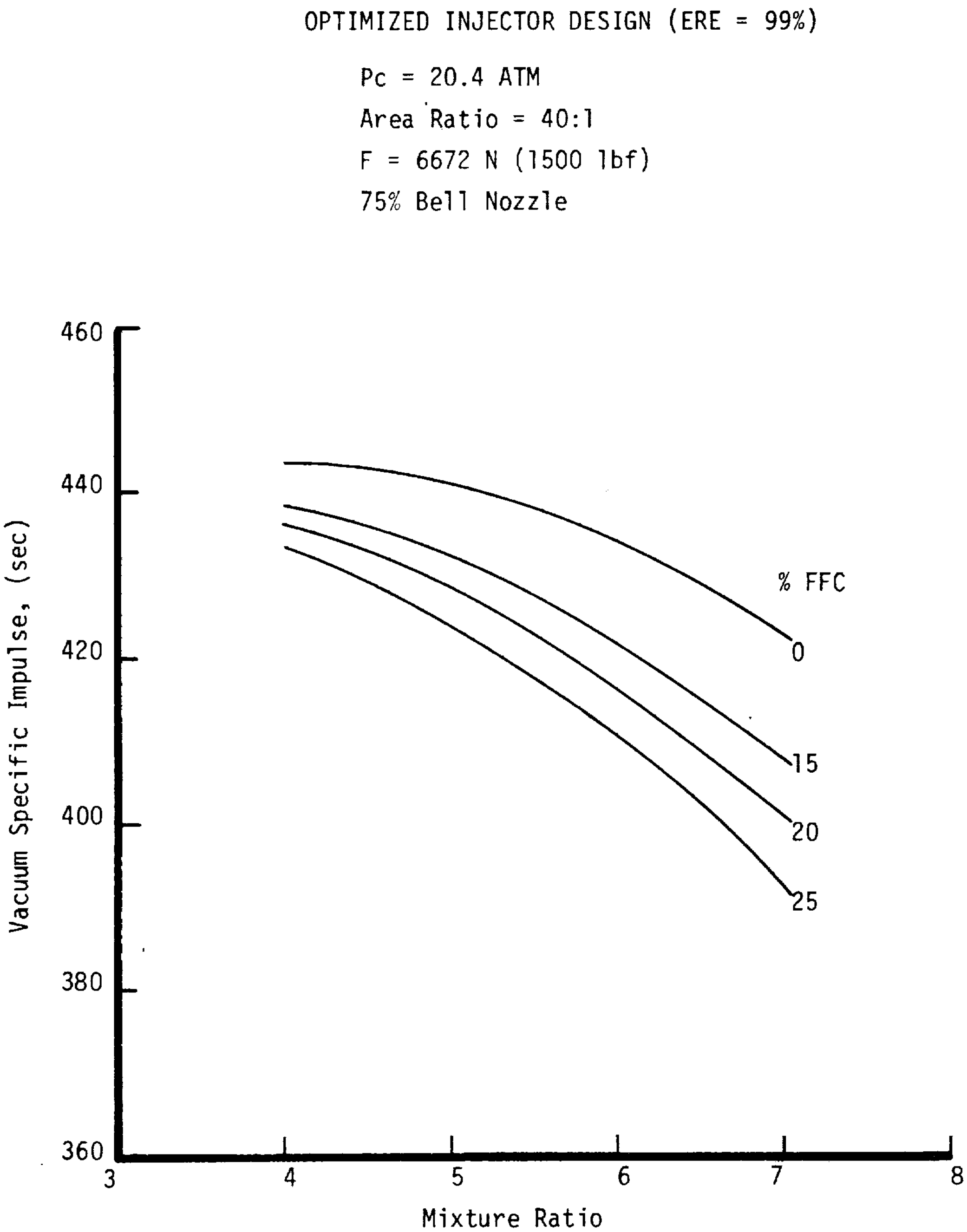

Figure 26. Module Delivered Specific Impulse for an Optimized Injector Design Operating at a Chamber Pressure of 20.4 ATM.

OPTIMIZED INJECTOR DESIGN (ERE = 99%)

Pc = 34.0 ATM

Area Ratio = 40:1

F = 6672 N (1500 lbf)

75% Bell Nozzle

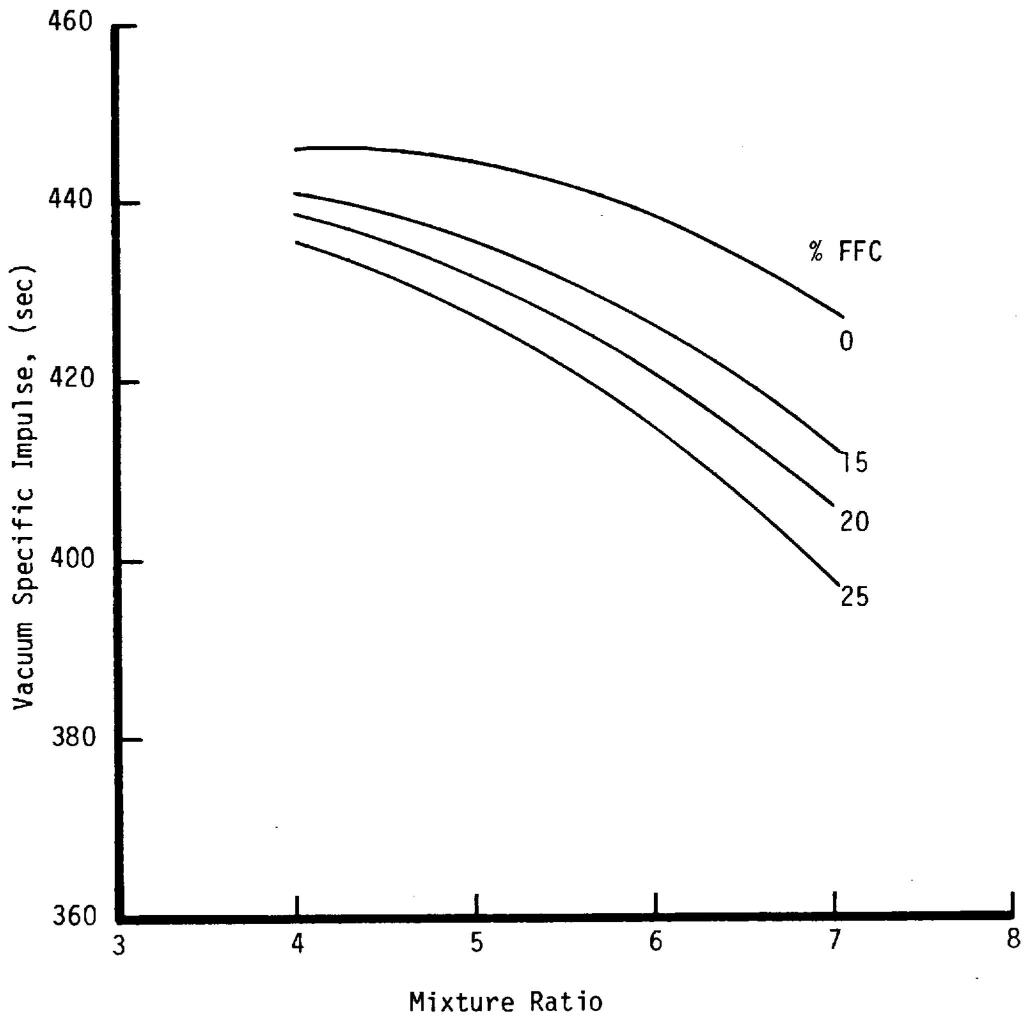

Figure 27. Module Delivered Specific Impulse for an Optimized Injector Design Operating at a Chamber Pressure of 34.0 ATM.

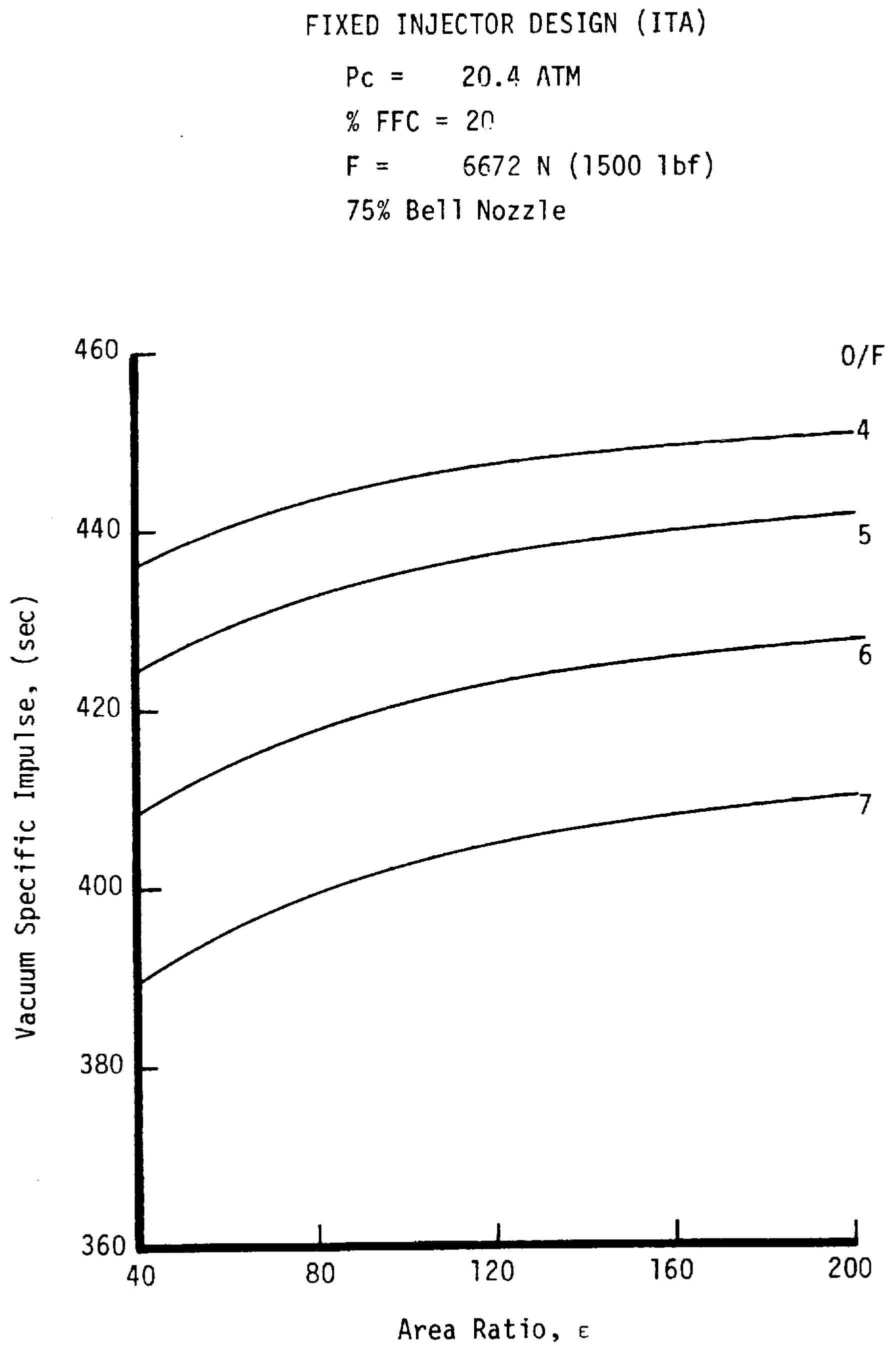

Figure 28. Influence of Expansion Area Ratio on Module Specific Impulse for a Fixed Injector Design.

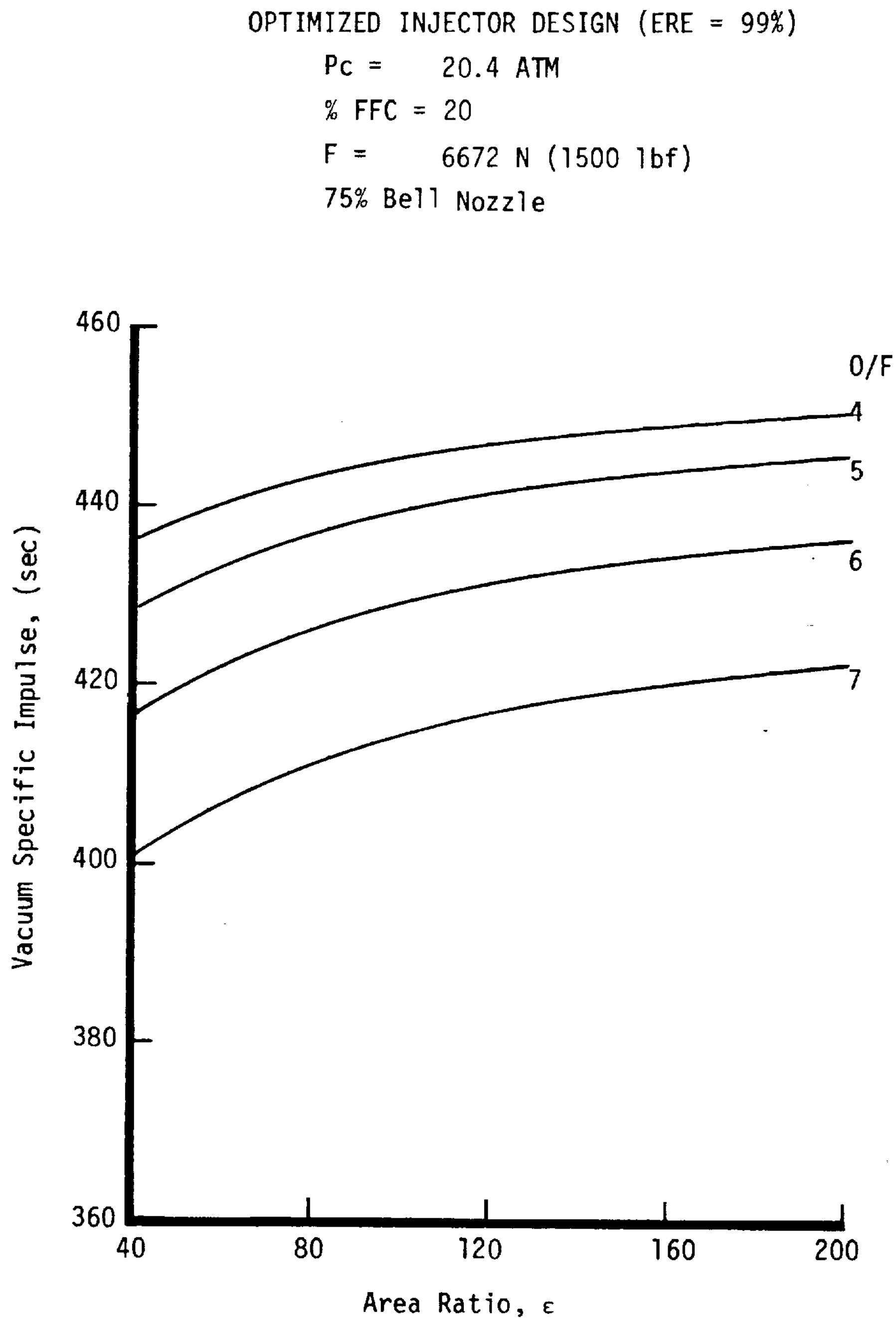

Figure 29. Influence of Expansion Area Ratio on Module Specific Impulse for an Optimized Injector Design.

OPTIMIZED INJECTOR DESIGN (ERE = 99%)

Pc = 20.4 ATM

% FFC = 20

O/F = 6.0

75% Bell Nozzle

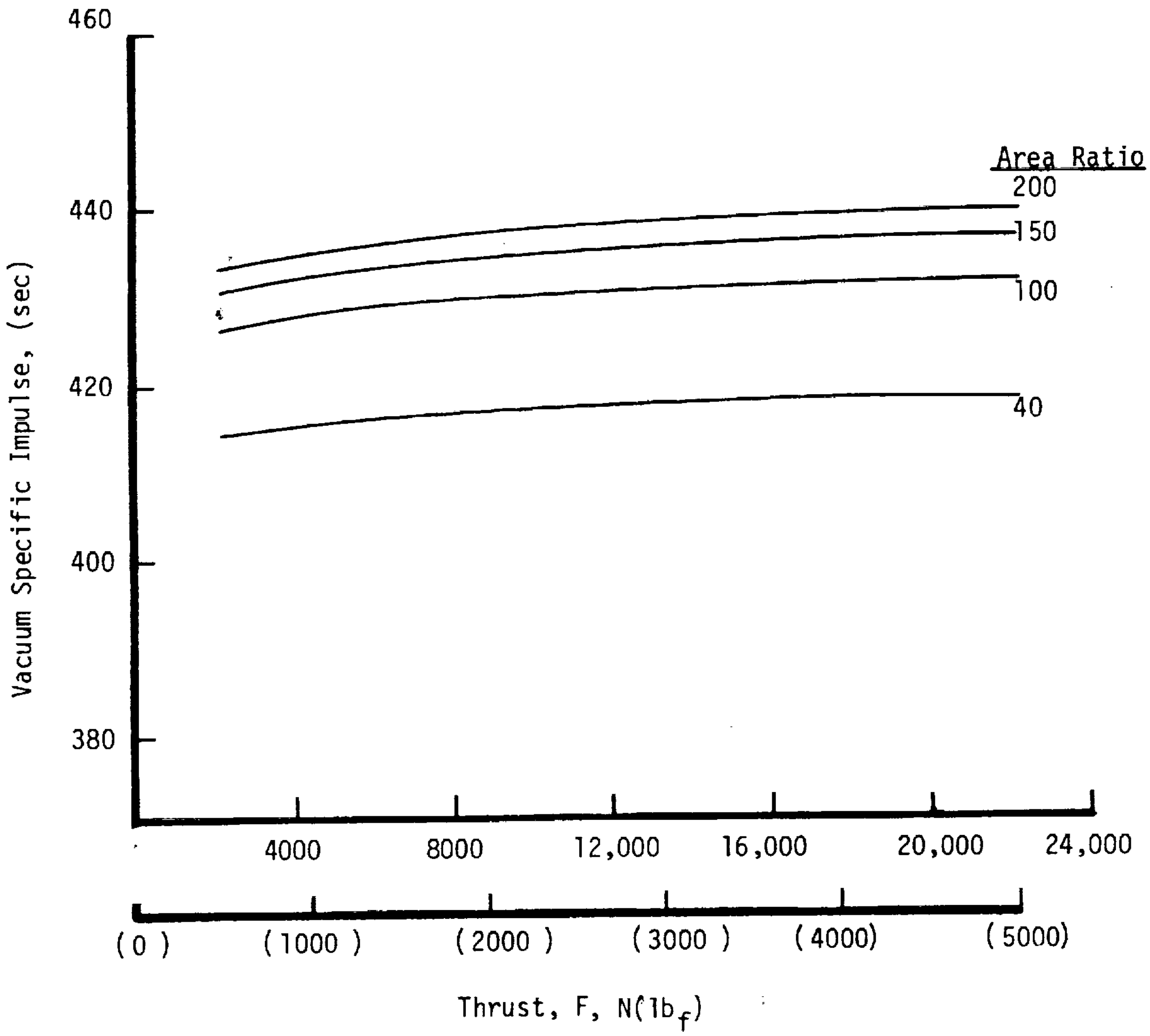

Figure 30. Variation of Module Specific Impulse With Thrust Level for an Optimized Injector Design

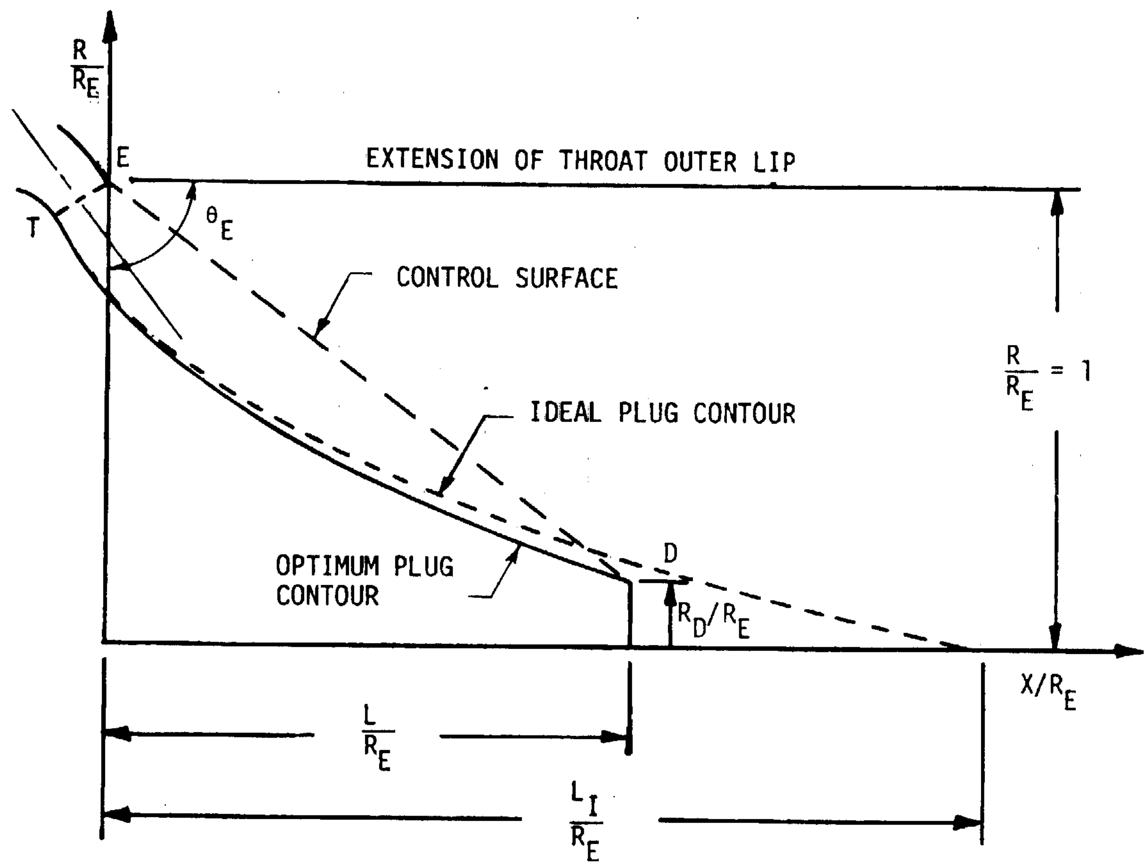

Figure 31. Sketch of a Plug Nozzle and Control Surface

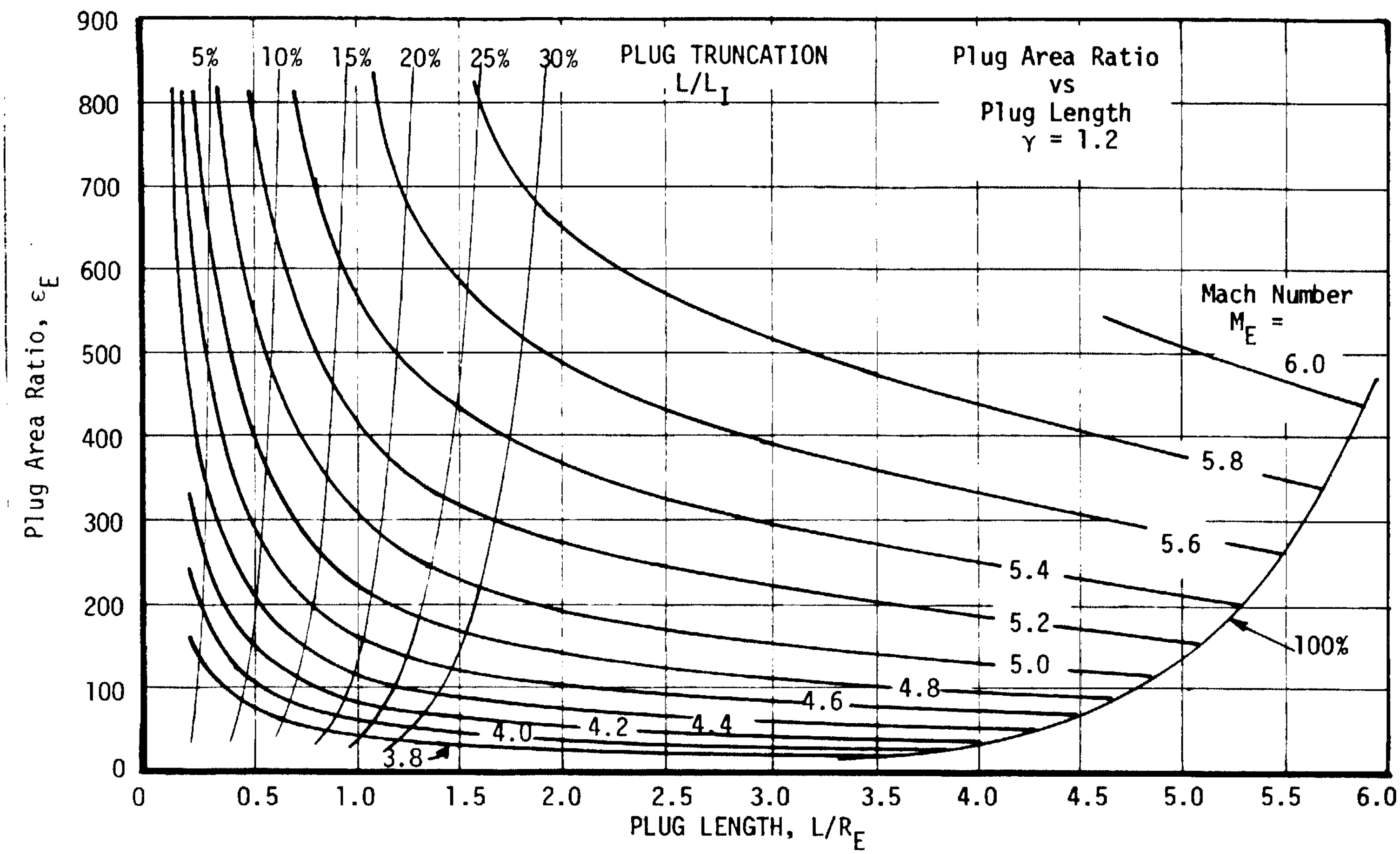

Figure 32. Plug Nozzle Design Map

The plug nomenclature is indicated in Figure 31. The ratio L/L_I is commonly referred to as the isentropic plug length percentage. The isentropic plug length is really a misnomer as all plug calculations are isentropic. In actuality, an isentropic plug is a plug in which the flow field is axial or effectively one-dimensional. All truncated plugs have flow fields which are not purely axial and thus contain divergence losses.

The calculated plug nozzle vacuum thrust coefficient can also be plotted as a function of plug length (L/R_E), area ratio (ε_E) and degree of truncation (L/L_I) as shown in Figure 33. This figure illustrates the effect of area ratio and truncation on achievable vacuum thrust coefficient assuming an isentropic expansion along the optimized plug contour from an annular throat.

The plug nozzle performance will be higher than indicated in Figure 33 due to a finite base pressure acting on the plug base. In vacuum, or at design pressure ratio, the wake behind the base will be closed (see Figure 34) and the base pressure, without base injection, will be a function of the expansion process along the plug wall. Experimentally obtained base pressures for both low and high area ratio plug nozzles follow the trend shown in Table X and Figure 35.

A relatively consistent correlation between P_B and P_E is evident from Figure 35, where the base pressure obtainable is defined as that in which the nozzle separation criteria holds. Base pressures above the nozzle separation criteria ($P_B/P_E \geq 3.6$, Ref. 42) cause an enlargement of the wake on the plug base, and thereby reduce the effective area ratio obtainable with a plug nozzle.

The data on plug nozzle base pressurization do not lead to a correlation between the base flow rate required to maintain a base pressure relationship, such as $P_B = 2.5\ P_E$. In some cases, no bleed flow was required. In other cases, percentage flows as high as one percent were required. Testing in facilities with finite volumes sometimes leads to conditions wherein wake closure is not achieved, unless a vacuum is pulled on the base region at the start of the experiment to "snap" close the wake. This phenomena could very well explain some of the variation in test data concerning base pressurization of truncated plug nozzles. The assumption was made, therefore, to utilize a bleed flow of 0.2% (see Table IV) of the engine flow, which is consistent with the latest test data on the Aerospike where the wake is closed (Ref. 6).

D. PLUG CLUSTER PERFORMANCE ANALYSIS

The selection of a performance model for the plug cluster engine proved to be the most difficult task in the study. This was due to the fact that the accepted, somewhat empirical, approach was based on utilizing a computer program for an annular plug with all external expansion. Experimental data indicated that the performance for a cluster of modules (internal expansion sections with discrete throats) could be very closely approximated by the annular plug model, providing the gap between the modules was close to

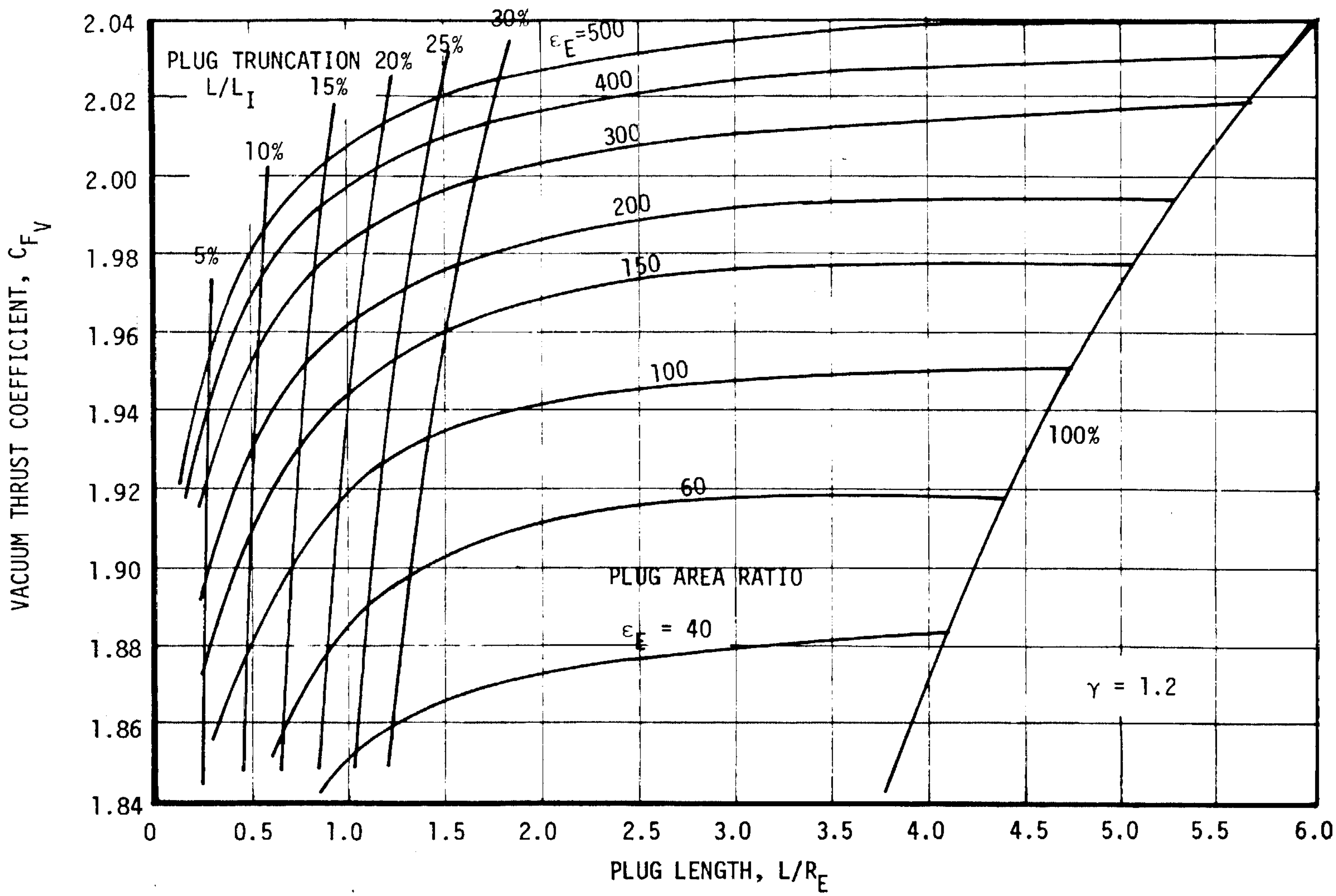

Figure 33. Plug Nozzle Two-Dimensional Thrust Coefficient

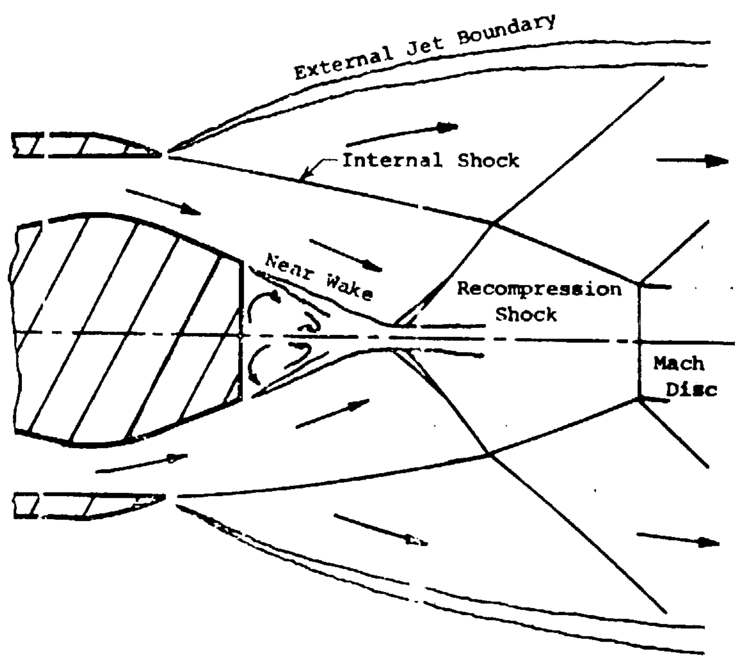

a. AT DESIGN PRESSURE RATIO

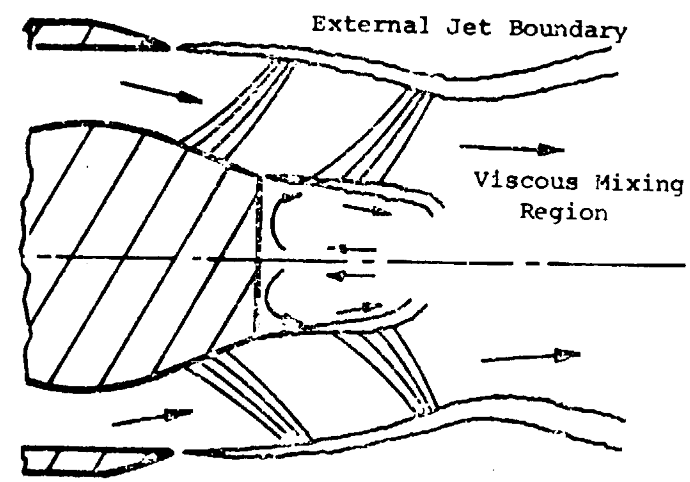

b. BELOW DESIGN PRESSURE RATIO

Figure 34. Features of Internal-External Expansion Axisymmetric Truncated Plug Nozzle Flow Fields.

TABLE X - BASE PRESSURIZATION DATA SUMMARY

Reference	P_c/P_a	ε	P_c/P_E	P_b/P_c	P_b/P_E	$\frac{\dot{W}\ base}{\dot{W}\ engine}$	Θ
NASA Plug Nozzle (C-5)*	850	16.56	290.	.0104	3.016	0	16.6°
"	870	"	"	.0120	3.480	.01	"
"	500	"	"	.0132	3.828	.01	"
Aerospike Report (C-8)	-	44.0	1200.	.0031	3.720	0	45°
"	-	"	1100.	.0036	3.960	.014	"
Aerospike Report (C-10)	1000	74.1	1030.	.0013	1.339	0	"
"	"	"	"	.0023	2.369	.014	"
"	"	"	"	.0027	2.781	.022	"
P&W Plug Cluster Report (C-11)	425	15.0	250.	.0117	2.925	0	18°
Cornell Lab Plug Cluster Report (C-12)	500	23.6	246.	.010	2.460	0	19°
Aerospike Report (6)	-	200.0	4200.	.0006	2.520	.0019	45°
"	-	"	"	.0006	2.638	.0017	"
NAS3-20104 Plug Cluster Cold Flow Data (46)	40,000	400.0	28,500	.00005	1.425	0	6.63°
"	"	"	"	.00009	2.565	.005	"
"	"	"	"	.00012	3.420	.010	"

P_c, Chamber Pressure

P_E, Isentropic (L_I) Plug Exit Pressure

P_b, Base Pressure (Truncated Plug)

P_a, Ambient Pressure of Test Cell

*Appendix C Bibliography or Reference

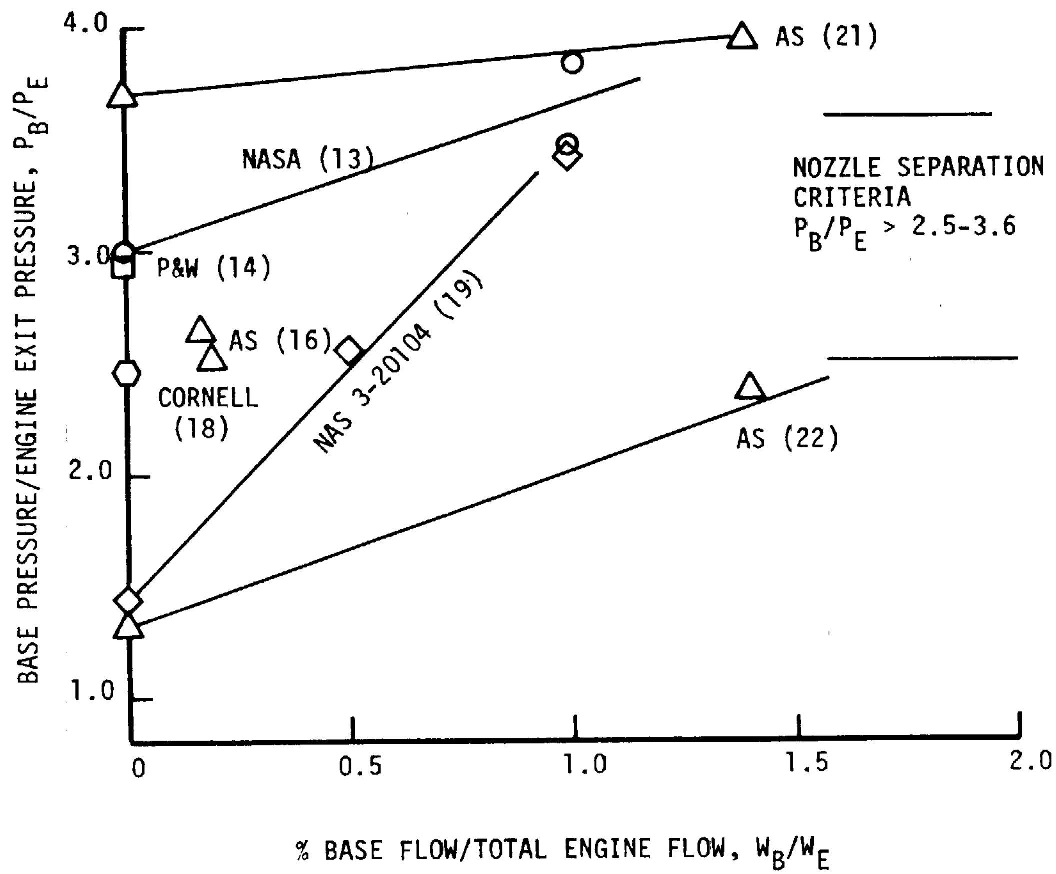

Figure 35. Base Pressurization Data Appear to Follow Nozzle Separation Criteria.

zero. At the start of the study, no method was available that could adequately represent a plug cluster where the gap was much greater than zero.

Several approaches were taken before a satisfactory plug cluster engine performance model was formulated. The initial approach relied heavily on defining the module performance accurately, and included the contribution provided by the plug. The plug contribution amounted to an area ratio increase factor and a base pressurization thrust component. An empirical performance improvement was added to account for the use of fairings in the gap between the modules.

The second approach incorporated the experimental results from Contract NAS 3-20104 into a revision of the initial model.

The final approach is based entirely on the JANNAF simplified procedures for bell nozzles. The method provides a straightforward estimate of the performance for plug cluster engines. The method is possible because the engine is envisioned to be formed from a cluster of high area ratio bell nozzles with zero gap (cf. Figure 4). A baseplate is provided, and the bells are scarfed. The plug cluster engine, therefore, resembles a cluster of modules, with large gaps, placed on a fluted plug. Since the aerodynamics of the flow from each module is identical to that for a scarfed bell nozzle, the JANNAF simplified procedures provide an accurate representation of the performance, providing the base contribution is included.

The progressive effort in defining the performance models was beneficial in obtaining an understanding of the weaknesses in some of the design approaches, and this understanding led to the formulation of the optimum plug cluster engine design configuration. Therefore, the rationale for each model will be summarized in the following sections to document the resulting performance associated with each design philosophy.

1. Plug Cluster Design Constraints

The nomenclature used to describe the plug cluster system is shown in Figure 36. Geometric constraints for the cluster have been identified (Ref. 4) in an equation which relates the area ratio amplification factor ($\varepsilon_E/\varepsilon_M$) to the number of modules, the module spacing, and the module tilt angle:

$$\frac{\varepsilon_E}{\varepsilon_M} = \frac{1}{N}\left[\frac{(1 + \delta/D_e)\cos\Theta}{\sin\left[\tan^{-1}\left(\cos\Theta\tan\frac{180}{N}\right)\right]} + \cos\Theta\right]^2 \qquad \text{(Eq. 1)}$$

where:

ε_E = cluster area ratio = $4\,(R_E^{\,2}/D_t^{\,2}\,N)$

ε_M = module area ratio = $(D_e/D_t)^2$

N = number of modules

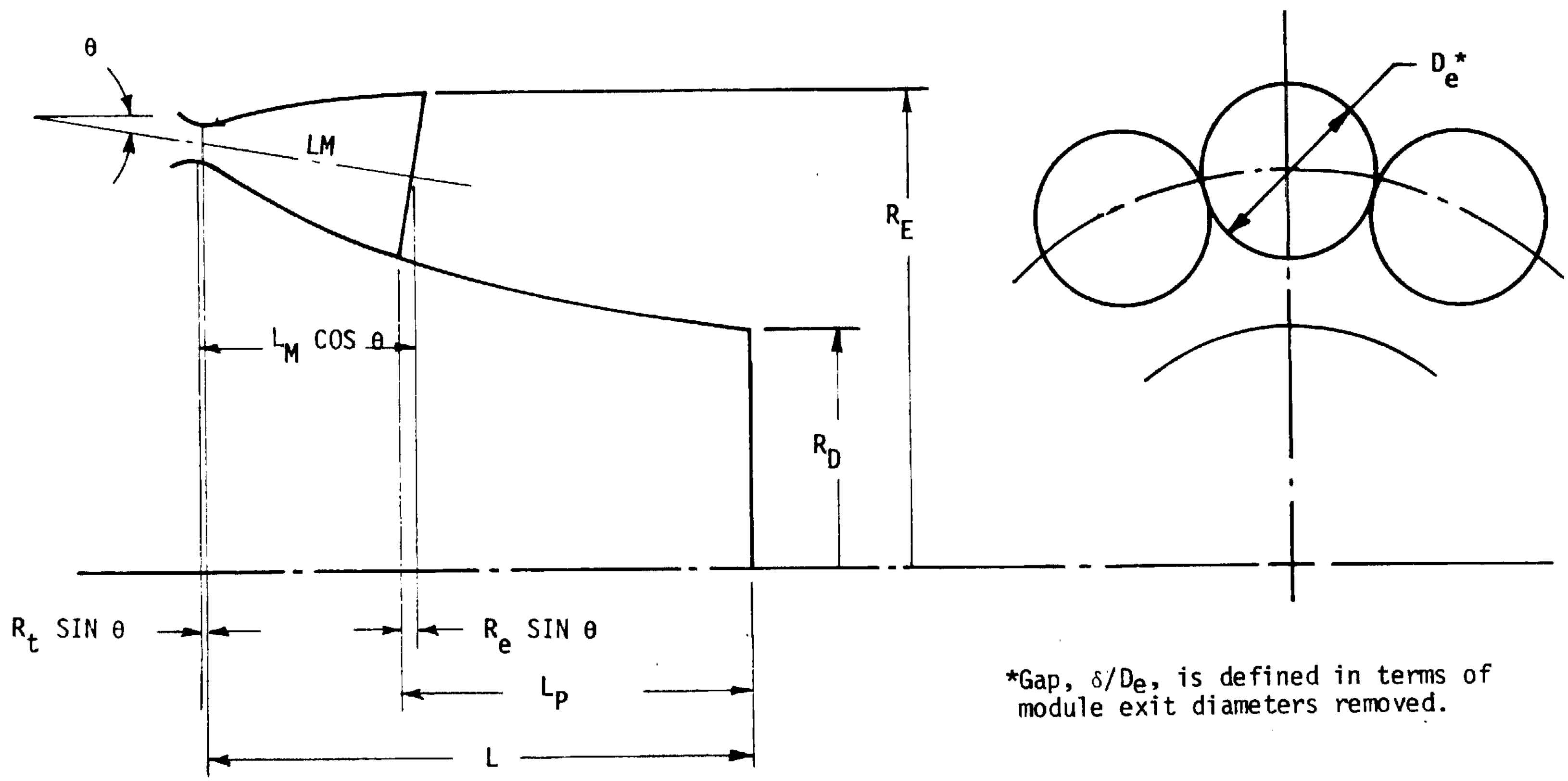

*Gap, δ/D_e, is defined in terms of module exit diameters removed.

Figure 36. Plug Cluster Geometry.

δ = gap between adjacent modules

D_e = module exit diameter

D_t = module throat diameter

R_E = cluster exit radius

A solution of the equation for a constant tilt angle of 10° is shown in Figure 37 to illustrate the cluster geometric constraint. As shown, the cluster amplification factor increases with both the number of modules and the gap between modules. Physically, for a fixed module size, the cluster radius (R_E) increases as the number of modules increase so that the exit area ($R_E{}^2$) increases at a greater rate than the cluster throat area (NA_t). Increasing the module tilt angle will decrease the amplification factor only slightly because of the reduced exit radius due to the module tilt.

A cluster of Bell nozzle modules around a truncated plug generates a complex three-dimensional non-isentropic flow field, which is presently too difficult to describe with a simple model (cf. Figure 34). However, some useful insight into the flow problem can be realized by assuming that the gas expands isentropically from the Mach number at the module exit to the Mach number at the cluster exit. Under this assumption, the tilt angle (Θ) is equal to the difference in the corresponding Prandtl angles.

$$\Theta = \nu_E - \nu_M \qquad \text{(Eq. 3)}$$

where:

ν_E = Prandtl-Meyer angle of plug exit Mach number M_E

$$= \left(\frac{\gamma+1}{\gamma-1}\right)^{1/2} \tan^{-1} \left[\left(\frac{\gamma-1}{\gamma+1}\right) (M_E{}^2 - 1)\right]^{1/2} - \tan^{-1} (M_E{}^2 - 1)^{1/2} \qquad \text{(Eq. 3a)}$$

ν_M = Prandtl-Meyer angle of module exit Mach number M_e

$$= \left(\frac{\gamma+1}{\gamma-1}\right)^{1/2} \tan^{-1} \left[\left(\frac{\gamma-1}{\gamma+1}\right) (M_e{}^2 - 1)\right]^{1/2} - \tan^{-1} (M_e{}^2 - 1)^{1/2} \qquad \text{(Eq. 3b)}$$

The allowable plug cluster configurations are thus defined by combining the geometric and Prandtl-Meyer constraints [Eqs. (1) and (3)]. These results are shown in Figures 38, 39, 40, 41, 42, and 43, respectively, for mdoule gaps (δ/D_E) of 0.0, 0.5, 1.0, 2.0, 3.0, and 4.0.

E. PLUG CLUSTER PERFORMANCE MODEL I

The initial plug cluster parametric model of this study approximated the performance of the plug cluster system by the performance of the module plus the added thrust generated on the exposed plug and plug base. This approach appears to be justified since the sum to the thrust generated by the modules comprises 95% or more of the total plug cluster engine thrust. (The result is valid for the Space Tug engine cluster system which utilizes

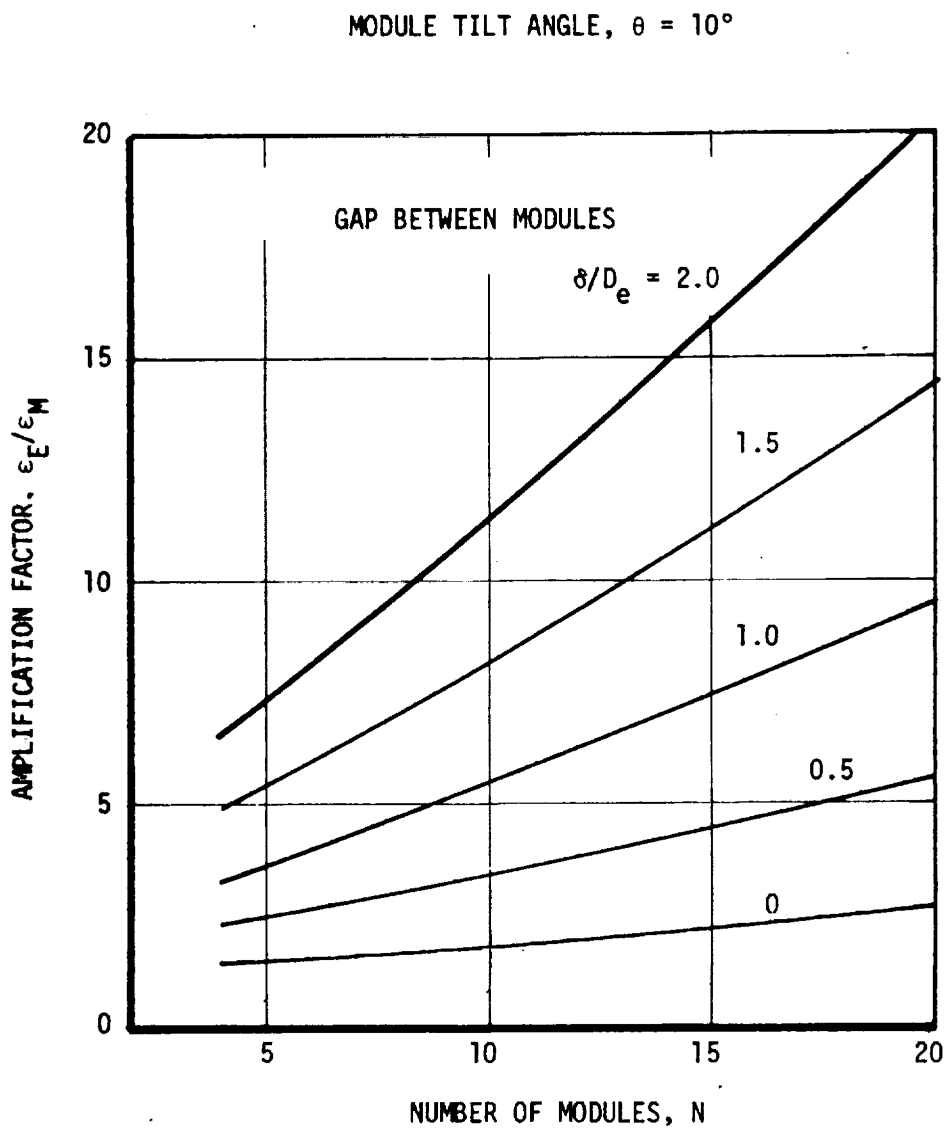

Figure 37. Variation of the Cluster Amplification Factor With Number of Modules.

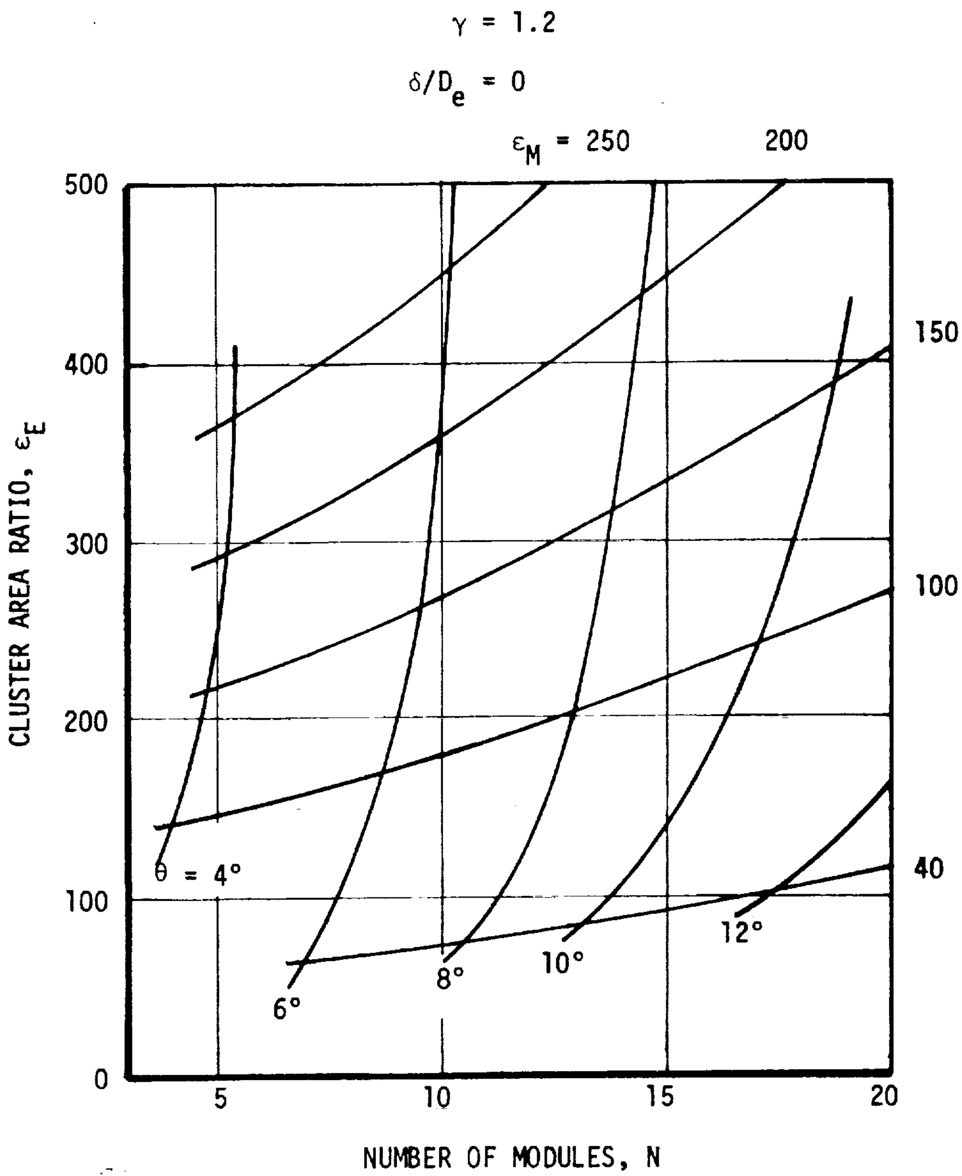

Figure 38. Allowable Plug Cluster Design Conditions for Modules with Zero Gap.

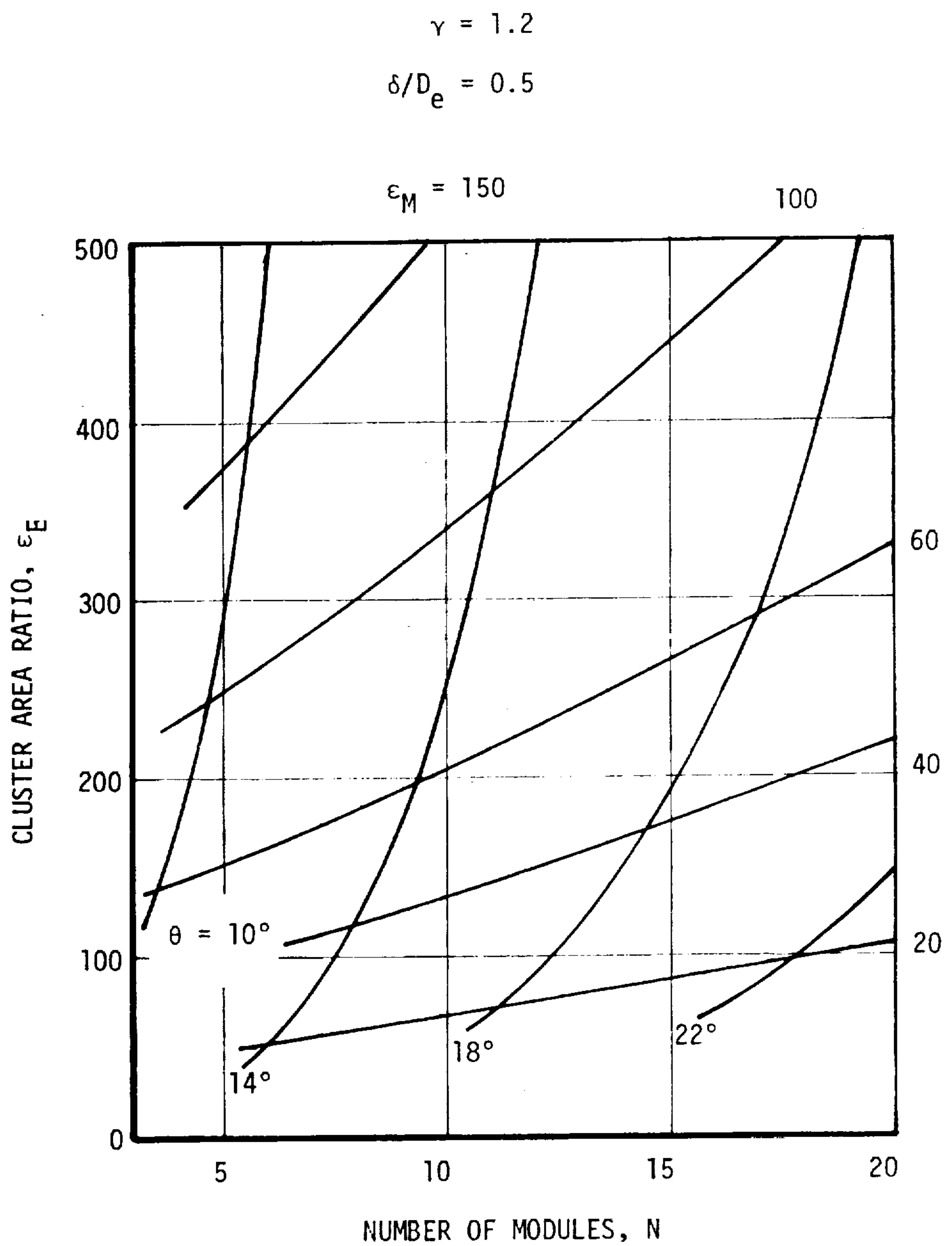

Figure 39. Allowable Plug Cluster Design Conditions for Modules with 0.5 GAP (δ/D_e).

CLUSTER AREA RATIO vs NUMBER OF MUDULES

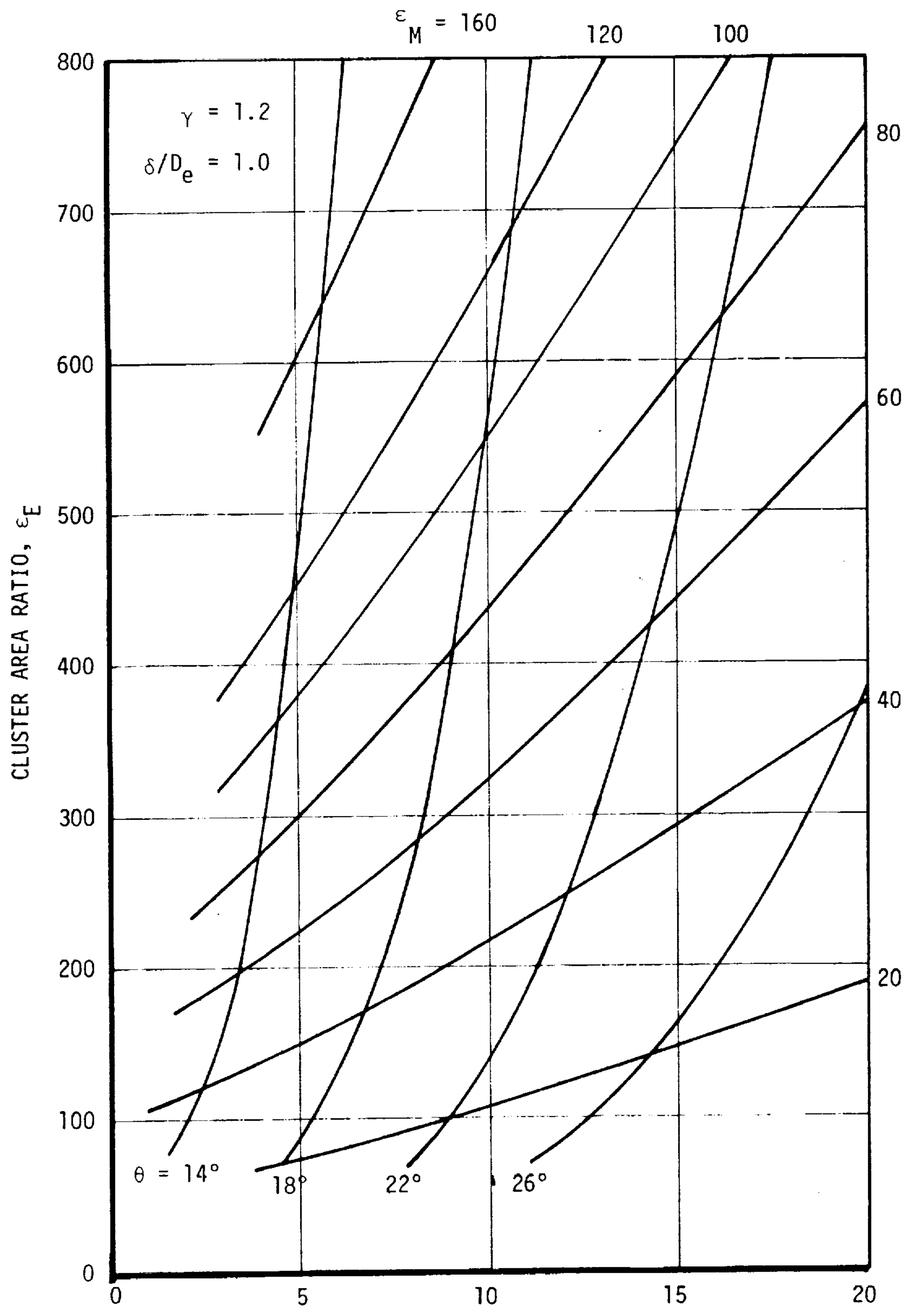

Figure 40. Allowable Plug Cluster Design Conditions for Modules with 1.0 GAP (δ/D_e)

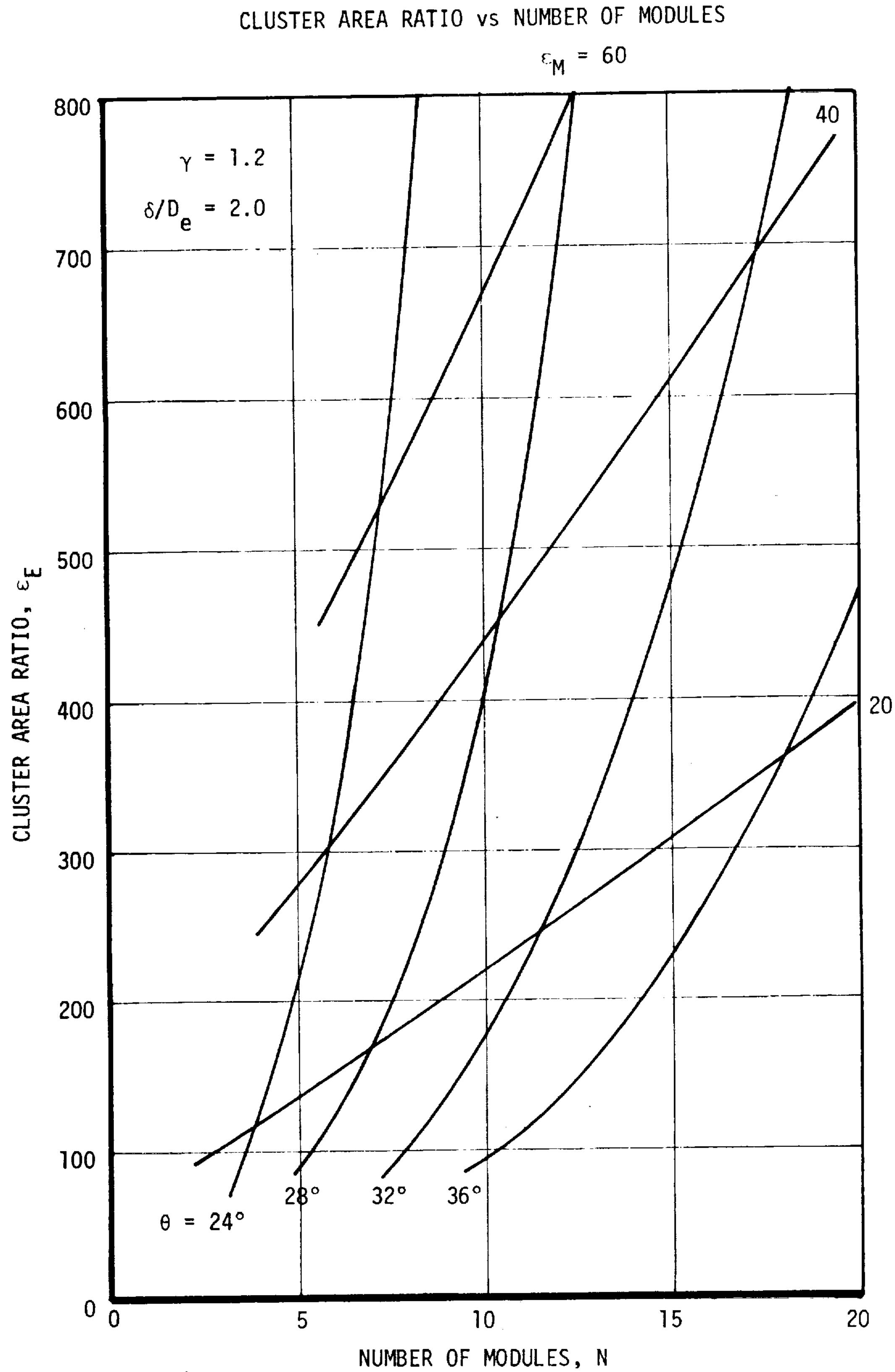

Figure 41. Allowable Plug Cluster Design Conditions for Modules with 2.0 Gap (δ/D_e)

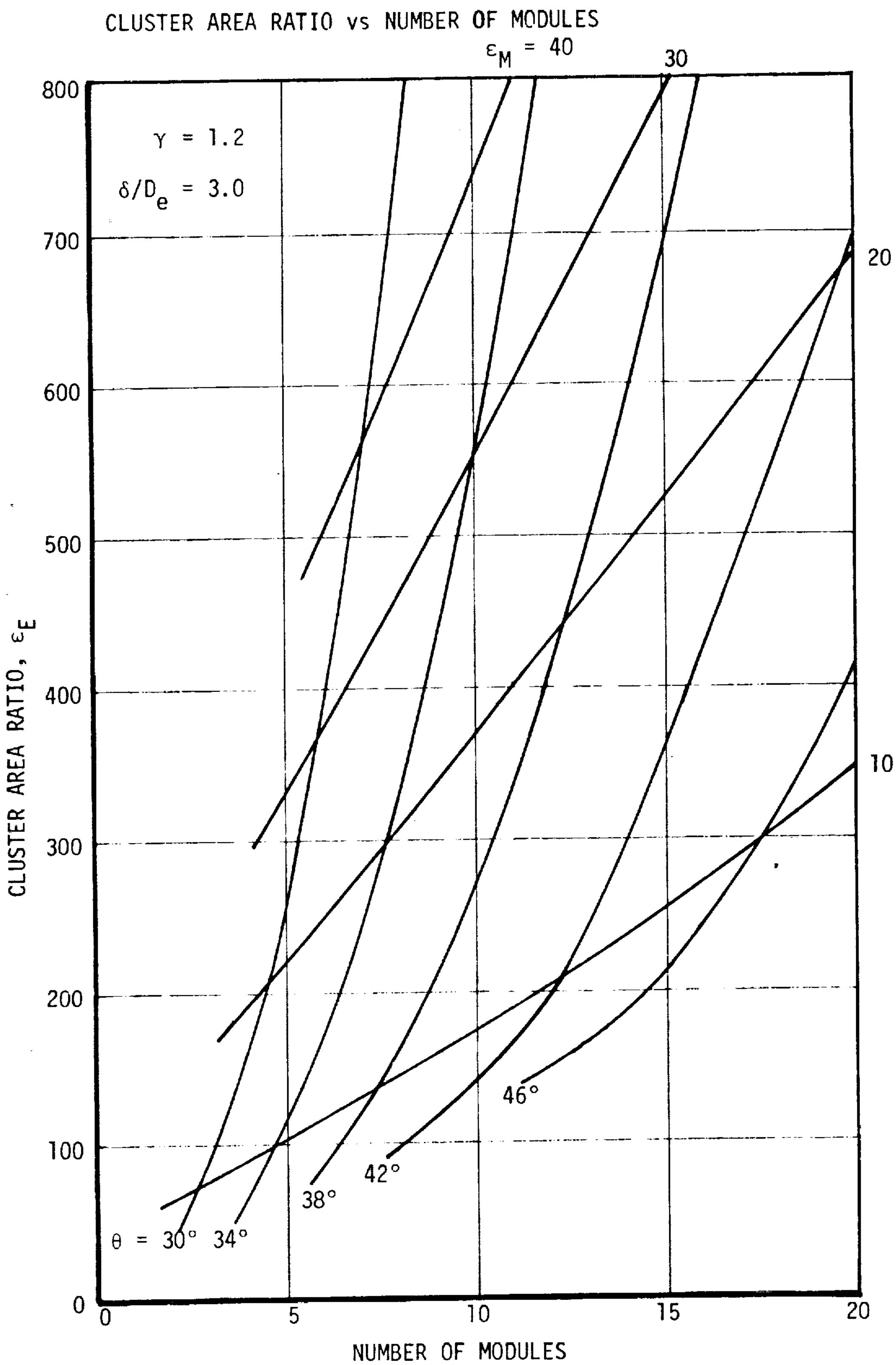

Figure 42. Allowable Plug Cluster Design Conditions for Modules With 3.0 GAP (δ/D_e)

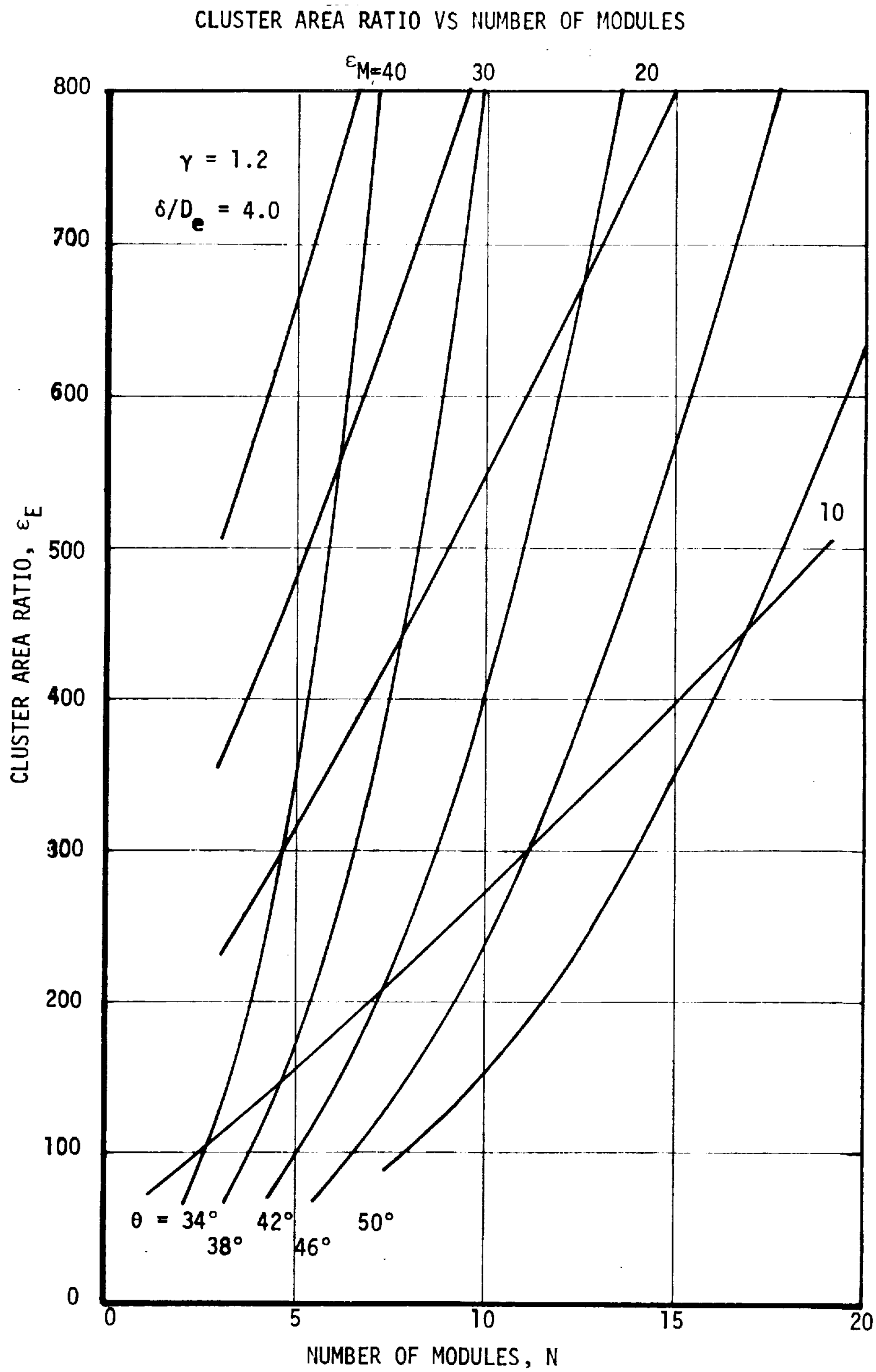

Figure 43. Allowable Plug Cluster Design Conditions for Modules with 4.0 GAP (δ/D_e)

relatively high area ratio modules (40-200) and operates in a vacuum environment. For booster systems, the module performance is about 91% of the total engine thrust.) Thus, the module performance contribution has a one to two order of magnitude greater effect on the total engine performance than the exposed plug contribution. In other words, a 1% error in the module thrust contribution will result in approximately a 1% error in the plug cluster engine performance, while a 10% error in the exposed plug thrust contribution will result in only a 0.5% or less error in the plug cluster engine performance.

Based on this criteria, the following assumptions were made in developing Plug Cluster Model I:

(1) Module performance is based on the JANNAF Simplified Performance Evaluation Procedure and thus includes the effects of operating conditions (O/F, Pc, propellant temperature), expansion kinetics, boundary layer losses, fuel film cooling losses, and incomplete energy release performance losses. The exposed plug thrust contribution can be estimated using the plug design C_F curve (Figure 33) and a base C_F contribution from an empirical correlation. The C_F curves are based on isentropic, constant gamma (perfect gas, frozen flow) flow conditions and are used only to ratio the total engine performance to the module performance. The throat of a module was assumed to coincide with the throat of the annular plug.

(2) For an isentropic plug (i.e., L/L_I = 100%) the module tilt angle is determined from the Prandtl-Meyer angle difference for an expansion from the module exit condition to the plug exit condition [Eq. (3)]. The module tilt angle is assumed to decrease linearly with the plug length as the exposed plug length is reduced from the isentropic value so that the tilt angle is zero when the exposed plug length is zero (i.e., there is no module tilt for a zero percent plug).

(3) No correction is made to the exposed plug thrust contribution for the effect of discreet module throats as opposed to the annular continuous throat configuration assumed in the calculation of the plug performance curves. This assumption is best for a large number of modules and small module gaps and worst for a small number of modules and large module gaps. The discreet throat effect must be determined from experimental data.

These assumptions lead to a reduced cluster efficiency with increasing module gap which is on the same order as the values reported in the literature. This effect is shown in the following derivation:

$$\frac{C_T \text{ with Gap}}{C_T \text{ without Gap}} = \frac{\left[\dfrac{C_F \text{ Plug with Gap}}{C_{F_I} \text{ Plug with Gap}}\right]}{\left[\dfrac{C_F \text{ Plug without Gap}}{C_{F_I} \text{ with Gap}}\right]} \qquad \text{(Eq. 4)}$$

$$\frac{C_T \text{ with Gap}}{C_T \text{ without Gap}} = \left[\frac{C_F \text{ with Gap}}{C_F \text{ without Gap}}\right]\left[\frac{C_{F_I} \text{ without Gap}}{C_{F_I} \text{ with Gap}}\right]$$

where it is assumed that the delivered C_F ratio (C_F with Gap/C_F without Gap) is approximately 1.0 and the ideal (C_{F_I}) ratio is a function of the plug area ratio increase with increasing module gap.

A special case for the comparison of gap effects can be obtained by engine-out operation of a module cluster without any module gap (i.e., constant module tilt angle, module area ratio, gap δ/D_E = 1.0 with every other module out). Under this condition, the plug area ratio will increase because of the reduced module throat area which will have the effect of reducing the plug cluster performance efficiency and total thrust without materially changing the delivered specific impulse. Thus, for all other design parameters constant except the module gap, the plug area ratio can be defined as follows:

$$\varepsilon_{\text{with Gap}} = \varepsilon_{\text{without Gap}} (1.0 + \delta/D_E) \qquad \text{(Eq. 5)}$$

and, $$\left[\frac{C_T \text{ with Gap}}{C_T \text{ without Gap}}\right] = \frac{C_{F_I} \text{ at } \varepsilon = \varepsilon_E \text{ without Gap}}{C_{F_I} \text{ at } \varepsilon = (\varepsilon_E \text{ without Gap})(1 + \delta/D_E)} \qquad \text{(Eq. 6)}$$

The efficiency ratio calculated in this manner is shown in Figure 44. Note that the efficiency ratio increases as the engine area ratio increases because of the diminishing effect of area ratio on performance. The general trend in the curve can be compared with the trend in Figures 11 and 12 for a 10 and 20 percent plug of 15 to 30 area ratio.

1. Model I Calculation Procedure

The Plug Cluster Computer Program Model I is set up to calculate performance based on a module arranged in a specific cluster configuration. The input consists of a desired gap, module, engine area ratio and number of modules for an isentropic plug as defined in Figures 38 through 43. As the plug is truncated, the number of modules and gap are held constant while the engine area ratio and tilt angle vary to accommodate the geometric requirements imposed by Equation 1. Physically, this has the effect of moving the cluster on the plug (by the amount $R_e \sin \Theta$) as the plug is shortened (Figure 45).

The working plug forward boundary is at L_0 where:

$$L_0 = L_M \cos \Theta - (R_e + R_t) \sin \Theta \qquad \text{(Eq. 7)}$$

The degree of truncation of the plug is defined in terms of the isentropic plug length (L/L_I). Plug truncation lengths are chosen in the program based

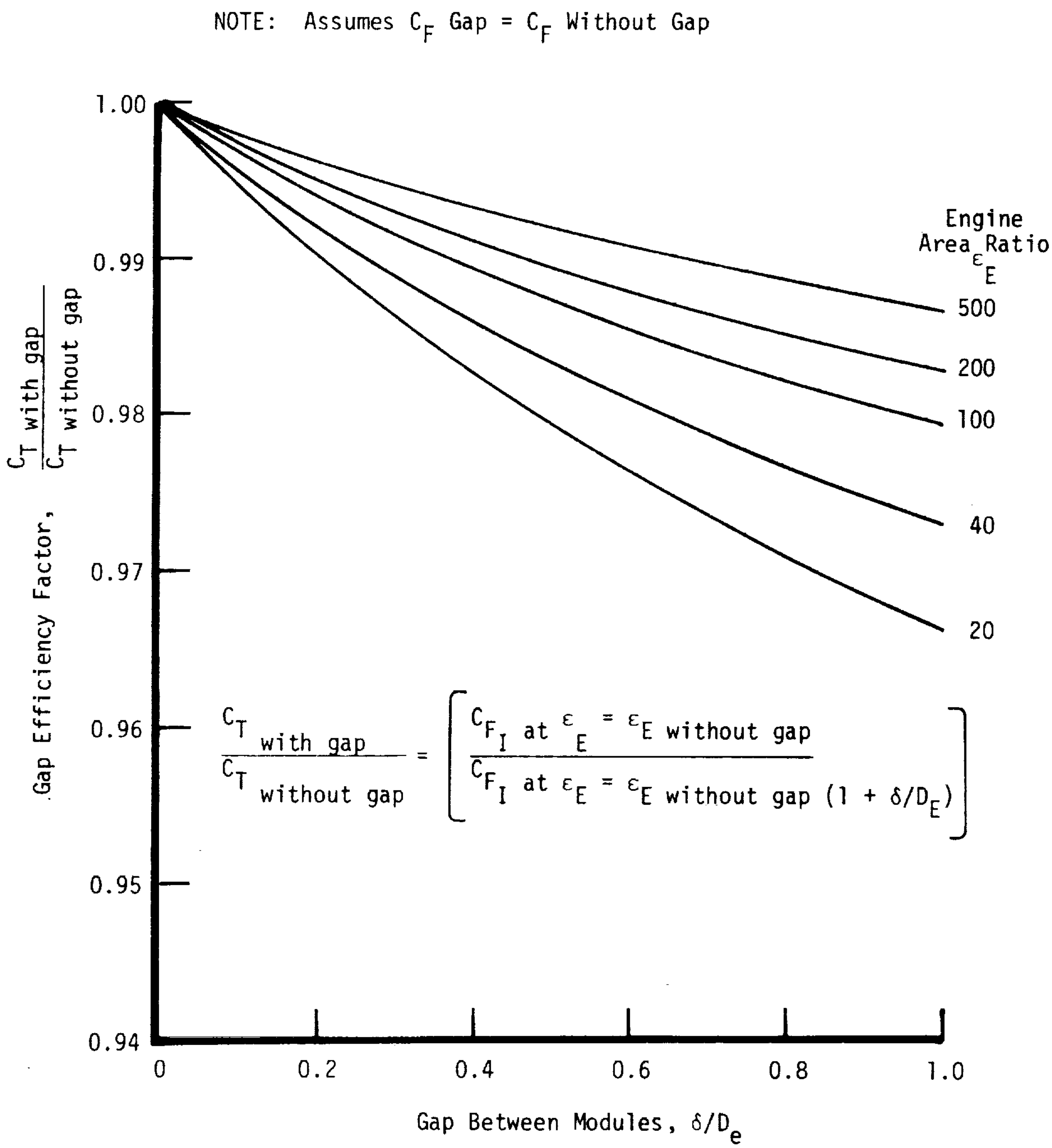

Figure 44. GAP Efficiency Factor for Constant Plug Cluster Performance.

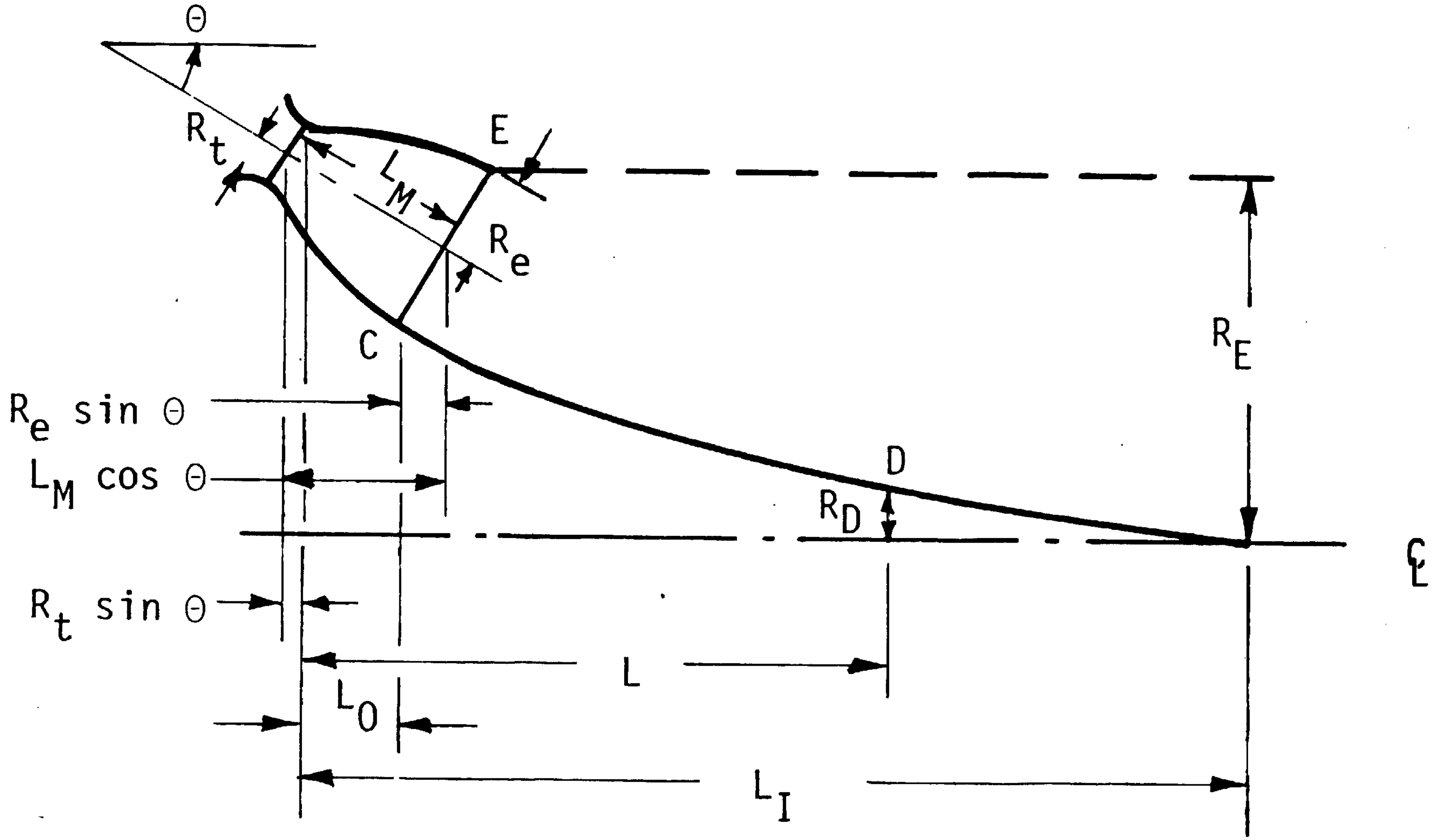

Figure 45. Sketch of Plug Showing Computer Model Nomenclature

on a percentage of isentropic lengths (5, 10, 15, 20, 25, 30).

The plug-cluster vacuum thrust coefficient is expressed as follows:

$$C_{F_E} = \left[C_{F_M} \times \left[\frac{C_{F_{PL}}}{C_{F_{PO}}} \right] + \Delta C_{F_F} + \Delta C_{F_B} \right] \frac{C_F}{C_F(\delta/D_E = 0)} \qquad \text{(Eq. 8)}$$

where:

C_{F_E} = Plug-cluster thrust coefficient

C_{F_M} = Module thrust coefficient calculated by means of JANNAF Simplified Analysis

$C_{F_{PL}}$ = Thrust coefficient of a plug of length L/L_I

$C_{F_{PO}}$ = Thrust coefficient of a plug of length L_0/L_I

ΔC_{F_B} = Increase in thrust coefficient due to base pressure

ΔC_{F_F} = Increase in thrust coefficient due to fairings

$\frac{C_F}{C_F\,(\delta/D_e = 0)}$ = Ratio of thrust coefficients with gap [assumed equal to 1.0 for this analysis as per Eq. (6)]

The value of C_{F_M} is obtained from the module parametric model and is equal to:

$$C_{F_M} = F_M/P_c\ A_t \qquad \text{(Eq. 9)}$$

The values of $C_{F_{PL}}$, $C_{F_{PO}}$, and the isentropic plug length are obtained by interpolation of Figure 33. The contributions from the fairings and base pressurization are obtained from empirical relationships to be described. Finally, the thrust, total mass flowrate and specific impulse of the plug cluster system are calculated as follows:

$$F_E = C_{F_E}\ P_c\ N\ A_t \qquad \text{(Eq. 10)}$$

$$\dot{m}_E = \dot{m}_M\ M + \dot{m}_{Base} \qquad \text{(Eq. 11)}$$

$$I_{sp_E} = F_E/\dot{m}_E \qquad \text{(Eq. 12)}$$

2. Model I Fairing Correction

The performance methodology indicates that the calculated engine efficiency (Figure 44) reflects the same trend as the experimental data (Figure 11) in showing a loss as a function of module gap. Therefore, it appeared reasonable to apply a fairing correction (ΔCF_F) to Eq. (8) to obtain the predicted delivered performance for the plug cluster engine.

Data for two different gaps (δ/D_e = 0.185 and 1.0) from Ref. (4) (p. II-53) are given in Table XI (see Figure 12). Utilizing these data, an

TABLE XI. - GAP PERFORMANCE (C_T) WITH FAIRINGS (Ref. 4)

Configuration	$\delta/D_E = 0$	$\delta/D_E = 0.185$	$\delta/D_E = 1.0$
Plug Length = 10%			
No Fairings	0.966	0.950	0.914
Straight Fairings	-	0.954	0.940

equation (curve fit) can be written of the form

$$C_{T_F} = \frac{C_T \text{ (without gap)} - C_T \text{ (with gap)}}{X} + C_T \text{ (with gap)} \qquad \text{(Eq. 13)}$$

where:

$$\Delta C_{F_F} = \left[C_{T_F} - C_T \text{ (with gap)}\right] C_{F_I} \qquad \text{(Eq. 14)}$$

and where X is equal to 4 and 2, respectively, for 0.185 gap and 1.0 gap. That is, the fairing correction becomes larger as the gap is increased.

Since no data were available on fairings for gaps greater than one, Eq. (13), with X equal to 2, was utilized for all of the gap calculations (δ/D_e = 1 to 4).

3. Model I Base Pressurization Correction

The base pressure can be 2.5 to 3.6 times the static pressure of the exhaust gas for the fully expanded plug as shown in Table X. This pressure is recognized to be the standard separation criteria ($P_e \geq 0.4$ P ambient) for DeLaval nozzles. The achievement of such a base pressure may require a finite mass flow into the base, the amount being presently determined from experiment. Base pressurization of the Aerospike (Ref. 6) annular plug engine amounts to 2.4% of the thrust as previously shown in Table IV. Utilization of these data for the 200:1 area ratio Aerospike plug allows the development of the equation.

$$\dot{w}_{base} = K \; P_{base} \; A_{base} \qquad \text{(Eq. 15)}$$

where the constant K = 1.731 (1.695×10^{-4}) was derived (Ref. 6) from $\dot{w}_{base}$ = 0.045 kg/s (0.10 lb/s), P_{base} = 0.041 atm (0.6 psia) and A_{base} = 0.634m^2 (983.1 in.^{2}).

Since the nozzle wake is closed, Eq. (15) would be expected to hold for small changes in the base area and/or tilt angle. It has been assumed to be valid for the larger area plugs of this study, but requires verification.

4. Model I Plug Cluster Engine Delivered Performance

Parametric performance data are given in Figures 46 through 50 for Model I engines. The figures include the module losses computed by JANNAF procedures, where the nomenclature is: ODE - one dimensional equilibrium, KL - kinetics loss, DL - divergence loss, BLL - boundary layer loss, and ERL - energy release loss. These losses are indicated by a bar giving a total loss of about 20 seconds in Figure 46. Because the plug nozzle is designed to turn the module exhaust, the module DL term is assumed zero in the plug cluster performance calculations. The true loss may be between that of zero and the module loss shown, giving an uncertainty band equivalent in thickness to the DL band shown for the module. The plug length was maintained essentially constant to be more representative of a practical application.

The lower performance line shown represents the engine performance for just the modules and truncated plug. Improvements provided by fairings and base pressurization increase the cluster performance as shown. For example, expansion (Figure 46) of the ε_M = 40 modules on an ε_E = 72 plug is seen to provide a 5% (23 second) improvement in engine performance. The method of combining the module and plug nozzle performance appears to be overly optimistic for the zero gap configuration, as the indicated losses are less than the module loss bar. At large gaps, the delivered performance appears correct, as the difference between the ODE line and the delivered line is equal to or greater than the module loss bar.

The base correction for the zero gap point in Figure 46 amounts to 1.5 seconds, or 0.3%. The maximum base pressurization correction shown at $\varepsilon \approx 400$ amounts to about seven seconds, or 1.5%.

No fairing correction is taken for a gap of zero, but for positive module gaps, the previously presented method was utilized. In Figure 46, the maximum fairing correction amounts to about nine seconds (2%) at $\varepsilon \approx 400$.

The gap = 3 point of Figure 46 shows engine losses considerably greater than those from the module alone. These differences can be attributed to gap and truncation terms in addition to the conventional losses.

In Figure 47, the (16%) film cooled module engine performance losses are described. The film cooling performance loss (2.7%) is seen to have a major impact on the engine performance.

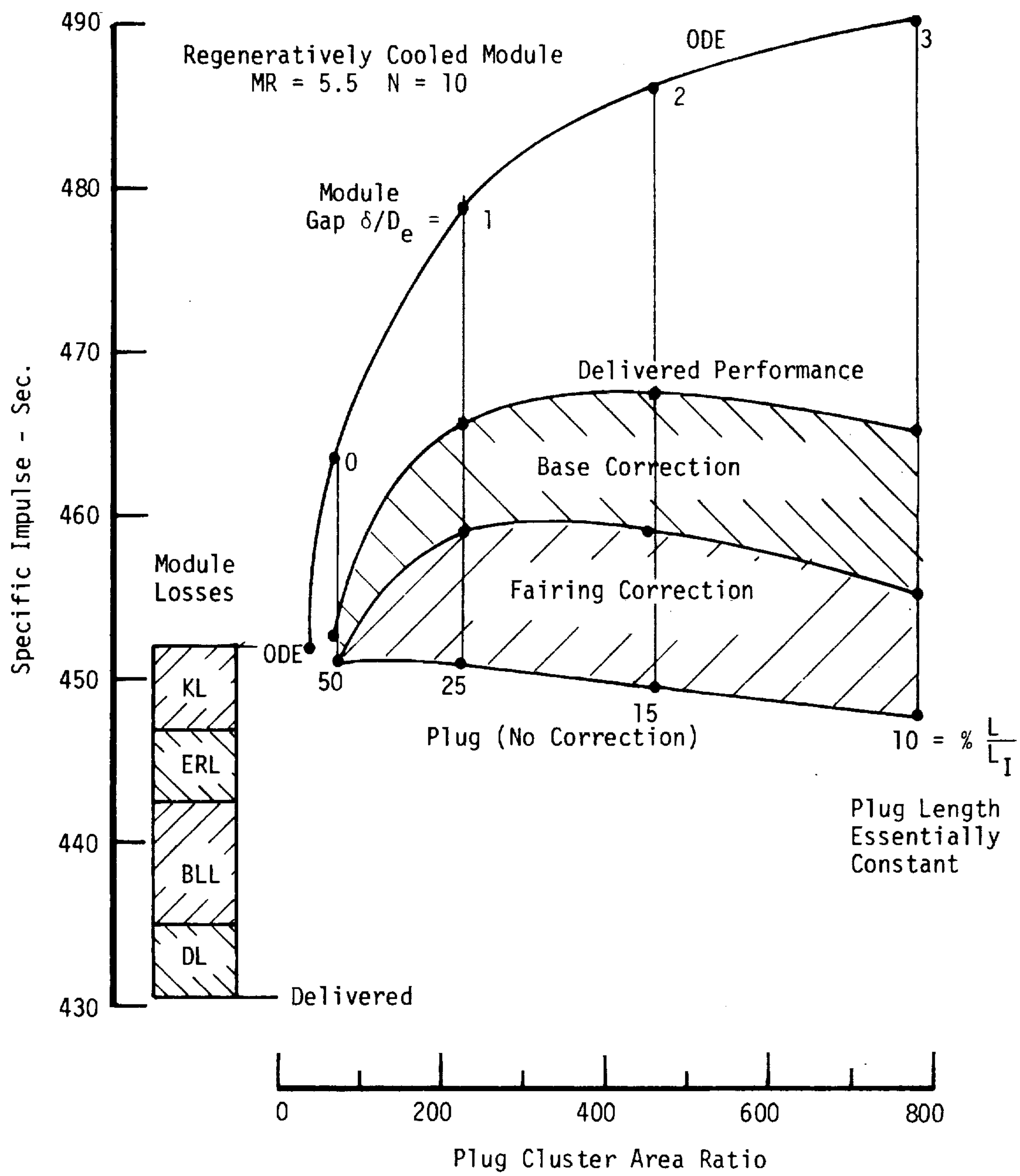

Figure 46. Plug Cluster Engine Performance Summary at P_c = 20.4 ATM and ϵ_M = 40

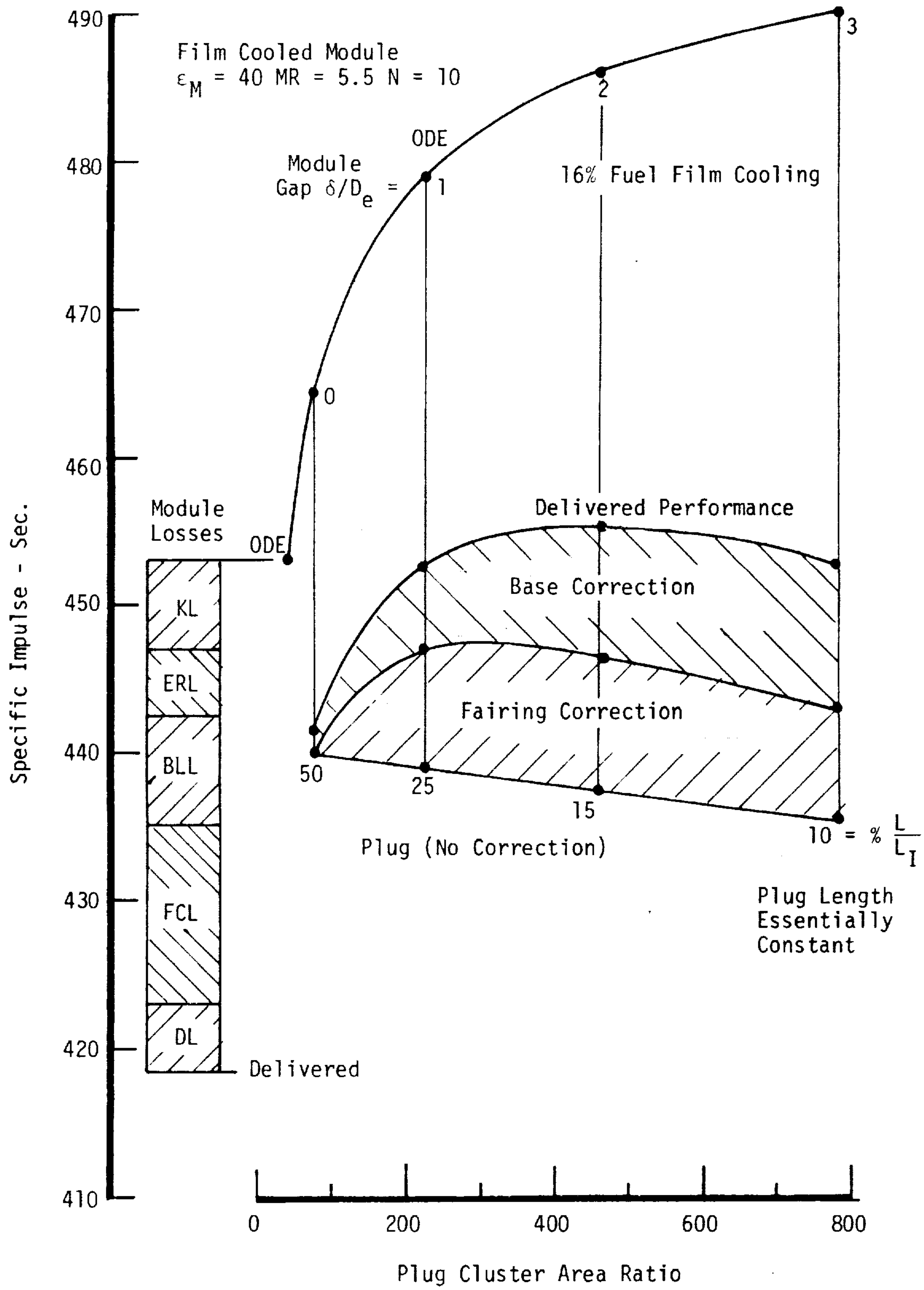

Figure 47. Plug Cluster Engine Performance Summary with ITA at P_c = 20.4 ATM.

C - 2

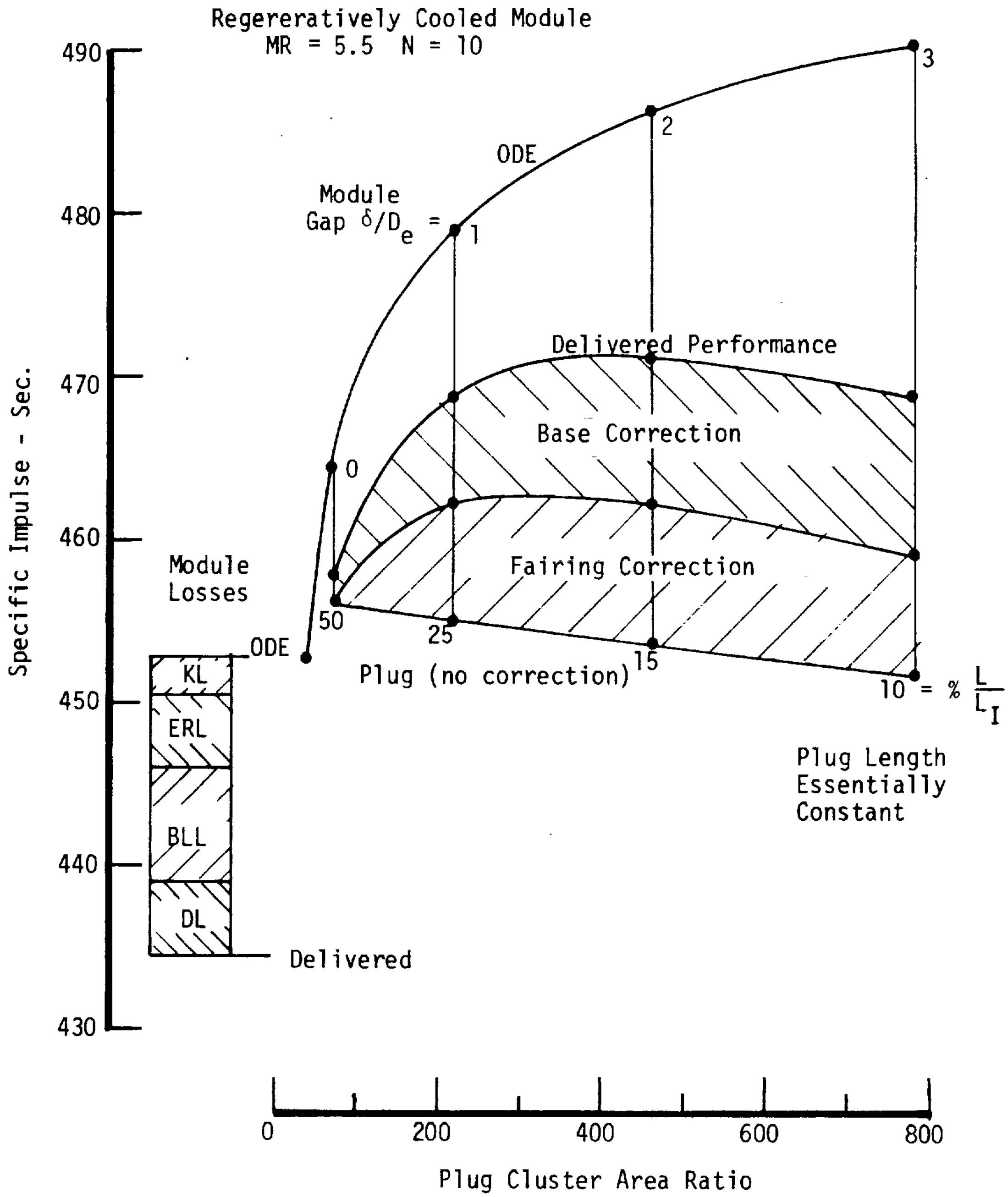

Figure 48. Plug Cluster Engine Performance Summary at P_c = 34 ATM and ε_M = 40

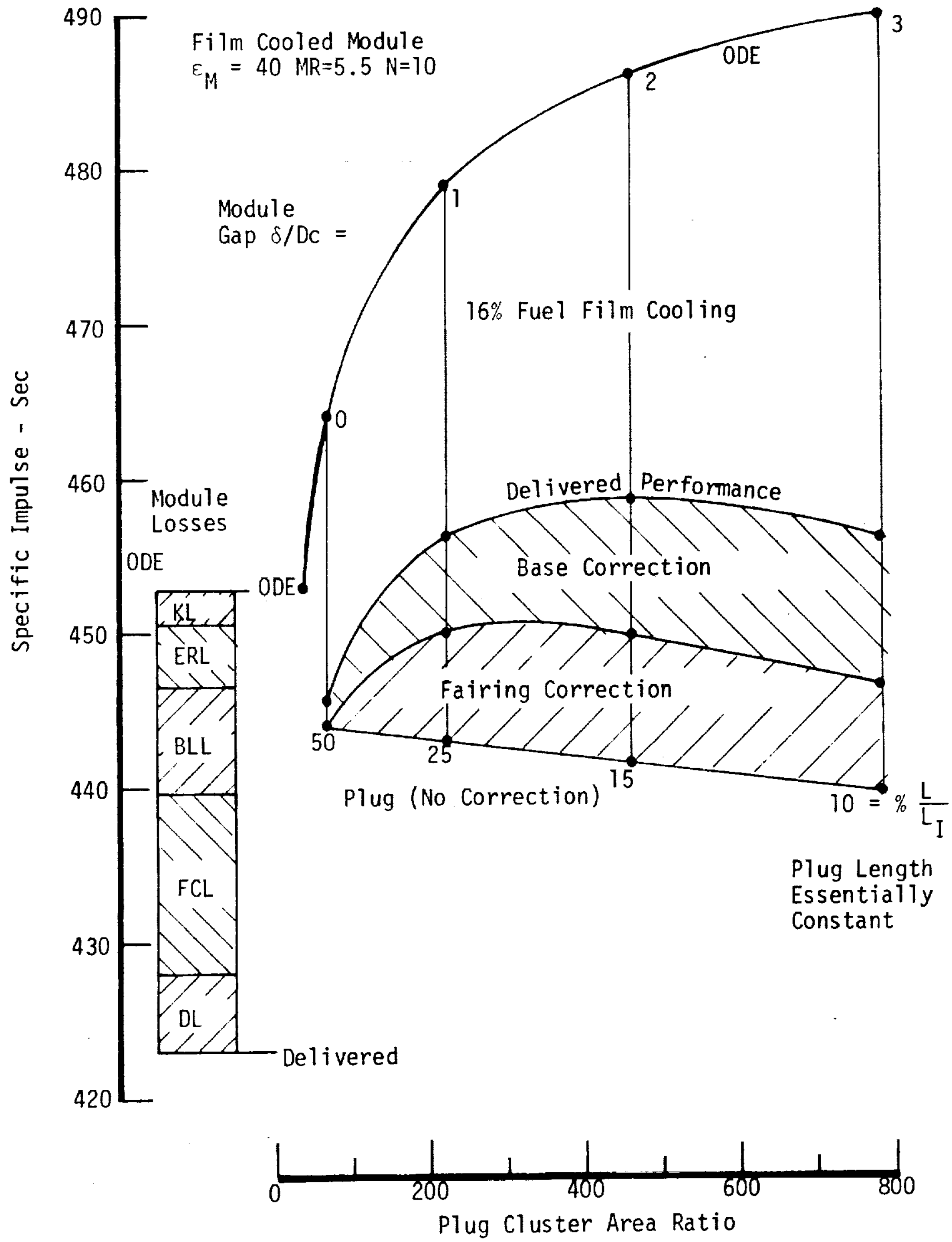

Figure 49. Plug Cluster Engine Performance Summary with ITA at P_c = 34 ATM.

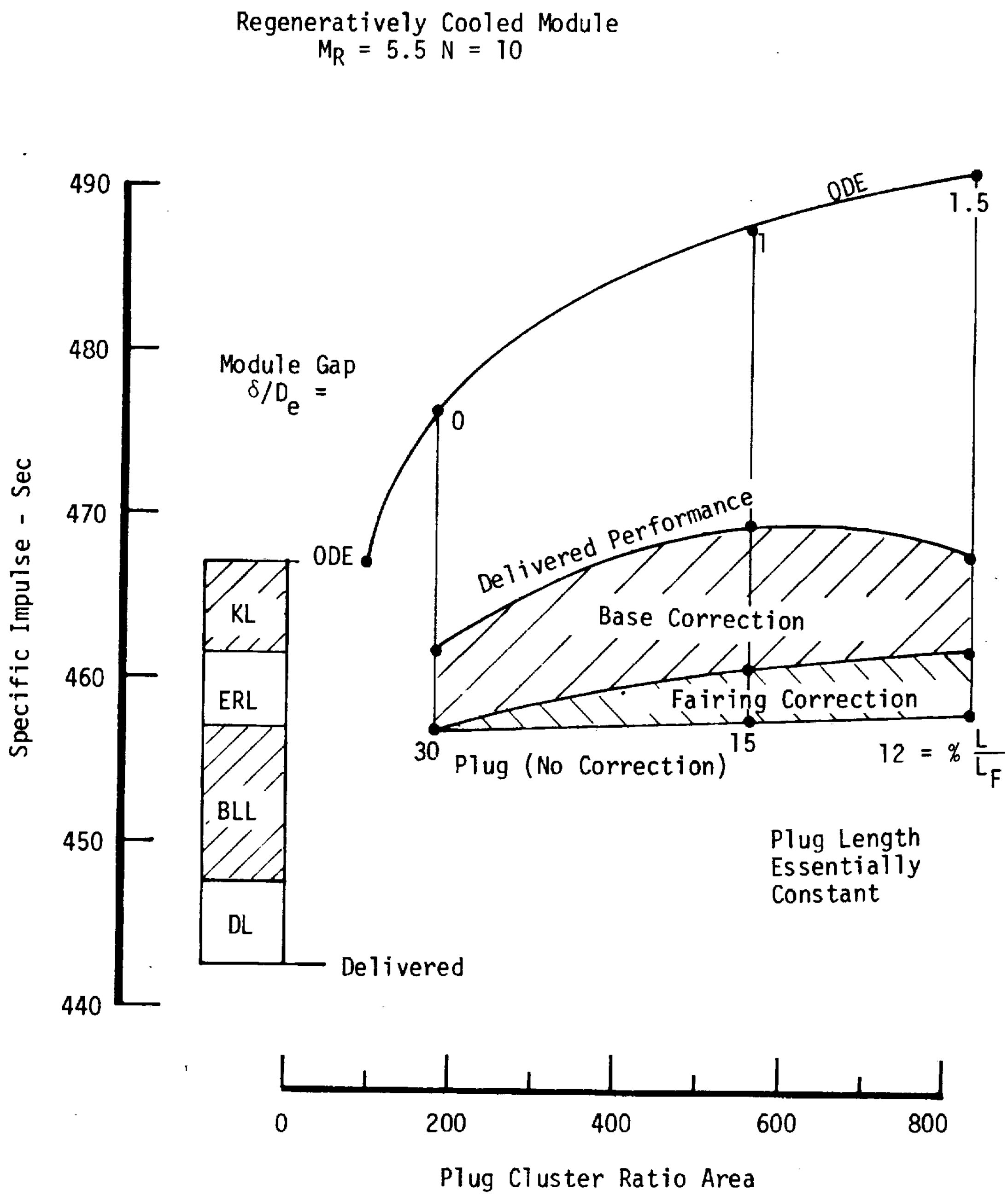

Figure 50. Plug Cluster Engine Performance Summary at P_c = 20.4 ATM and ε_M = 100.

Figures 48 and 49 depict the proceding two cases at the higher chamber pressure of 34.0 atm (500 psia). A corresponding case for ϵ_M = 100 modules, is given in Figure 50.

Examination of the data presented in Figures 46 and 50 for Model I, shows that the clustered plug performance improvement for a $\epsilon_M = 40$ and a $\epsilon_M = 100$ module is 7.8% and 5.7%, respectively, at the large area ratios of this study.

F. ANALYSIS OF EXPERIMENTAL PLUG CLUSTER DATA (NAS 3-20104)

Module-plug cluster performance Model II, presented in the next section, incorporates the results of the cold flow experiments conducted under Contract NAS 3-20104 (Ref. 46). Prior to the use of these data, however, it was a requirement of this contract to make an appraisal of the data and to compare the results with those available in the literature. This section documents the work performed to analyze the test data.

Tests were performed on twelve different cluster configurations shown in Table XII. Freon or air were used as the test medium to determine the effects of gap, module area ratio, cluster area ratio, fairings, fences, tilt angle, and base pressurization on cluster performance. Validity of the air data is questionable because condensation shocks could have had an effect on the results. In addition, the applicability of the air data is questionable because the tilt angles and module-match points were designed based on the use of Freon. Figure 51 shows that the change in the ratio of specific heat capacities has a strong influence on these design parameters.

A comparison of the experimental data from Contract NAS 3-20104 with that given in Reference 4 is shown in Table XIII. It is seen that there is general agreement with the engine performance based on the efficiency (η_{Is}) of the engine for zero gap cases, but that either the base or module performance derived from the data do not agree. For example, the Contract NAS 3-20104 results in the table indicate a negative recovery of the tilt angle (cosine Θ) loss, whereas the Contract NAS 8-11023 results indicate some recovery even for a zero length plug. It is not expected that the large difference in area ratio between the cited cases should have any effect for zero gap cases.

For a fixed number of modules and module area ratio, the test data in Figure 52 show that increasing the cluster area results in a decrease in performance and efficiency. This decrease in performance and efficiency is due to the mismatch of aerodynamic flow fields for discrete bell nozzles exhausting onto an annular plug contour, as indicated in Figure 53. The loss in performance is conventionally reported as due to the increase in gap associated with the increase in cluster area ratio.

The trend in the data is what would be expected for a plug cluster configuration based on an annular plug nozzle, where the contour has not been optimized for discrete internal expansion sections (bell nozzles) with a gap between the nozzles. Typical static pressure data are shown on a

TABLE XII - AERODYNAMIC VARIABLES FOR TEST MODELS

Config.	ε_c	$\bar{\varepsilon}_M$	N	δ/DE	θ_T EXPTL	θ_T Eq.(3) (FREON)	$\varepsilon_c/\varepsilon_M$ EXPTL	$\varepsilon_c/\varepsilon_M$ Eq.(1)
				Based on γ = 1.15				
A-11	500	40	12	1.96	27.9	31.9	12.48	12.36
A-10	400	40	12	1.62	26.93	29.4	10.01	9.92
D-10	400	40	20	1.06	25.93	29.4	9.85	9.80
E-10	400	40	5	2.88	26.93	29.4	10.60	10.34
B-10	400	80	12	.77	17.2	19.5	5.04	5.01
C-10	400	200	12	.01	6.63	8.0	2.00	1.99
A-7	200	40	12	.77	19.23	21.5	5.02	4.99
				Based on γ = 1.4 (AIR)				
A-11	500	40	12	1.96	27.9	19.9	12.48	12.67
A-10	400	40	12	1.62	25.93	18.6	10.01	10.15
D-10	400	40	20	1.06	25.93	18.6	9.85	9.94
E-10	400	40	5	2.88	25.93	18.6	10.60	11.05
B-10	400	80	12	.77	17.2	11.9	5.04	5.08
C-10	400	200	12	.01	6.63	4.6	2.00	2.00
A-7	200	40	12	.77	19.23	14.0	5.02	5.06

$$\theta_T = \nu_E - \nu_M \qquad \text{Eq. (3)}$$

$$\nu = \sqrt{\frac{\gamma + 1}{\gamma - 1}} \tan^{-1} \sqrt{\frac{\gamma - 1}{\gamma + 1} (M^2 - 1)} - \tan^{-1} \sqrt{M^2 - 1} \qquad \text{Eq (3a,}$$

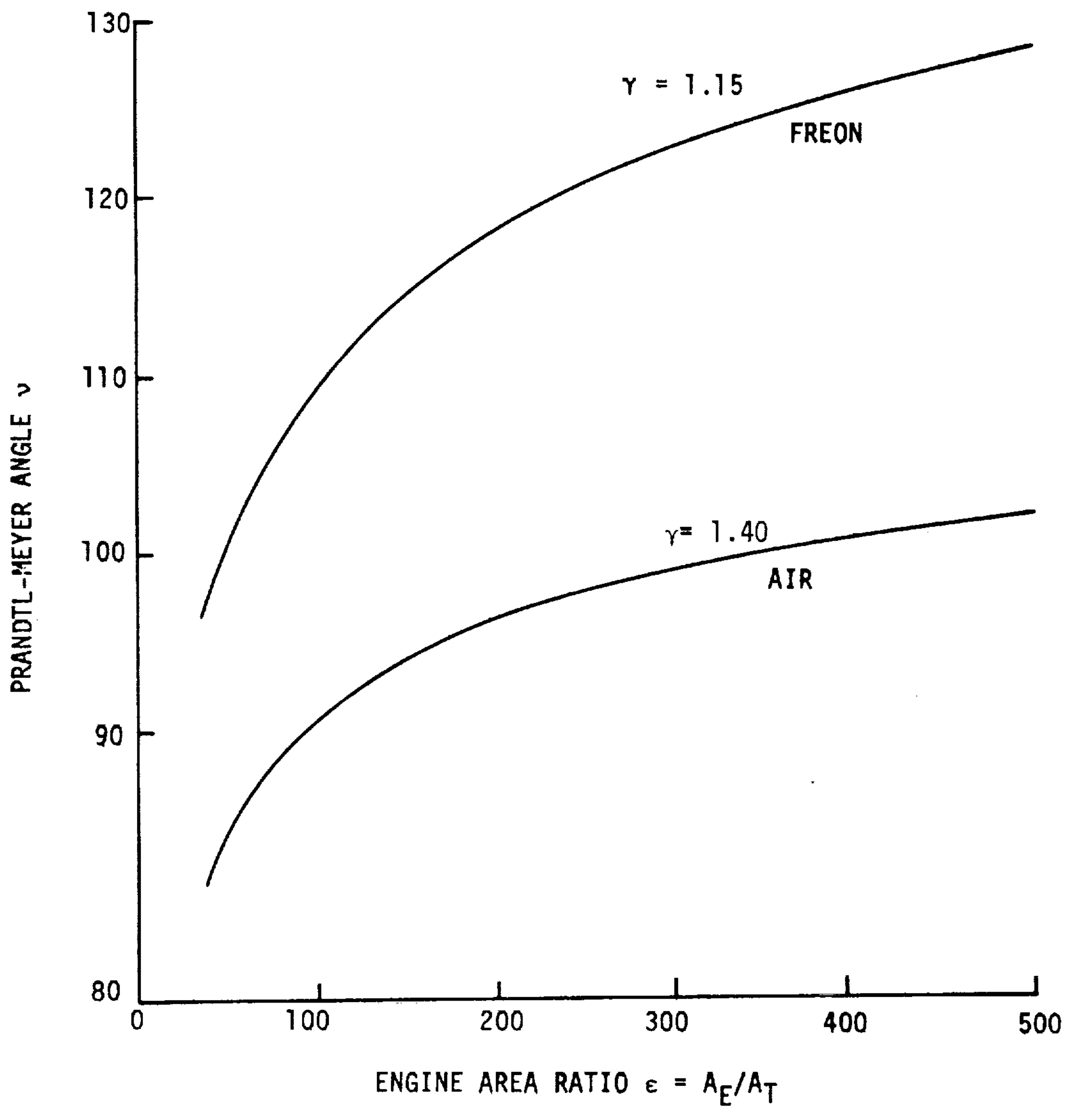

Figure 51. Effect of Gas Properties on Required Tilt Angle.

TABLE XIII- COMPARISON OF EXPERIMENTAL PLUG CLUSTER PERFORMANCE

PARAMETER	NAS 8-11023*			NAS 3-20104**
N	24	24	12	12
ε_M	4.85	4.85	7.7	195.6
ε_E	15.0	15.0	15.0	386.5
Θ	18	18	10	6.63
PLUG LENGTH	0	9.4	0	0
I_{ODE} (MODULE)	63.72	63.72	66.62	94.78
I_{ODE} (ENGINE)	69.66	69.66	69.66	95.65
$\dot{W}$ (ENGINE)	3.48	3.48	3.48	0.574
I_{DEL} (ENGINE)	66.45	67.29	67.15	91.46
η_{IS} (ENGINE)	0.954	0.966	0.964	0.956
I_{DEL} (BASE)	3.99	3.43	1.25	0.47
P_B/P_E	2.93	2.5	1.48	1.60
% BASE I_S	6.0	5.1	1.9	1.7
$\dot{W}_{BASE}$	0	0	0	0
I_{DEL} (MODULE)***	62.47	63.86	65.90	90.99
η_{IS} (MODULE)	0.980	1.002	0.989	0.960
I_{ODE} (MODULE) . cos Θ	60.60	60.60	65.61	94.14
% cos Θ loss recovered****	59.9	104.5	28.7	<0

* Reference 4: Base area estimated from photographs of hardware; flow rate assumed from sample case given in Appendix A.

** Test 35.01; Configuration C-10; Air Media

*** I_{DEL} (ENGINE)- I_{DEL} (BASE) $\simeq$ I_{DEL} (MODULE)

**** [I_{DEL} (MODULE) - I_{ODE} (MODULE) x cos Θ]/[I_{ODE} (MODULE) - I_{ODE} MODULE) x cos Θ]

CONTRACT NAS 3-20104 (REFERENCE 46)

TEST NO.	CONFIG.	ϵ_E	γ/D_e	θ_T	Isp	C_T
49.02	A-7	200	0.77	19°	63.39	0.919
28.01	A-10c	400	1.62	26°	63.07	0.897
46.01	A-11	500	1.96	28°	62.29	0.895

$\epsilon_M = 40$ $N = 12$

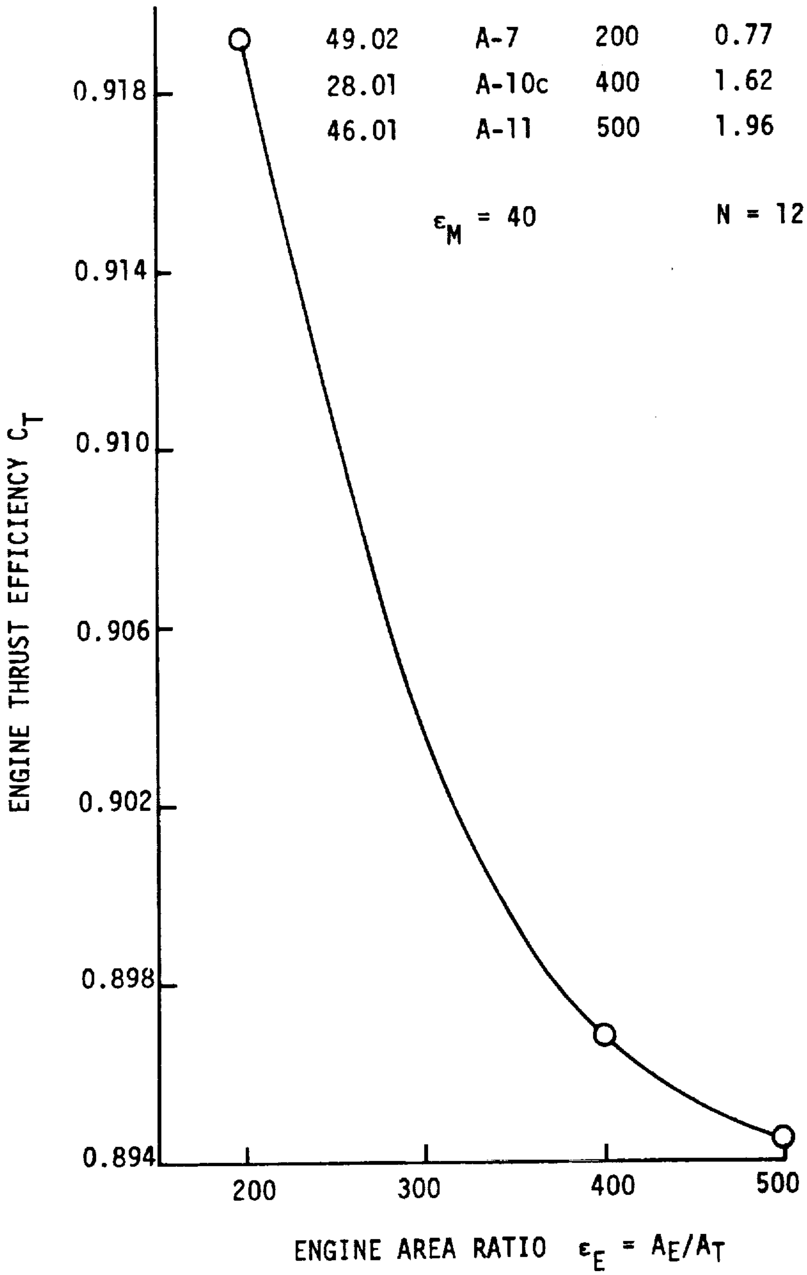

Figure 52. Cluster Performance as a Function of Engine Area Ratio.

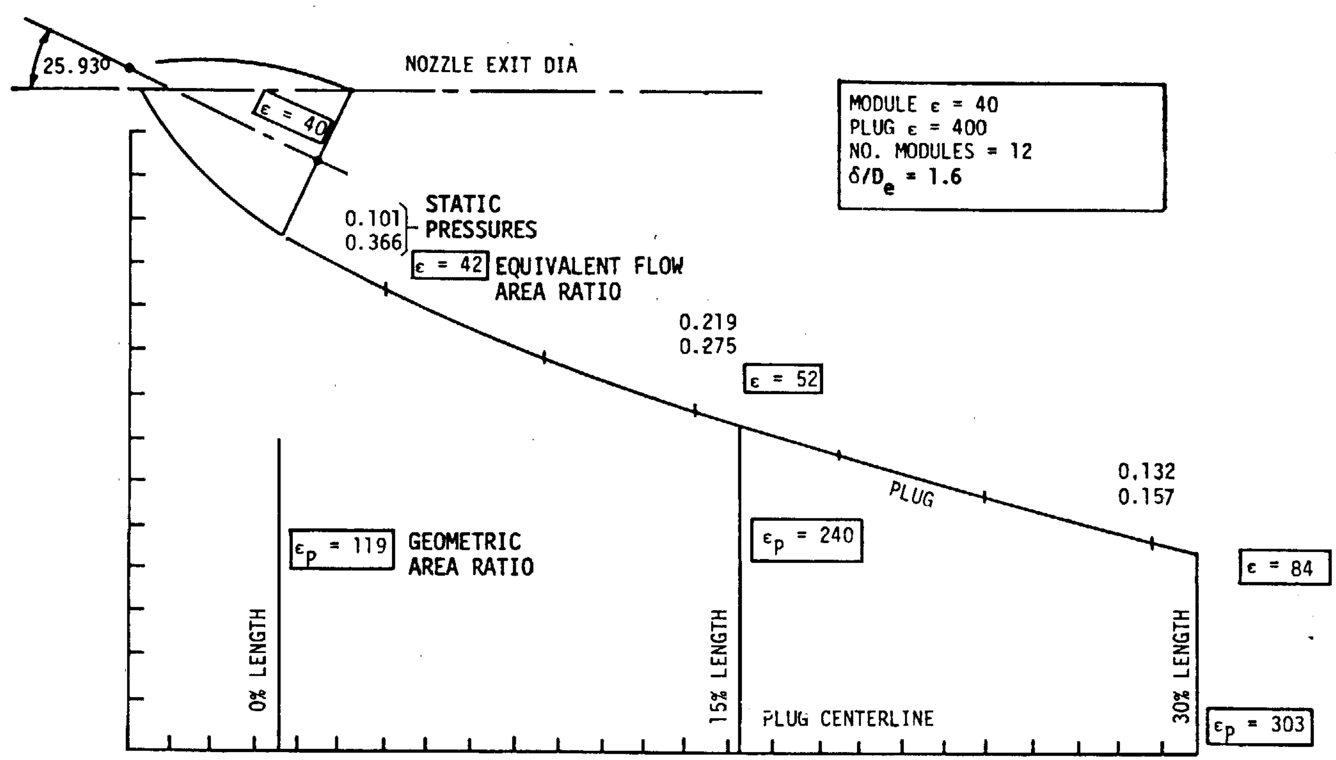

Figure 53. Pressure Tap Data Indicate the Effective Area Ratio Achieved by the Flow of Gas on the Plug Nozzle.

schematic of the plug cluster in Figure 53. The two values listed refer to pressures measured on the plug nozzle wall between two modules (gap of 1.6 module exit diameters) and on the center line of one module exit. We would expect the static pressure values to be lower as the gas expands on the plug nozzle, and to approximate the isentropic relationship. Correspondingly, we would expect to be able to calculate the effective area ratio using the isentropic relations (with suitable two dimensional corrections).

The calculated aerodynamic area ratios based on the pressure measurements are shown on Figure 53 for 0, 15, and 30 percent plugs, and also on Figure 54. It is seen that the gas expands from the module area ratio of 40 to an equivalent area ratio of 84 at the plug exit. Now, by definition, this plug cluster configuration has an area ratio of 400. However, since we are examining the gas flow data on the surface of the plug, we must compare the data with the geometric plug flow area ratio. This area ratio is determined by taking the defined engine area, subtracting the area occupied by the plug, and dividing this value by the sum of the module throat areas. Three such area ratios are indicated on Figure 53.

It is seen, therefore, that less than one-third (84/303) of the available geometric plug flow area ratio was actually achieved with the 30% plug test configuration of Figure 53. This result is consistent with the one-third (40/119) value expected for a zero length plug, the larger plug flow area being the result of the gap between the modules. We thus have a gross discontinuity in area ratio at the match point.

The results from Contract NAS 3-20104 may be interpreted by examining the geometric flow area for a zero gap version of Figure 53. Despite the fact that an even number of modules cannot be added to change this configuration to zero gap, the assumption can be verified by examining a cluster with a $\delta/D_e = 1$ gap, for example. The addition of more modules increases the sum of the throat areas, and thus decreases the geometric plug flow area ratio to that shown in Figure 54 at zero gap. It is seen that the aerodynamic area ratio based on the pressure measurements more closely fits the zero gap geometric plug flow area ratio. Thus it can be concluded that the stream tubes emanating from the nozzles (modules) apparently follow essentially the same aerodynamic path regardless of the area available. The performance at large gaps (for the tested configuration) is thus about the same as at low gaps (area ratios).

The test results from Contract NAS 3-20104 indicate a serious flaw in the design criteria of high area ratio plug clusters based on methodologies developed from low area ratio testing. The low area ratio, low gap, methodology stipulates a one-dimensional matching of the module Mach number with that of an annular plug Mach number, as shown in Figure 55. But this approach becomes unsatisfactory at gaps much greater than zero, because we have a three dimensional problem. Geometric remedies, such as the addition of fairings between the modules, offer a partial solution for large gaps, as shown in Contract NAS 3-20104 and also indicated in Figure 12.

As shown in Table XIV the effective specific impulse of the base injection flow (Isp Base) is from 6 to 13% less than the specific impulse

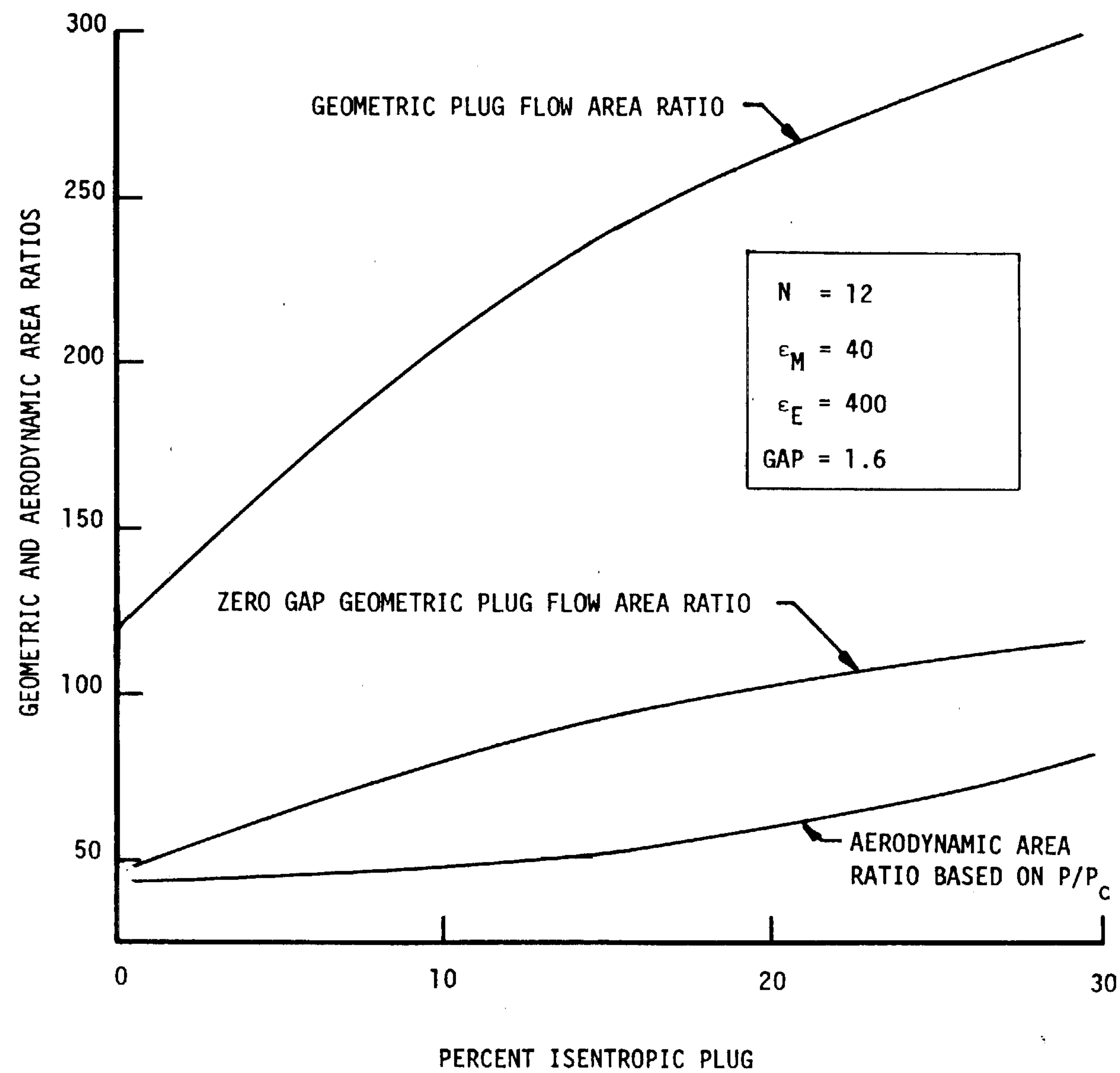

Figure 54. Effective Area Ratio of Plug Cluster is Less Than Geometric Area Ratio.

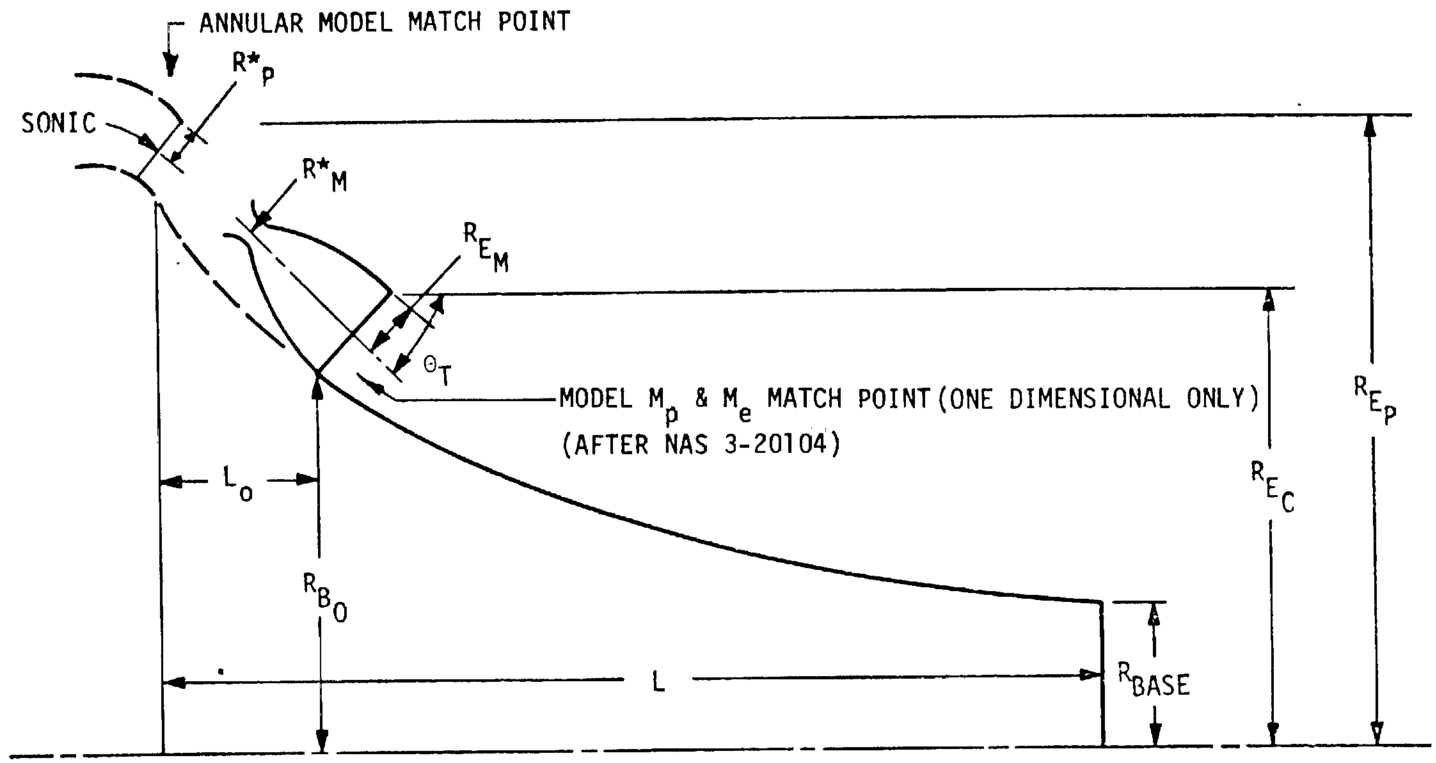

Figure 55. MACH Number Match Configuration for Model II.

TABLE XIV. - BASE PRESSURE AND SECONDARY EFFECTS (NAS 3-20104)

Test	Config.	F_{VAC}	$\dot{W}_s/\dot{W}_p$	I_{SPE}	F_{Base}	% Total	P_B	$I_{SP_{Base}}$	% Plug
29.01	A-10b	59.72	0	64.93	.2317	0.4	.014	-	30
29.02	A-10b	60.30	.0107	64.86	.8303	1.4	.051	61.08	30
28.01	A-10c	58.94	0	63.84	.8445	1.4	.035	-	15
28.03	A-10c	59.59	.0109	63.63	1.4685	2.5	.061	61.78	15
30.01	A-10d	56.33	0	61.17	2.6872	4.8	.062	-	0
30.02	A-10d	56.93	.0107	61.05	3.2050	5.6	.074	52.91	0

$$I_{SPE} = \frac{F_{vac}}{\dot{W}_p\ (1 + \dot{W}_s/\dot{W}_p)} \qquad I_{SP_{BASE}} = \frac{\Delta F_{Base}}{\dot{W}_s} \qquad F_B = P_B A_B$$

generated by the primary flow. The overall specific impulse with secondary injection for Contract NAS 3-20104 testing was always less than the Isp without base injection. This result differs from that found in Reference 4, where the efficiency of the zero gap plug cluster was slightly better or equal to that for no base flow up to a secondary flow of about two percent. It also differs from that found for the annular throat (Aerospike) configuration, where the secondary flow specific impulse amounted to 6056 seconds (Table IV) for flows as low as 0.2 percent. The base pressurization results from Contract NAS 3-20104 correspond to those obtained for below design point testing of plug nozzles, where the wake is not closed. The results indicate the possibility that the flow did not provide a closed wake, making secondary injection not as effective.

The results from the testing on Contract NAS 3-20104 represent selected point design plug cluster configurations, as resources did not allow a systematic investigation of the many variables. Nevertheless, the data and their comparison with related test data from the literature, indicate that low performance will be obtained with large gap cluster configurations of bell nozzles on annular plug designs. The results conclusively define the problem as being one of assuring an aerodynamic flow match between the bell and the plug. Solution of the problem leads to unconventional plug contours that resemble a fluted plug, and provide much higher performance than conventional type clusters.

G. MODULE-PLUG CLUSTER PERFORMANCE MODEL II

The initial computer model (Model I) represented an engine configuration in which the cluster throat location coincided with the equivalent area ratio annular plug throat location. In order to provide a better approximation of the test data from Contract NAS 3-20104, Model I was revised to incorporate a Mach number match point. The configuration model is that shown in Figure 55. Uncorrected plug performance is calculated in a similar manner to that for Model I, except that CF_{LO} is now evaluated at the point of Mach number match.

The uncorrected plug performance is multiplied by a gap efficiency factor (see Figure 44), which is defined as the ratio of the uncorrected cluster efficiency to the efficiency of a zero gap configuration at the given cluster radius (R_{E_C}).

Correction for base pressurization was provided by a correlation derived from Contract NAS 3-20104 data utilizing the effective base pressure P_B as a function of the plug exit pressure P_E.

Application of Model II to a cluster configuration used in Contract NAS 3-20104 resulted in predicted performance of C_F = 1.927 compared to the measured C_F = 1.928 - 1.933. Plug cluster engine performance computed for the baseline case is shown in Table XV for both Models I and II. Cold flow test information are included in the table for comparison.

It is seen from Table XV that Model II, based on Contract NAS 3-20104 test data correlations, predicts that a plug cluster engine will be only 91% efficient. Model II is not considered to be an accurate representation of a plug cluster engine, because of the approximations that have been utilized. The model, however, does provide engine performance consistent with the cold flow results for Contract NAS 3-20104 configurations. The model will require revision to predict the performance of optimum cluster designs.

H. MODULE-PLUG CLUSTER PERFORMANCE MODEL III

The problem of achieving highly efficient aerodynamic flow for the plug cluster engine concept was solved by joining high area ratio, partially scarfed, bell nozzles in the manner shown in Figure 56. Discussions concerning the performance of the scarfed-bell or fluted-plug cluster engine concept are presented in this section.

Since the JANNAF simplified performance methodology is well established for full bell nozzles, Model III includes the analysis of the configuration shown in Figure 57. The performance of the scarfed-bell plug cluster engine is expected to very closely approach that for the clustered bell concept shown in Figure 57.

In order to make a direct comparison (in Section VIII of this report) between the plug cluster engine and candidate Space Tug engines, such as the RL10 and the Advanced Space Engine (ASE), this section also includes the calculated performance for these engines.

1. Model III Description

The JANNAF simplified methodology, as utilized in this study, reduces to the equation

$$Isp_{delivered} = Isp_{ODE} \left(\eta_{KIN}\ \eta_{NOZ}\ \eta_{ERE} - \frac{\Delta F_{BL}}{F}\right)$$

TABLE XV - PLUG CLUSTER PERFORMANCE MODEL COMPARISONS

	Model I	Model II	NAS 3-20104 Test 46.01 Config. A-11
Vacuum Thrust, KN (Klb)	72.5 (16.3)	68.7 (15.5)	--
Chamber Pressure, atm (psia)	20.4 (300)	20.4 (300)	10.7 (157)
Vacuum Specific Impulse, s	467.4	443.8	--
Mixture Ratio (O/F)	5.44	5.5	--
Engine Area Ratio (A_E/A_t)	458	458	493
Module Area Ratio (A_e/A_t)	40	40	40
Number of Modules	10	10	12
Module Gap (δ/De)	2	2.05	1.96
Engine Diameter, cm (in)	320 (126)	320 (126)	--
Plug Base Diameter, cm (in)	218 (86)	173 (68)	--
Engine Length, cm (in)	86 (34)	91 (36)	--
Percent (L/L_I) Plug	15	20	15
Tilt Angle, deg.	3.5	27.7	27.9
Base Flow Ratio %	0.2	0	0
Uncorrected I_s, s	449.5	454.6	--
Base Correction ΔI_s, s	+ 8.9	+ 0.6	--
Gap/Fairing Correction ΔI_s, s	+ 9.0	- 11.4	--
Delivered I_s, s	467.4	443.8	--
Engine Efficiency η_{I_s}	0.962	0.914	0.895

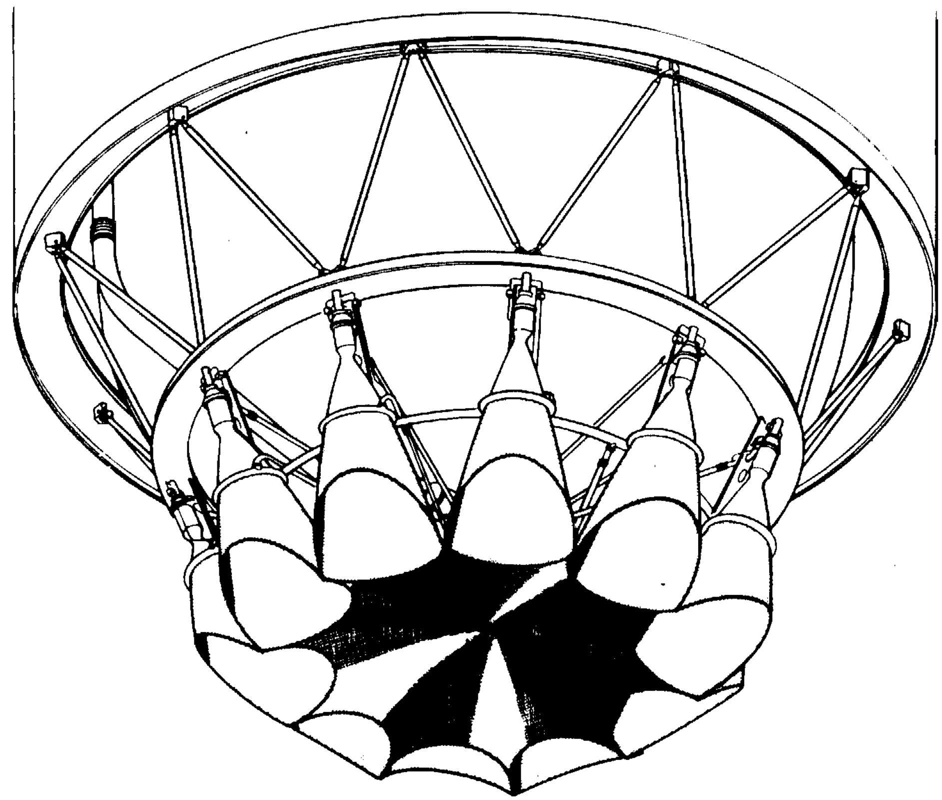

Figure 56. Scarfed Bell/Plug Cluster Engine Concept.

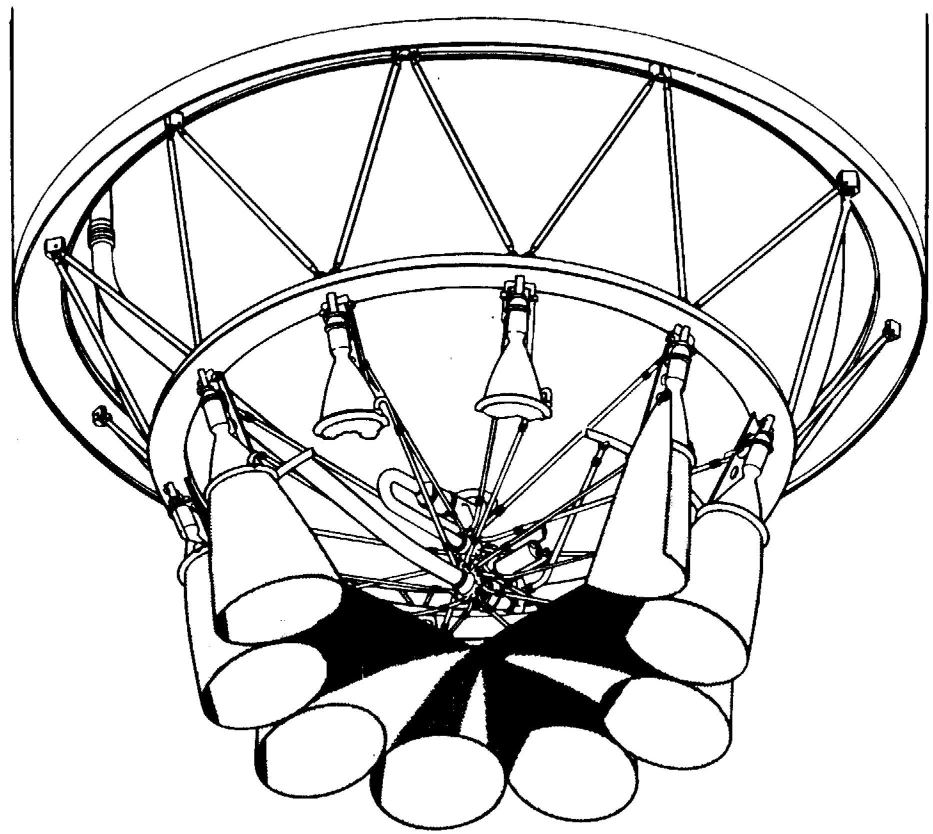

Figure 57. Clustered Bell Nozzle Concept.

where Isp_{ODE} is the one dimensional equilibrium specific impulse, η_{KIN} is the kinetic efficiency (Isp_{ODK}/Isp_{ODE}), η_{NOZ} is the nozzle or divergence efficiency, η_{ERE} is the energy release efficinecy, ΔF_{BL} is the boundary layer thrust decrement, and F is the nominal engine thrust.

The values of Isp_{ODE} and Isp_{ODK} are generated by the JANNAF ODE-ODK-TDK computer program, and η_{NOZ} and ΔF_{BL} are found using the charts and methodology from Reference 17. The value of η_{ERE} = 0.995 was used in the performance calculations for all of the engines.

Because the plug cluster engine (PCE) is not strictly a bell nozzle configuration, its performance required additional calculations as follows:

- Determine the $Isp_{delivered}$ for scarfed nozzles.
- Calculate exit pressure (P_E) corresponding to overall PCE area ratio.
- Determine base pressure (P_B) as a function of P_E (normally assumed to be 2.5 x P_E but can be as high as 3.6 x P_E).
- Determine base area (A_B) of PCE.
- Calculate thrust loss ($\Delta F_{\Theta T}$) due to module tilt angle (Θ_T); equals Fm (1 - $\cos\Theta_T$).
- Calculate delivered thrust of PCE; $F_{PCE} = N\ Fm + P_B\ A_B - N\ \Delta F_{\Theta T}$, where N is the number of modules in the cluster.
- Calculate the delivered specific impulse; $Isp_{del} = F_{PCE}/\dot{w}_{ENGINE}$, where the flow rate to the engine, $\dot{w}_{ENGINE}$, may include a base bleed contribution.

The rationale and assumptions used in the calculations for the PCE are described in the following.

2. MODEL III Nozzle Efficiency

Nozzle divergence efficiency is obtained in the standard manner from the following equation

$$\eta_{NOZ} = \frac{1 + \cos\alpha}{2}$$

where α is the nozzle divergence angle.

In the case of the plug cluster engine, there is some question regarding the use of the module nozzle efficiency, since the module is tilted toward the axis of the engine. For the case when the tilt angle equals the nozzle divergence angle, the flow from the outer portion of the nozzle is aligned with the axis of the engine. The flow from the inner portion of the nozzle is turned aerodynamically in forming the wake on the base of the plug. Since the method of calculation includes a tilt angle (cos Θ) loss, inclusion of the module nozzle divergence loss does not appear to be warranted. Since there is some uncertainty, however, the PCE delivered performance will be presented with and without this loss.

3. Scarfed Nozzle Performance

The scarfed bell/plug cluster nozzle concept (Figure 56) can be envisioned to be a fluted plug nozzle with both internal and external expansion components. As such, the performance would very closely approach that for the full bell cluster shown in Figure 57. Were the scarfed bell/plug cluster nozzle to operate as a cluster of scarfed nozzles with a small amount of base thrust contribution, the performance would be less. In order to present this degree of uncertainty, PCE calculations were made assuming the module thrust contribution to be only that from a scarfed nozzle.

The first step in determining the performance of a scarfed nozzle is to determine the area ratio (ε_{eff}) of an equivalent unscarfed nozzle. In this manner it is assumed that the delivered performance of a scarfed nozzle corresponds to the area ratio at the intersection of the scarfing plane and the lengthwise nozzle axis. This method of scarfing is shown in Figure 58, along with the method chosen for the PCE design.

The analytical expression for ε_{eff} is obtained by assuming a 15-degree conical nozzle and by specifying the two area ratios (ε_1 and ε_2) between which the nozzle is scarfed.

$$\mathrm{eff} = \frac{4\varepsilon_1\varepsilon_2}{(\sqrt{\varepsilon_1} + \sqrt{\varepsilon_2})^2}$$

For the two scarfed nozzles considered, the expression yields:

When Nozzle is Scarfed From	ε_{eff}
$\varepsilon_1 = 40$ to $\varepsilon_2 = 500$	97
$\varepsilon_1 = 100$ to $\varepsilon_2 = 500$	191

Using these values of ε_{eff}, the kinetics and boundary layer losses were obtained from Figures 59 and 60, respectively.

As seen in Figure 58, the PCE scarfed nozzle is not as severely scarfed as the one utilized in this analysis. However, the more conservative ε_{eff} was utilized for this analysis.

4. Model III Base Pressurization

A relatively consistent correlation between P_B and P_E was previously cited in Table X and Figure 35 (Section IV,C), where the base pressure obtainable is defined as that in which the nozzle separation criteria

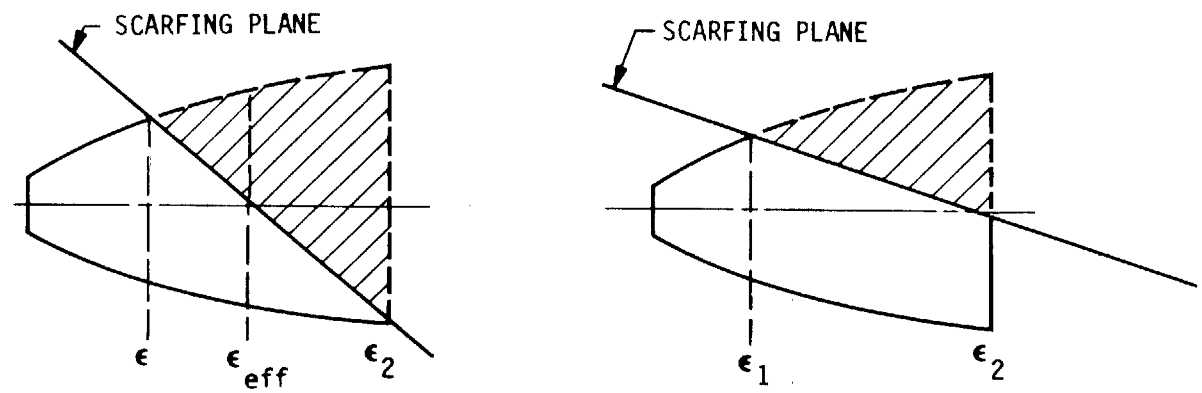

(a) ANALYTICAL SCARFED NOZZLE

(b) PCE SCARFED NOZZLE

Figure 58. Scarfed Nozzle Geometry.

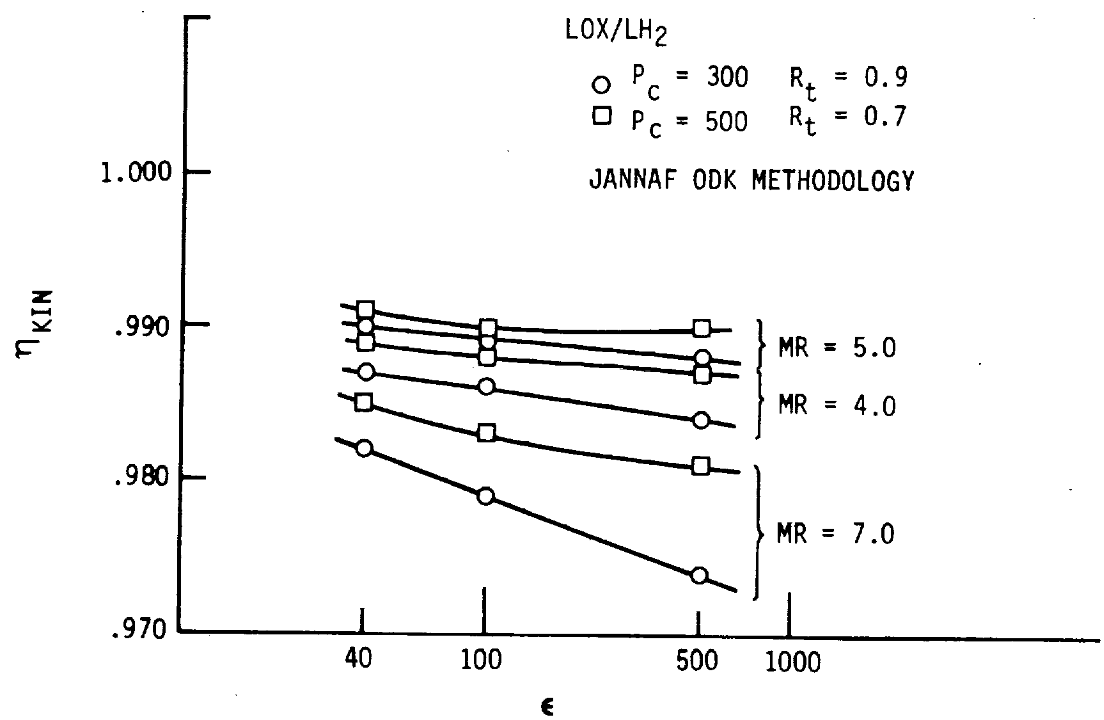

Figure 59. Kinetics Loss for Scarfed Nozzle.

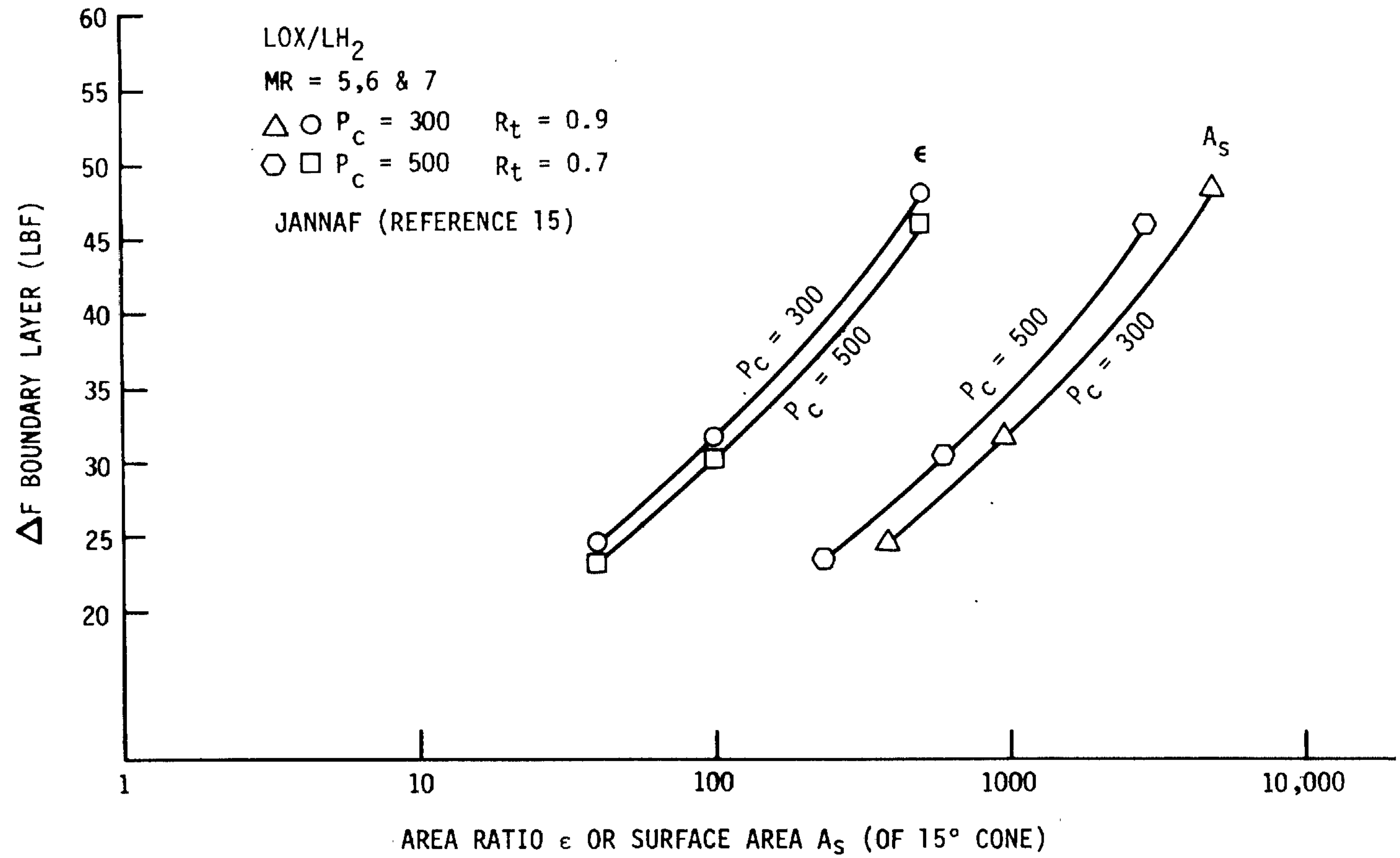

Figure 60. Boundary Layer Loss for Scarfed Nozzle.

holds. Base pressures above the nozzle separation criteria ($P_B/P_E \geq 3.6$) cause an enlargement of the wake on the plug base, and thereby reduce the effective area ratio obtainable with a plug nozzle.

The assumption was made, as cited in Section IV,C to utilize bleed flows of 0.2% of the engine flow.

5. Model III Plug Cluster Engine Delivered Performance

The plug cluster engine performance calculated by the outlined methodology is summarized in Table XVI. Calculated values are given for chamber pressures of 20.4 atm (300 psia) and 34.0 atm (500 psia), and for mixture ratios of 5 and 6. Three types of nozzles are assumed: (1) performance equivalent to a full bell nozzle, (2) performance equivalent to a scarfed bell at $\varepsilon = 40$, and (3) performance equivalent to a scarfed bell at $\varepsilon = 100$.

Table XVII gives a comparison of the three performance models.

In order to estimate the possible uncertainty in the calculated values of performance, a base case was selected, and the assumptions were modified to determine their effect on performance. The result of the uncertainty analysis is summarized in Table XVIII.

The lower limit in performance is achieved by a cluster of bell nozzles with zero tilt angle. For this case, it is assumed that the base pressure is equal to P_E, and that there is zero base bleed. The nozzle efficiency is now 0.994 as the divergence loss of the bell nozzle must be taken into account. The resultant performance is found to be 460.7 seconds ($\eta_{I_S} = 0.943$). A possible upper limit for the cluster is found to be 471.7 seconds ($\eta_{I_S} = 0.965$). Zero base bleed and the maximum base pressure consistent with nozzle separation criteria is assumed. Also a smaller boundary layer loss is assumed, which is consistent with more rigorous calculations. A loss of 0.6 second in specific impulse is required for a gas generator cycle plug cluster engine.

In order to further evaluate the validity of the performance prediction for the plug cluster engine, calculations were made for the RL10 and ASE using the same JANNAF simplified procedures. The results of these calculations are given in Table XIX. Comparisons with the performance values presently accepted for these engines are shown.

TABLE XVI - JANNAF SIMPLIFIED PERFORMANCE FOR PLUG CLUSTER ENGINES

N = 10   90% Bell F_M = 1.5K lbf   Expander Cycle θ_T = 5.3° ε_E = 895

	Pc	300	300	300	300	300	300	500	500	500	500	500	500
	MR	5	5	5	6	6	6	5	5	5	6	6	6
	ε	500	40-500 ε_{eff} = 97	100-500 ε_{eff} = 191	500	40-500 ε_{eff} = 97	100-500 ε_{eff} = 191	500	40-500 ε_{eff} = 97	100-500 ε_{eff} = 191	500	40-500 ε_{eff} = 97	100-500 ε_{eff} = 191
	R_t	.9	.9	.9	.9	.9	.9	.7	.7	.7	.7	.7	.7
	Isp_{ode}	485.3	468.6	476.5	486.8	467.0	477.0	485.5	469.0	477.0	487.1	467.5	477.0
Module	Isp_{odk}	479.4	463.4	471.2	478.6	460.5	469.8	480.3	464.3	472.2	480.6	461.9	471.0
	η_{ERE}	.995	.995	.995	.995	.995	.995	.995	.995	.995	.995	.995	.995
	η_{KIN}	.988	.989	.988	.984	.986	.985	.990	.990	.990	.987	.988	.988
	η_{NOZ}	1.000	1.000	1.000	1.000	1.000	1.000	1.000	1.000	1.000	1.000	1.000	1.000
	ΔF_{BL}^{Module}	48.2	42.0	43.5	47.9	42.0	43.5	46.2	40.	41.5	45.9	40.0	41.5
	$\eta_{overall}$	.951	.956	.955	.947	.953	.951	.954	.958	.957	.951	.956	.955
	Isp delivered Module	461.5	448.0	455.0	461.1	445.1	453.7	463.3	449.5	456.7	463.5	447.1	455.5
	$\dot{W}_{mod}$	3.250	3.348	3.297	3.253	3.370	3.306	3.238	3.337	3.285	3.237	3.355	3.293
	$F_{ENGINE}^{NOMINAL}$	15K	15K	15K	15K	15K	15K	15K	15K	15K	15K	15K	15K
	Engine Description	PCE	PCE	PCE	PCE	PCE	PCE	PCE	PCE	PCE	PCE	PCE	PCE
Plug Cluster	A_{base}	7348.2	7358.2	7358.2	7358.2	7358.2	7358.2	4446.1	4446.1	4446.1	4446.1	4446.1	4446.1
	Isp_{ode}^{ENGINE}	489.0	489.0	489.0	491.6	491.6	491.6	489.2	489.2	489.2	491.9	491.9	491.9
	P_{EENG}	.0085	.0085	.0085	.0109	.0109	.0109	.0143	.0143	.0143	.0179	.0179	.0179
	$\dot{W}_{ENGINE}$	32.50	33.48	32.97	32.53	33.70	33.06	32.38	33.37	32.85	32.37	33.55	32.93
	$\dot{W}_{BASE}$	.065	.067	.066	.065	.067	.066	.065	.067	.066	.065	.067	.066
	F_{BASE}	156.4	156.4	156.4	200.5	200.5	200.5	158.9	158.9	158.9	199.0	199.0	199.0
	$F_{LOSS-\theta T}$	64.9	64.9	64.9	64.9	64.9	64.9	64.9	64.9	64.9	64.9	64.9	64.9
	$F_{ENG}^{delivered}$	15,091.5	15,091.5	15,091.5	15,135.6	15,135.6	15,135.6	15,094.0	15,094.0	15,094.0	15,134.1	15,134.1	15,134.1
	$Isp_{ENGINE}^{delivered}$	463.4	449.9	456.8	464.4	448.2	456.9	465.2	451.4	458.6	466.6	450.2	458.7
	$\eta_{DELIVERED}$	.948	.920	.934	.945	.912	.929	.951	.923	.937	.949	.915	.933

TABLE XVII - PLUG CLUSTER PERFORMANCE MODEL COMPARISONS

	Model I	Model II	Model III
Vacuum Thrust, KN (Klb)	72.5 (16.3)	68.7 (15.5)	67.1 (15.1)
Chamber Pressure, atm (psia)	20.4 (300)	20.4 (300)	20.4 (300)
Vacuum Specific Impulse, s	467.4	443.8	463.9
Mixture Ratio (O/F)	5.44	5.5	5.5
Engine Area Ratio (A_E/A_t)	458	458	895
Module Area Ratio (A_e/A_t)	40	40	500
Number of Modules	10	10	10
Module Gap (δ/De)	2	2.05	0
Engine Diameter, cm (in)	320 (126)	320 (126)	433 (170)
Plug Base Diameter, cm (in)	218 (86)	173 (68)	246 (97)
Engine Length, cm (in)	86 (34)	91 (36)	82 (32)
Percent (L/L_I) Plug	15	20	0
Tilt Angle, deg.	3.5	27.7	5.3
Base Flow Ratio %	0.2	0	0.2
Uncorrected I_s, s	449.5	454.6	459.3
Base Correction ΔI_s, s	+ 8.9	+ 0.6	+ 4.6
Gap/Fairing Correction ΔI_s, s	+ 9.0	- 11.4	0
Delivered I_s, s	467.4	443.8	463.9
Engine Efficiency η_{I_s}	0.962	0.914	0.947

TABLE XVIII. - UNCERTAINTY IN PLUG CLUSTER ENGINE PERFORMANCE

Expander Cycle

$MR = 6.0$ $\quad \varepsilon_M = 500$ $\quad N = 10$

$Pc = 300$ $\quad \varepsilon_E = 895$

Base Case: $\eta_{NOZ} = 1.0$ $\dot{W}_B = .065$ (0.2%)

$P_B = 2.5\ P_E$ $\Theta_T = 5.3°$

$\Delta F_{BL} = 47.9$

Variable	Delivered Isp Performance	Difference From Base Case Isp
Base Case	464.4	-
$\eta_{NOZ} = 0.994$	461.5	-2.9
$\dot{W}_B = 0$	465.3	+0.9
$\dot{W}_B = 0.33$ (1%)	460.6	-3.8
$P_B = 3.6\ P_E$	467.1	+2.7
$P_B = 1.5\ P_E$	463.9	-0.5
$\Theta_T = 0$ $\dot{W}_B = 0$ $P_B = P_E$ $\eta_{NOZ} = 0.994$	460.7	-3.7
$\Delta F_{BL} = 38$	467.5	+3.1
Gas Generator Cycle	463.8	-0.6

The JANNAF simplified procedure is seen to give conservative performance prediction for the ASE, and to give correct performance prediction for the RL10, providing a more conservative nozzle efficiency and other losses are utilized in the calculation. It is anticipated, therefore, that the preceding methodology for the plug cluster engine will provide a reasonably accurate assessment of the performance potential.

TABLE XIX. JANNAF SIMPLIFIED PERFORMANCE FOR RL10 AND ASE

Engine Description	RL10 IIB	RL10 IIB	ASE	ASE
Cycle	Exp.	Exp.	SC	SC
Pc	400	400	2000	2000
MR	5	6	5	6
ε	200	200	400	400
% Bell	75	75	90	90
F nom (lbf)	15K	15K	20K	20K
I_{sp}ode	477.3	477.2	484.0	485.8
η_{ere}	0.995	0.995	0.995	0.995
η_{kin}	0.998	0.998	0.996	0.996
η_{noz}	0.996	0.992	0.994	0.994
ΔF_{BL}	300.92	299.0	380.35	380.35
$\eta_{overall}$	0.969	0.965	0.966	0.966
I_{sp} delivered	462.5	460.6	467.6	469.3
		(Ref. 26) 456.2*		(Ref. 27) 473.0

*Includes dump cooled nozzle loss and η_{NOZ} = 0.982

SECTION V

SUBSYSTEM EVALUATION

A. OBJECTIVES AND GUIDELINES

Analyses were conducted for the four major subsystems of the plug cluster engine to determine the configurations, operating conditions, and weights that must be considered for the complete engine system analysis. The subsystems analyzed are:

- Base Pressurization
- Engine Cooling (Thruster Module and Base Region)
- Turbomachinery and Power
- Thrust Vector Control

The extent of the subsystem analysis was carried out only to determine the effect on engine performance limitations imposed on engine design, and to define the geometry for the subsequent weight estimates.

The design point for the plug cluster engine evaluation was assumed to be that given in Table I, commensurate with the baseline Space Tug requirements. Upon completion of the analysis, the selected configurations and associated rationale were reviewed with the NASA LeRC Project Manager to select the specific configurations to be carried into the conceptual design phase.

B. ENGINE CYCLE ANALYSIS

Candidate cycles that were evaluated include expander topping and gas generator cycles (Figures 61 to 70). Parallel turbine arrangements and single turbine arrangements with a direct-drive fuel pump and a gear-driven oxidizer pump were compared. The cycle analysis was conducted utilizing a preliminary version of the 66.7 kN (15,000 pound) thrust plug cluster engine at the baseline design point (Table XX). Conclusions derived for the design point are essentially applicable for the thrust levels (between 44.5 kN and 111.2 kN [10,000 and 25,000 pounds force]) under consideration and for chamber pressures to 34 atm (500 psia).

TABLE XX. PLUG CLUSTER ENGINE BASELINE DESIGN POINT

Vacuum Thrust	66,723 N (15,000 lbf)
Chamber Pressure	20.4 atm (300 psia)
Mixture Ratio	6
Engine Area Ratio	∿400
Number of Modules	10

The expander topping cycle is basically a closed cycle because the turbine flow can be included in the main chamber flow. A small portion (about 0.2%) is directed through the nozzle base to maximize the base pressure thrust contribution. The gas generator cycle is an open cycle. The turbine

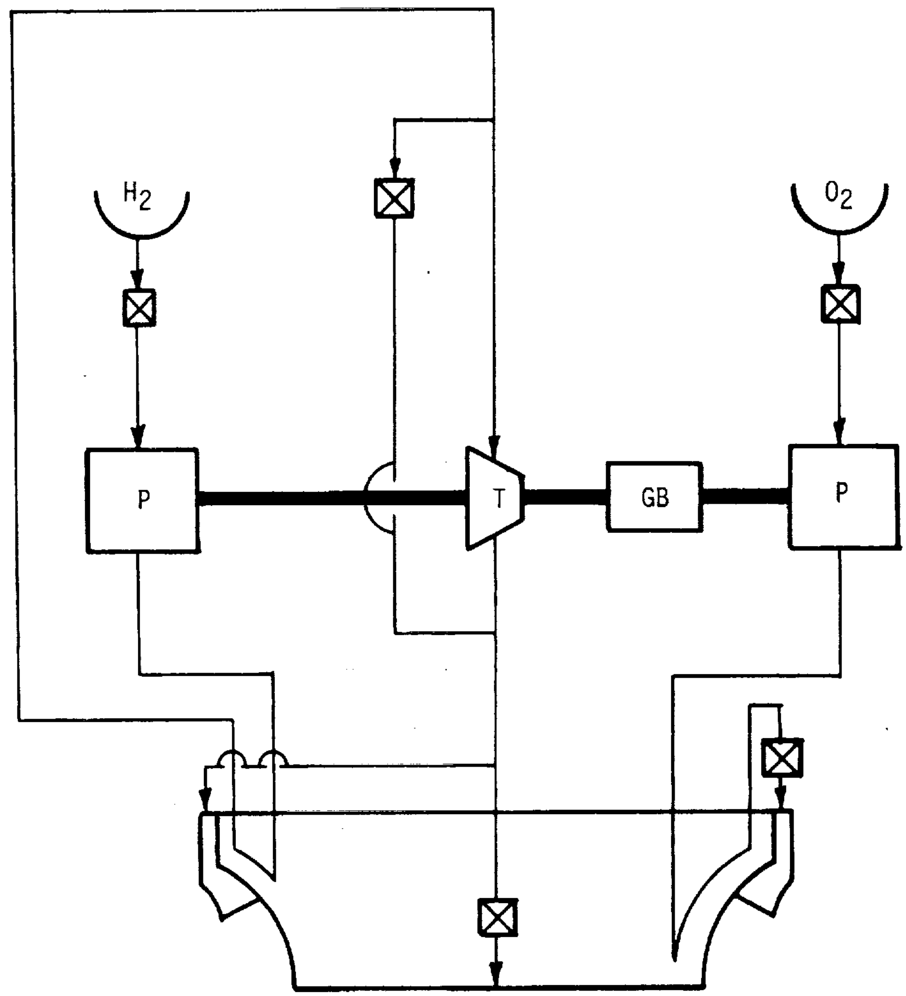

Figure 61. Cycle EX01: Expander Topping Cycle, H_2-Cooled TCA, O_2-Cooled Plug, Single Turbine TPA, Base Pressurization with H_2

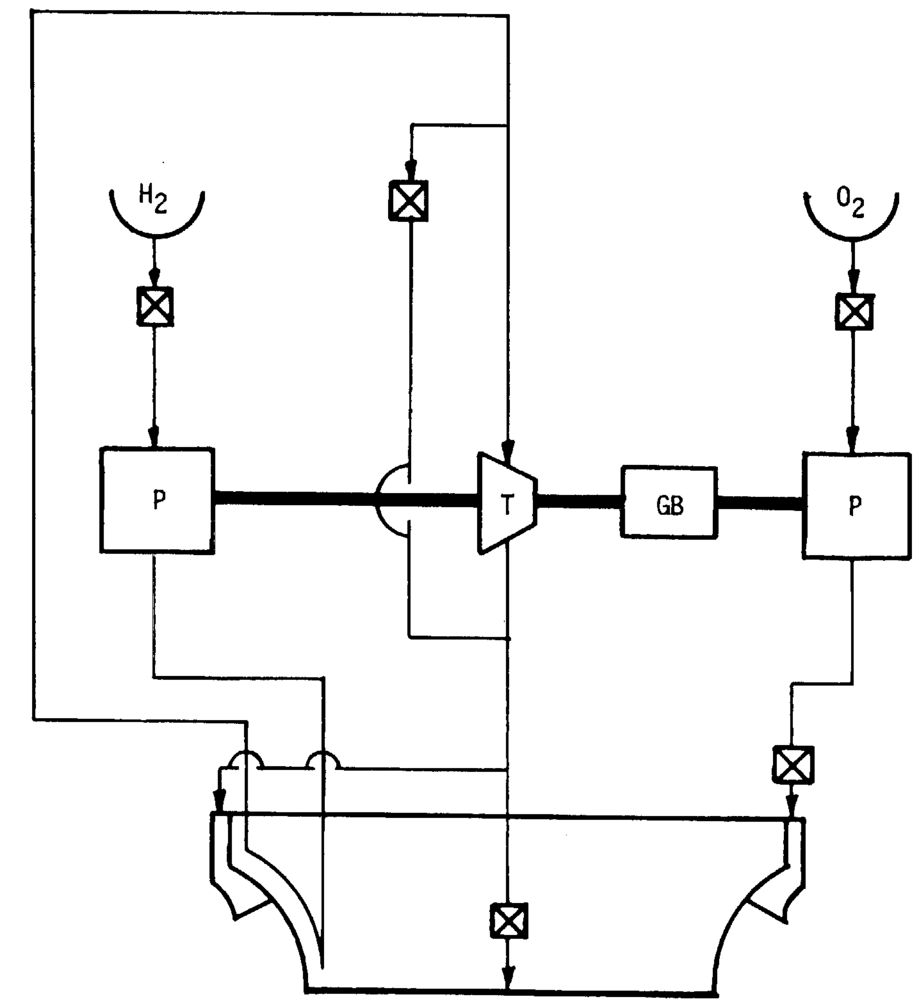

Figure 62. Cycle EX02: Expander Topping Cycle, H_2-Cooled TCA, H_2-Cooled Plug, Single Turbine TPA, Base Pressurization with H_2.

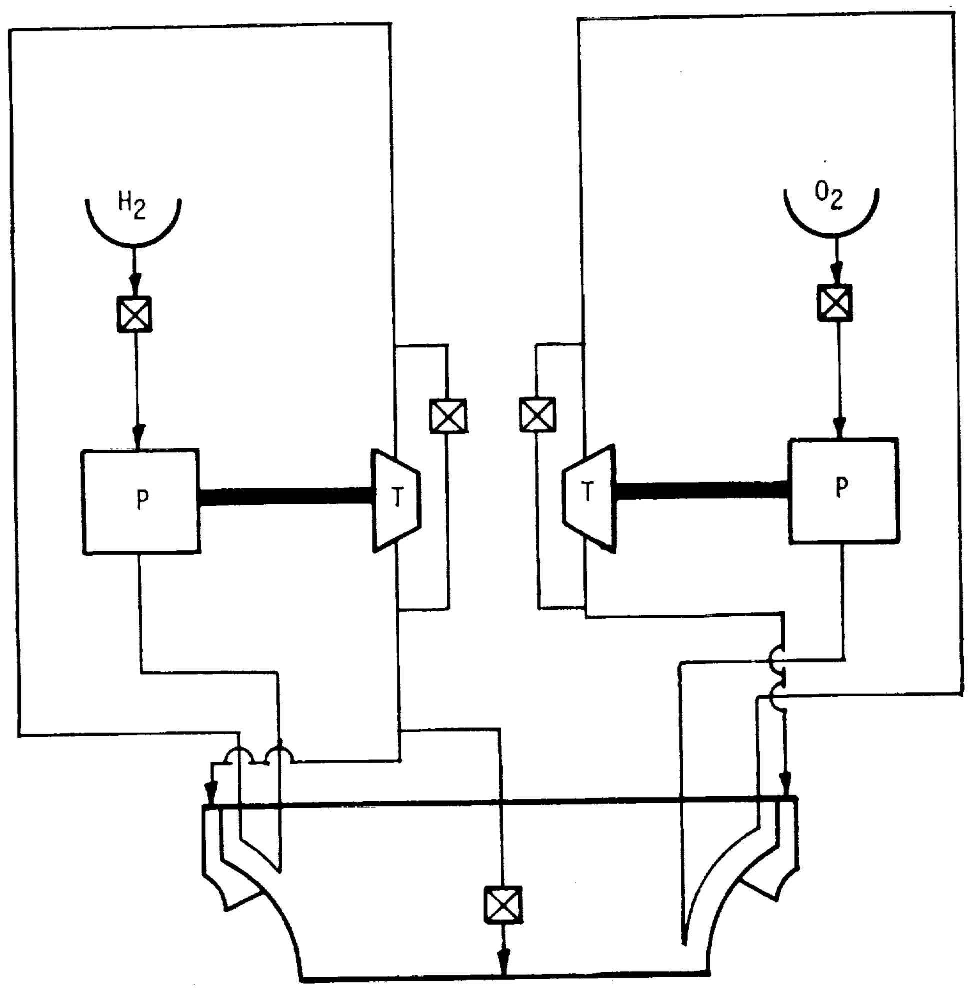

Figure 63. Cycle EX03: Expander Topping Cycle, H_2-Cooled TCA, TPA with Separate Gas Driven Turbine, Base Pressurization with H_2

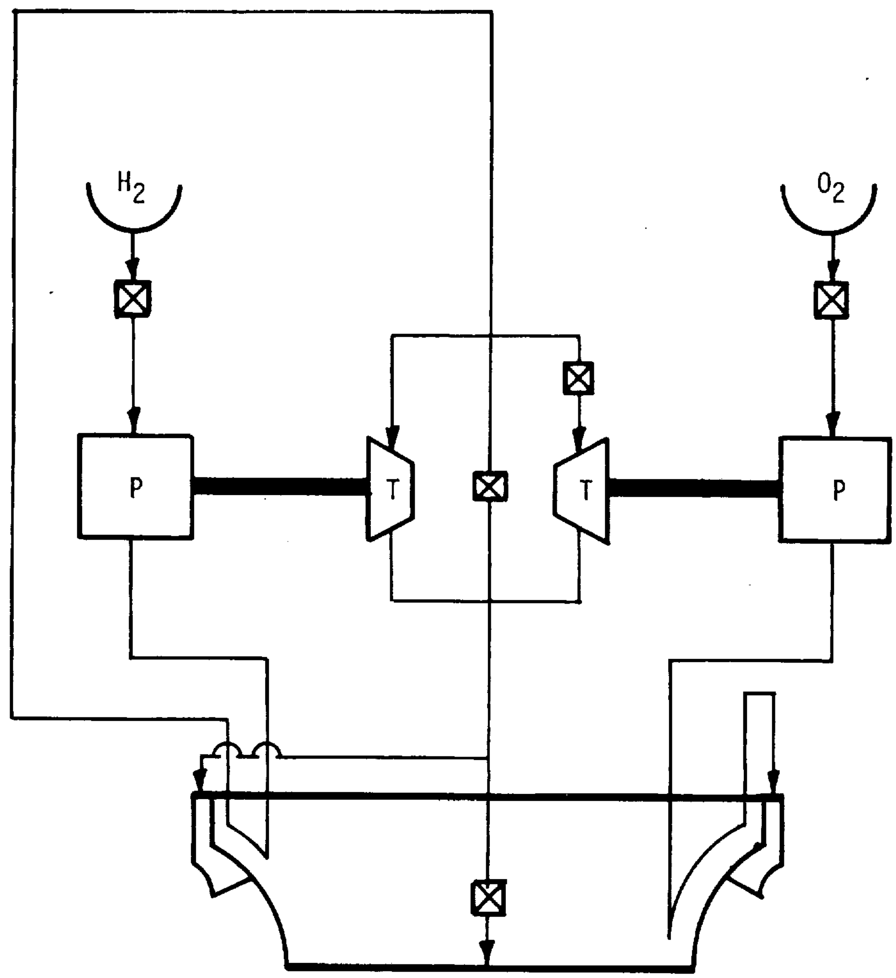

Figure 64. Cycle EX04: Expander Topping Cycle, H_2-Cooled TCA, O_2-Cooled Plug, Parallel Turbine TPA, Base Pressurization with H_2

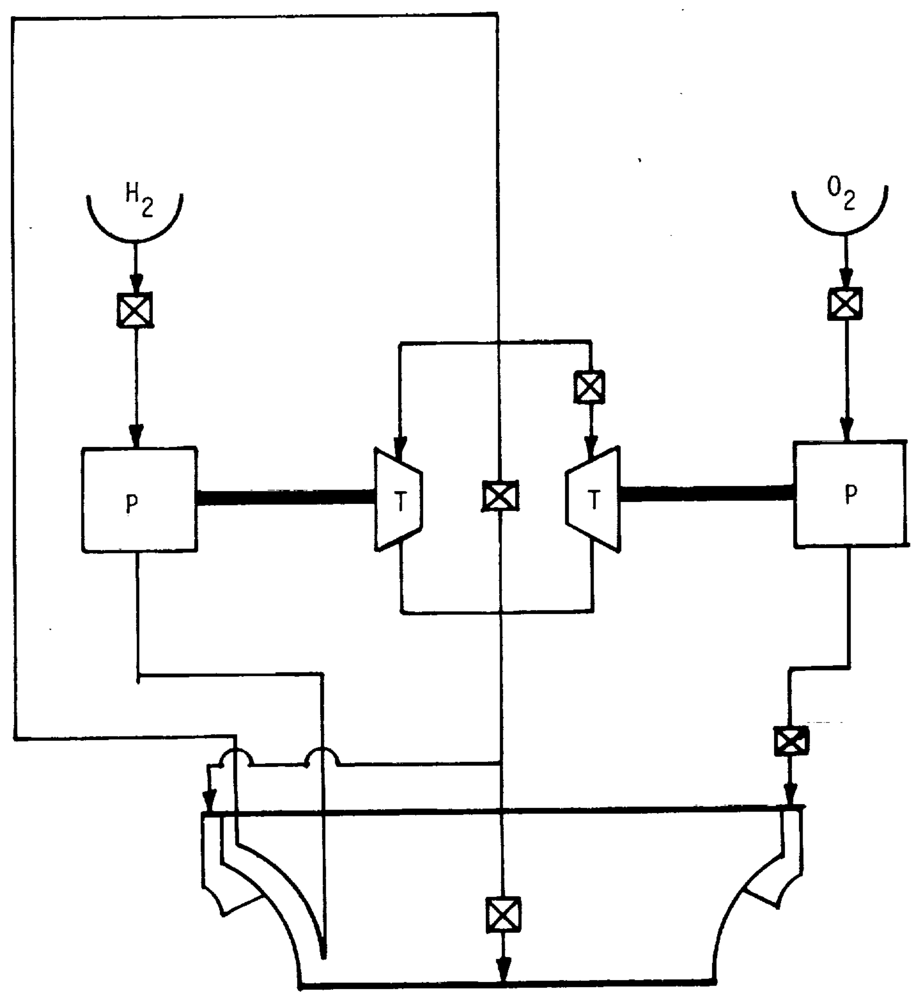

Figure 65. Cycle EX05: Expander Topping Cycle, H_2-Cooled TCA, H_2-cooled Plug, Parallel Turbine TPA, Base Pressurization with H_2.

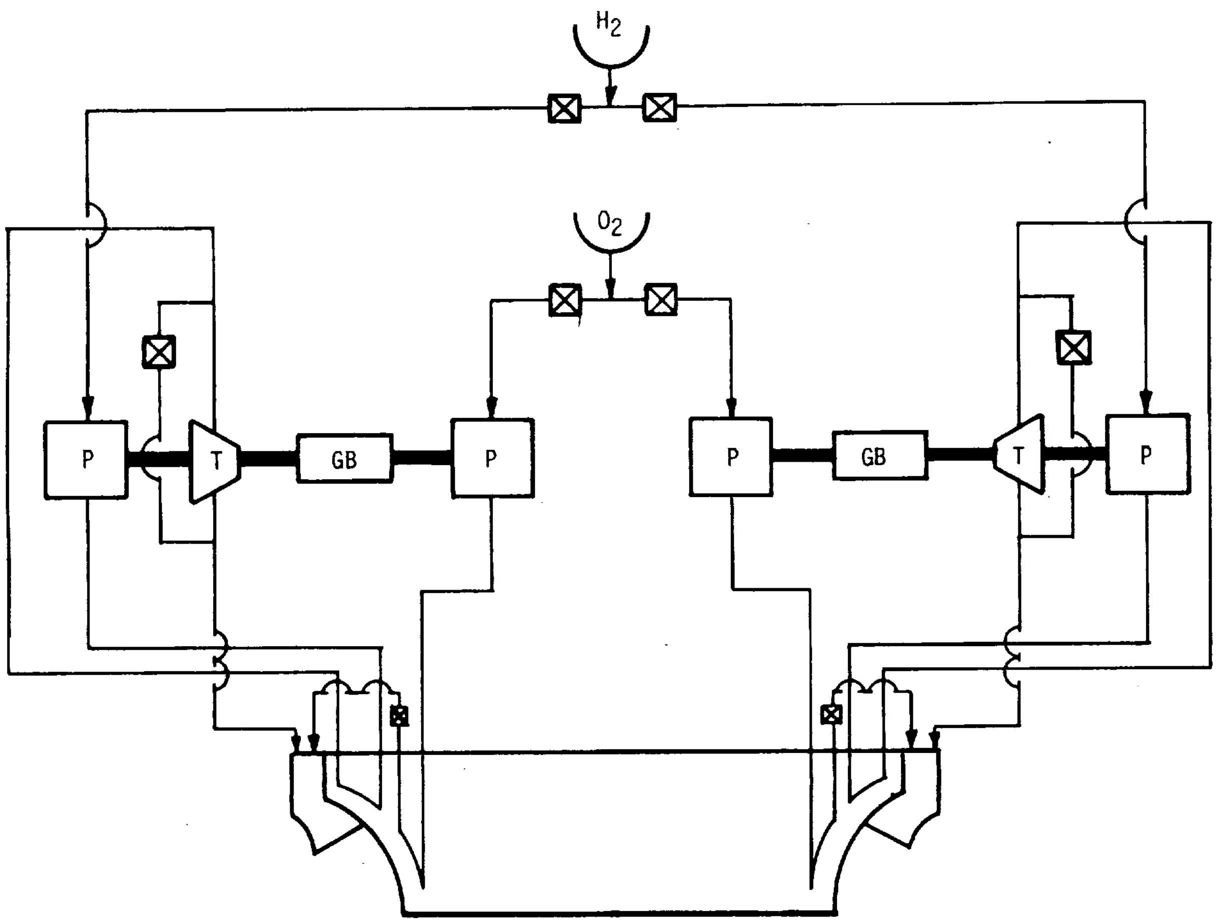

Figure 66. Cycle EX11A: Expander Topping Cycle, H_2-Cooled TCA, O_2-Cooled Plug, Dual Single Turbine TPAs, Base Pressurization with H_2 (Not Shown)

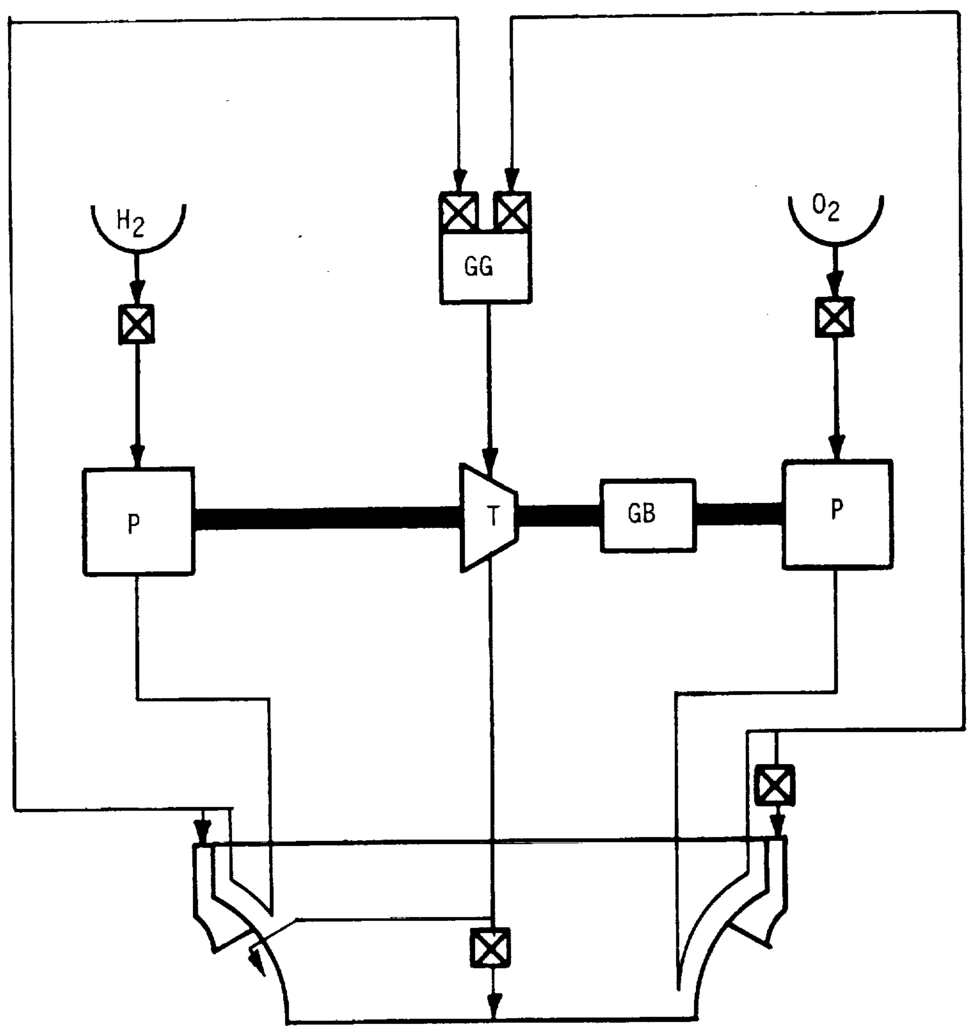

Figure 67. Cycle GG01: Gas Generator Cycle, H_2-Cooled TCA, O_2-Cooled Plug, GG Exhaust on Plug, Single Turbine TPA, Base Pressurization With Partial GG Exhaust.

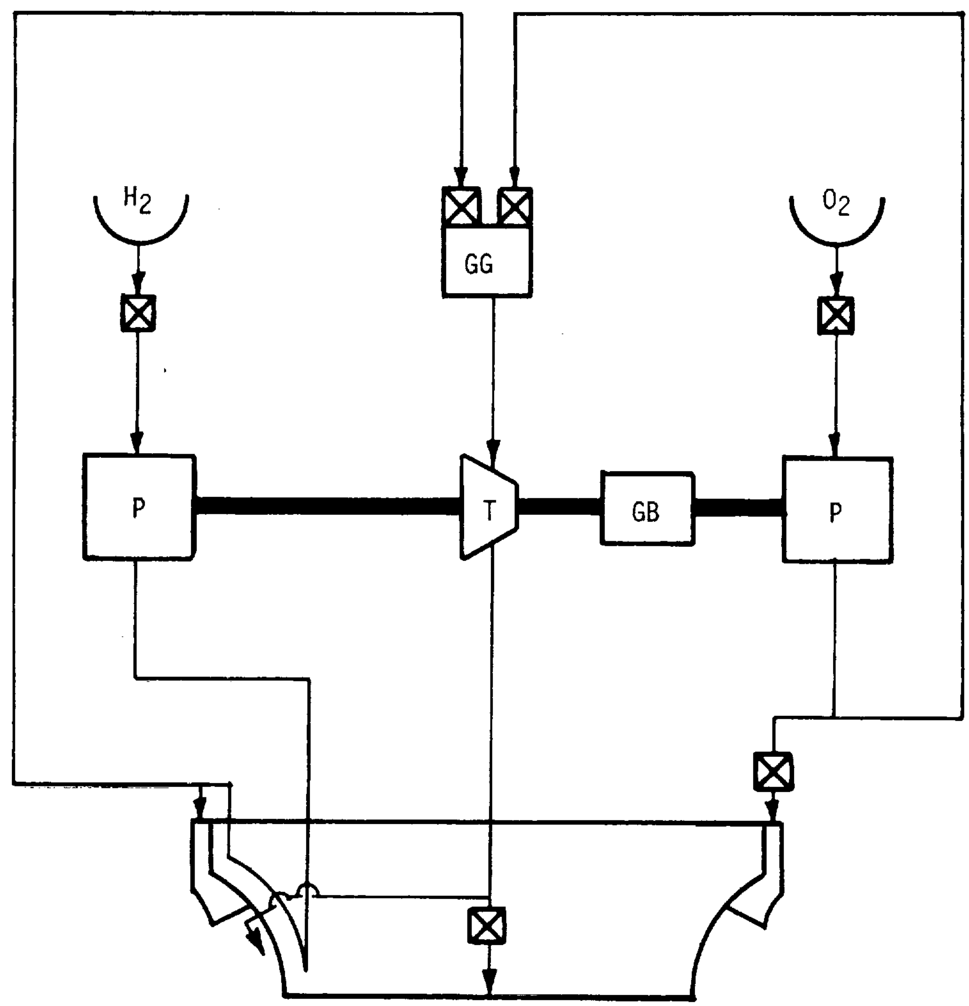

Figure 68. Cycle GG02: Gas Generator Cycle, H_2-Cooled TCA, H_2-Cooled Plug, GG Exhaust on Plug, RL10 TPA, Base Pressurization with Partial GG Exhaust.

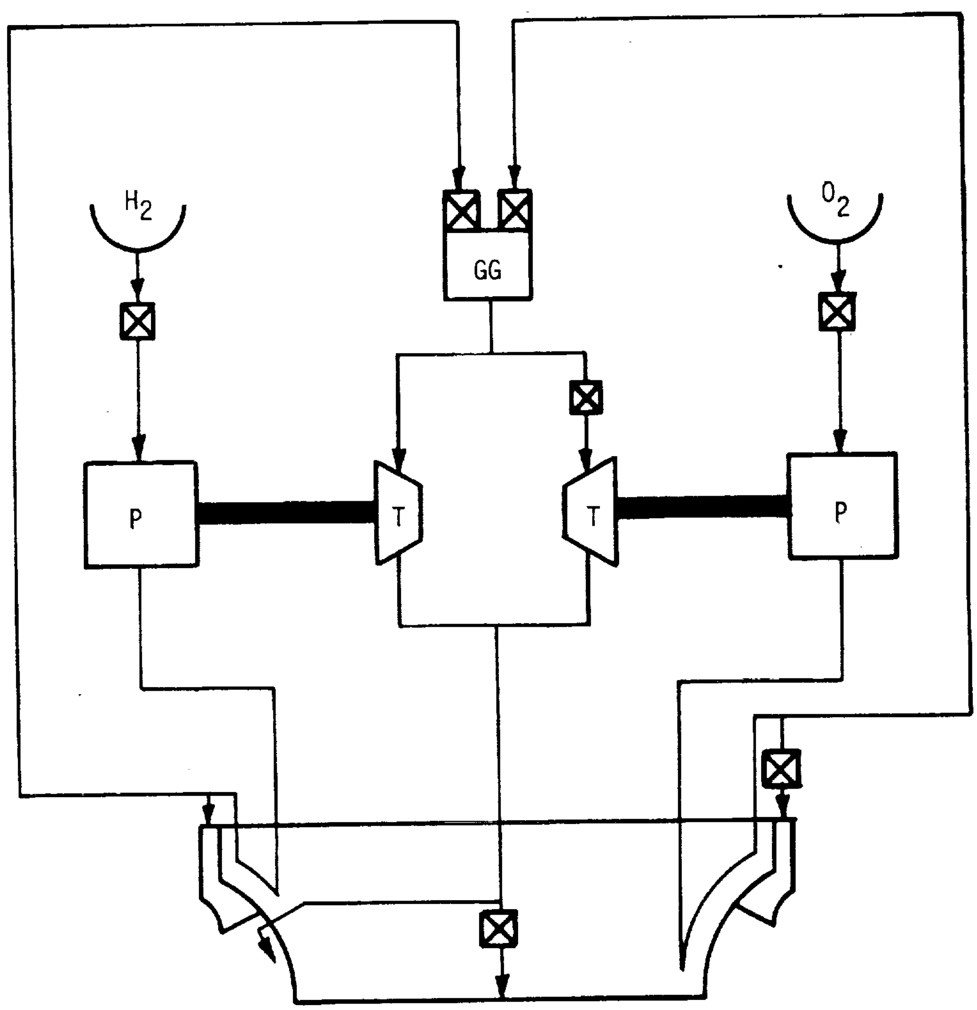

Figure 69. Cycle GG03: Gas Generator Cycle, H_2-Cooled TCA, O_2-Cooled Plug, GG Exhaust on Plug, Parallel Turbine TPA, Base Pressurization With Partial GG Exhaust.

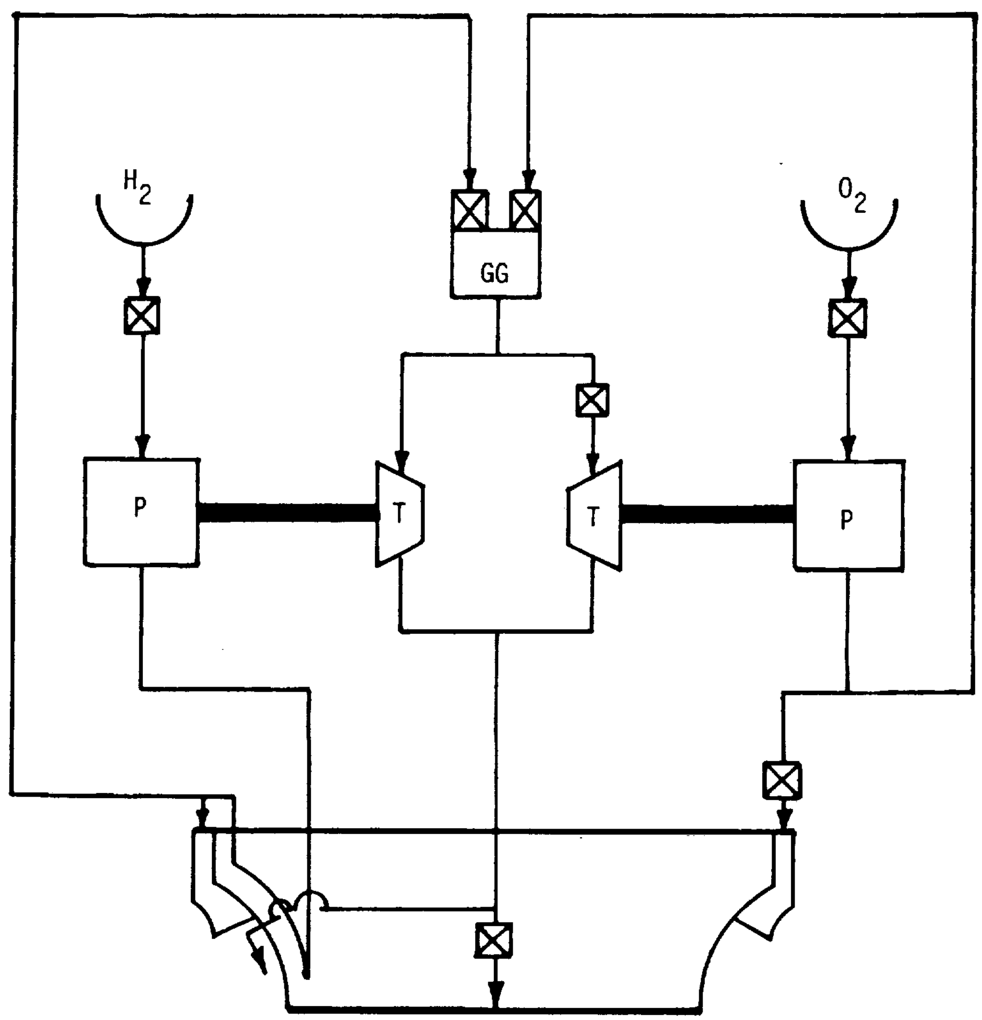

Figure 70. Cycle GG04: Gas Generator Cycle, H_2 Cooled TCA, H_2-Cooled Plug, GG Exhaust on Plug, Parallel Turbine TPA, Base Pressurization With Partial GG Exhaust

exhaust flow is greater than the optimum base flow required for base pressurization with the result that the majority of the flow is dumped from the engine, producing a low thrust contribution. Since the chamber pressure is relatively low for the plug cluster engine, the turbine flow rate, which is determined by the turbomachinery requirements, is relatively small, such that the thrust loss is only on the order of 0.6%. A portion of this loss can be regained by dumping the gases on the plug in the gaps between the module exits.

In the expander cycle, turbine power is derived from passing most of the hot hydrogen (and hot oxygen in some variations) from a cooling jacket through low pressure ratio turbines. A control reserve can be obtained when 5 to 20% of the available turbine flow bypasses the turbine. The combined hydrogen flow, minus a small amount (0.2%) providing base pressurization, is injected into the main combustion chamber.

Several types of expander cycles were examined. Cycle EX01, depicted in Figure 61, represents a plug cluster engine utilizing an RL10 type turbopump assembly (TPA). Note that hydrogen is used to cool the modules, and oxygen the plug and base. A discussion concerning modification of this pressure schedule to best utilize an existing RL10 TPA is presented in the next section (Section V.C.). The pump discharge pressures are 34.0 and 39.5 atm (500 and 580 psia) for the oxygen and hydrogen pumps, respectively.

Cycle EX02, shown in Figure 62, is identical to that in Figure 61 except that hydrogen replaces oxygen as the plug coolant. The pump discharge pressures are 26.8 and 43.2 atm (394 and 635 psia) for the oxygen and hydrogen pumps. This cycle was one of those selected for conceptual design study. The pressure schedule for a baseline engine, utilized in the preliminary cycle evaluations, is given in Table XXI.

Cycle EX03 (Figure 63) with oxygen and hydrogen pump discharge pressures of 40.5 and 35.7 atm (595 and 525 psia) utilizes both hot hydrogen and hot oxygen-driven turbines. The feasibility of obtaining sufficient heat input to the oxygen at the baseline pressure conditions, and at a short plug length, is marginal, as discussed in Section V.D. on engine cooling. This cycle, and those depicted in Figures 64 and 65 offer the potential of lighter weight turbomachinery. Cycle EX05 (Figure 65) was selected for further design analysis.

An expander cycle configuration, utilizing two TPAs, is shown in Figure 66. This cycle provides an approach to a fail-operational mode as opposed to a fail-safe failure mode designated for the single engine baseline Space Tug. Each TPA of Cycle EX11A delivers propellant to one-half of the modules. The propulsion system, therefore, has the capability of operating at full thrust (all modules firing), at 50% thrust (one-half of the modules firing), or at in-between thrust levels, depending upon the throttle capability of the final design. Failure of component(s) in one TPA-fed subsystem would allow a minimum of 50% thrust capability for the Space Tug to return to a service station for repair. Since a weight penalty would be associated with Cycle EX11A, it is included here only to show a further potential that a module cluster can offer.

TABLE XXI - CYCLE EX02 PRELIMINARY PRESSURE SCHEDULE

Pressure, atm (psia)	O_2	H_2
Main Pump Discharge	26.8 (394)	43.2 (635)
ΔP Line (2%)	0.5 (8)	0.9 (13)
ΔP Plug Coolant Jacket	--	3.4 (50)
Plug Coolant Jacket Outlet	--	38.9 (572)
ΔP Line (1%)	--	0.3 (5)
ΔP Fuel Shutoff Valve (1%)	--	0.3 (5)
Valve Outlet	--	38.2 (561)
Orifice Outlet	--	37.7 (554)
Coolant Jacket Inlet	--	36.5 (537)
ΔP Coolant Jacket	--	6.7 (98)
Coolant Jacket Outlet	--	29.6 (435)
ΔP Line (1%)	--	0.3 (4)
Turbine Inlet	--	29.3 (431)
ΔP Turbine (Total to Static)	--	4.9 (72)
Turbine Outlet	--	24.4 (359)
ΔP Line (1%)	0.3 (4)	0.3 (4)
Shutoff Valve Outlet (1%)	26.0 (382)	24.0 (352)
Orifice Outlet	23.8 (350)	23.7 (348)
Main Injector Inlet	23.1 (340)	22.9 (337)
ΔP Injector (10%)	2.7 (40)	2.5 (37)
Chamber Pressure	20.4 (300)	

In the gas generator cycles shown in Figures 67-70, a small amount of propellant (about 1% of the engine flowrate) is burned in a gas generator to power high pressure ratio turbines. The mixture ratio is selected to give a gas temperature of about 922°K (1660°R) (MR = 0.7 to 0.9, depending upon the heat input to the propellants in the cooling circuit). In the cases evaluated, the required turbine flowrate exceeds the optimum base pressurization flowrate (0.2%) by a factor of five.

Cycle GG01, depicted in Figure 67, represents a plug cluster engine utilizing an RL10 type TPA. The oxygen and hydrogen pump discharge pressures are 33.9 and 27.7 atm (498 and 407 psia), respectively.

In Cycle GG02, shown in Figure 68 hydrogen is used as the coolant for both modules and plug, with oxygen and hydrogen pump discharge pressures of 27.1 and 31.8 atm (398 and 467 psia). This cycle was selected for conceptual design analysis. A Typical pressure schedule for this cycle is given in Table XXII (next page).

In Cycles GG03 and GG04, Figures 69 and 70, a lighter weight parallel turbine arrangement is utilized. Cycle GG04 was one of the all hydrogen-cooled cycles selected for further study.

1. Cycle Analysis Summary

The results of the cycle analysis are presented in Table XXIII and XXIV. There appear to be no limitations in the power balance for the regeneratively cooled plug and modules, even at chamber pressures to 34 atm. However, no expander cycle power balance was possible for an ITA module with an expansion ratio of $\varepsilon_M = 100$. This was due to the lack of sufficient LH_2 coolant temperature rise in the shortened plug and the chamber portion of the module.

TABLE XXIII. CYCLE ANALYSIS SUMMARY

Cycle	EX02 Regen-Cooled	EX02 ITA (16% FFC)	GG04 Regen-Cooled	GG04 ITA (16% FFC)
Pc atm	20.4	20.4	20.4	20.4
ε_M	40	40	40	40
Is sec	467.4	454.9	466.8	454.4
ΔIs sec	0	0	0.6 (0.13%)	0.5 (0.10%)
$\dot{w}_{GG}$	0	0	0.38	0.36
Pc atm	34.0	Not Calculated	34.0	34.0
ε_M	40		40	40
Is sec	471.1		470.1	457.7
ΔIs sec	0		1.0 (0.21%)	0.8 (0.17%)
$\dot{w}_{GG}$	0		0.57	0.57
Pc atm	20.4	20.4	20.4	Not Calculated
ε_M	100	100	100	
Is sec	469.2	No Power Balance	468.5	
ΔIs sec	0		0.7 (0.15%)	
$\dot{w}_{GG}$	0		0.40	

TABLE XXII - CYCLE GG02 PRELIMINARY PRESSURE SCHEDULE

Pressure, atm (psia)	TCA		GG	
	O_2	H_2	O_2	H_2
Main Pump Discharge	27.1 (398)	31.8 (467)	27.1 (398)	31.8 (467)
ΔP Line (2%)	0.5 (8)	0.6 (9)	0.5 (8)	0.6 (9)
ΔP GG Valve (10%)	--	--	2.7 (39)	3.1 (46)
Valve Outlet	--	--	23.9 (351)	28.0 (412)
GG Inlet	--	--	23.2 (341)	25.7 (377)
ΔP GG (10%)	--	--	2.3 (34)	4.8 (70)
Turbine Inlet	--	--	20.9 (307)	
ΔP Turbine (Total to Static)	--	--	17.9 (263)	
Turbine Outlet	--	--	3.0 (44)	
ΔP Line (20%)	--	--	0.6 (9)	
Plug Dump	--	--	2.4 (35)	
ΔP Shutoff Valve (2%)	0.5 (8)	--		
Valve Outlet	26.0 (382)	--		
Orifice Outlet	23.8 (350)	--		
Plug Coolant Jacket Inlet	--	31.2 (458)		
ΔP Plug Jacket	--	3.4 (50)		
Plug Coolant Jacket Outlet	--	27.8 (408)		
ΔP Line (1%)	--	0.3 (4)		
Fuel Shutoff Valve Inlet	--	27.5 (404)		
ΔP Shutoff Valve (1%)	--	0.3 (4)		
Valve Outlet	--	27.2 (400)		
Coolant Jacket Inlet	--	26.7 (392)		
ΔP Module Coolant Jacket	--	2.7 (40)		
Coolant Jacket Outlet	--	24.0 (352)		
Orifice Outlet	--	23.7 (348)		
Main Injector Inlet	23.1 (340)	22.9 (337)		
ΔP Injector (10%)	2.7 (40)	2.5 (37)		
Chamber Pressure	20.4 (300)			

TABLE XXIV - CYCLE ANALYSIS SUMMARY DATA

PARAMETER	GG01	GG02	EX01	EX02	EX02	EX02	EX02	GG04	GG04	GG04	ITA EX02	GG04
Chamber Pressure, psia	300	→					500	300	300	500	300	300
Module Area Ratio	40	→				100	40	40	100	40	40	40
Vacuum Specific Impulse, sec	466.8	466.8	467.4	467.4	467.4	469.2	471.1	466.8	468.5	470.1	454.9	454.4
LH_2 Pump Discharge Pressure, psia	407	467	580	635	540	555	982	410	426	727	656	405
LO_2 Pump Discharge Pressure, psia	498	398	500	394	400	400	640	400	400	640	400	400
Turbine Inlet Pressure, psia	314	307	432	431	464	463	812	96	95	95	584	95
Turbine Inlet Temperature, °R	1660	1660	474	500	677	721	485	1660	1660	1660	188	1660
Turbine Pressure Ratio	7	7	1.2	1.2	1.3	1.3	1.4	5.9	5.9	5.9	1.6	5.9
Turbine Flow Rate, lb/sec	0.29	0.31	5.15	5.15	2.32	2.24	4.94	0.38	0.40	0.57	5.6	0.36
% Turbine Bypass	0	→			57	58	8	0	0	0	0	0
Turbine Efficiency	0.60	0.60	0.71	0.71	→			0.32/0.62	0.32/0.62	0.32/0.62	0.71	0.32/0.62
LH_2 Pump Efficiency	0.52	→						0.75	0.75	0.75	0.52	0.75
LO_2 Pump Efficiency	0.62	→						0.68	0.68	0.68	0.62	0.68
LH_2 Coolant ΔP, psi	38	90	102	148	65	82	152	65	82	152	60	60
LO_2 Coolant ΔP, psi	100	0	100	0	0	→						

C. TURBOMACHINERY ANALYSIS

The turbomachinery selection and design studies were conducted by giving consideration to the following system capabilities:

- Idle mode engine firing to provide thrust for propellant settling in the tanks and thermal conditioning (chill) of the propellant feed system.

- Two-phase flow pumping capability in both oxidizer and fuel pumps.

These capabilities are essentially the same as those provided by the RL10 derivative IIA configuration. The existing RL10 TPA, however, has a 5-hour life limit.

1. RL10 IIA Turbopump Assembly Analysis

The fuel and oxidizer pump performance curves used for RL10 derivative IIA turbopump performance predictions are shown in Figures 71 and 72. The turbine flow parameter is shown in Figure 73.

These curves were constructed utilizing the information in Reference 14 Appendices. Application of this pump to the various plug cluster engine cycles requires certain modifications, which are outlined in the following.

- Cycle EX01

A modified RL10 derivative IIA turbopump was selected for this engine. The modification consists of a 10% reduction in fuel pump head coefficient accomplished by impeller trimming. No changes are anticipated in the turbine, the low speed or the high speed oxidizer pump. Cycle power balance was achieved with a turbine speed of 27,850 rpm and a turbine bypass flow of 39% (Fig. 74).

- Cycle EX02

As with Cycle EX01, a modified RL10 derivative IIA turbopump was selected. The turbopump modification consists of a 19% reduction in oxidizer pump head accomplished by trimming the oxidizer impeller. Cycle balance was achieved with a turbine speed of 27,500 rpm and a turbine bypass flow of 40% (Fig. 75). As an alternate, the turbine could be modified by increasing its flow area. This modification would reduce turbine speed and turbine bypass flow. In addition, less trimming of the oxidizer pump would be required.

- Cycle EX11A

The turbomachinery for this cycle either combines scaled versions of the turbopumps selected for Cycle EX01, or represents a plug cluster of double the thrust level. The dual turbopumps provide a redundancy with reduced thrust capability in the event of one turbopump failure

- Cycle GG01

This cycle utilizes a modified RL10 derivative IIA turbopump. A redesigned turbine is required to accommodate the hot combustion products from the gas generator. The fuel pump impellers are trimmed (similar to EX01) or redesigned to provide the required propellant pressures. Heat shields may be required to avoid excessive heat flux into the gearbox.

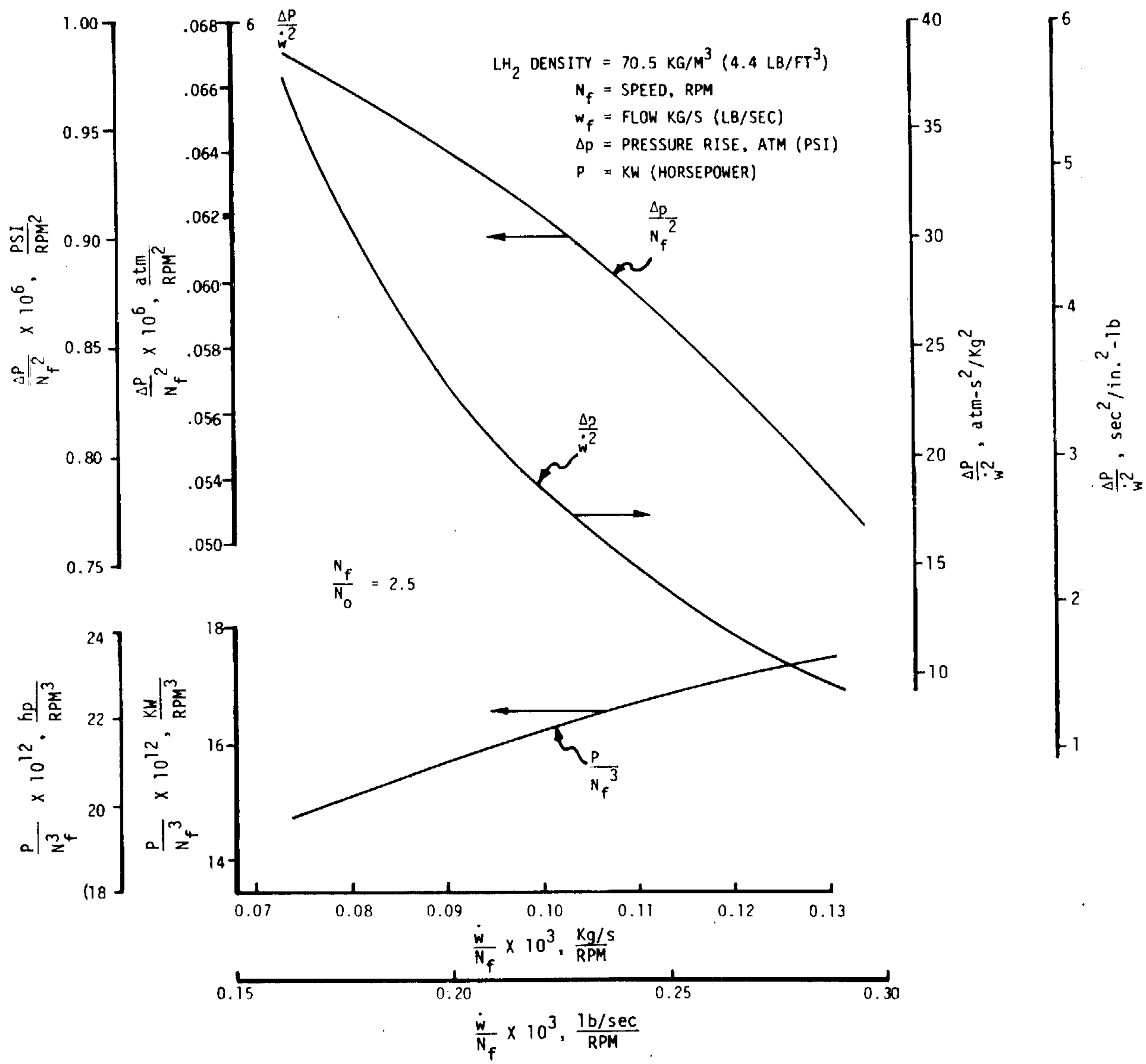

Figure 71. RL10 Derivative IIA Fuel Pump Characteristics.

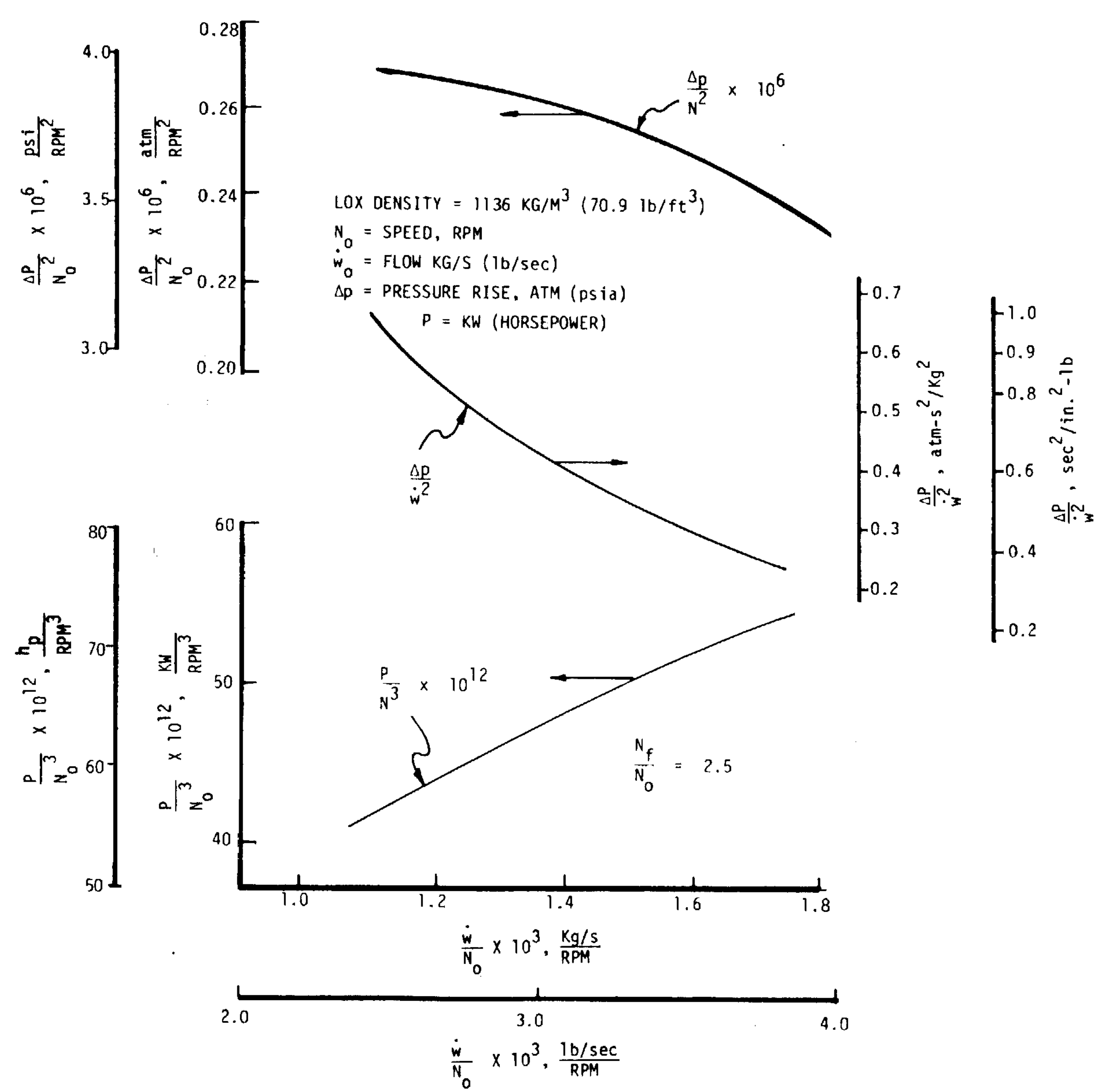

Figure 72. RL10 Derivative IIA and IIB Oxidizer Pump Characteristics.

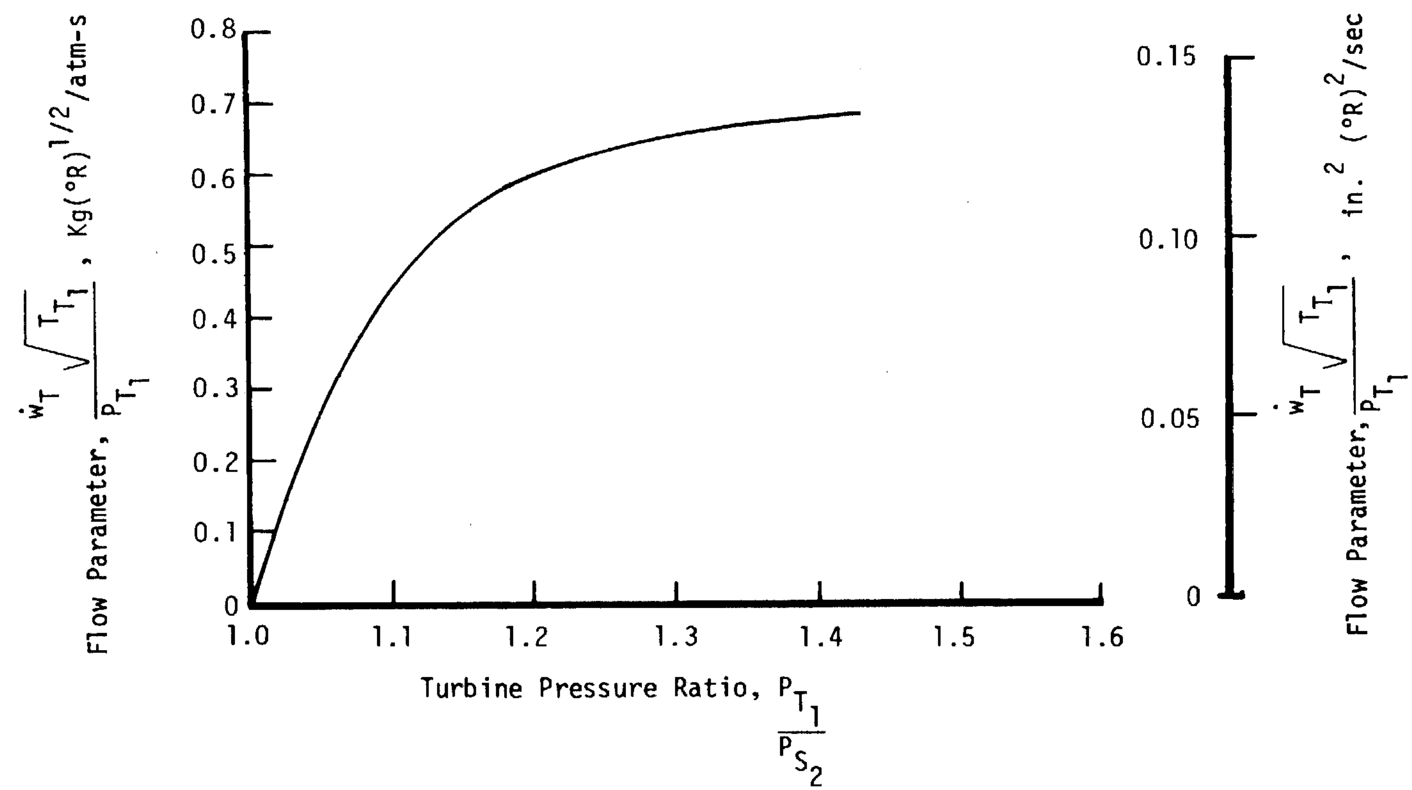

Figure 73. Approximate RL10 Turbine Flow Parameter.

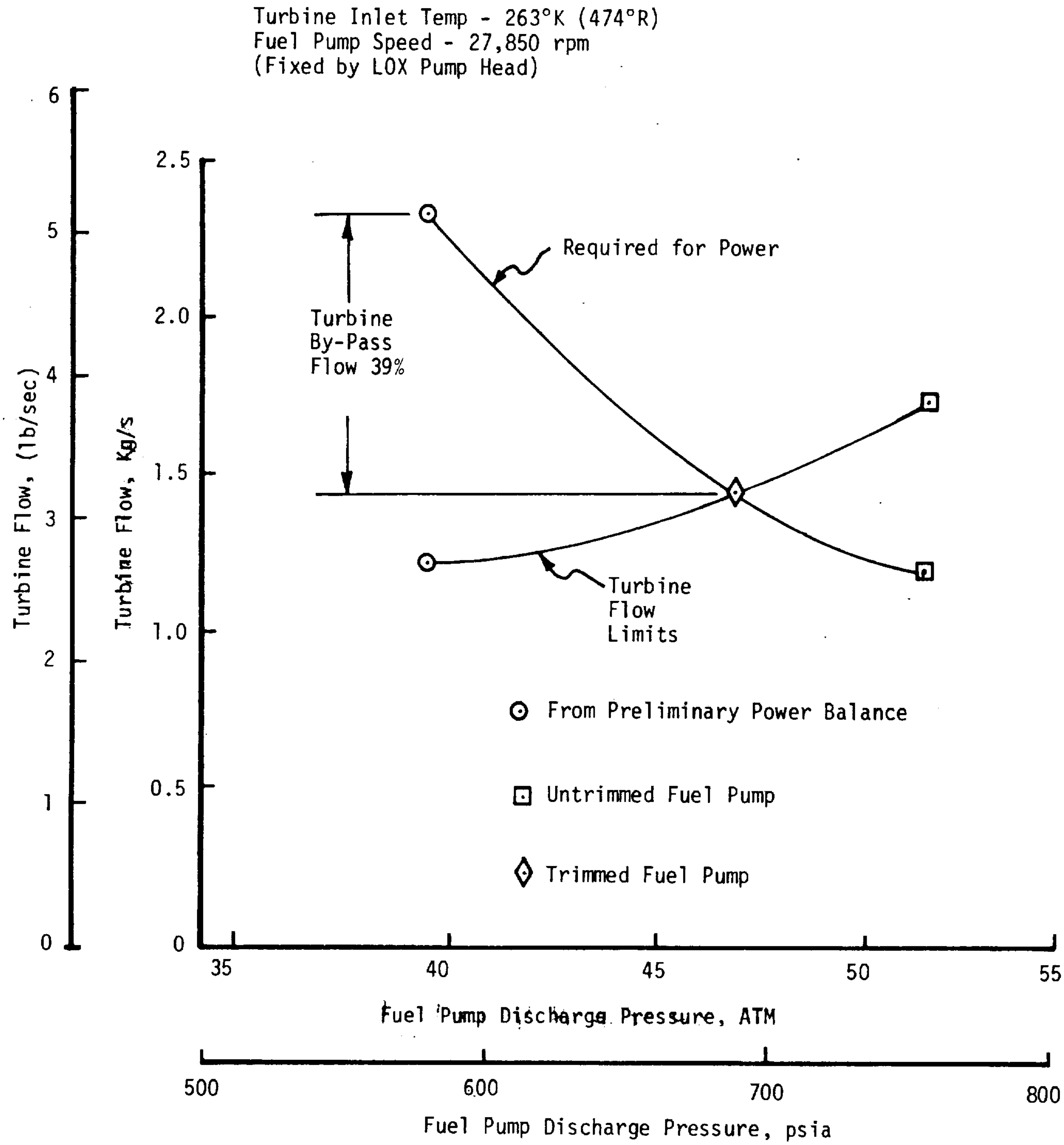

Figure 74. Expander Cycle EX01 Power Balance With RL10 Turbine.

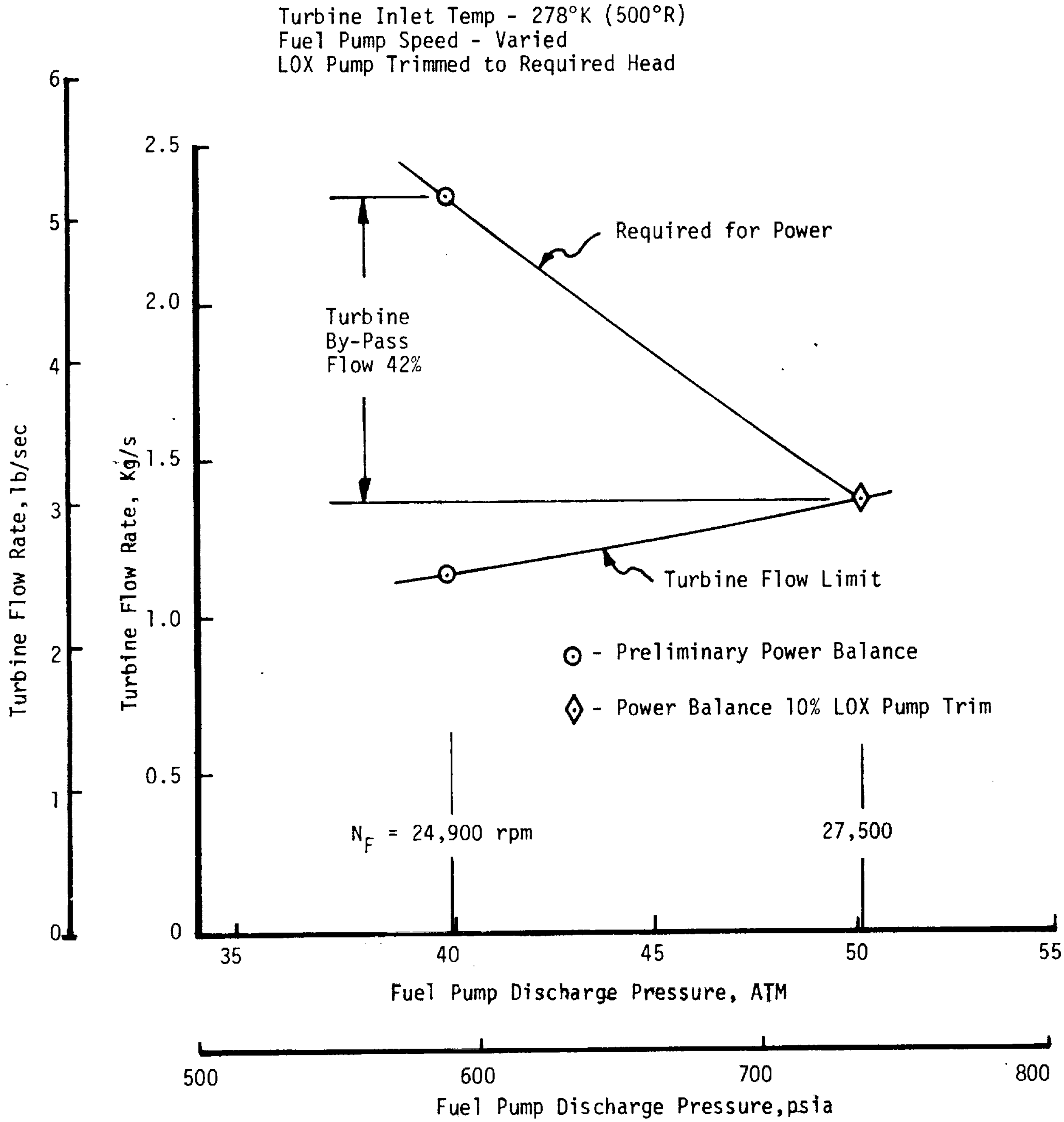

Figure 75. Expander Cycle EX02 Power Balance With RL10 Turbine.

° Cycle GG02

This cycle utilizes a modified RL10 derivative IIA turbopump. As with Cycle GG01, a redesigned hot gas turbine is required. A heat shield may be required to reduce the heat flux to the gearbox.

2. Conceptual Turbopump Design Analysis

Section III,E, established the state-of-the-art of turbopumps required for this application. Utilizing these data and the NASA guidelines from References 21 and 22, pumps were conceptually designed to meet the baseline Space Tug requirements including a 10-hour life expectancy. Table XXV summarizes the design criteria.

The low speed LOX pump consists of a high head inducer driven by a five-stage hydraulic turbine, with the turbine drive fluid being taken from the discharge of the high speed LOX pump. The design parameters are listed in Table XXVI. The nondimensional pump performance map is shown in Figure 76, and the hydraulic turbine efficiency performance is presented in Figure 77. The turbopump cross-section is shown in Figure 78.

It is anticipated that the low speed pump will be cooled to liquid oxygen temperature prior to full speed operation.

The high speed LOX turbopump consists of a full shrouded single stage centrifugal pump driven by a velocity compounded gas turbine such as shown in Figure 70. The shaft is supported by a spring-loaded angular contact ball bearing cooled by liquid oxygen. The design parameters are listed in Table XXVII. The nondimensional pump head-flow and efficiency performance is shown in Figure 79 and the turbine efficiency performance is shown in Figure 80. It is anticipated that the pump will be cooled to liquid oxygen temperature prior to full speed operation. Tank head idle-mode and pump idle-mode are a logical sequence. The turbopump cross-section is shown in Figure 81.

The liquid hydrogen turbopump consists of a fully shrouded single stage centrifugal pump driven by a velocity compounded gas turbine. The pump impeller has an inducer stage designed to provide a zero NPSH pumping capability. The shaft is supported by two sets of spring-loaded angular contact ball bearings. The rotor axial thrust is supported by a self-compensating thrust balance incorporated in the impeller back shroud.

The turbopump design parameters are listed in Table XXVIII. The nondimensional pump head-flow and efficiency characteristics are shown in Figure 79. The drive turbine efficiency is shown in Figure 80. The pump cross-section is shown in Figure 82.

Application of the conceptual turbopump designs to the various plug cluster engine cycles are outlined in the following:

° Cycle EX03

For this cycle, low speed pumps with a hydraulic turbine drive are used for both the oxidizer and fuel to provide two-phase flow pumping capability. The high speed turbopumps incorporate single-stage centrifugal

TABLE XXV - TURBOPUMP DESIGN CRITERIA

GENERAL PUMP REQUIREMENTS

1. Pump Zero Tank NPSH
2. TPA Life Expectancy 10 hours - 1200 Engine Starts

PUMPS

$150\ (1000) < N_s > 600\ (4000)$

$N_s \cong 225\ (1500)$ Preferred

$N_s = \frac{N\sqrt{Q}}{(H)^{3/4}}$ N - rpm
Q - m^3/min (gpm)
H - m (ft)

TURBINES

Full Admission
$A_aN^2 < 258 \times 10^9\ (40 \times 10^9)$ - (Blade Stress Consideration) -
$cm^2 \times rpm^2\ (in^2 \times rpm^2)$ (Ref. 21)

INDUCERS NASA LIMITS

$C_m \cong \sqrt{\frac{(NPSH)\ 2g}{C}}$, $\phi = \frac{C_m}{U_t} > 0.06$

Fluid	C
LOX	2.3
LH_2	1.3

Design Limits S = 3,000 (20,000) - High Speed LOX
= 15,000 (100,000) - High Speed LH_2
= 4,500 (30,000) - Low Speed LOX

$S = \frac{N\sqrt{Q}}{(NPSH)^{3/4}}$
N - rpm
Q - m^3/min (gpm)
NPSH - m (ft)

SHAFTING

$N_{c_1} > 1.5\ N_{Design}$ N_{c_1} - Lowest Shaft Critical Speed

(Watt) $N^2 = \frac{\sigma\ (DN)^3}{4.8 \times 10^5}$, $\sigma <$ 1,361 atm; D - mm, N - rpm (Ref. 22)

[(Horsepower) $N^2 = \frac{\sigma\ (DN)^3}{5.26 \times 10^9}$, $\sigma <$ 20,000 psi]

BEARINGS NASA LIMITS

Fluid	DN Limit
LOX	1.3×10^6
LH_2	2×10^6

D - mm, N - rpm

TABLE XXVI. LOW SPEED LOX TURBOPUMP DESIGN PARAMETERS

<u>PUMP</u> - High Head Inducer

Flow, $\dot{\omega}$ Kg/s (lb/sec) = 14.1 (31)

Pressure Rise, $\frac{N}{m^2}$, (psi) = 0.14×10^6 (20)

Flow, Q $\frac{m^3}{s}$ (gpm) = 0.0122 (193)

Head Rise, m (ft) = 12.2 (40)

Specific Speed = 3500

Design Speed, rpm = 4000

Tip Speed, $\frac{m}{s}$ (ft/sec) = 18.1 (59.4)

Head Coefficient = 0.37

Tip Diameter, cm (in) = 8.64 (3.4)

Efficiency, η = 0.68

NPSH, m (ft) = 0.68 (2.25)

Suction Specific Speed = 30,000

Inlet Flow Coefficient = 0.13

<u>TURBINE</u> - Five-Stage Hydraulic

Flow, $\dot{\omega}$ Kg/s (lb/sec) = 2.77 (6.1)

Pressure Drop $\frac{N}{m^2}$ (psi) = 1.54×10^6 (223)

Flow, Q $\frac{m^3}{s}$ (gpm) = 0.0024 (38.6)

Head, m (ft) = 135 (445)

Pitch Line Velocity m/s (ft/sec) = 9.3 (30.5)

Pitch Diameter cm (in) = 4.39 (1.73)

Blade Height, cm (in) = 0.254 (0.1)

Efficiency, η = 0.66

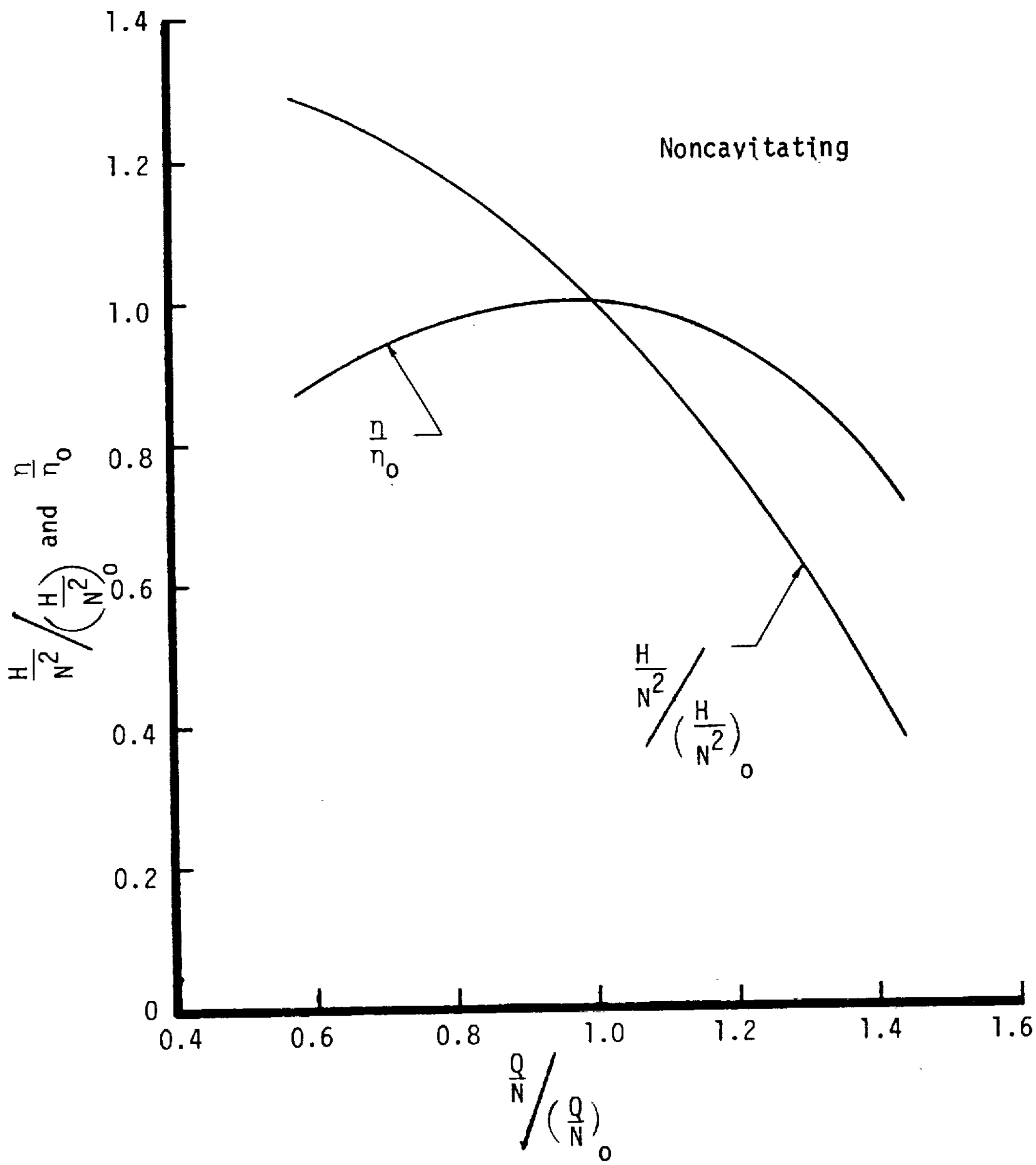

Figure 76. Low Speed LOX Pump Dimensionless Performance Characteristics.

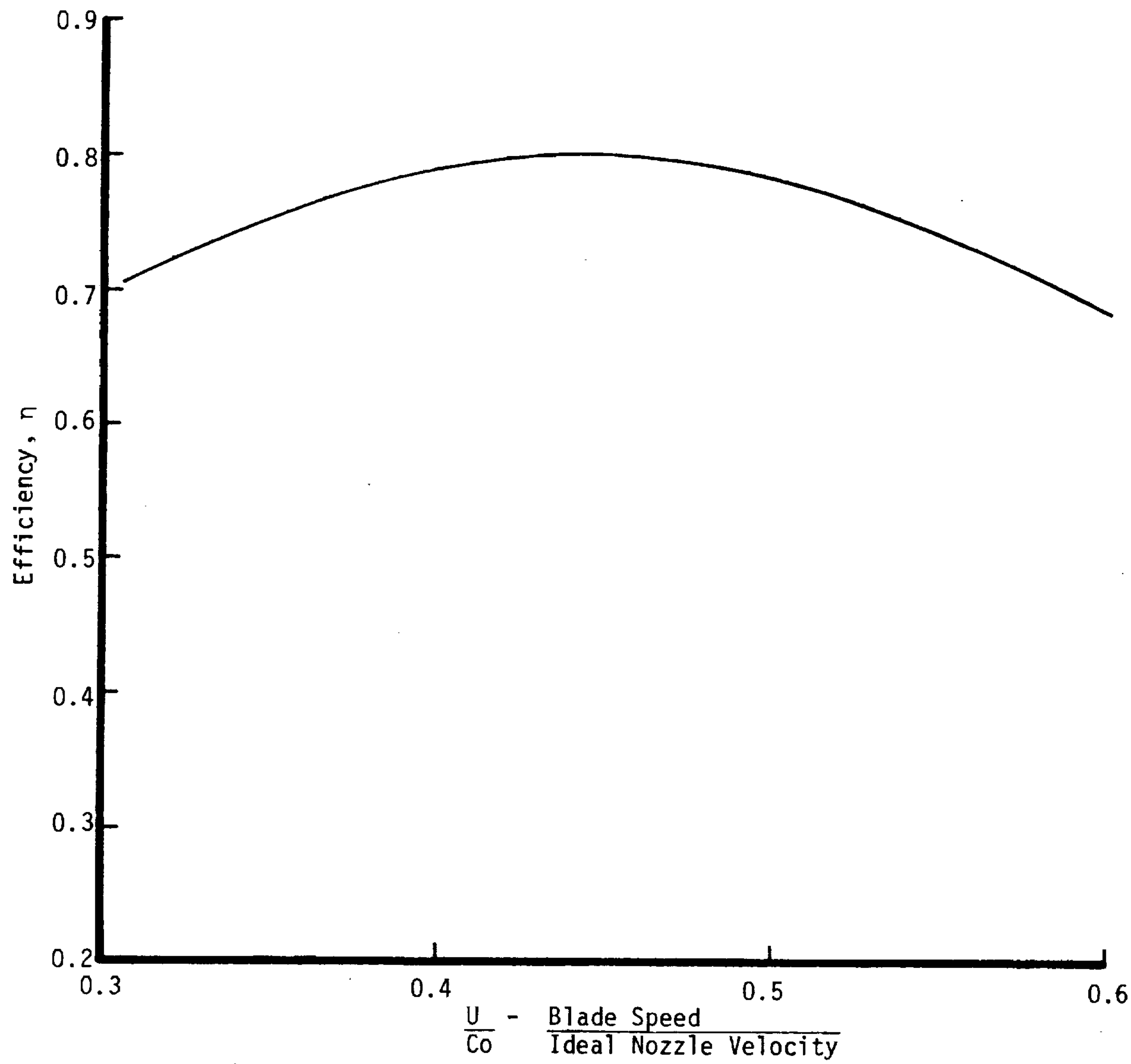

Figure 77. Effect of U/C_o on Turbine Efficiency, Single Impulse Stage.

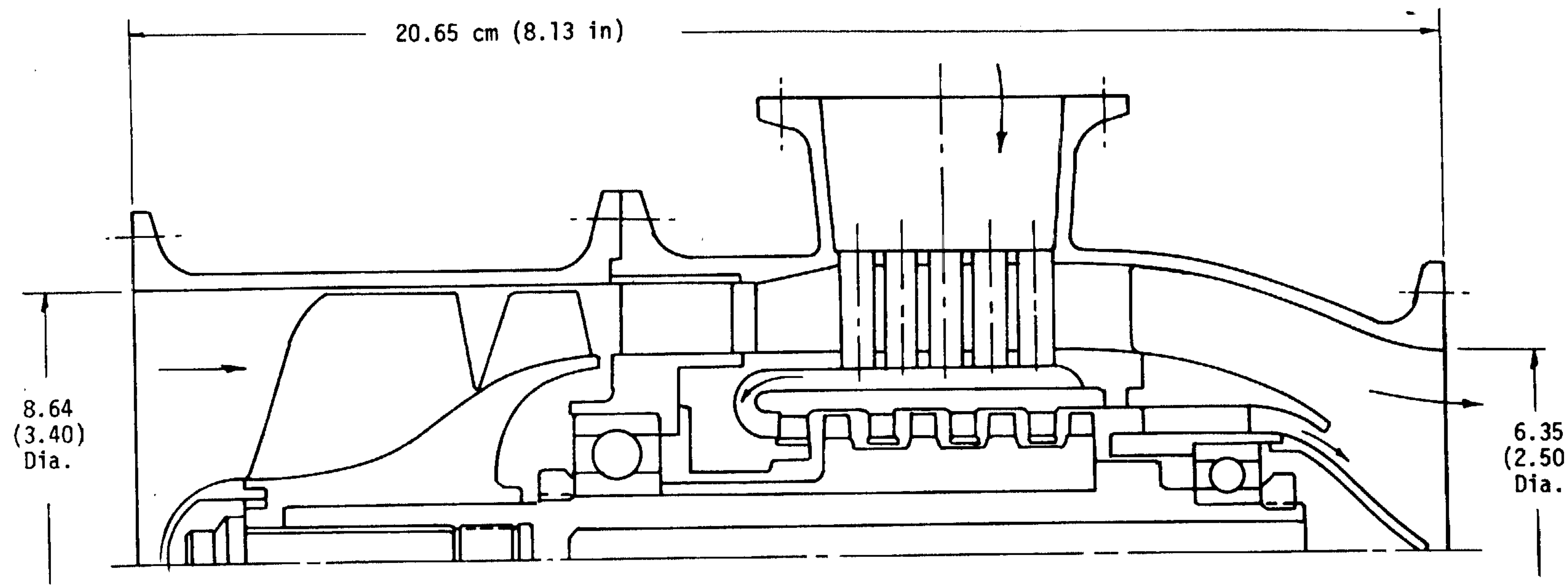

PUMP

Flow - 14.1 Kg/s (31 lb/sec)
Head - 12.2 m (40 ft.)

TURBINE

Flow - 2.77 Kg/s (6.1 lb/sec)
Head - 135 m (445 ft)

N = 4000 RPM

Weight = 1.8 Kg (4 lb)

Figure 78. Conceptual TPA Design, LOX Boost Pump.

TABLE XXVII - HIGH SPEED LOX TURBOPUMP DESIGN POINT PARAMETERS

PUMP - Single Stage Centrifugal (Fully Shrouded)

Flow, $\dot{\omega}$ Kg/s (lb/sec) = 16.83 (37.1)

Pressure Rise, $\frac{N}{m^2}$ (psi) = 3.1×10^6 (450)

Flow, Q $\frac{m^3}{s}$ (gpm) = 0.0146 (231)[1]

Head Rise m, (ft) = 274.3 (900)

Specific Speed, Ns = 1,589

Design Speed, rpm = 17,176

Tip Speed $\frac{m}{s}$ (ft/sec) = 75.3 (247)

Head Coefficient, ψ = 0.475

Efficiency, η = 0.68

Tip Diameter, cm (in) = 8.38 (3.3)

INDUCER

NPSH, m (ft) = 9.37 (31)

Suction Specific Speed, S = 20,000

Tip Diameter cm (in) = 5.00 (1.97)

Tip Speed m/s (ft/sec) = 45.1 (148)

Inlet Flow Coefficient = 0.18

Flow, Q $\frac{m^3}{s}$ (gpm) = 0.0146 (231)

TURBINE

Velocity Compounded - Full Admission

Pitchline Blade Speed, U_m, m/s (ft/sec) = 137 (450)

Pitch Diameter, cm (in) = 15.24 (6)

Inlet Pressure $\frac{N}{m^2}$ (psi) = 0.325×10^6 (47.2)

Inlet Temperature °K (°R) = 922 (1660)

Exit Pressure (static) $\frac{N}{m^2}$ (psi) = 0.109×10^6 (15.8)

Ideal Nozzle Velocity, C_o m/s (ft/sec) = 1936 (6351)

$\frac{U_m}{Co}$ = 0.071

Estimated Efficiency, η = 0.32

Flow Kg/sec, (lb/sec) = 0.11 (0.245)

Exit Annular Area Aa, cm^2 (in^2) = 102 (15.8)

AaN^2, $cm^2 \times rpm^2$ ($in^2 \times rpm^2$) = 30.6×10^9 (4.60×10^9)

BEARINGS

Bore m (in) = 25 (0.984)

DN mm x rpm = 0.429×10^6

SHAFT CRITICAL SPEEDS

Not Determined

[1]Includes flow to hydraulic turbine drive for low speed pump.

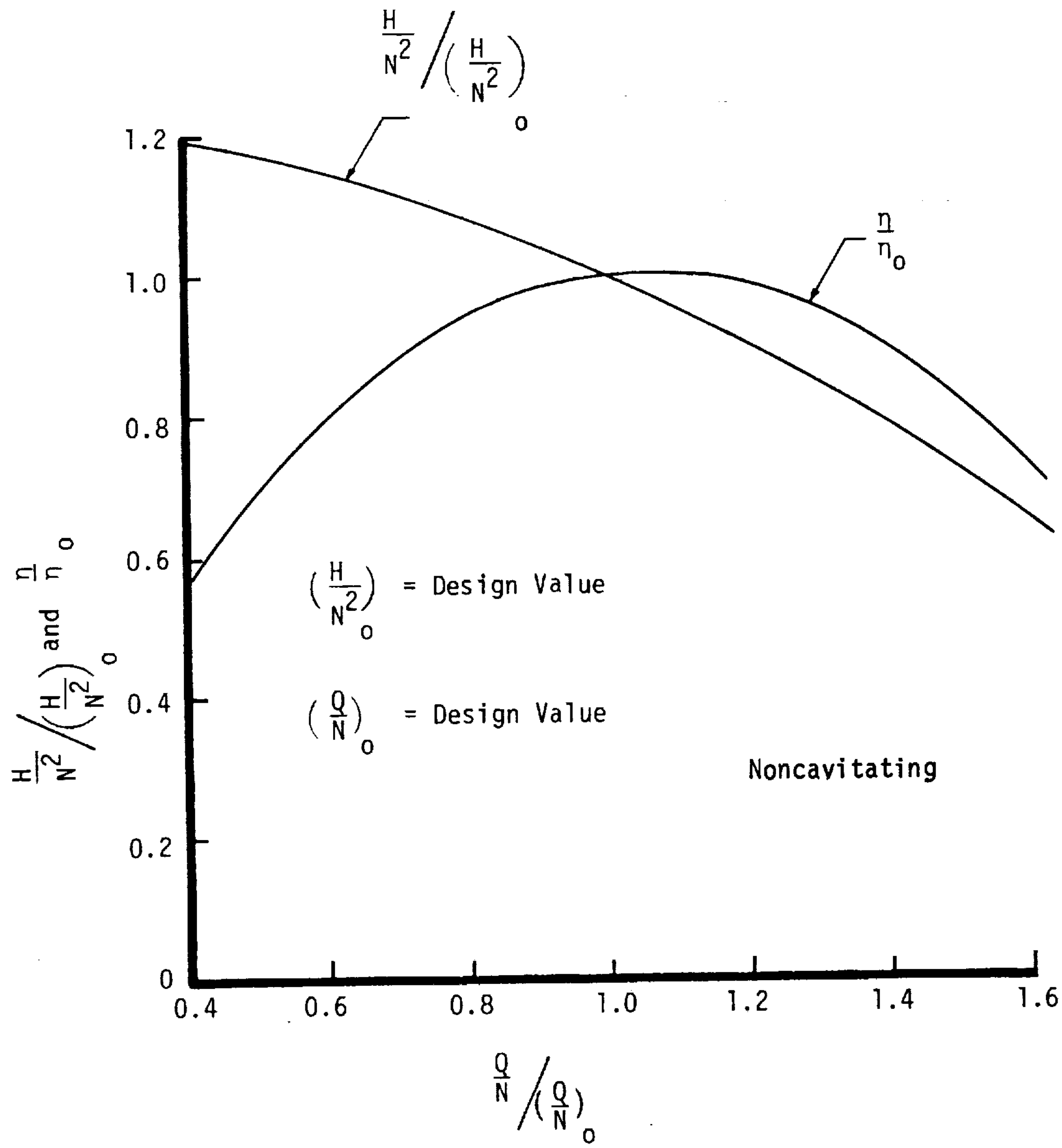

Figure 79. High Speed LOX and LH_2 Pump Dimensionless Performance Characteristics.

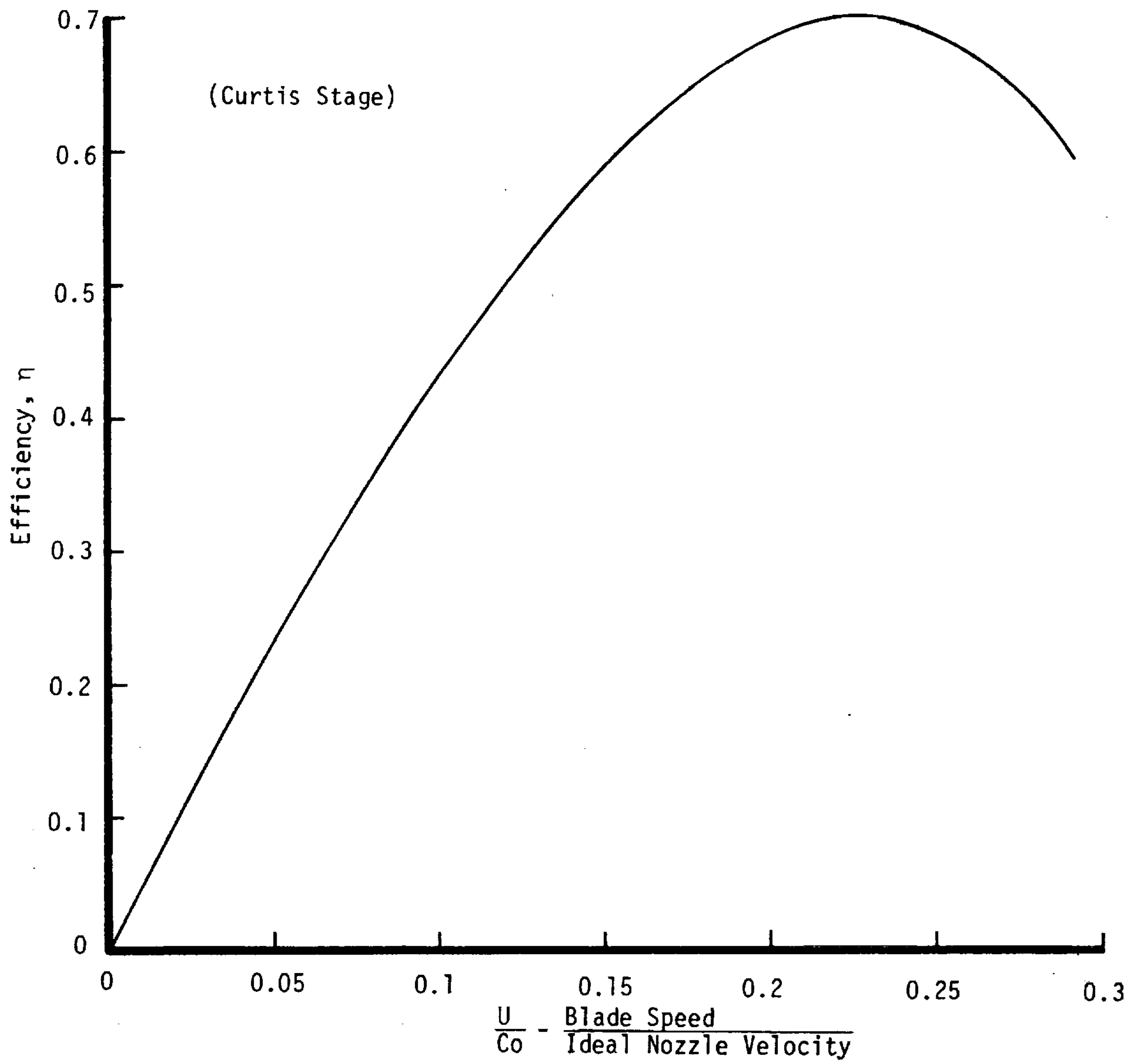

Figure 80. Effect of U/C_0 of Turbine Efficiency, Velocity Compounded Stage.

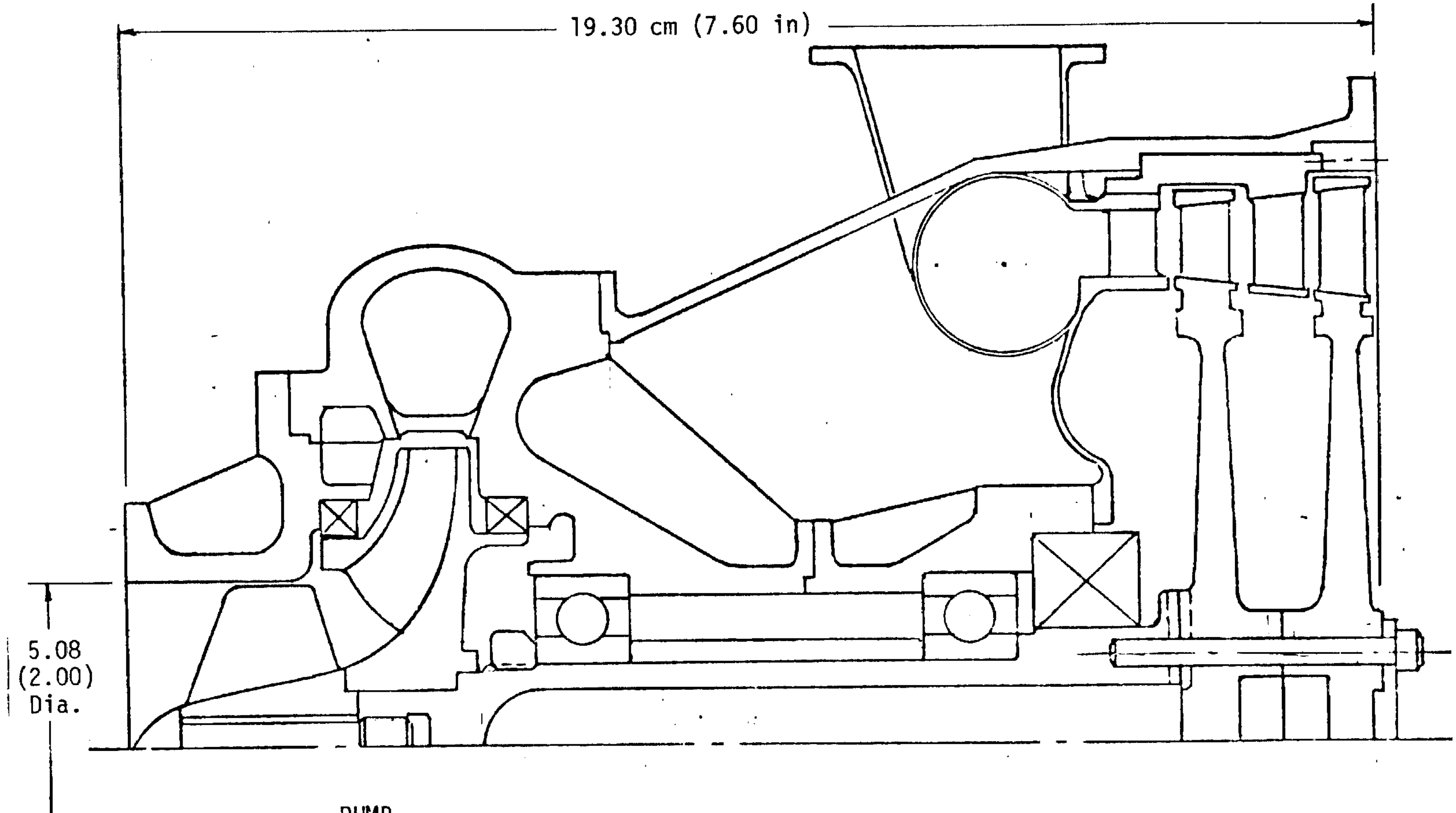

PUMP

Flow-16.83 Kg/s (37.1 lb/sec)
Head-274.3m (900 ft)

N = 17,176 RPM
Weight = 7.26 Kg (16 lb)

TURBINE

Flow - 0.11 Kg/s (0.24 lb/sec)
Inlet Pressure - 3.21 atm (47 psia)
Inlet Temp - 922°K (1660°R)
Exit Pressure -1.08 atm (15.8 psia)

Figure 81. Conceptual TPA Design, LOX Pump.

TABLE XXVIII - LH_2 TURBOPUMP DESIGN POINT PARAMETERS

PUMP - Single Stage Centrifugal (Fully Shrouded)

Flow - $\dot{\omega}$ Kg/sec (lb/sec) = 2.45 (5.4)

Pressure Rise, $\frac{N}{m^2}$ (psi) = 2.67×10^6 (391)

Flow - $\frac{m^3}{sec}$ (gpm) = 0.0355 (563)

Head Rise, m (ft) = 3992.9 (13,100)

Specific Speed, Ns = 1500

Design Speed, N = 77,400 rpm

Tip Speed m/s ft/sec = 295 (967)

Head Coefficient ψ = 0.45

Efficiency, η = 0.75

Tip Diameter, D_T, cm, (in) = 7.37 (2.9)

INDUCER

NPSH m (ft) = 15.7 (52)

Suction Specific Speed = 95,000

Tip Diameter cm (in) = 5.84 (2.3)

Tip Speed m/s (ft/sec) = 237 (777)

Inlet Flow Coefficient, ϕ = 0.065

TURBINE

Velocity Compounded - Full Admission

Pitch Line Blade Speed, U_m m/s (ft/sec) = 427 (1400)

Pitch Diameter cm (in) = 10.5 (4.14)

Inlet Pressure $\frac{N}{m^2}$ (psi) = 6.55×10^5 (95)

Inlet Temperature, K (°R) = 922 (1660)

Exit Pressure (static), $\frac{N}{m^2}$ (psi) = 0.109×10^5 (15.8)

Ideal Nozzle Velocity, C_o m/s (ft/sec) = 2,219 (7,281)

$\frac{U_m}{C_o}$ = 0.192

Estimated Efficiency = 0.62

Flow, Kg/sec (lb/sec) = 0.0837 (0.185)

Exit Annular Area, Aa, cm^2 (in^2) = 33.55 (5.2)

AaN^2, $cm^2 \times rpm^2$ ($in^2 \times rpm^2$) = 210×10^9 (31×10^9)

BEARINGS

Bore mm (in) = 20 (0.787)

DN mm x rpm = 1.55×10^6

SHAFT CRITICAL SPEEDS

Not Determined

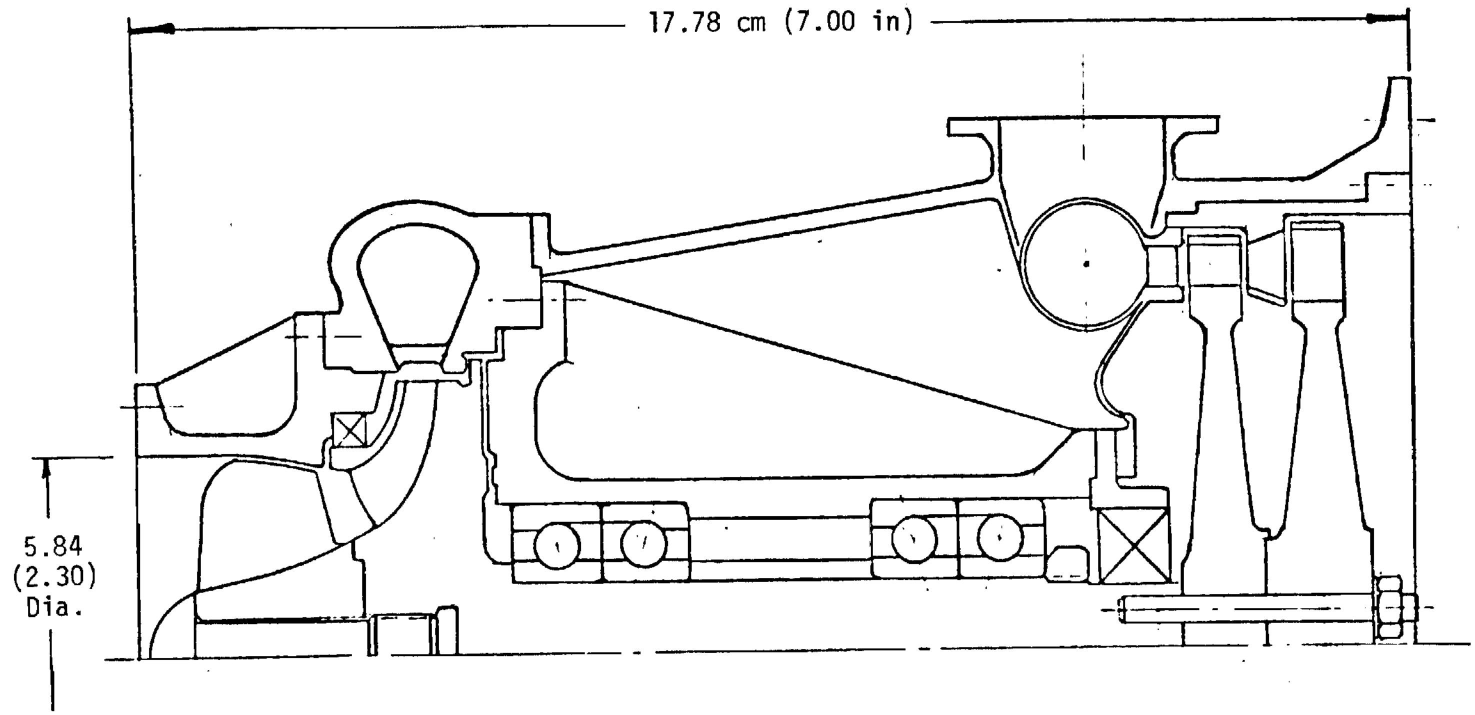

PUMP

Flow - 2.45 Kg/s (5.4 lb/sec)
Head - 3993 m (13,100 ft)

TURBINE

Flow - 0.084 Kg/s (.185 lb/sec)
Inlet Pressure - 6.46 ATM (95 psia)
Inlet Temp - 922°K (1660°R)
Exit Static Press - 1.01 ATM (15.8 psia)

N = 77,400 RPM

Weight = 7.26 Kg (16 lb)

Figure 82. Conceptual TPA Design, LH_2 High Speed Pump.

pumps and two-stage turbines. At the design point, the turbine bypass flow is no greater than 20 percent. A bypass around the plug cooling passages, rather than the turbine, could be used if the heat flux from the plug should prove inadequate to heat all the oxidizer flow.

° Cycle EX04

The turbomachinery for this cycle is similar to that used for Cycle EX03 except that both turbines are provided with gaseous hydrogen. An oxygen seal package similar to that used in the RL10 is required between the oxidizer pump and its drive turbine.

° Cycle GG03

The turbopumps utilized for this cycle are single-stage, centrifugal, high speed pumps, and hydraulic, turbine driven, low speed pumps. An oxygen seal package is required for the high speed oxidizer pump. The hot gas turbine is a velocity compounded or Curtis stage.

D. ENGINE COOLING ANALYSIS

1. ITA-Type Module

Cooling analyses conducted early in the program on film-cooled skirts for both 40:1 and 200:1 nozzles (Figure 83) led to recommended design points of 21.5% FFC (fuel film cooling) and 24% FFC, respectively, for a 2560°R wall with cycle life of 1200. A reexamination of the film cooling requirements of the 40:1 nozzle was made using the results obtained on Contract NAS3-20107 (Plug Cluster Module Demonstration Program).

The effect of increasing the module area ratio from 40 to 200 on module film cooling requirements was evaluated using the entrainment fraction model. There is some uncertainty as to how to apply the entrainment fraction, k, data obtained with a 40:1 nozzle to a 200:1 design so results for two representative assumptions were obtained as shown in Figure 83. The "k vs x" model assumes that the axial entrainment fraction distribution in the 200:1 nozzle is the same as in the 40:1 nozzle. This assumption yields maximum nozzle wall temperature about equal to the 40:1 nozzle prediction, thereby indicating that the film cooling requirements are about the same.

The "k vs x/L" model assumes that the entrainment fraction correlates with non-dimensional axial position rather than the absolute value of axial position. This assumption yields high nozzle temperature for a 200:1 design which means that higher film coolant flow rates are required.

It is believed that the "k vs x/L" model is most likely to represent the entrainment fraction distribution in a 200:1 nozzle because the entrainment is strongly influenced by wall curvature which tends to correlate with x/L. Therefore, it is believed that a 2 - 3% FFC percentage increase would be required if the module area were increased from 40:1 to 200:1.

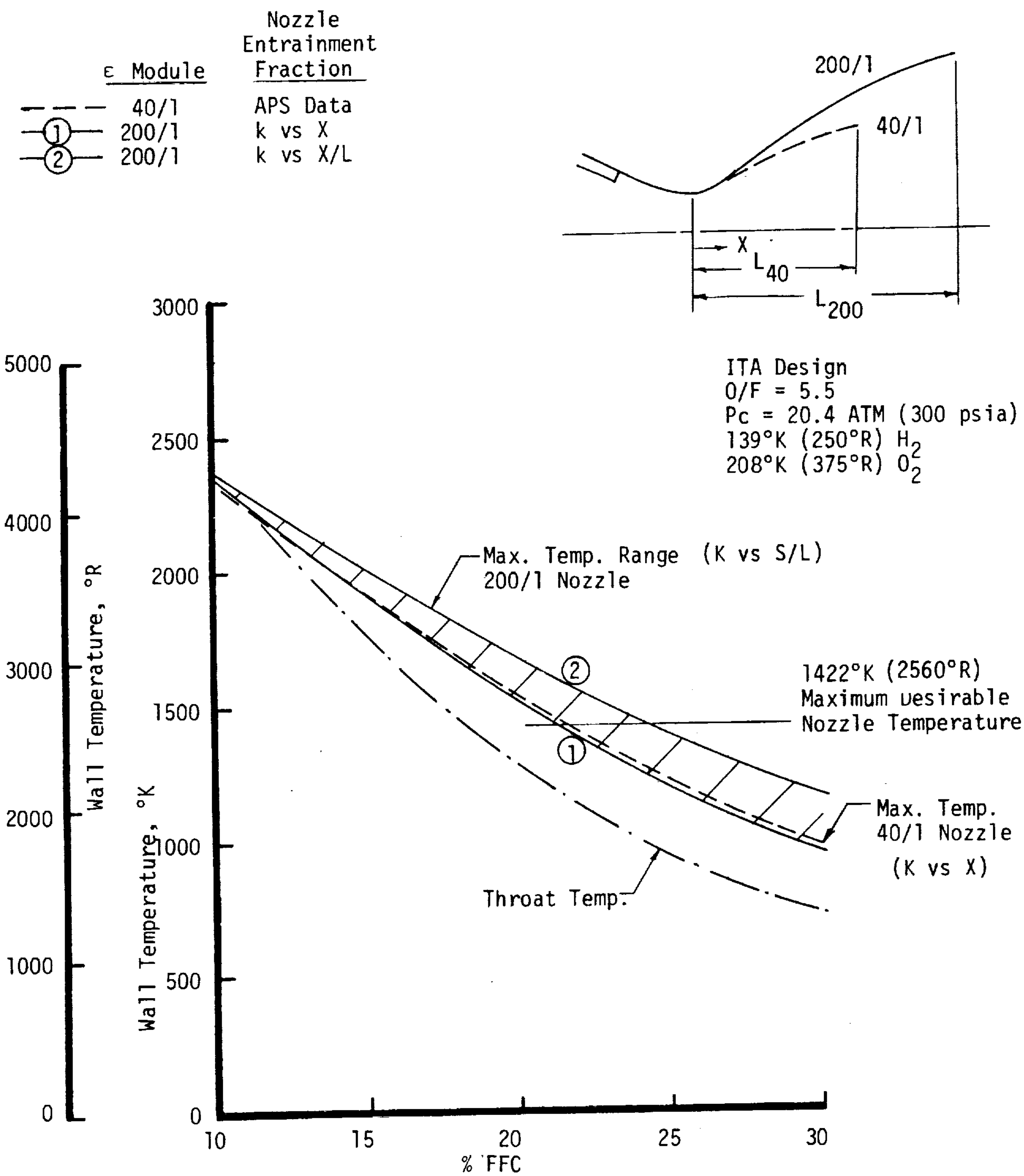

Figure 83. ITA Wall Temperatures Based on Entrainment Fraction Model.

The effect of overall module mixture ratio on film cooling requirements and the parametric relationship between film-cooling-performance loss, mixture ratio, and fuel film cooling percent are shown in Figure 84. These results were obtained for the ITA engine configuration but the APS film coolant injection sleeve design was assumed because it is more efficient (less coolant mixing). The analysis was performed using the HOCOOL computer program and the post-test entrainment fraction model. The design criteria used for defining the film coolant requirements are: cyclic life of 1200 cycles (throat limit - includes safety factor of 4), 1% maximum creep in 10 hour (nozzle limit), 2560°R maximum nozzle temperature, and 1660°R film coolant injection sleeve temperature (copper material).

2. Regeneratively Cooled Module

Preliminary regenerative cooling analysis of a module with a 40:1 nozzle area ratio was conducted using the following ground rules: (1) chamber and nozzle are entirely fuel cooled with no film cooling, (2) chamber pressure is 20.4 atm (300 psia) or 34.0 atm (500 psia), (3) mixture ratio is 5.5, and (4) total cycle life is 1200 cycles. A zirconium copper chamber with rectangular coolant passages, similar to the ITA design was used.

Gas-side boundary conditions were based on data generated in Ref. 18, in which heat fluxes were calculated from gas-side thermocouple responses by means of a two-dimensional SINDA model. Test hardware was comparable to the ITA design, i.e., premix injector, identical chamber contour. The present analysis was based on the reactive gas-side model and a reference temperature equal to the mean of the wall and the recovery temperature. The correlating factor, C_g, was adjusted to make the predicted flux profile agree with the data of Ref. 18, as shown on Figure 85.

Coolant side heat transfer was based on the Hess and Kunz correlation with a constant correlating factor, C_L, of 0.0208. The wall temperature distribution in the coolant correlation was based on the bulk temperature over the land and external wall and on the centerline wall temperature over the internal wall. As described in Ref. 23, this formulation matched the results of two-dimensional SINDA analyses reasonably well.

Channel geometry was not varied extensively. The sixty channel ITA design, with a channel width of 0.152 cm (0.060 in) was used as a starting point, and when found satisfactory, the channel depth was varied to obtain the change in wall temperature with channel depth. In the expansion section, both constant channel width and constant land width configurations were investigated. Both are satisfactory, but the constant channel width design will be excessively heavy, while the constant land width design leaves a large span across the coolant passage. Although not modeled, a bifurcation to double the number of channels will reduce both the weight and the span.

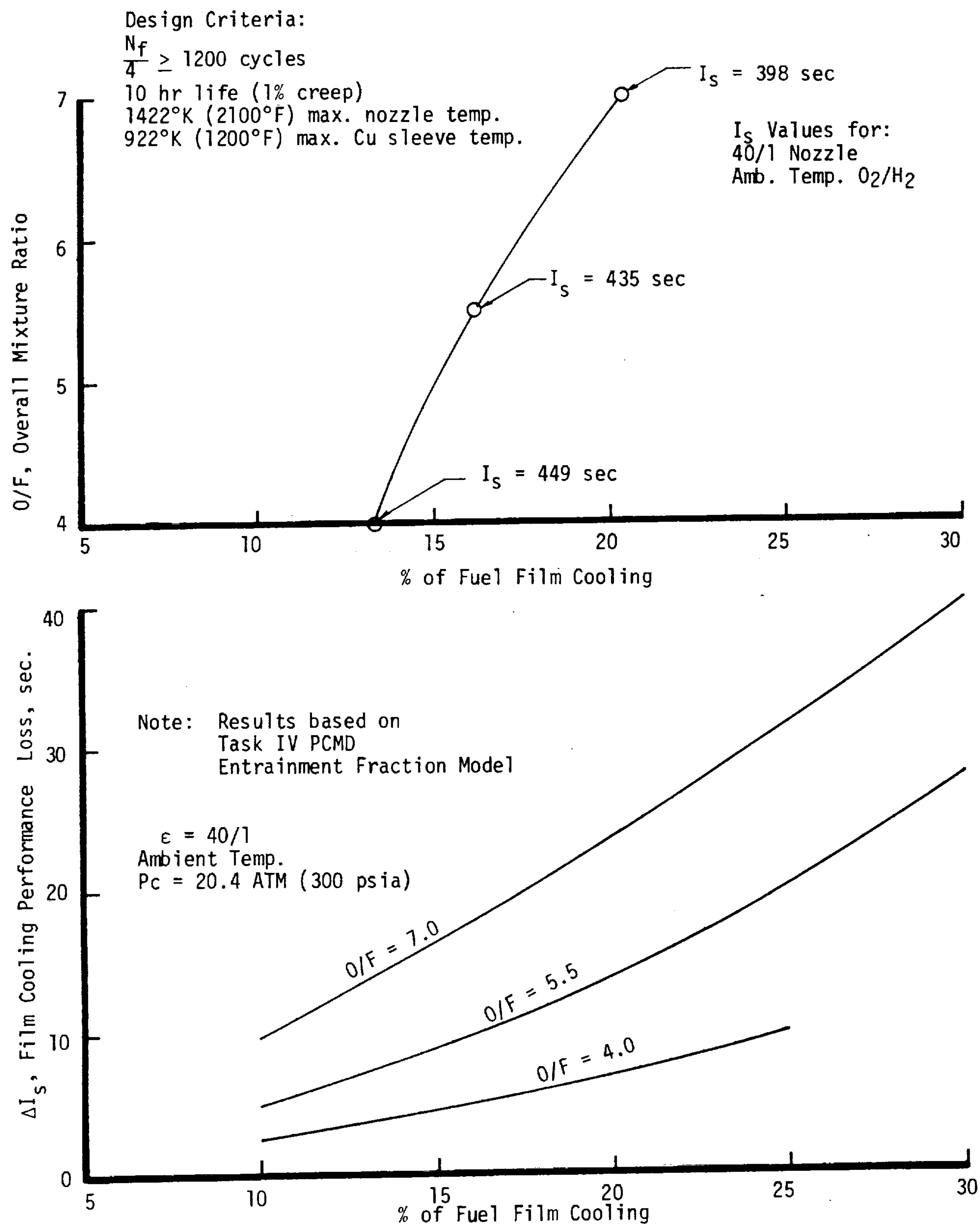

Figure 84. Film Cooling Requirements for 1200 Cycle Life at Mixture Ratios from 4 to 7.

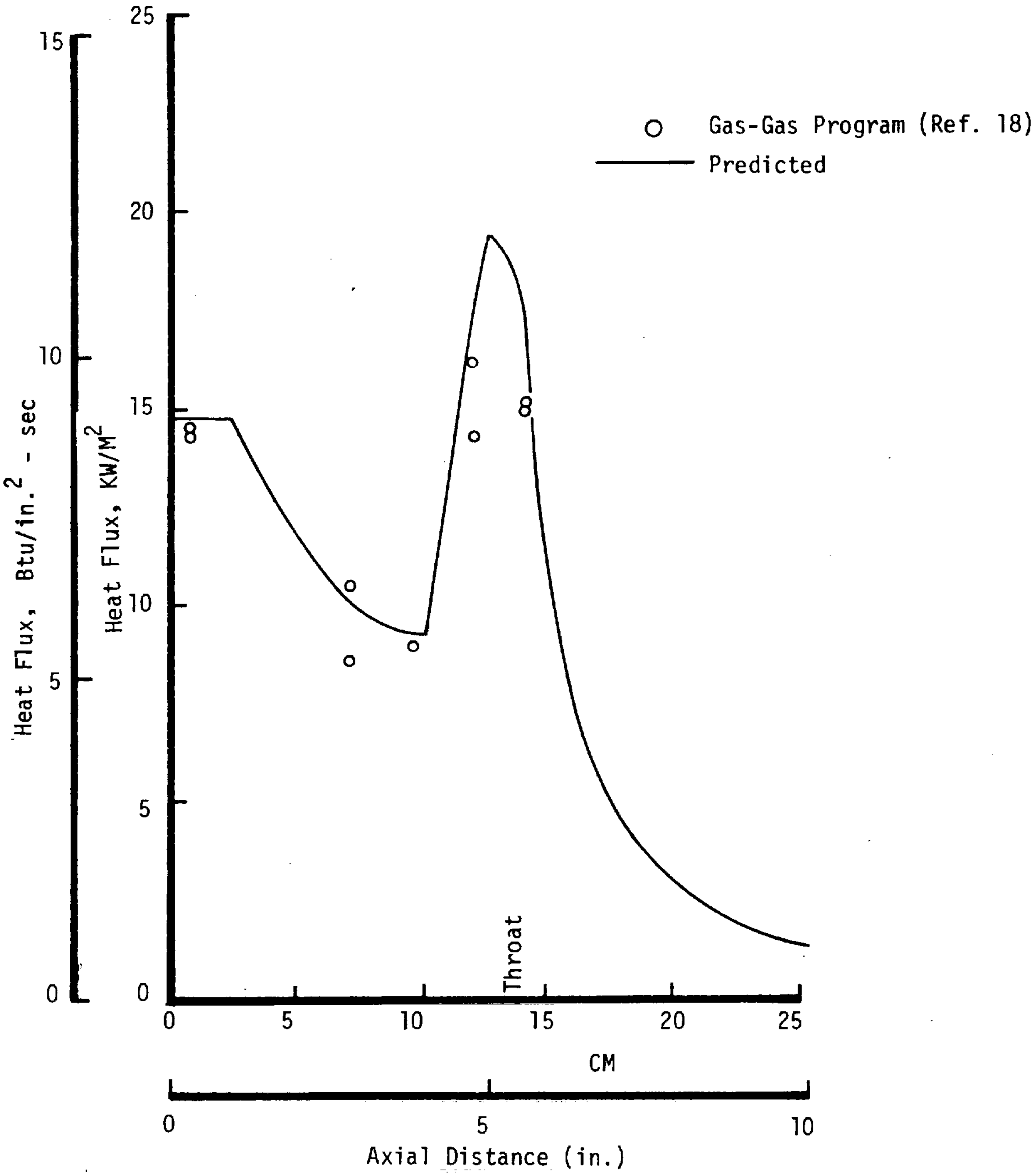

Figure 85. Gas-Side Heat Flux Profile.

Figure 86 shows a partial computer program output for a 0.508 cm (0.20 in) channel depth coflow design in which the channel width is constant between the injector and a point 8.89 cm (3.5 in) past the throat, and the land width is constant at 0.508 cm (0.20 in) thereafter.

The results of the analysis are summarized in Figures 87-92 for the 20.4 atm (300 psia) chamber pressure case.

Figure 87 presents the predicted gas-side wall temperature and temperature drop from gas-side to back-side at the maximum temperature point -- 1.27 cm (0.5 in) forward of the throat -- as a function of channel depth for the coflow design.

Figure 88 shows similar data at the same location in the counterflow design. Temperatures and gradients are comparable to those of the coflow design. However, at the injector and the gas-side, temperatures are considerably higher than near the throat, as shown in Figure 89, although the gradients are much reduced.

The predicted coolant pressure drop for both the coflow and counterflow design is shown in Figure 90. The loss coefficients at the entrance and exit are taken to be 0.5 and 1.0 respectively, with the friction drop based on a surface roughness of 0.000163 cm (0.000064 in).

The corresponding data for a module operating at a 34 atm (500 psia) chamber pressure is compared in Figure 91 at the injector (forward) end and near the throat.

From the standpoint of thermal considerations, there is an ample margin on wall temperature, pressure drop, and flow velocity for the regeneratively cooled zirconium copper module with a gas-side wall thickness of 0.152 cm (0.06 in.). Thus, the mechanical design (see Section VI,F) can concentrate on integration of the module most effectively into the entire system, minimizing module weight, cost and fabrication complexity.

Nickel and stainless steel chambers were also considered on a preliminary design basis. Figure 92 shows the maximum wall temperatures predicted for Nickel-200 as a function of channel depth, for a counterflow 60 channel design. The pressure drops are low and a reduction in wall temperature appears feasible within a reasonable pressure schedule.

The stainless steel design produced wall temperatures in excess of 1422°K (2100°F) above the throat for a channel depth of 0.406 cm (0.160 in); it is not apparent that reasonable temperatures can be achieved without an extensive design effort.

3. Regeneratively Cooled Plug Nozzle

The geometry of the plug cluster engine analyzed was assumed to consist of ten 40:1 area ratio modules distributed around a 400:1 area ratio plug. The configuration is summarized in Figure 93 and Table XXIX.

02/11/77 08:14:57 F00115 C427AA070 000027 559 100 DATE 021177 PAGE 8

AEROJET LIQUID ROCKET COMPANY

HEAT

A HEAT TRANSFER ANALYSIS OF REGENERATIVE COOLING

THE STUDY IS FOR

UNTS 40:1 REGEN DESIGN--COFLOW

THE COOLANT IS HYDROGEN (NBS) FLOWING IN RECTANGULAR SLOTS

MR = 5.56, PC = .207+07 N/M2, TC = 3396. K, WGSTAR = 1.5 KG/SEC, PIN = .386+07 N/M2, TIN = 106. K

FLOW SUMMARY TABLE

STATION NO	POS M	FLOW RATE KG/SEC	* * LIQUID * * PRESSURE N/M2	TEMP DEG K	VELOCITY M/SEC	MACH NO.	FILM COEFFICIENTS LIQUID W/M2-K	GAS W/M2-K	TOTAL W/M2-K	WALL TEMPERATURES LIQUID DEGREE K	METAL DEGREE K	GAS DEGREE K	* * HEAT TRANSFER * * Q/AI W/M2	Q/AO W/M2	QSUM J	G/ -
-	INLET	-	.386+07	105.6	0.0											
1	.000	.239	.384+07	105.9	56.1	.070	.159+05	.569+04	.882+04	640.2	650.0	657.4	.47+07	.15+08	.00	.0
2	.025	.237	.383+07	135.6	76.8	.065	.162+05	.566+04	.994+04	623.3	633.3	641.0	.45+07	.15+08	.11+03	.0
3	.051	.239	.381+07	161.1	91.9	.094	.191+05	.446+04	.114+05	538.8	547.7	554.6	.43+07	.12+08	.20+03	.0
4	.076	.239	.380+07	181.6	104.0	.100	.193+05	.359+04	.126+05	484.9	492.7	499.0	.36+07	.10+08	.28+03	.0
5	.102	.239	.379+07	201.1	115.6	.106	.193+05	.404+04	.128+05	528.0	536.6	544.3	.42+07	.11+08	.36+03	.01
6	.114	.239	.379+07	213.1	102.1	.091	.165+05	.536+04	.106+05	623.4	632.4	643.6	.44+07	.14+08	.41+03	.01
7	.127	.239	.378+07	227.6	109.2	.094	.164+05	.768+04	.104+05	720.3	731.0	755.7	.51+07	.19+08	.46+03	.0
8	.141	.239	.378+07	240.7	115.4	.097	.164+05	.701+04	.109+05	672.3	682.2	706.6	.47+07	.18+08	.51+03	.0
9	.152	.239	.378+07	246.7	118.3	.098	.164+05	.385+04	.124+05	502.1	508.6	520.3	.32+07	.10+08	.53+03	.0
10	.165	.239	.377+07	254.1	122.0	.099	.163+05	.249+04	.133+05	439.5	444.5	450.3	.25+07	.66+07	.56+03	.0
11	.178	.239	.376+07	259.3	150.0	.121	.190+05	.174+04	.162+05	398.5	403.1	406.9	.23+07	.47+07	.58+03	.0
12	.203	.239	.374+07	267.3	158.5	.125	.190+05	.106+04	.171+05	371.7	375.3	377.4	.18+07	.29+07	.61+03	.0
13	.229	.239	.375+07	277.2	162.7	.127	.189+05	.692+03	.176+05	356.3	359.2	360.9	.14+07	.19+07	.64+03	.0
14	.254	.239	.376+07	284.5	60.1	.046	.739+04	.547+03	.658+04	403.1	404.7	401.6	.78+06	.14+07	.66+03	.00
15	.279	.239	.376+07	290.2	48.8	.037	.602+04	.444+03	.539+04	406.1	407.3	403.6	.62+06	.12+07	.68+03	.00
16	.305	.239	.376+07	295.3	42.2	.032	.523+04	.354+03	.473+04	400.4	401.4	397.6	.50+06	.93+06	.70+03	.00
17	.330	.239	.376+07	299.7	37.6	.028	.466+04	.301+03	.424+04	398.8	399.7	395.8	.42+06	.79+06	.72+03	.00
18	.356	.239	.376+07	303.8	34.8	.026	.431+04	.278+03	.395+04	402.3	403.1	399.0	.39+06	.73+06	.73+03	.00
19	.381	.239	.376+07	307.7	31.7	.023	.393+04	.249+03	.360+04	403.4	404.1	399.9	.34+06	.65+06	.74+03	.00
20	.406	.239	.376+07	311.4	29.9	.022	.370+04	.227+03	.340+04	403.6	404.3	400.1	.31+06	.59+06	.76+03	.00
21	.432	.239	.376+07	314.9	28.4	.021	.351+04	.206+03	.324+04	402.8	403.4	399.4	.29+06	.54+06	.77+03	.00
22	.457	.239	.376+07	318.2	27.3	.020	.335+04	.187+03	.312+04	401.3	401.8	397.9	.26+06	.49+06	.78+03	.000
23	.483	.239	.376+07	321.3	26.2	.019	.321+04	.168+03	.301+04	396.7	399.2	395.5	.23+06	.44+06	.79+03	.000
24	.597	.239	.376+07	324.2	25.4	.018	.310+04	.151+03	.292+04	396.1	396.5	393.0	.21+06	.39+06	.80+03	.000
-	EXIT	-	.376+07	324.2	0.0											

Figure 86. Heat Transfer Computer Printout for Co Flow Regenerative Cooling (1 of 2)

ORIGINAL PAGE IS OF POOR QUALITY

02/11/77 08:14:57 F00115 0027AA070 000027 559 100 DATE 021177 PAGE 5

AEROJET LIQUID ROCKET COMPANY

HEAT

A HEAT TRANSFER ANALYSIS OF REGENERATIVE COOLING

THE STUDY IS FOR

OETS 4011 REGEN DESIGN--COFLOW

THE COOLANT IS HYDROGEN (NBS) FLOWING IN RECTANGULAR SLOTS

MR= 5.50 PC= 300. PSIA TC=6022. R WGSTAR= 3.39 LB/SEC PIN= 560. PSIA TIN= 190. R

FLOW SUMMARY TABLE

STATION NO.	POS IN.	FLOW RATE LBM/SEC	LIQUID PRESSURE PSIA	LIQUID TEMP DEG F	LIQUID VELOCITY FT/SEC	MACH NO.	FILM COEFFICIENTS LAND BTU/IN2-SEC-R HL	GAS	LIQUID	WALL TEMPERATURES LIQUID DEGREE F TWLC	METAL T2	GAS TWG3	HEAT TRANSFER Q/A1 BTU/IN2-SEC QAIC	Q/A1 QAI3	QSUM BTU	Q/..
-	INLET	-	560.0	-249.7	0.0											
1	.00	.55	556.4	-249.9	190.6	.070	.542-02	.193-02	.300-02	692.7	710.4	723.6	2.69	9.12	.0000	[illegible]
2	1.00	.55	554.6	-215.0	252.1	.085	.618-02	.192-02	.338-02	662.2	680.3	694.1	2.97	9.13	.1074+03	[illegible]
3	2.00	.55	553.0	-169.7	301.4	.094	.649-02	.151-02	.387-02	510.2	526.1	538.6	2.63	7.42	.2048+03	[illegible]
4	3.00	.55	551.3	-132.8	341.1	.100	.657-02	.122-02	.426-02	413.2	427.2	438.5	2.33	6.10	.2844+03	[illegible]
5	4.00	.55	549.6	-97.7	379.4	.106	.657-02	.137-02	.436-02	490.7	506.2	520.1	2.57	6.76	.3603+03	.
6	4.55	.55	550.1	-70.0	334.9	.091	.561-02	.182-02	.361-02	662.4	678.7	698.9	2.67	8.64	.4166+03	[illegible]
7	5.00	.55	548.2	-49.7	358.1	.094	.559-02	.261-02	.355-02	836.8	856.2	900.7	3.13	11.82	.4605+03	.
8	5.55	.55	548.1	-20.3	374.8	.097	.557-02	.238-02	.372-02	750.5	768.2	815.7	2.84	10.79	.5075+03	.
9	6.00	.55	547.9	-15.0	388.3	.096	.556-02	.131-02	.422-02	444.1	455.7	476.8	1.94	6.14	.5291+03	.
10	6.50	.55	547.2	-2.3	400.3	.099	.555-02	.845-03	.450-02	331.4	340.4	350.9	1.50	4.04	.5560+03	[illegible]
11	7.00	.53	543.8	7.1	492.2	.121	.646-02	.592-03	.549-02	257.7	266.0	272.8	1.38	2.86	.5758+03	[illegible]
12	8.00	.55	542.7	25.1	519.9	.125	.644-02	.360-03	.582-02	209.4	215.8	219.7	1.07	1.74	.6122+03	[illegible]
13	9.00	.55	540.9	39.4	535.8	.127	.643-02	.235-03	.597-02	181.7	186.8	190.0	.85	1.14	.6407+03	[illegible]
14	10.00	.55	545.6	52.4	197.3	.046	.251-02	.186-03	.224-02	265.9	268.8	263.2	.48	.8-	.6637+03	[illegible]
15	11.00	.55	545.8	62.7	169.9	.037	.205-02	.151-03	.185-02	271.3	273.5	266.8	.38	.71	.6836+03	[illegible]
16	12.00	.53	545.7	71.6	135.5	.032	.178-02	.120-03	.161-02	261.0	262.9	256.0	.30	.57	.7011+03	[illegible]
17	13.00	.55	545.9	79.7	123.3	.028	.158-02	.102-03	.144-02	258.3	259.8	252.7	.26	.48	.7163+03	[illegible]
18	14.00	.55	545.9	87.1	114.1	.026	.146-02	.945-04	.133-02	264.4	265.8	258.5	.24	.44	.7304+03	.
19	15.00	.55	545.9	94.2	104.0	.023	.133-02	.845-04	.122-02	266.4	267.6	260.1	.21	.40	.7459+03	[illegible]
20	16.00	.55	545.9	100.8	98.2	.022	.126-02	.771-04	.116-02	266.9	268.0	260.6	.19	.36	.7565+03	[illegible]
21	17.00	.53	545.9	107.1	93.3	.021	.119-02	.701-04	.110-02	265.4	266.5	259.2	.17	.33	.7686+03	[illegible]
22	18.00	.53	545.9	113.1	89.5	.020	.114-02	.636-04	.106-02	262.7	263.7	256.6	.16	.30	.7799+03	[illegible]
23	19.00	.53	545.9	118.7	85.9	.019	.109-02	.570-04	.102-02	258.0	258.8	252.2	.14	.27	.7905+03	[illegible]
24	19.95	.53	545.9	123.8	83.3	.018	.105-02	.514-04	.995-03	253.2	254.0	247.7	.13	.24	.8003+03	[illegible]
-	EXIT	-	545.9	123.9	0.0	.										

Figure 86. Heat Transfer Computer Printout for Co Flow Regenerative Cooling (2 of 2)

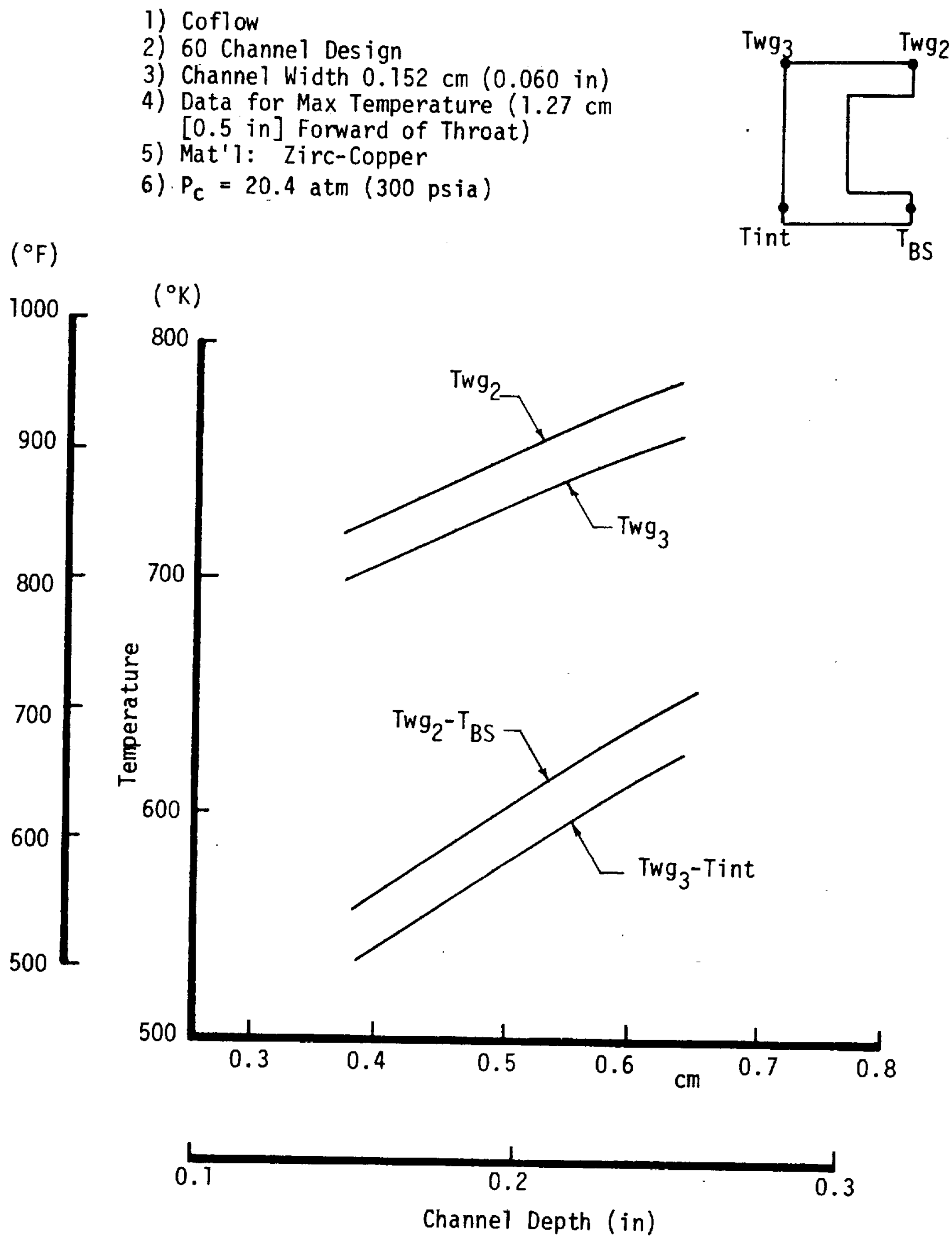

Figure 87. Predicted Coolant Passage Temperatures, Down Pass (CoFlow) Design.

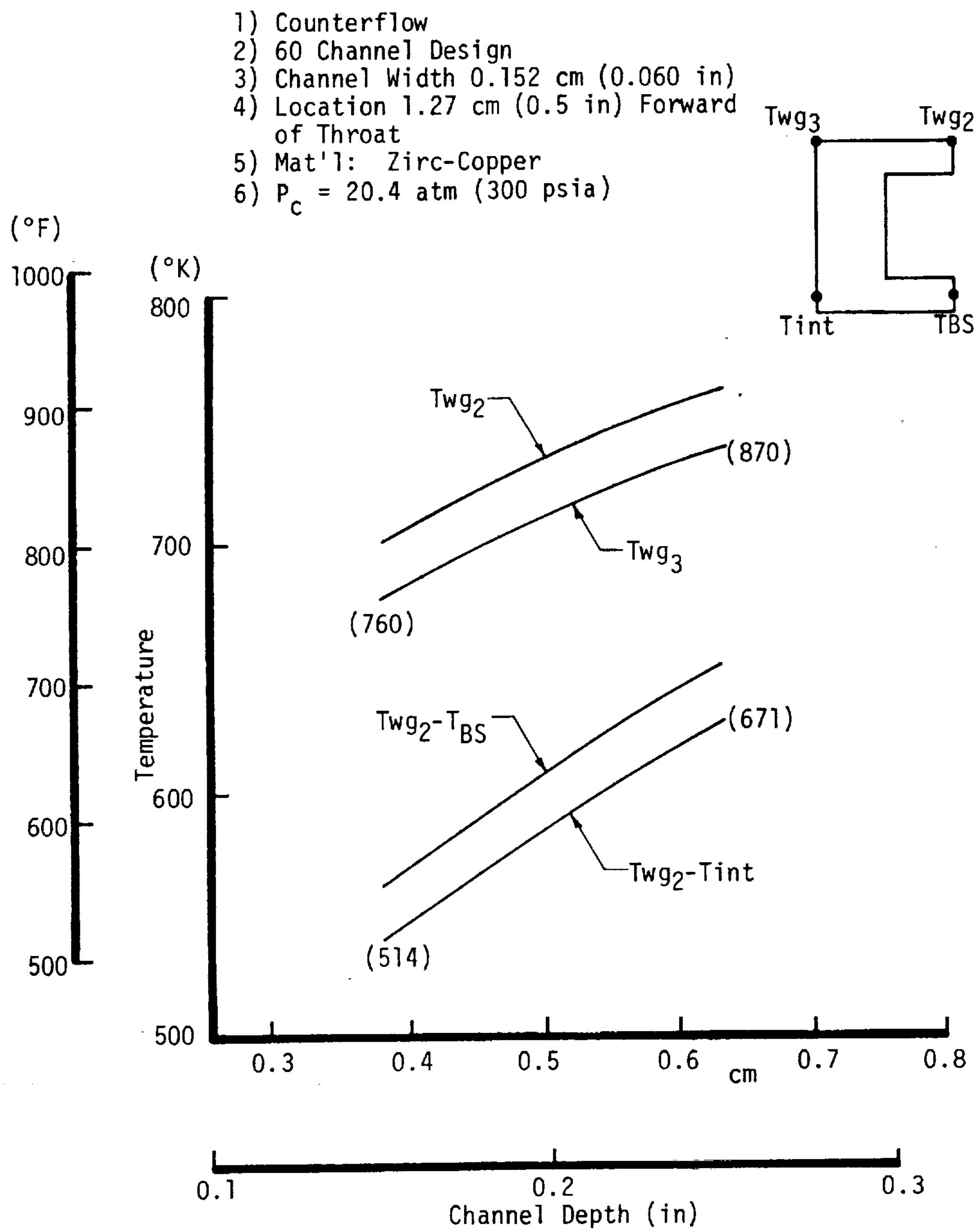

Figure 88. Predicted Coolant Passage Temperatures, Up-Pass (Counterflow) Design.

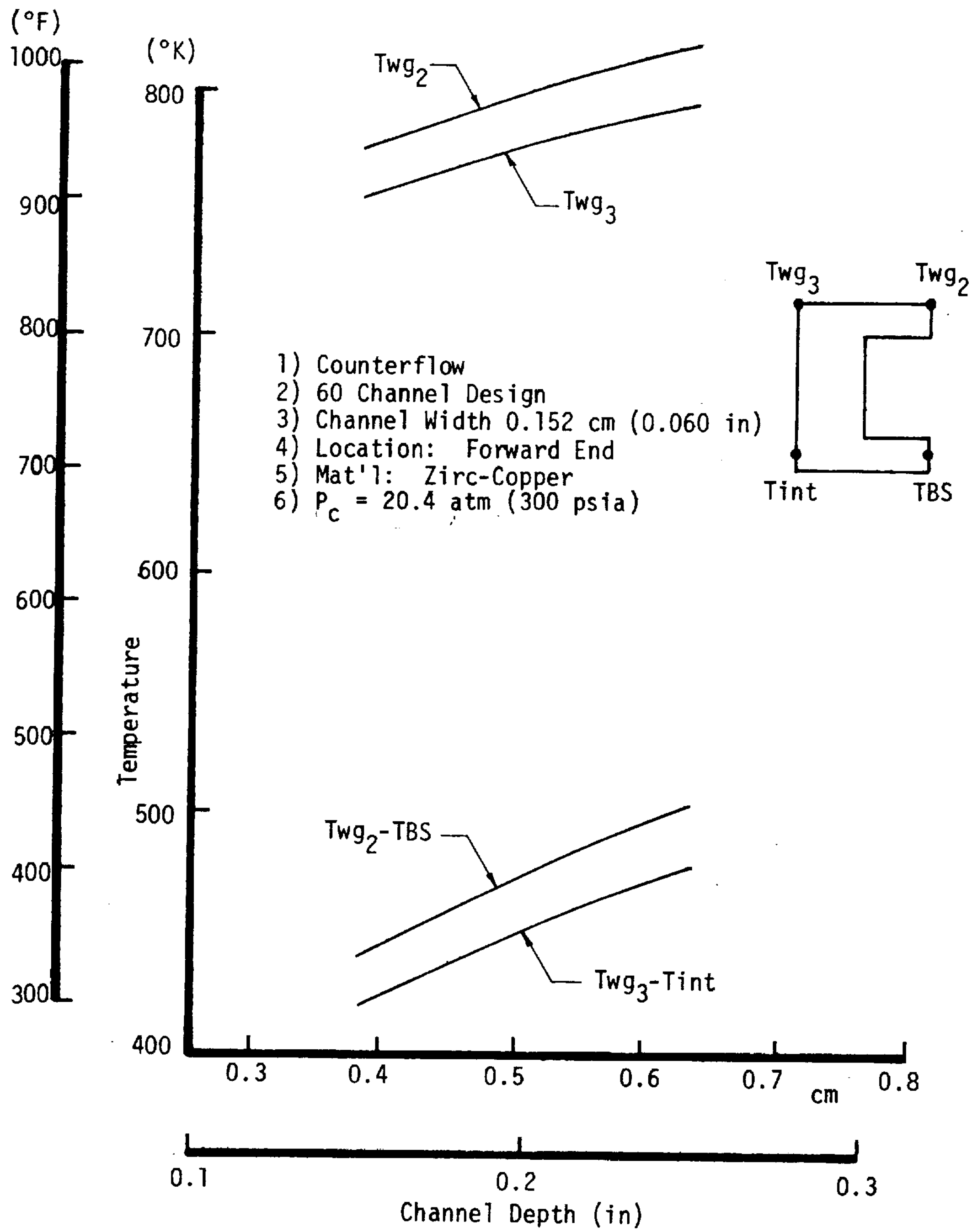

Figure 89. Injector End Predicted Coolant Passage Temperatures, Up-Pass Design.

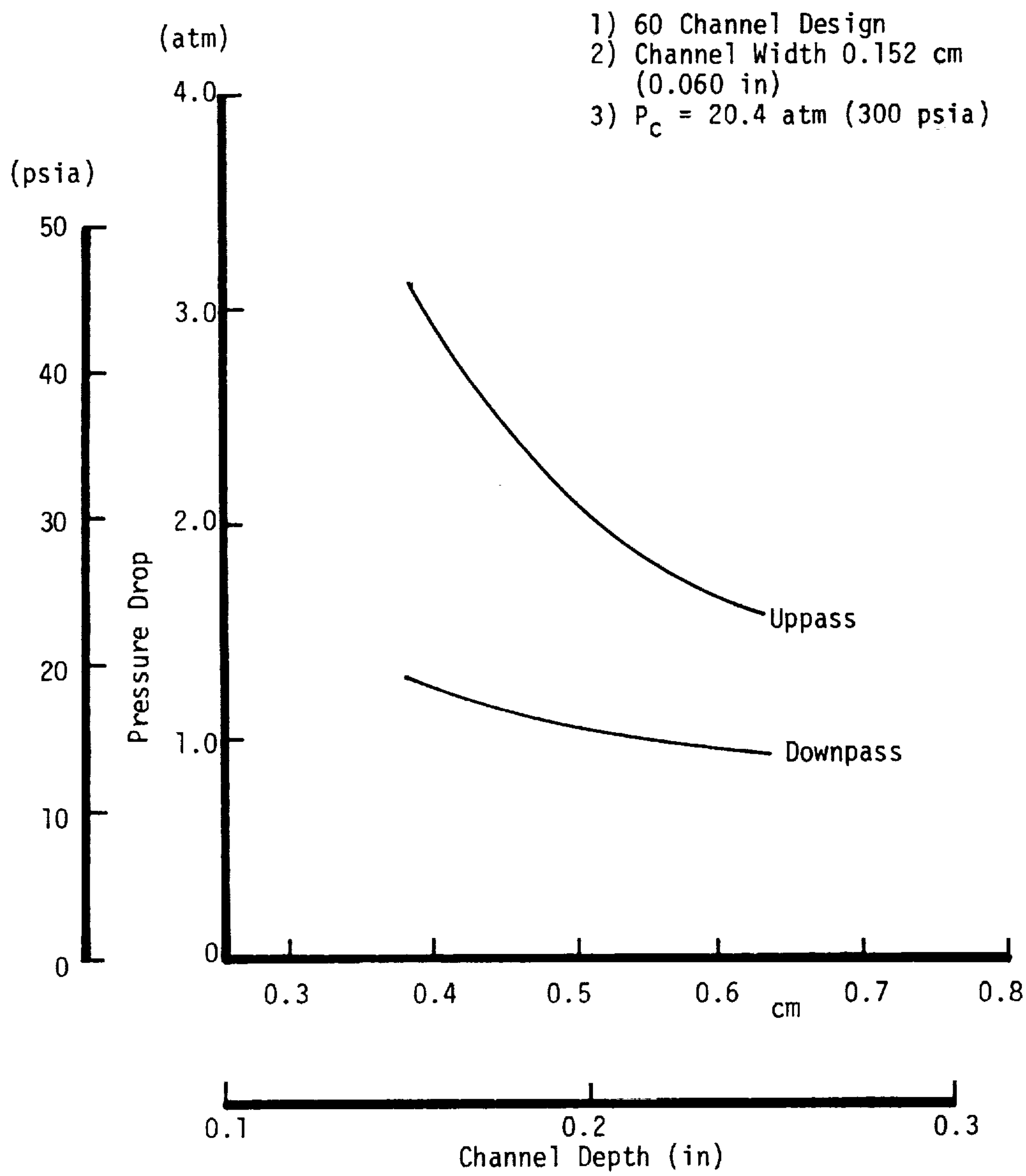

Figure 90. Predicted Coolant Pressure Drop.

Counterflow

Channel Depth 0.51 cm (0.2 in)

Pc = 20.4 atm (300 psia)	Pc = 34 atm (500 psia)
ΔP = 2.04 atm (30 psi)	ΔP = 5.58 atm (82 psi)
ΔT = 223°K (402°F)	ΔT = 194°K (350°F)

At Injector

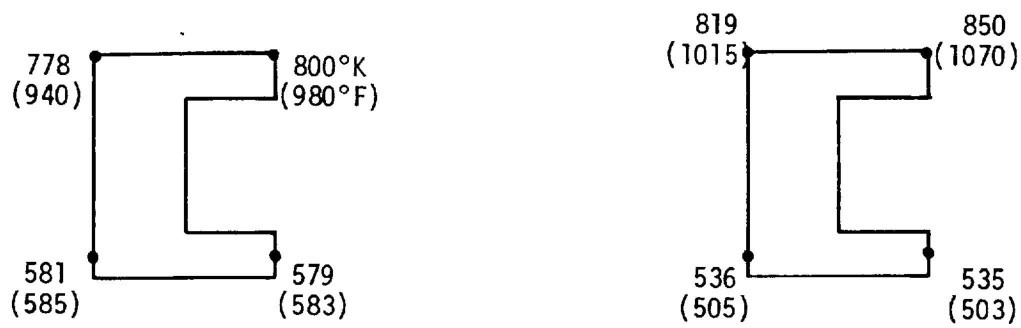

1.27 cm (0.5 in) Forward of Throat

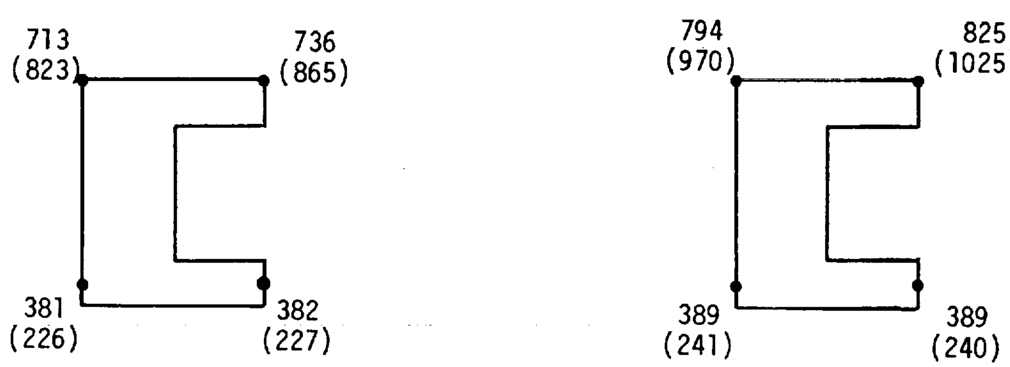

Figure 91. Comparison of Counterflow Design Temperatures at Chamber Pressures of 20.4 and 34 ATM.

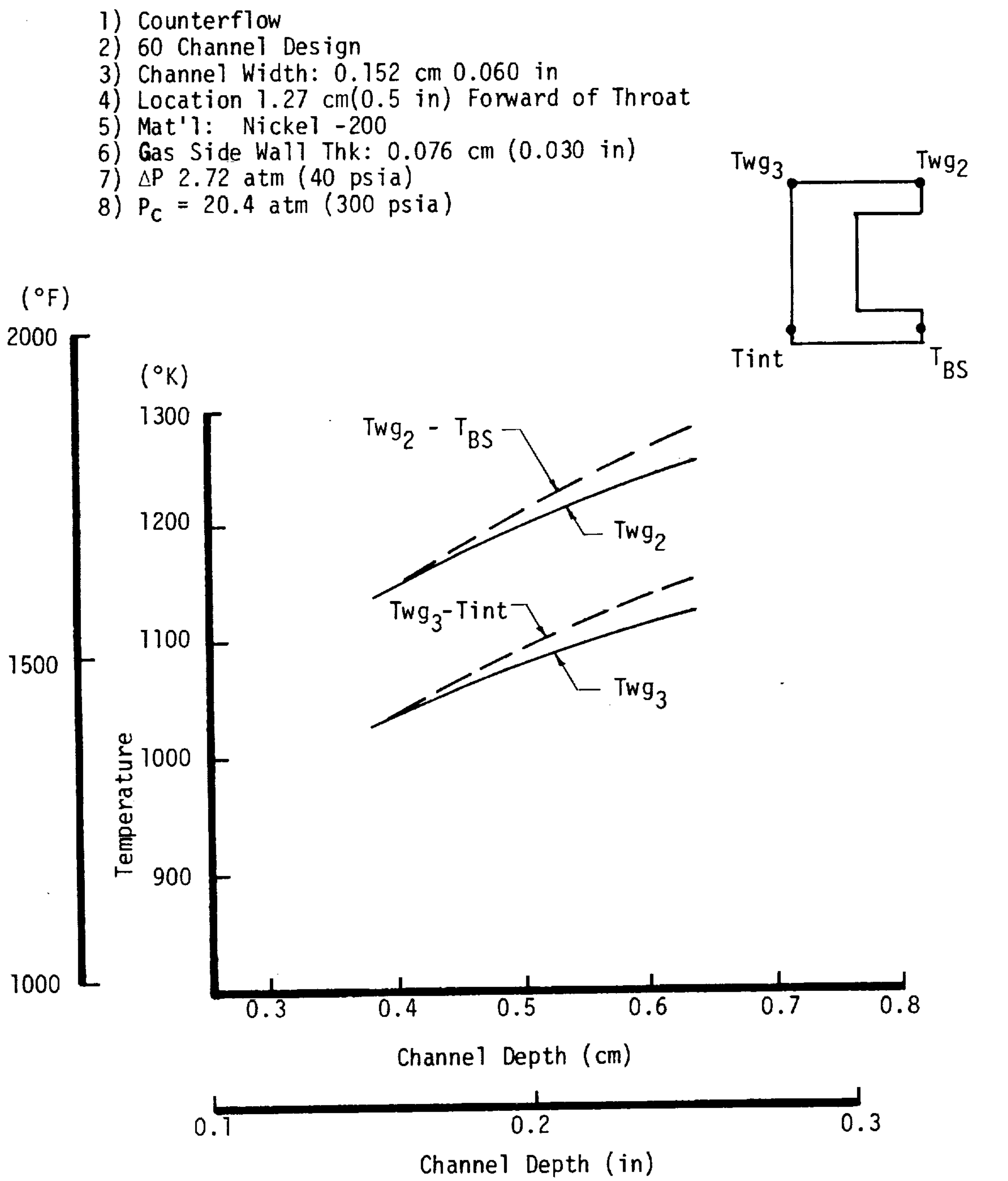

Figure 92. Predicted Coolant Passage Temperatures, Up-Pass (Counterflow) Design Using Nickel - 200.

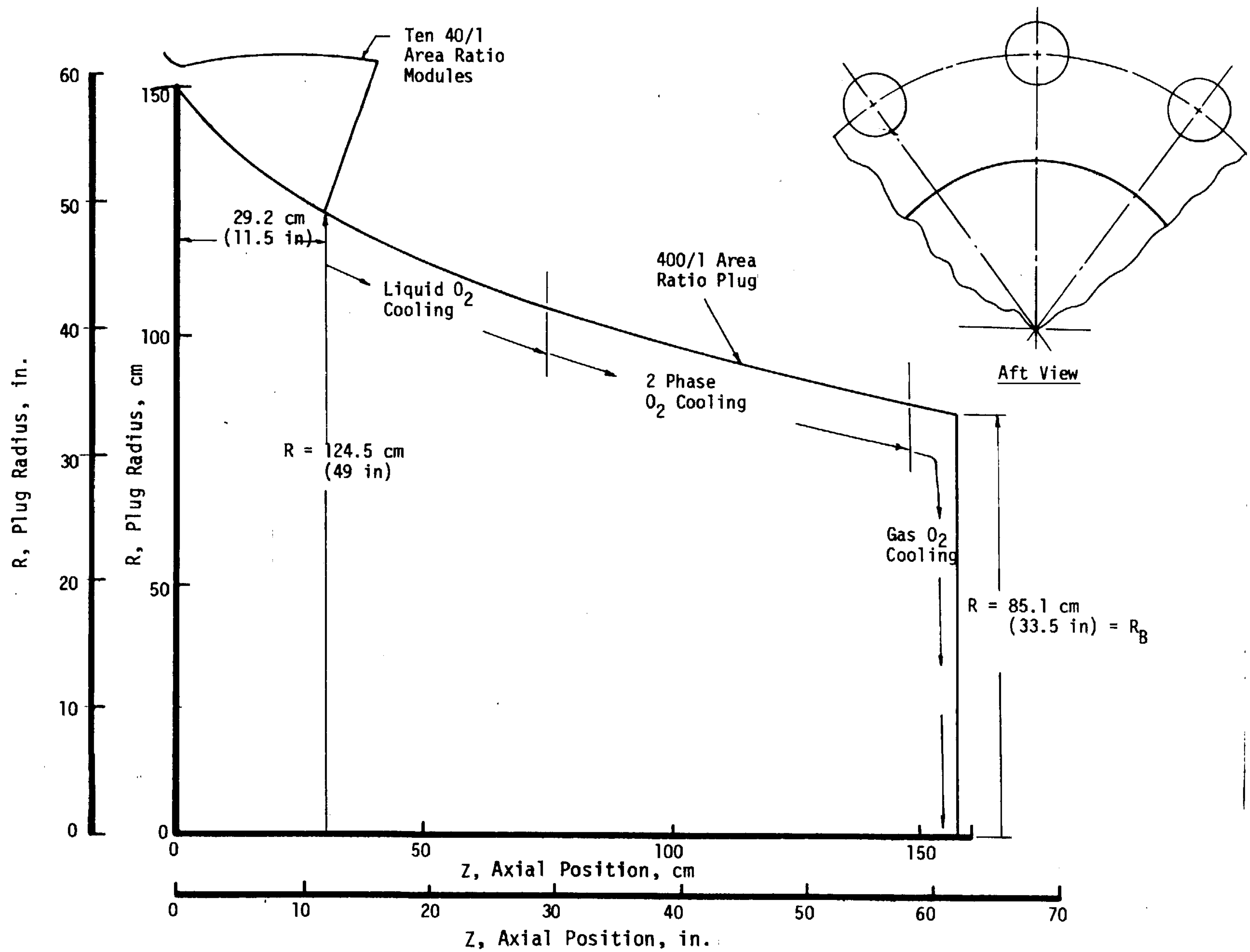

Figure 93. Plug Contour for Cooled Plug Analysis.

TABLE XXIX- PLUG HEAT TRANSFER DATA

$\varepsilon_{Module} = 40/1$ $\varepsilon_{Plug} = 400/1$

Location	Axial Position, Z, cm (in)	Radius, R cm (in)	(ρV) kg/s-m^2 wall (lb/sec in^2)	(1) TFS/To	(2) Tr °K (°F)	(2) hg x 10^4 kW/m^2-s-°K (Btu/in^2-sec-F)	(Twg=500F) q/A kW/m^2 (Btu/in^2 sec)	Radiation Cooled Plug Temp. °K(°F)
Plug Wall	29.2 (11.5)	124.5 (49)	26.9 (.0382)	.368	3007 (4953)	2839 (.965)	703 (0.43)	1875 (2915)
Plug Wall	50.8 (20)	114.3 (45)	18.3 (.026)	.335	2989 (4921)	1956 (.665)	474 (0.29)	1656 (2520)
Plug Wall	76.2 (30)	105.4 (41.5)	13.6 (.0193)	.314	2978 (4901)	1447 (.492)	343 (0.21)	1531 (2295)
Plug Wall	101.6 (40)	97.8 (38.5)	11.0 (.0157)	.3	2971 (4887)	1200 (.408)	294 (0.18)	1456 (2160)
Plug Wall	127 (50)	91.4 (36)	9.5 (.0135)	.29	2966 (4878)	1035 (.352)	261 (0.16)	1402 (2063)
Plug Wall	157.5 (62)	85.1 (33.5)	8.2 (.0116)	.282	2961 (4870)	894 (.304)	229 (0.14)	1353 (1975)
Base	157.5 (62)	85.1 (33.5)	--	--	2961 (4870)	--	(3) 85 (0.052)	1067 (1460)
Base	157.5 (62)	0 (0)	--	--	2961 (4870)	--	(3)180 (0.11)	1294 (1870)

Notes: (1) TFS = free stream static temperature.

(2) Film cooling effects assumed negligible.

(3) Calculated from HGC = 5 equation of HOCOOL (Ref. 24).

$Cg = 1.0$

$Wt/D^{1.8} = (.785\ \rho V)^{0.8}/De^{.2}$

De = Module Exit Diameter

$Tref = T_{film} = 1500°K\ (2700°R)$

$O_2/H_2 = 5.5$, Pc = 20.4 atm (300 psia), To = 3346°K (6022°R)

Base Heat Flux Distribution per CAL Data (Ref. 25)

r/R_B	$(q/A)_{Base}/(q/A)_{Wall,\ plug\ exit}$
0 - .15	0.80
.15 - .6	.95 = .97 (r/R_B)
.6 - 1.0	0.37

Average $(q/A)_{Base}$ = 83.3 kW/m^2 (.051 Btu/in^2-sec)

A heat flux distribution for the plug nozzle was estimated using a Bartz-type equation for heat transfer coefficient (Ref. 24), and Cornell data for the base heat flux distribution (Ref. 25), as indicated on Table XXIX. The heat fluxes estimated range from 703 kW/m^2 (0.43 Btu/in^2 sec) at the module exit to 85 kW/m^2 (.052 Btu/in^2 sec) at the base outer radius. These heat fluxes were calculated using the mass flux adjacent to the plug wall along the centerline of a module and circumferential heat flux variations were neglected. Data relative to the variation in mass flux between modules was not available; however, it is conceivable that a lower mass flux, normally conducive to a lower heat flux, will exist along the centerline between modules. On the other hand, it appears that shock phenomena will tend to increase the plug wall heat flux between modules. Due to these uncertainties, the accuracy of the estimated heat flux is probably on the order of $\pm$ 50%. Experimental plug heat flux data are needed to determine the extent of circumferential variations and to verify the heat flux magnitude along the module centerline. The Ref. 25 heat flux data are for a plug cluster engine with zero gap and are therefore not entirely applicable.

A radiation cooled plug was also considered. The wall temperatures estimated for a radiation cooled plug are listed in Table XXIX. These temperatures range from 1067-1867°K (1460-2900°F).

Table XXX presents the results of plug energy balance calculations which yielded coolant outlet temperature for two plug cluster engine configurations: 1) a 40:1 area ratio module and a 400:1 area ratio plug, and 2) a 200:1 area ratio module and a 400:1 area ratio plug. Oxygen and hydrogen coolants were considered. For the oxygen cooled case, the entire plug can be cooled with liquid oxygen if the module area ratio is 200:1, but a two-phase cooling system is required if the module area ratio is 40:1. If all of the hydrogen is utilized as a plug coolant, the outlet temperature would range from 40-106°K (80-190°R) depending on the module area ratio.

The feasibility of oxygen cooling of the plug cluster engine depicted in Figure 93 (40:1 module, 400:1 plug) was investigated. The correlations used to evaluate the oxygen heat transfer coefficient were obtained from Refs. 26-29 and are summarized in Table XXXI. The estimated critical heat flux for subcooled and two-phase oxygen is also plotted in Figure 94. These critical heat flux estimates are a crucial factor in evaluating the stainless steel coolant channel design and need to be verified experimentally.

° Counter Flow vs Parallel Flow

The initial analysis objective was to determine the best inlet location for the oxygen since it enters the cooling passages as a liquid and exits as a gas. It was found that the counterflow arrangement indicated in Figure 93 is best. This is demonstrated on Figures 95 and 96 which show plug

TABLE XXX - PLUG ENERGY BALANCE CALCULATIONS

ε_m	ε_{plug}	ΣQ_{plug} kW (Btu/sec)	Coolant	Δh KJ/kg (Btu/lb)	T_{in} °K(°R)	T_{out} °K(°R)
40	400	3278 (3109)	all O_2	237 (102)	92 (165)	157 (283) (G)
40	400		all H_2	1302 (560)	22 (40)	104 (188)
40	400		75% H_2	1732 (745)	22 (40)	132 (237)
40	400		50% H_2	2603 (1120)	22 (40)	185 (333)
40	400		25% H_2	5207 (2240)	22 (40)	354 (638)
200	400	1034 (981)	all O_2	75 (32.2)	92 (165)	132 (238) (L)
200	400		all H_2	411 (177)	22 (40)	46 (83)
200	400		75% H_2	549 (236)	22 (40)	53 (95)
200	400		50% H_2	823 (354)	22 (40)	71 (127)
200	400		25% H_2	1646 (708)	22 (40)	127 (229)

(1) $P_{in}O_2$ = 40.8 atm (600 psia), h_{in} = -129 KJ/Kg (-55.4 Btu/lb),
$\dot{w}$ = 13.83 Kg/s (30.48 lb/sec)

$P_{in}H_2$ = 43.2 atm (635 psia), h_{in} = -188 KJ/Kg (-81 Btu/lb),
$\dot{w}$ = 2.51 Kg/s (5.54 lb/sec)

(2) $P_{out}O_2$ = 34 atm (500 psia), $P_{out}H_2$ = 36.4 atm (535 psia)

Major Assumptions:
1. Plug Twall - 533°K (500°F).
2. No film cooling effects on plug.
3. Heat flux proportional to ρV at the plug wall along module $\mathbb{C}_L$ to the 0.8 power.
4. No circumferential heat flux variation on plug.
5. Oxygen Tsat = 147°K (265 °R) at 37.4 atm (550 psia).

TABLE XXXI - OXYGEN HEAT TRANSFER CORRELATIONS USED FOR THE OXYGEN COOLED PLUG ANALYSIS

Oxygen Heat Transfer Correlations

1. Subcooled Liquid O_2 Heat Transfer

   a. Forced Convection

   ALRC O_2 Correlation (Ref. 26) evaluated at typical T_{bulk} and T_{wall}

   $p = 34$ atm (500 psia), $T_b = 111°K$ (200°R), $T_w = 139°K$ (250°R)

   $hd^{.05}/(\rho V)^{.95} = 2.30 \times 10^{-2}$ (1.09×10^{-4})

   h - kW/m^2-°K (Btu/in^2 sec °F)

   d - cm (in)

   ρV - Kg/m^2-s (lb/sec ft^2)

   b. Burnout or critical heat flux (nucleate-to-film-boiling transition) based on N_2O_4 data and per correlation (Ref. 27):

   $\phi_{Bo} = A + B\ V\Delta T_{sub}$, kW/$m^2$ (Btu/in^2 sec)

   $V\ \Delta T_{sub}$

m°K/s	(ft °F/sec)	A	B
<1097	(2000)	981 (0.6)	1.85 (.00062)
>1097	(2000)	2451 (1.5)	0.507 (.00017)

   c. Nucleate Boiling: $T_{wL} = T_{sat} + \Delta T_{SH}$, ($\Delta T_{SH}$ = 283°K or 50°F)

2. Gas O_2 Heat Transfer

   Approximation of ALRC correlation (Ref. 26) prediction for

   $P = 34$ atm (500 psia), $T_b = 153°K$ (275°R)

   $$\frac{hd^{.05}}{(\rho V)^{.95}} = 1.82 \times 10^{-2} (8.65 \times 10^{-5})\ [0.7\ (T_w/T_b)^{-.8}]$$

   h - kW/m^2-°I (Btu/in^2 sec°F)

   d - cm (in)

   ρV - Kg/m^2-s (lb/sec ft^2)

   T_w, T_b - °K (°R)

3. Two-Phase O_2 Heat Transfer

   a. Film boiling based on Giarratano and Smith Correlation (Ref. 28)

x, quality	h_{2ph}/h_{gas}
0 - .01	0.25
0.1	0.35
0.5	0.65
1.0	1.0

   b. Burnout or Critical Heat Flux

   Based on shippingport correlation for water (Ref. 29)

   $p = 37.4$ atm (550 psia)

   $\phi_{BO} = 981.\ (0.6)\ [\frac{H' - H}{H' - H_o}]$, kW/$m^2$ (Btu/in^2 sec)

   $H_o = H_f = -16.5$ KJ/Kg (-7.1 Btu/lb)

   $H' = H_f + .724\ \Delta H_{fg}\ [(1 - \frac{12.9}{\Delta H_{fg}})\ \frac{0.395}{\rho V}\ ]$ KJ/Kg

   $H' = H_f + .724\ \Delta H_{fg}\ [(1 - \frac{30}{\Delta H_{fg}})\ ^{1.93/\rho V}\ ]$ (Btu/lb)

   c. Nucleate Boiling: $T_{wl} = T_{sat} + \Delta T_{sh}$, ($\Delta T_{SH}$ = 283°K or 50°F)

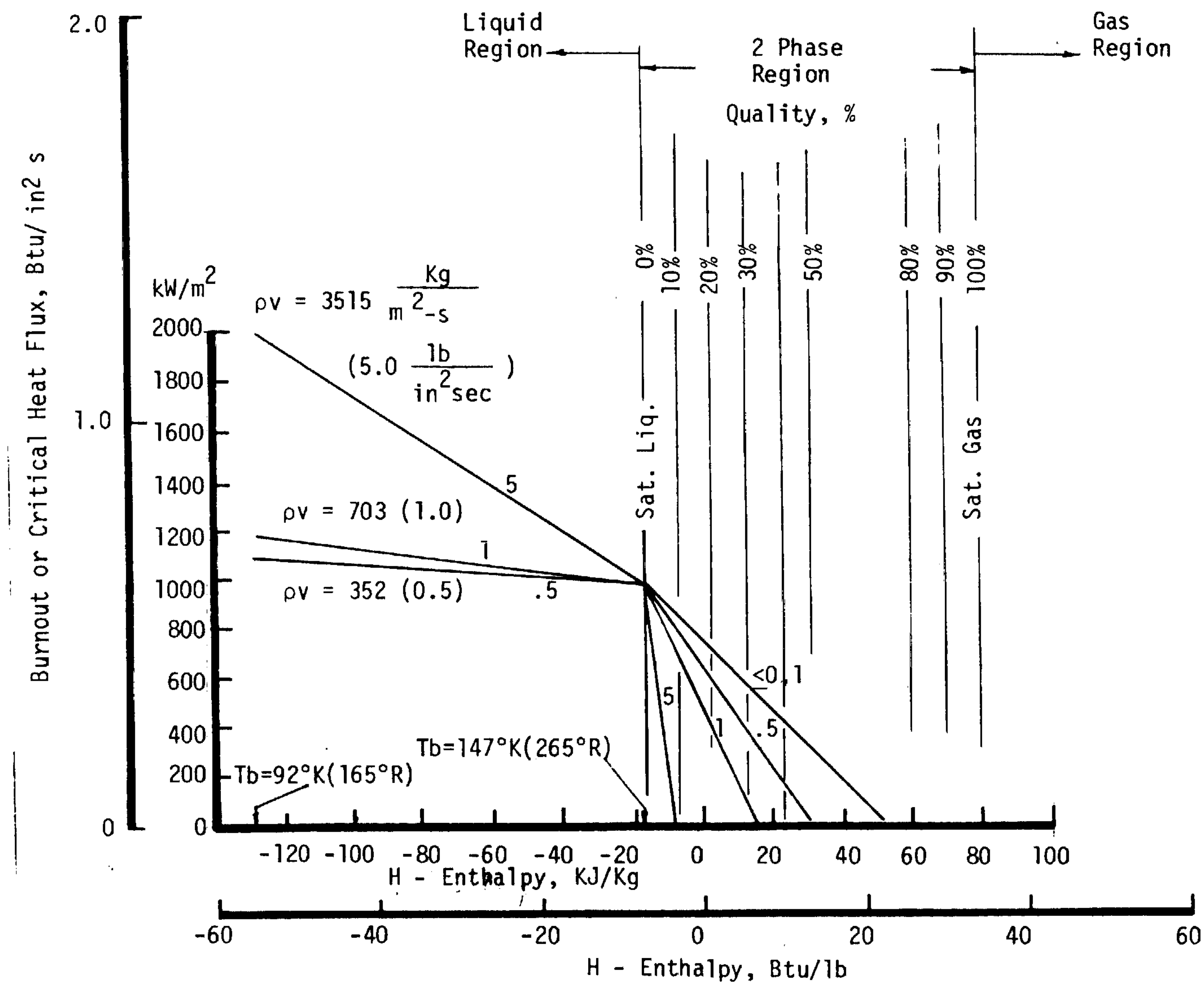

Figure 94. Estimated Critical Heat Flux Characteristics of Oxygen.

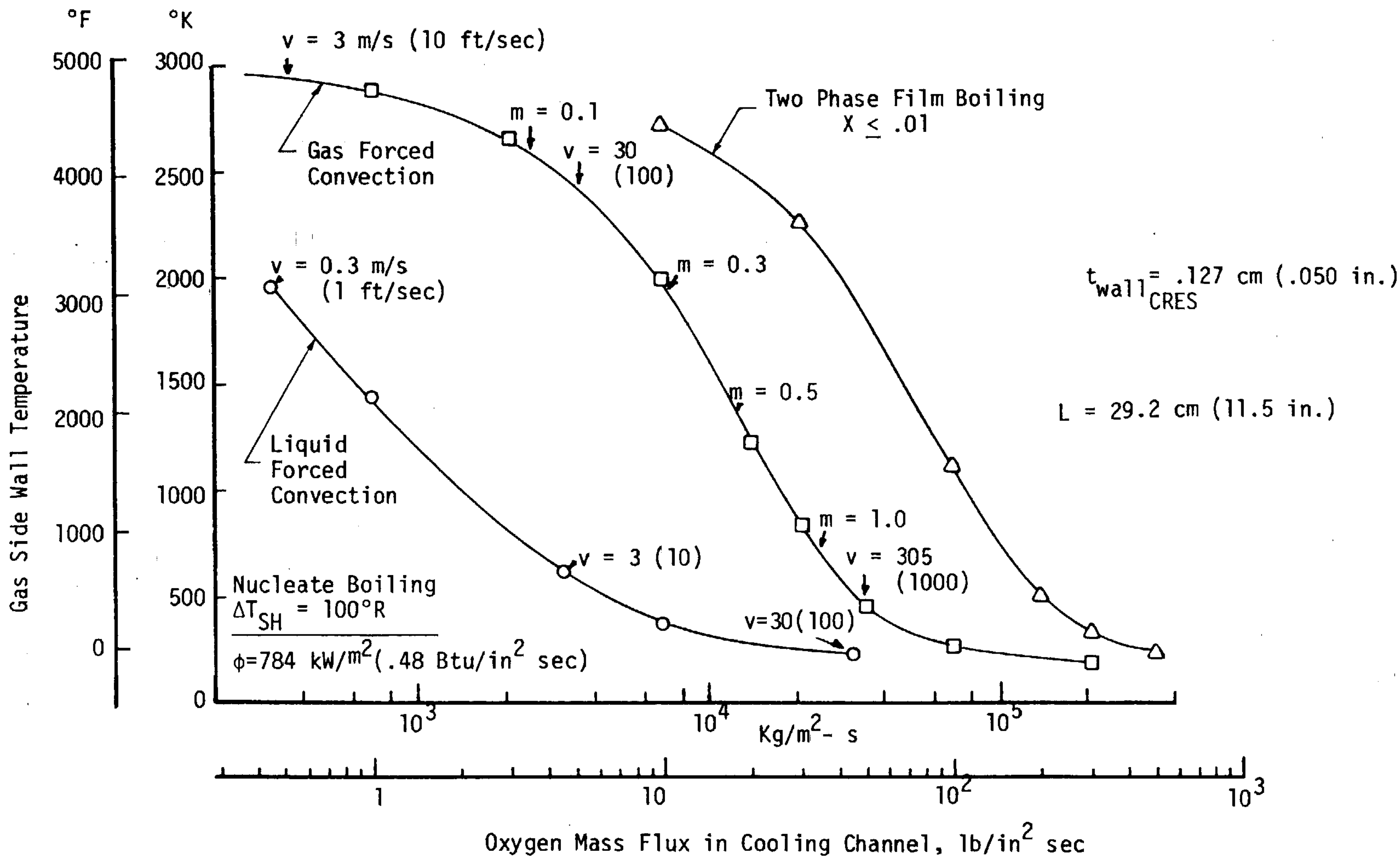

Figure 95. Gas-Side Wall Temperature Versus O_2 Mass Flux, Module Exit Plane.

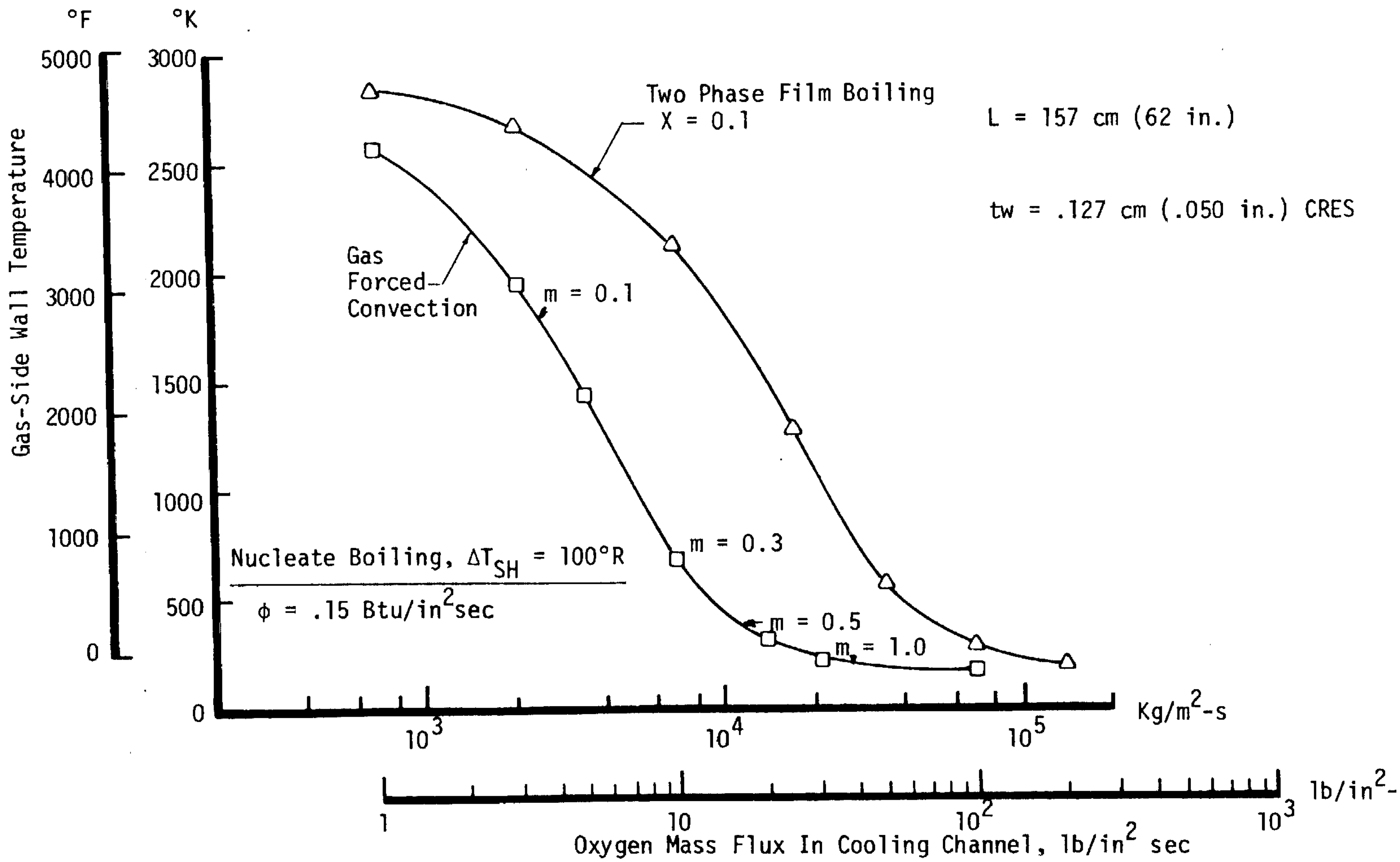

Figure 96. Gas-Side Wall Temperature Versus O_2 Mass Flux, Downstream End of Plug.

wall temperature at the module exit and at the downstream end of the plug as a function of coolant oxygen mass flux and the coolant state. At the module exit (Figure 95) acceptable wall temperature can be maintained by liquid oxygen cooling with a nucleate boiling of a forced convection mechanism but excessive Mach number (>0.5) are required for gas. The results plotted on Figure 96 shows that gas cooling is feasible at the downstream end of the plug as a wall temperature of about 811 °K (1000°F) can be maintained with a coolant Mach number less than 0.3.

° Coolant Channel Design

Preliminary design calculations for sizing the cooling channels of an oxygen cooled (counter flow) plug are summarized in Table XXXII. A 92°K (165°R) liquid oxygen inlet temperature was assumed.

At the coolant inlet (z = 29.2 cm or 11.5 in), the oxygen is a subcooled liquid and it is desirable to avoid film boiling. Consequently, the coolant velocity is governed by critical heat flux consideration. A 0.6 m/s (2 ft/sec) velocity is sufficient to yield an adequate burnout safety factor (1.5). The required mass flux is 0.07 Kg/cm^2s (1.0 lb/in^2 sec).

At the next analysis station (z = 50.8 cm or 20 in), the heat flux is lower and the oxygen is still significantly subcooled. As a result, the required velocity is lower 0.37 m/s (1.2 ft/sec).

At the third analysis point (z = 76.2 cm or 30 in), the oxygen bulk temperature has reached the saturation temperature (147°K at p = 37.4 atm, or 265°R at p = 550 psia assumed) and bulk boiling is beginning to occur.

As long as the oxygen remains slightly subcooled, nucleate boiling can be easily maintained. However, after a certain amount of bulk boiling occurs, it is difficult to maintain nucleate boiling on the coolant channel walls.

For the fourth analysis point, z = 101.6 cm (40 in), the coolant is 48% vapor and the estimated critical heat flux characteristic (Figure 94) indicates that reduced mass fluxes are required to maintain nucleate boiling and avoid film boiling. This is necessary to avoid annular flow where the liquid does not touch the wall. The approach is indicated by option (a) for the z = 101.6 cm analysis point where the channel area has been increased by a factor of 5. Options (b) and (c) are film boiling designs in which the wall is cooled to a 811-1367°K (1000-2000°F) temperature by decreasing the channel flow area (by a factor of 28-52) so that annular flow does occur but the gas velocity adjacent to the wall is sufficient to provide the required cooling.

TABLE XXXII - COOLING CHANNEL DESIGN CALCULATIONS, OXYGEN COOLED PLUG

Parallel Flow - Ox Cooled Plug
$\epsilon_m = 40:1$ $\epsilon_{plug} = 400:1$

Analysis Point	(Z) Location(1) cm (in)	T_{bulk} °K (°R)	Coolant(2) State	Cooling(3) Mechanism	q/A_2 kW/m^2 (Btu/in^2 sec)	$\dot{w}/A_2$ kg/m^2-s (lb/in^2 sec)	Remarks
1	29.2 (11.5)	92 (165)	Subcooled Liquid	N.B.	784 (0.48)	703(1.0)(min)	V = 0.61 m/s (2 ft/sec), BOSF = 1.5
2	50.8 (20)	125 (225)	Subcooled Liquid	N.B.	539 (0.33)	352 (0.5)	V = 0.37 m/s (1.2 ft/sec), BOSF = 1.9
3	76.2 (30)	147 (265)	Saturated Liquid	a) N.B. b) F.B.	392 (0.24)	352 (0.5) 29,500 (42)	V = 0.49 m/s (1.6 ft/sec), BOSF = 2.5 Twg = 1367°K (2000°F)
4	102 (40)	147 (265)	2-phase x = .48	a) N.B. b) F.B. c) F.B.	327 (0.20)	70 (0.1)(max) 9,840 (14) 18,280 (26)	Twg = 228°K (-50°F) Twg = 1367°K (2000°F) Twg = 811°K (1000°F)
5	127 (50)	147 (265)	2-phase x = .84	a) N.B. b) F.B. c) F.B.	278 (0.17)	No solution 4,900 (7) 9,840 (14)	(Quality too high for N.B.) Twg = 1367°K (2000°F) Twg = 811°K (1000°F)
6	157 (62)	150 (270)	Gas	G.F.C.	131 (.08) 180 (.11)	3,800 (5.4) 6,300 (9.0)	Twg = 1367°K (2000°F) Twg = 811°K (1000°F)
7	Base at outer radius	150 (270)	Gas	G.F.C. G.F.C.	57 (.035) 82 (.05)	1,550 (2.2) 2,740 (3.9)	Twg = 1367°K (2000°F) Twg = 811°K (1000°F)
8	Base at Center	156 (280)	Gas	G.F.C. G.F.C.	131 (.08) 180 (.11)	3,800 (5.4) 6,300 (9)	Twg = 1367°K (2000°F) Twg = 811°K (1000°F)

Notes: (1) z = Axial position from module throat.

(2) x = Quality = wt. % of gas in mixture.

(3) N.B. = Nucleate boiling
F.B. = Film boiling
G.F.C. = Gas forced convection

At the fifth analysis point, the quality is 84% and it is no longer possible to maintain nucleate boiling. However, adequate wall temperatures can be maintained with the film boiling mode as indicated in options (b) and (c).

The results obtained for analysis points 3, 4 and 5 show there are two choices for the coolant channel design in the two-phase region: (1) a design which includes a two-phase nucleate boiling region, and (2) a design which does not. The design which does not include two-phase nucleate boiling is considered most practical for fabrication purposes. A design which does include a nucleate boiling region would have a lowest pressure drop but would be extremely difficult to design and fabricate since it would be necessary to first increase the flow area by a factor of five (decrease the mass flux from 0.035 to 0.007 kg/cm^2 s or 0.5 to 0.1 lb/in^2 sec), and then decrease it by a factor of at least 70 (increase mass flux from 0.007 to 0.49 kg/cm^2 s or 0.1 to 7 lb/in^2 sec).

Cooling of the plug base region is relatively straight-forward since it involves only gas-forced convection heat transfer.

° Pressure Drop Estimate

The pressure drop in an oxygen cooled plug was estimated by assuming that the coolant channels would be designed for film boiling in the two-phase region. The coolant channel geometry and pressure drop calculations are summarized in Table XXXIII.

The estimated loss was over 47.6 atm (700 psi) which is so large that it probably rules out oxygen plug cooling as a practical concept. Most of the pressure drop is estimated for the two phase region where the estimated friction loss is 39.8 atm (585 psia). The two-phase flow ΔP was estimated using the Ref. 30 water data as indicated in Figure 97.

E. BASE PRESSURIZATION ANALYSIS

The early literature, summarized in Section III.C.1, Figures 15 and 16 and Table IV, indicates that only a small relative base flow rate (about 0.2%) is required for a large area ratio plug nozzle operating in vacuum conditions where the wake is closed aft of the plug base. Analysis of these data for vacuum operation reveals that the base pressure, corresponding to the 0.2% flow, is 2.5 times the static pressure of the exhaust gas on the edge of the expansion section of the plug. This value is recognized to be the standard separation criteria ($P_e \geq 0.4\ P_{ambient}$) for DeLaval nozzles. (Also given as $P_e \geq 0.28\ P_{ambient}$ for high area ratio nozzles in Reference 42.)

Achievement of the optimum base pressure may or may not require a finite mass flow into the base, the amount presently being determined from experiment (See Table X and Figure 35). Since the amount of flow should be dependent upon both the diameter of the base and the pressure level, an equation (Eq. 17, Section IV,E.3) was formulated for the parametric analysis using Aerospike (Ref. 6) data.

TABLE XXXIII - PRESSURE DROP ESTIMATE, OXYGEN COOLED PLUG

Coolant Channel Design Assumed: L/W = 4.0 305 Channels

Z Plug Axial Location cm(in)	R cm(in)	T_b °K(°R)	State	Cooling Mechanism °K (°F)	$\dot{w}/A$ kg/m^2-s (lb/in^2 sec)	w cm (in)	d cm (in)	L cm (in)
29.2 (11.5)	124 (49)	92 (165)	Sub. Liq.	NB	703 (1.0)	.51 (.2)	1.3 (.5)	2.0 (.8)
50.8 (20)	114 (45)	125 (225)	Sub. Liq.	NB	703 (1.0)	.51 (.2)	1.3 (.5)	1.8 (.72)
76.2 (30)	105 (41.5)	147 (265)	Sat. Liq.	NB FB 1367(2000)	703 (1.0) 29,500 (42)	.51 (2) .12 (.049)	1.3 (.5) .12 (.049)	1.7 (.65) 2.0 (.80)
102 (40)	98 (38.5)	147 (265)	2 phase x = .48	FB 1089(1500)	11,950 17	.31 (.121)	.12 (.049)	1.69 (.665)
127 (50)	91 (36)	147 (265)	2 phase x = .84	FB 811 (1000)	9,840 14	.31 (.121)	.15 (.0595)	1.56 (.614)
157 (62)	85 (33.5)	150 (270)	Gas	FC 811 (1000)	6,300 9	.31 (.121)	.24 (.0926)	1.43 (.563)
Base	85 (33.5)	150 (270)	Gas	FC 811 (1000)	2,800 4	.31 (.121)	.53 (.208)	1.43 (.563)
Base	38 (15)	154 (278)	Gas	FC 811 (1000)	6,300 9 (min)	.31 (.121)	.24 (.0926)	0.47 (.185)
Base	15 (5.88)		Gas	FC 811 (1000)	6,300 9 (min)	.31 (.121)	.24 (.0926)	
Base	0	156 (280)	Gas					

w = Cooling Channel Width   d = Channel Depth T_b = Bulk Temperature

L = Land Width T_w = Wall Temperature

Region	Plug Axial Location cm(in)	Inlet ΔP, atm (psia)	Friction ΔP, atm (psia)	Exit ΔP, atm (psia)	Turn ΔP, atm (psia)	Total ΔP, atm (psia)
Liquid Cooled	29.2-76.2 (11.5-30)	.002 (03)	.16 (2.4)	--	--	0.2 (2.4)
2 Phase Cooled	76.2-147.3 (30-58)	2.4 (36)	39.8 (585)	--	--	42.3 (621)
Gas Cooled	>147.3 (58) (includes base)	--	5.8 (85)	1.2 (18)	0.8 (12)	7.8 (115)
					Total Pressure Drop:	50.2 (738)

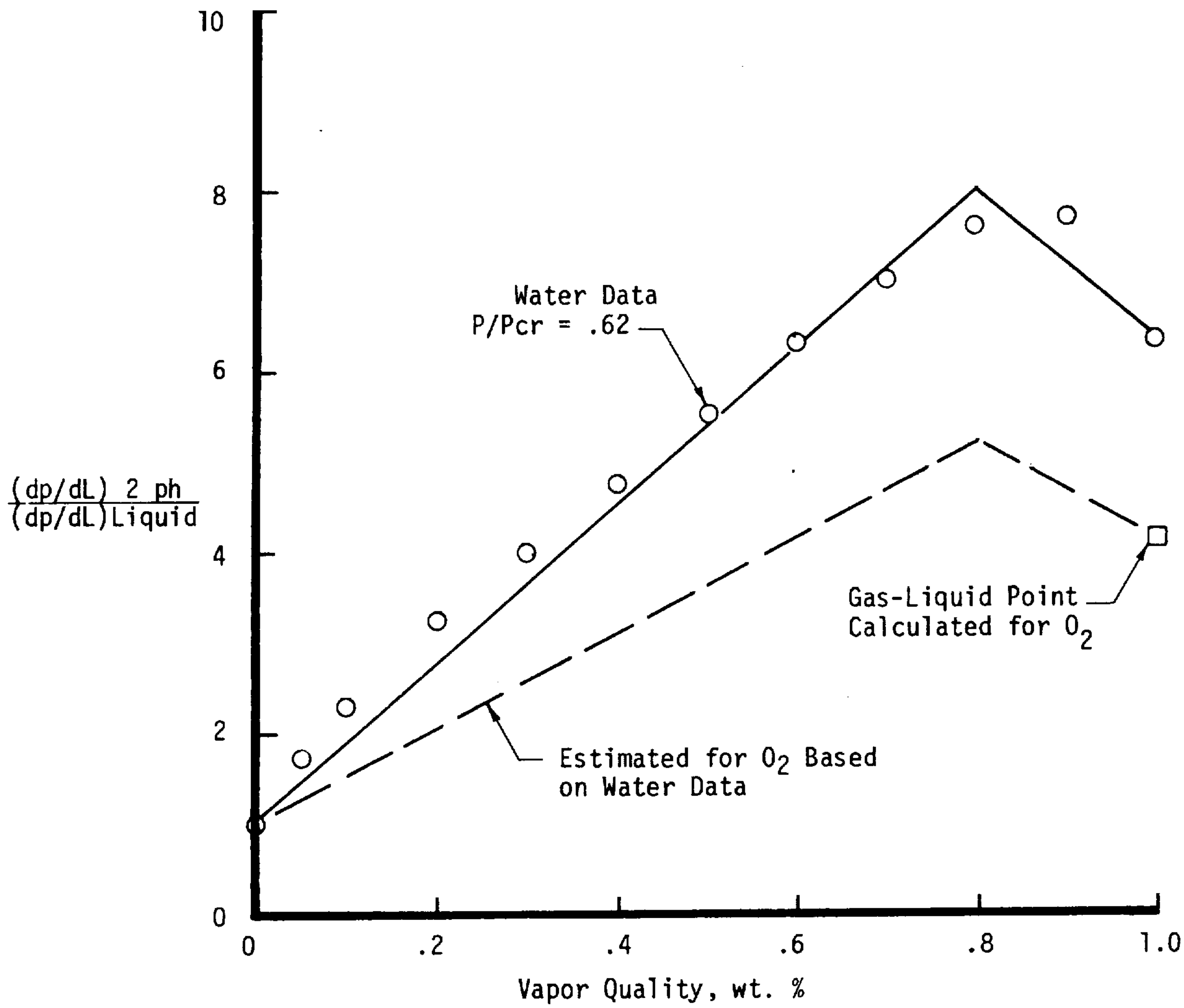

Figure 97. Two-Phase Pressure Drop Correlation.

$$\dot{w}_{base} = K\, P_{base}\, A_{Base} \qquad \text{(Eq. 15)}$$

In solving this equation for the flow rate, it is assumed that the flow pressure is given by

$$P_{base} = 2.5\, P_e$$

where P_e is the ODE pressure at the engine area ratio.

The performance improvement obtained by a base pressurization correction using Eq. 15 is seen to be between 0.3 to 2.1% 1 to 10 seconds specific impulse as shown in Figures 46-50 of Section IV. This improvement seems reasonable when compared with the 2.4% thrust increase due to base pressurization of the Aerospike (see Section IV,E.3.)

The schematics for the various engine cycles utilizing base pressurization are given in Figures 61-70 (Section V.B.) In all cases, the performance improvement was sufficient to justify the additional weight (2 to 5 lbs) required to achieve pressurization (see Section VI.)

F. CONFIGURATION ANALYSIS

Plug cluster engine configuration layouts were prepared for candidate cycles utilizing modules with area ratios of 40,100 and 200:1. These layouts (Section VI.B), in conjunction with the parametric weight analysis (Section V.G.), and the parametric engine performance (Section IV.E.), led to the selection by the NASA Project Manager of the configurations:

- ITA Module (ε_M = 40), δ/D_e = 2
- Minimum Change ITA, δ/D_e = 2
- Regeneratively Cooled Modules (ε_M = 100), δ/D_e = 1

The cycles selected for these configurations were the expander cycle (EX02) with an RL10 turbopump assembly and a gas generator cycle with a state-of-the-art technology turbopump design. Both cycles were to utilize an H_2-cooled plug.

G. PARAMETRIC WEIGHT ANALYSIS

For purposes of the parametric weight study, the plug cluster engine was assumed to be composed of a combination of the following components:

- Regeneratively Cooled Combustion Chamber (WCC)
- Regeneratively Cooled Thrust Chamber Nozzle (WTCN)
- Thrust Chamber Nozzle Extension (WNOZ)
- Main Injector (WINJ)

- ° Ignition System (WIGN)
- ° Main Turbopump (with Gear Box) (WTPA)
- ° Main Turbopump (Parallel Turbines) (WTPA)
- ° Valves and Actuators (WV)
- ° Propellant/Gas Lines (WL)
- ° Gas Generator (WGG)
- ° Miscellaneous (Electrical Harness, Instrumentation, Brackets, Engine Mount, Gimbal (WMISC)
- ° Plug Nozzle (WPN)

The engine dry weights do not include:

- ° Gimbal Actuators and Actuation System
- ° Engine Controller
- ° Pre-Valves
- ° Tank Pressurant Heat Exchangers and Associated Equipment
- ° Contingency (a total contingency is normally included in the vehicle weight statement)

Baseline engine weight statements were established for the expander and gas generator cycle engines by comparing like components with the RL10 IIB, the single- and double-panel Aerospike, and the Advanced Space Engine. These baseline weights were revised during the program to conform to the preliminary conceptual design layouts. The initial component weights utilized in the parametric analysis, are given in Table XXXIV (see Section VI for revised weights and a detailed breakdown by component).

TABLE XXXIV. PLUG CLUSTER BASELINE WEIGHT SUMMARY FOR PARAMETRIC ANALYSIS

Component	Baseline Weight kg (lb) Expander Cycle		Baseline Weight kg (lb) Gas Generator Cycle		Comments
WCC (per module)	2.12	(4.68)	2.12	(4.68)	All modules
WTCN (per module)	3.2	(7.0)	3.2	(7.0)	Regen Module Only
WNOZ (per module)	1.6	(3.6)	1.6	(3.6)	ITA Module Only
WINJ (per module)	1.88	(4.14)	1.88	(4.14)	All Modules
WIGN	9.9	(21.9)	11.9	(26.3)	All Chambers
WTPA (Gear Box)	31.8	(70.0)	31.8	(70.0)	RL10 TPA
WTPA (Parallel Turbines)	21.3	(47.0)	21.3	(47.0)	All Cycles
WV	10.4	(22.9)	10.4	(22.9)	Will Vary for GG
WL	17.4	(38.3)	17.4	(38.3)	Will Vary for GG
WGG			2.5	(5.6)	GG Cycle Only
WMISC	27.4	(60.5)	27.4	(60.5)	All Cycles
WPN	38.8	(85.5)	38.8	(85.5)	All Cycles

With the baseline engine weight established, engine component weight scaling relationships were derived as a function of thrust, chamber pressure, and nozzle area ratio. These scaling relationships were used to calculate the weights over the parametric ranges of interest. The equations, which were established through geometry considerations and empirical data fits of historical data (References 23, 31, 32), were modified to obtain the best fit for a variety of engine types (References 5, 9, 14, 23, 32-34).

The results of the parametric weight analysis are presented in Figures 98 and 99 for chamber pressure of 20.4 and 34 atm respectively. It is seen that the engine weight for a module area ratio of 200 becomes excessive. For this reason, configurations with 200:1 modules were not selected for further study. The inclusion of AGCarb nozzle extensions later in this study, however, showed that area ratios as high as 500:1 could be utilized.

H. THRUST VECTOR CONTROL ANALYSIS

Preliminary analytical evaluation of four basic thrust vector control (TVC) concepts for the plug cluster rocket engine was accomplished. The four concepts are gimbaling, throttling or engine out, hinged panels, and secondary injection.

The initial evaluation involved an assessment of the moment generating capability for all the concepts. The required TVC moment generating capability is identical to that moment which would be generated by a 66.7 KN (15,000 lbf) thrust engine operating at a gimbaled angle of 4 degrees or 21,280 joules (188,342 inch-pounds). The analysis and test information contained in Pratt and Whitney Aircraft Report PWA FR-1013, Reference 4, formed the basis for this portion of the study. The information was manipulated to yield the lateral force, the axial force, and the moment producing displacement of the axial force for the following TVC concepts:

- Gimbaling - The only mode of operation considered is the so-called hinged motion of a modular engine in a plane which intersects the plug nozzle centerline. The corresponding moment generating capability is shown in Figure 100 for 1, 2, and 3 hinged modular engines. The required moment of 21,280 joules (188,342 inch-pounds) can be achieved by this TVC scheme with one module at a hinge angle of 52 degrees.

- Throttling or Engine Out - The differential throttling of modules will result in the moment generating capability shown in Figure 101 for 2, 3, and 5 throttled modular engines. The required moment can be achieved by throttling 3 engines to approximately 12% nominal thrust.

- Hinged Panels - The hinging of a panel or flap consisting of a 60 degree sector of the plug surface located at the upstream end of the plug nozzle will result in an estimated longitudinal force of 71,981 N (16, 182 pounds) for a panel or flap hinge angle of 18 degrees. The assumed relationship between moment generating capability and hinge angle is shown in Figure 102. Note that the desired moment can be achieved with an estimated hinge angle of 34 degrees.

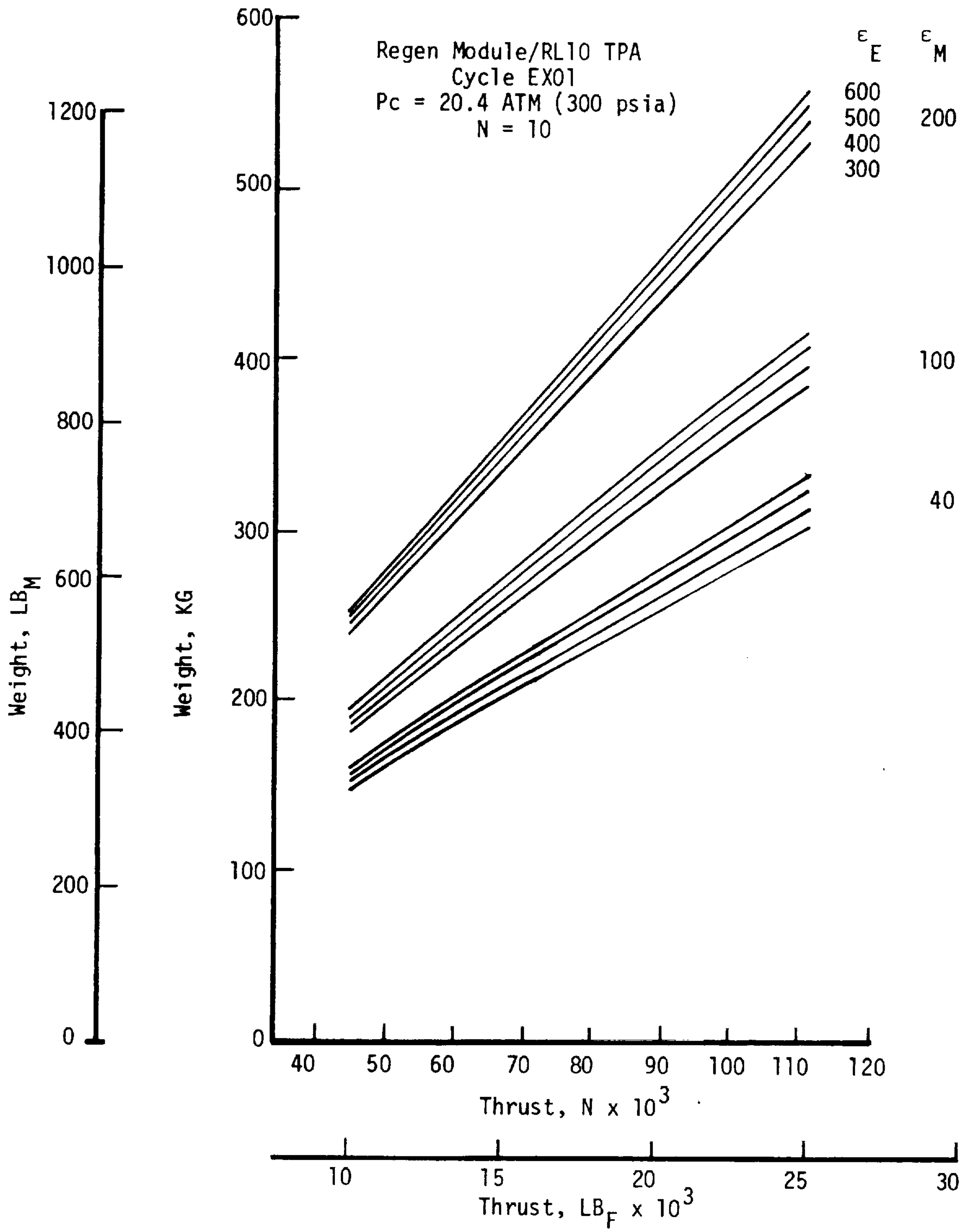

Figure 98. Plug Cluster Engine Dry Weight, Pc = 20.4 ATM.

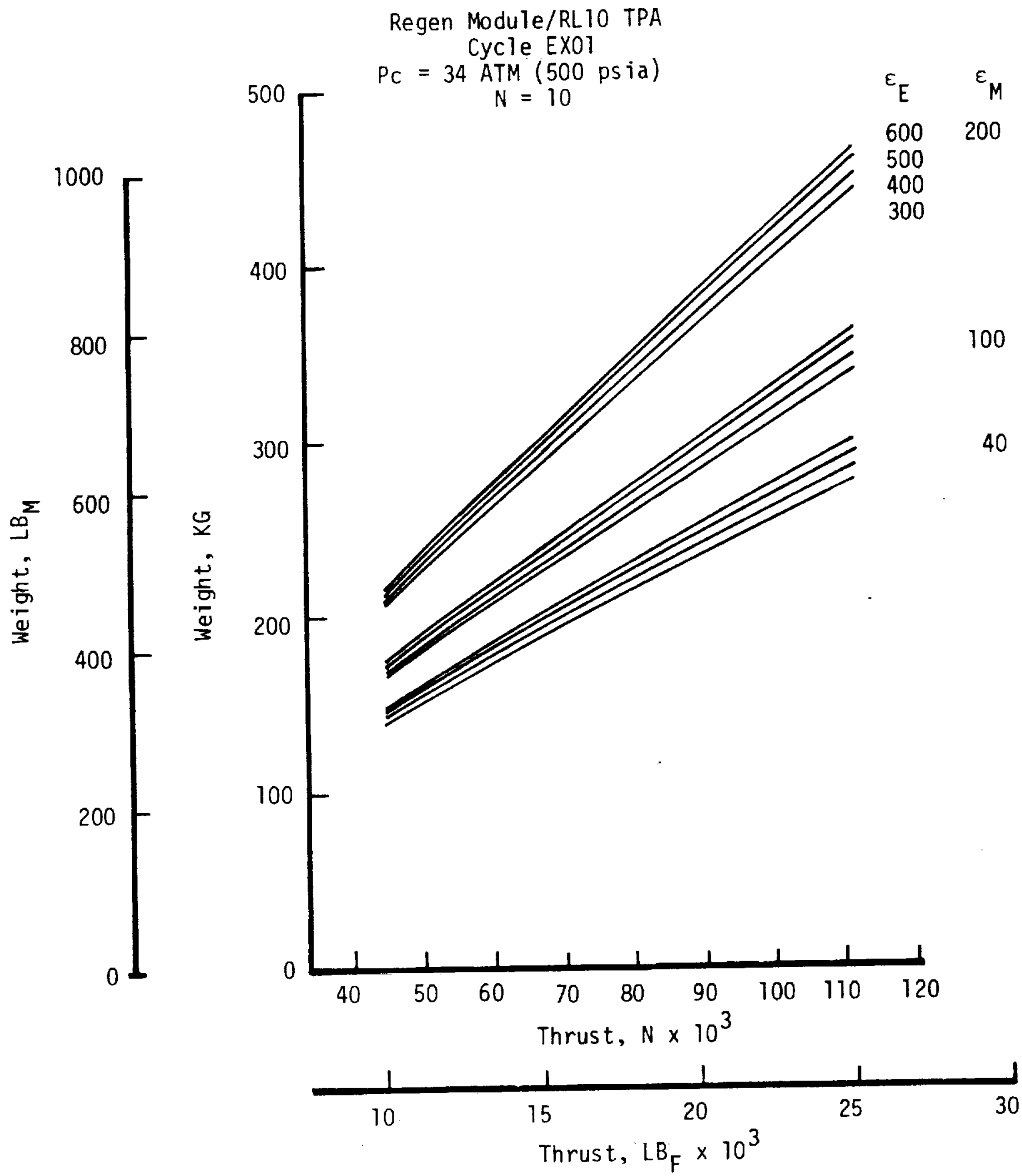

Figure 99. Plug Cluster Engine Dry Weight, Pc - 34 ATM.

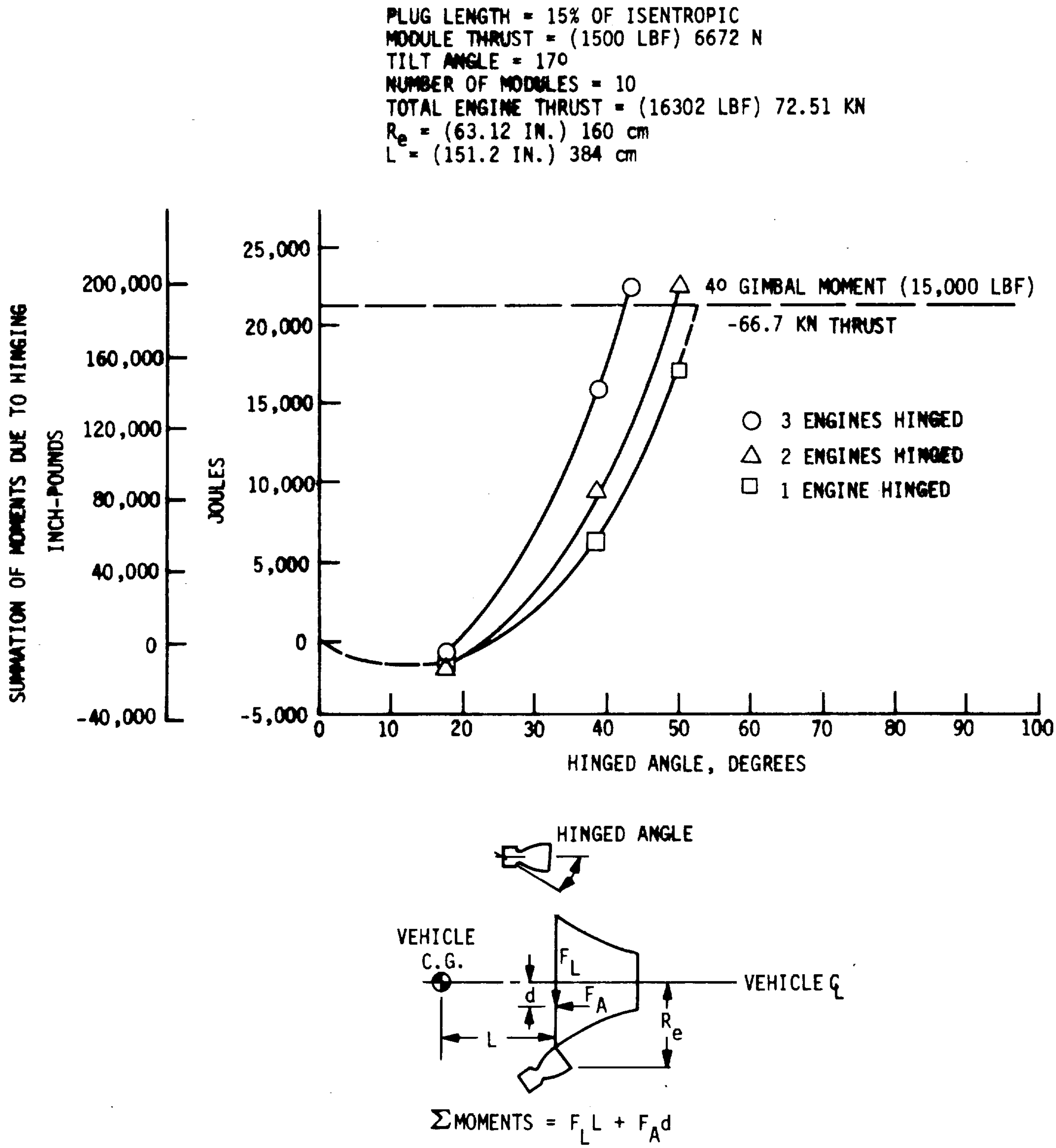

Figure 100. Moment Generating Capability for Hinged Engine Model Concept.

PLUG LENGTH = 15% OF ISENTROPIC
MODULE THRUST = (1500 LBF) 6672 N
TILT ANGLE = 17°
NUMBER OF MODULES = 10
TOTAL ENGINE THRUST = (16,302 LBF) 72.51 KN
R_e = (63.12 IN) 160 cm
L = (151.2 IN) 3.84 cm

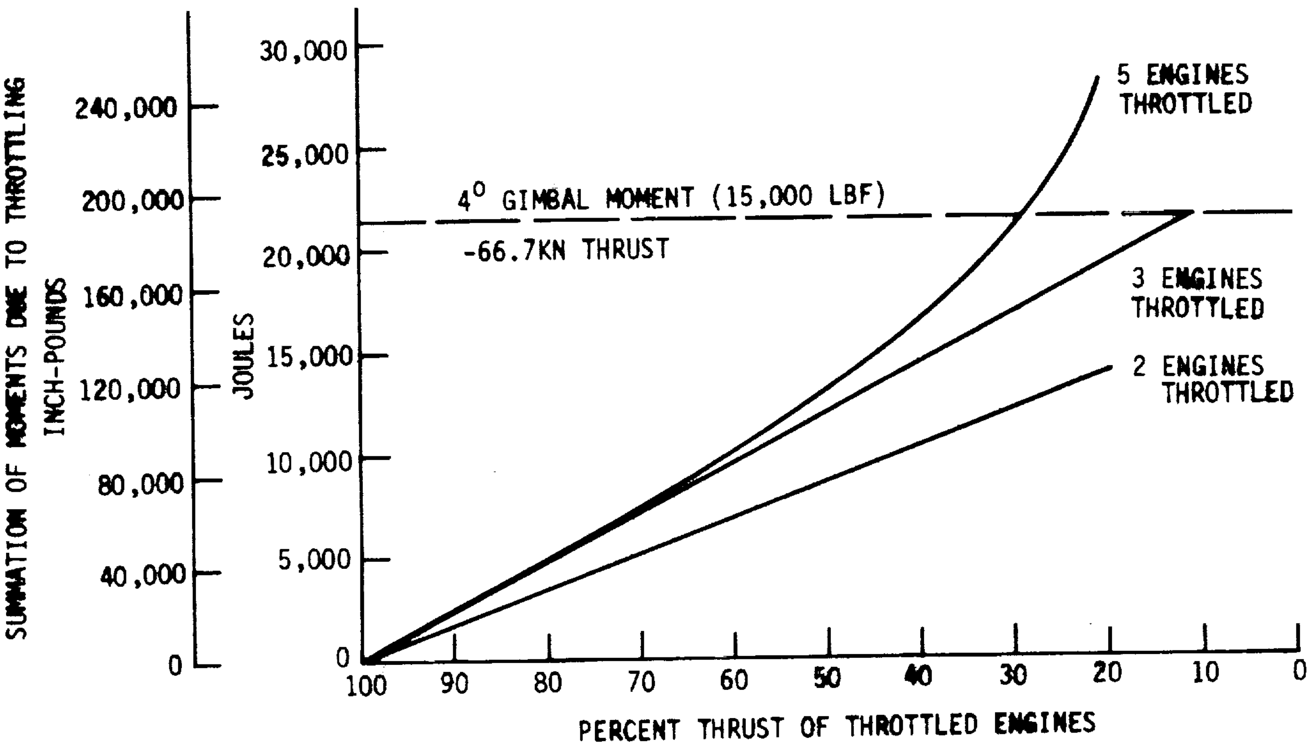

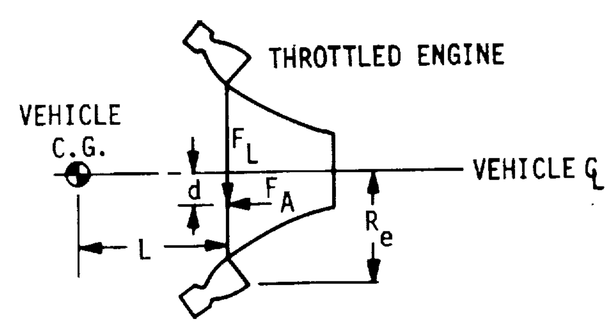

ΣMOMENTS = $F_L L + F_A d$

Figure 101. Moment Generating Capability for Throttled Engine Module Concept.

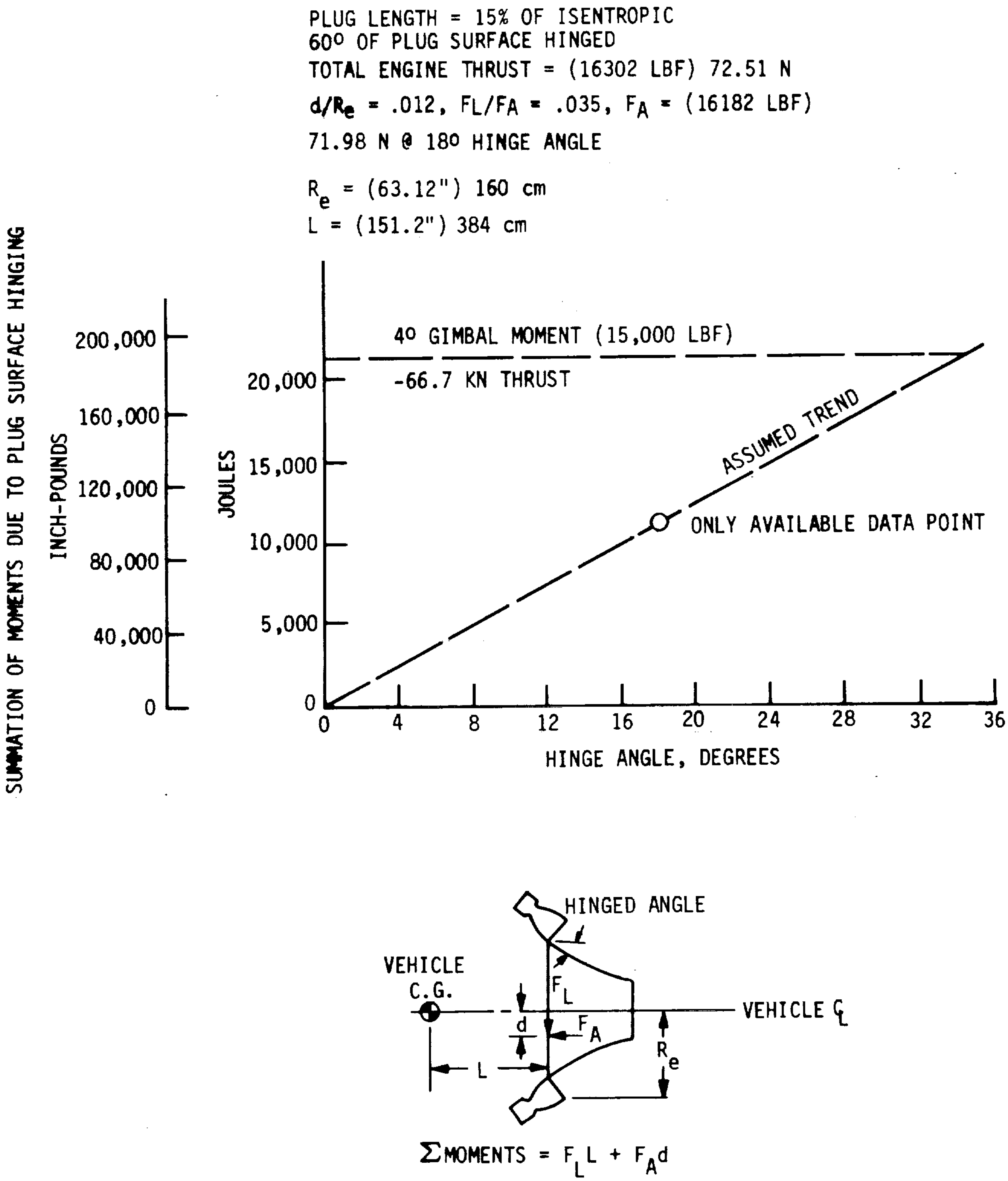

Figure 102. Moment Generating Capability for Hinged Panel Concept.

° Secondary Injection - The injection of fluids into the supersonic primary stream produces a shock wave which causes an asymmetrical pressure distribution on the plug nozzle wall. The resulting lateral force and axial force displacement characteristics were evaluated for both gas slot injection at the end of the plug and for gas injection at the outside diameter (OD) of 50 percent of the modules. The moment generating capability for slot injection is shown in Figure 103. Only slot injection yields the required moment and this occurs at a relative weight flow of 4.5 percent. Relative weight flow is defined as the ratio of secondary injection flow to total primary flow converted to percent.

The next phase of the preliminary evaluation of the four basic TVC concepts involved an estimation of the control hardware characteristics necessary to achieve the equivalent of the following gimbaled single engine requirements.

- Gimbal angle = 4 degrees
- Rate = 4 deg/sec
- Frequency Response = flat to 5 hertz

Table XXXV contains a tabulation of the estimated control hardware characteristics. The actuation system estimated weights for hinged modules were found to be similar for both hydraulic (including pump) and electromechanical systems using historical data from past programs. The throttling, engine out, and secondary injection systems will require flow control valves which, in turn, must be operated by an actuation device. The estimated pressure drop and weight flow requirements were converted to a fluid K_W requirement [K_W = weight flow/(pressure drop x specific gravity)$^{1/2}$]. An array of historical data regarding the use of LOX and LH_2 valves and actuation devices on past engine programs was likewise arranged as a function of K_W and provided the basis for the estimation of both the weight and envelope dimensions. Electromechanical actuation was presumed for the valves in this study based upon past actuation trade studies.

A Summary evaluation of the TVC schemes proceeds as follows:

° Gimbaling - A minimum of four hinged modular engines are required to achieve pitch and yaw control with a total actuation system weight of approximately 36.3 Kg (80 pounds). The required maximum module hinge angle is approximately 53 degrees. There are questions involving the mechanics of hinging the modules through a large angle that remain to be answered.

° Hinged Panels - A minimum of four hinged panels are required to achieve pitch and yaw control with a total hydraulic actuation system weight of approximately 83.5 Kg (184 pounds). The required maximum panel hinge angle of 34 degrees is based upon very little data and more information is necessary to determine the effects of panel shape, size, location and hinge angle. A 34 degree panel hinge angle raises questions concerning the erosion of the panel while deflecting the combustion gases.

C-7

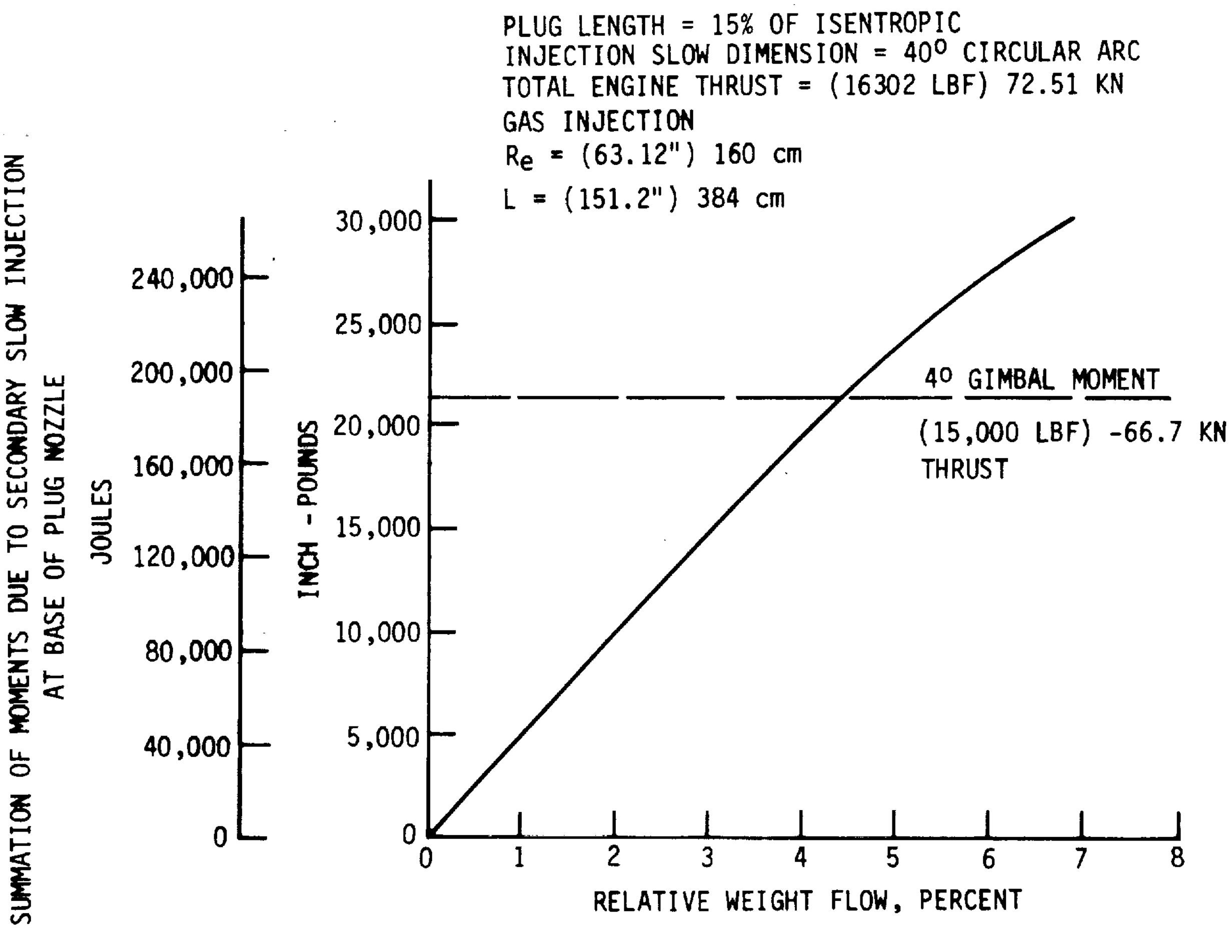

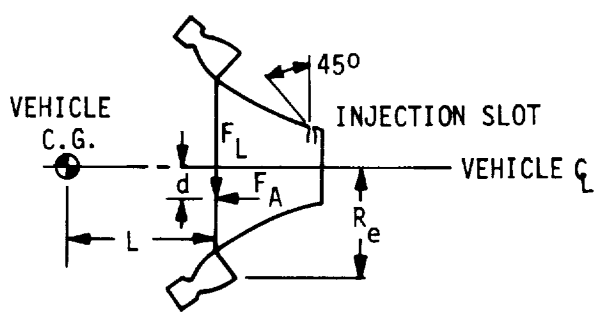

ΣMOMENTS = $F_L L + F_A d$

Figure 103. Moment Generating Capability for Secondary Injection Concept.

TABLE XXXV - ESTIMATED CONTROL HARDWARE CHARACTERISTICS

		ACTUATION SYSTEM			FLOW CONTROL POPPET VALVE/ACTUATOR COMBINATION					
TCV CONCEPT	MINIMUM* NUMBER OF CONTROL UNITS	STROKE Cm(in.)	RATE Cm/s (in/sec)	WEIGHT Kg (lb)	FLUID K_w $\frac{Kg\text{-}Cm}{s\text{-}N^{1/2}}$ $\frac{lb\text{-}in.}{s\text{-}lbf^{1/2}}$	DIA. Cm (in)	WEIGHT Kg (in)	DIA. Cm (in)	LENGTH Cm (in)	AVERAGE POWER (WATTS)
Gimbal (Hinged Modules	1 Module	16.0 (6.3)	16 (6.3)	9.1 (20)/module						
Hinged Panels	1 Panel	8.9 (3.5)	8.9 (3.5)	20.9 (46)/panel						
Throttling	3 Modules									
Fuel Circuit					0.91 (1.67)	1.80 (0.71)	5.9 (13)	10.2 (4)	15.2 (6)	35
Oxidizer Circuit					2.11 (3.87)	2.74 (1.08)	9.1 (20)	15.2 (6)		40
Total							15 (33)/ Module			75/Module
Engine Out	3 Modules									
Fuel Circuit					Same as for Throttling					
Oxidizer Circuit					Same as for Throttling					
Secondary Injection (Gas)	1 Injection Slot at Plug Base				6.7 (12.3)	4.90 (1.93)	17.2(38)/ Slot	22.9 (9)	35.6 (14)	50/Slot

*Required to achieve a moment of 21,280 Joules (188,342 inch-pounds) in a single direction.

° Throttling or Engine Out - A minimum of three deeply throttled engine modules are required to achieve the required moment in a pitch or yaw plane. As a result, all ten engine modules must either be operated in a throttled mode or in an on-off mode to achieve the full pitch and yaw control. In either case, there will be two modules which will be required to respond to both a pitch and a yaw command. This overlap of control for two modules is not a problem if engine out or on-off control is used. In addition, engine out operation eliminates the potential combustion stability problem associated with deep throttling of engine modules. The total weight for the ten flow control valve/actuator combinations is approximately 150 Kg (330 pounds). The average power required to obtain adequate valve transient response is estimated to be 75 watts per module.

° Secondary Injection - A minimum of four gas injection slots located at the plug base are required to achieve pitch and yaw control. The total weight for the four flow control valve/actuator combinations is approximately 69 Kg (152 pounds). The average power required to obtain adequate valve transient response is estimated to be 50 watts per slot. Past tests at ALRC on the Minuteman secondary injection system indicate that the generated side forces are directly responsive to changes in injectant flow rate for frequencies up to 20 hertz. This concept raises questions concerning the weight and complexity associated with the hardware necessary to deliver the injectant to the flow control valve.

In conclusion, it appears from this preliminary analysis that hinging engine modules to achieve the required pitch and yaw control moments would be the most desirable concept from the standpoint of axial force capability, weight, and reliability. If weight reductions of 20% are made in the near future through the use of composite materials, the hinged module approach still appears the most promising.

SECTION VI

PRELIMINARY CONCEPTUAL DESIGN

A. OBJECTIVES AND GUIDELINES

Preliminary conceptual designs of selected plug cluster engine systems were generated based on the information developed in Tasks I-III for film and regeneratively cooled systems. The detail of the designs allowed the approximation of complete engine weights from which perturbations or tradeoffs could be conducted to optimize the plug cluster engine.

Tradeoff and sensitivity factors between subsystem operating points, plug cluster engine geometry, plug cluster engine performance, and installed engine weight, were established for the nominal configurations of the plug cluster engine.

An engine component list was prepared and compared with those for candidate engines in past Space Tug studies to assure that similar components and requirements were included in the weight statement. A common frame of reference was thus established for the weight of the plug cluster engine.

Consideration of AGCarb, carbon-carbon cloth, lightweight structures led to modification of portions of the conceptual designs. An AGCarb uncooled plug nozzle was investigated in depth. A cluster of large area ratio scarfed bell nozzles, with AGCarb nozzle extensions from $\varepsilon = 40$ to $\varepsilon = 500$, was also investigated.

B. CONCEPTUAL DESIGN

Conceptual design layouts were made for the expander and gas generator cycle configurations. Typical layouts are shown in Figures 104-106. These layouts contain individual valving for the igniters and two additional main propellant valves. This number of control elements is more than considered necessary for the minimum valve configuration. The selection of the more conservative system is based on the preliminary controls analysis presented in Section VI,E.

The RL10 turbopump assembly is shown for the expander cycle configurations (Figures 104 and 105), and a parallel turbine state-of-the-art TPA is shown for the gas generator cycle configuration (Figure 106).

Four different modules are utilized in the conceptual designs: (1) Integrated Thruster Assembly (ITA), (2) Minimum Modification ITA, and (3) Regeneratively cooled ITA with both a 40:1 and a 100:1 module area ratio. These are discussed in Section VI.F.

Three types of fairings are shown in the figures: (1) straight fairings, which historically have shown the highest performance, (2) contoured fairings, which appear to add excessive weight, and (3) scarfed nozzles, where the uncut portion of the nozzle becomes the contoured fairing.

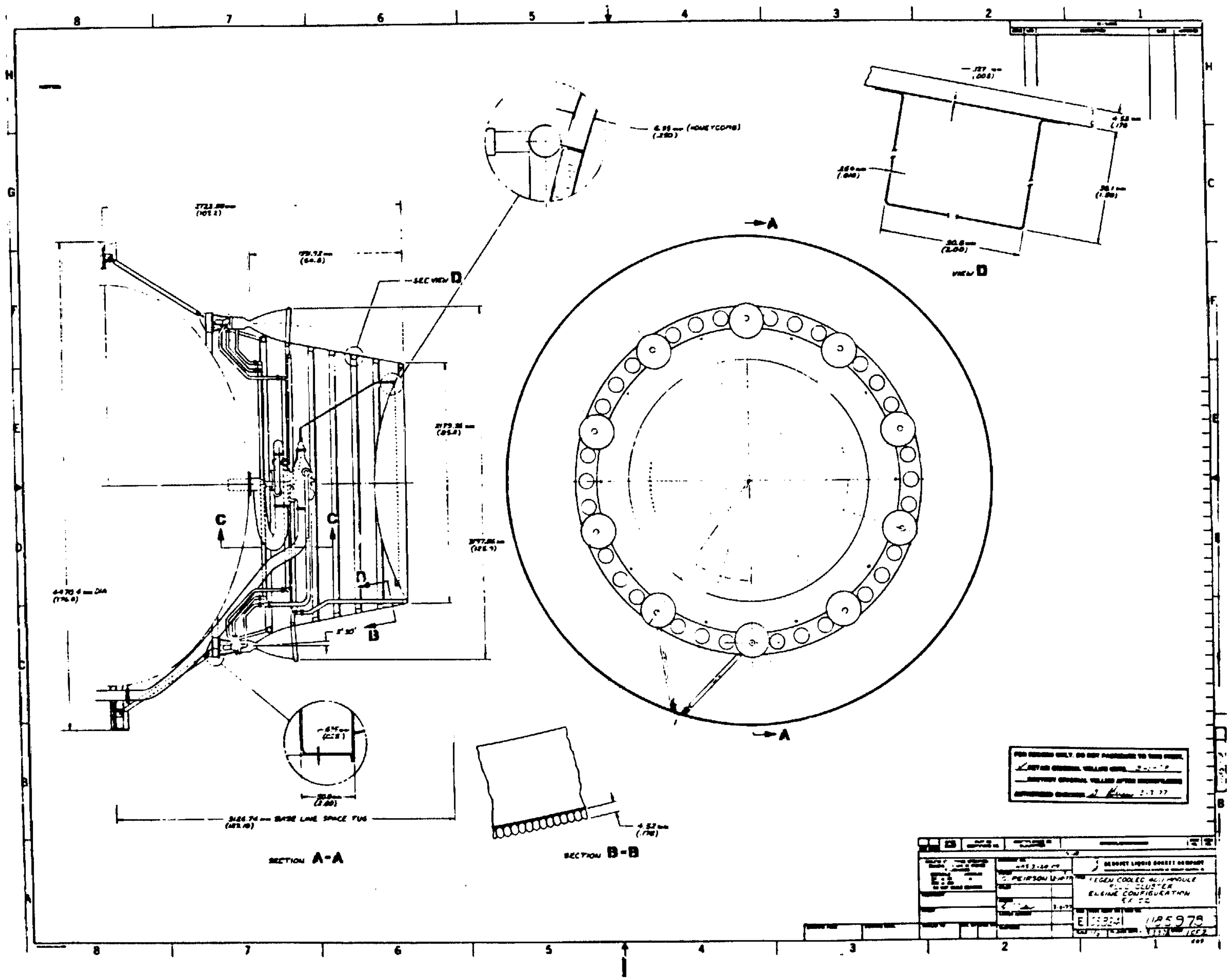

Figure 104. Regen-Cooled 40:1 Module Plug Cluster Engine Configuration EX02, Dwg No. 1185978 (Sheet 1 of 2)

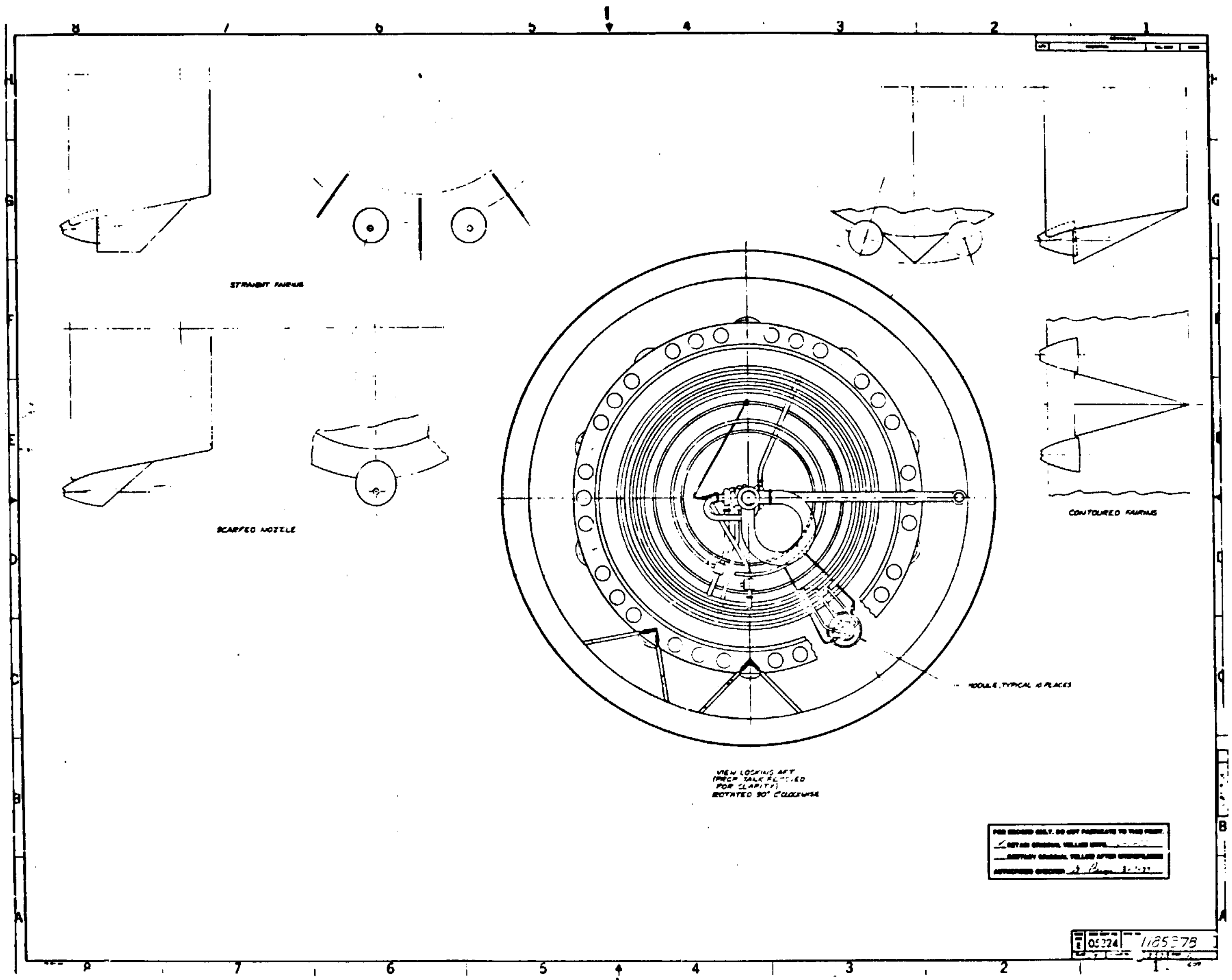

Figure 104. Regen-Cooled 40:1 Module Plug Cluster Engine Configuration EX02, Dwg No. 1185978 (Sheet 2 of 2)

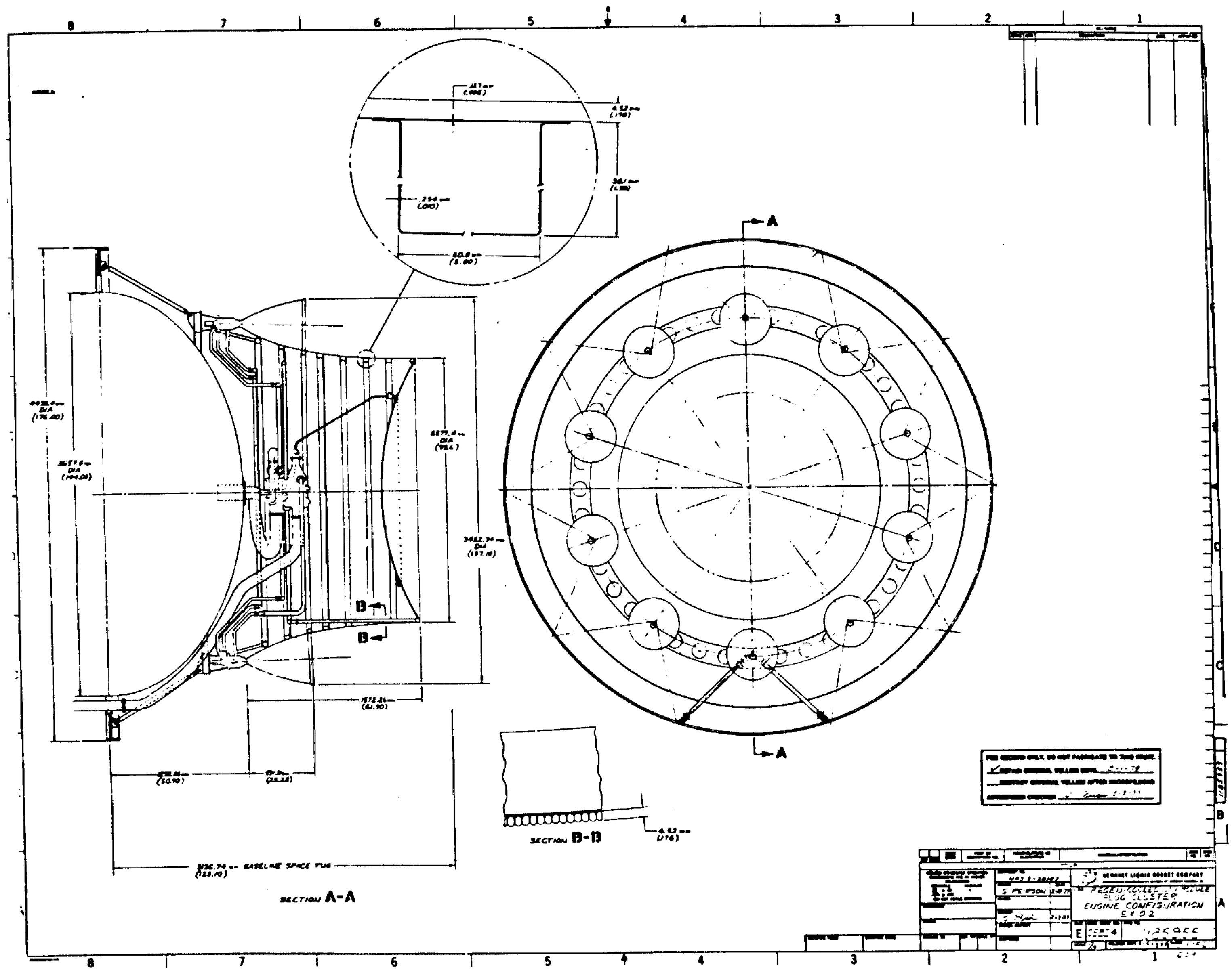

Figure 105. Regen-Cooled 100:1 Module Plug Cluster Engine Configuration EX02, Dwg No. 1185955 (Sheet 1 of 2)

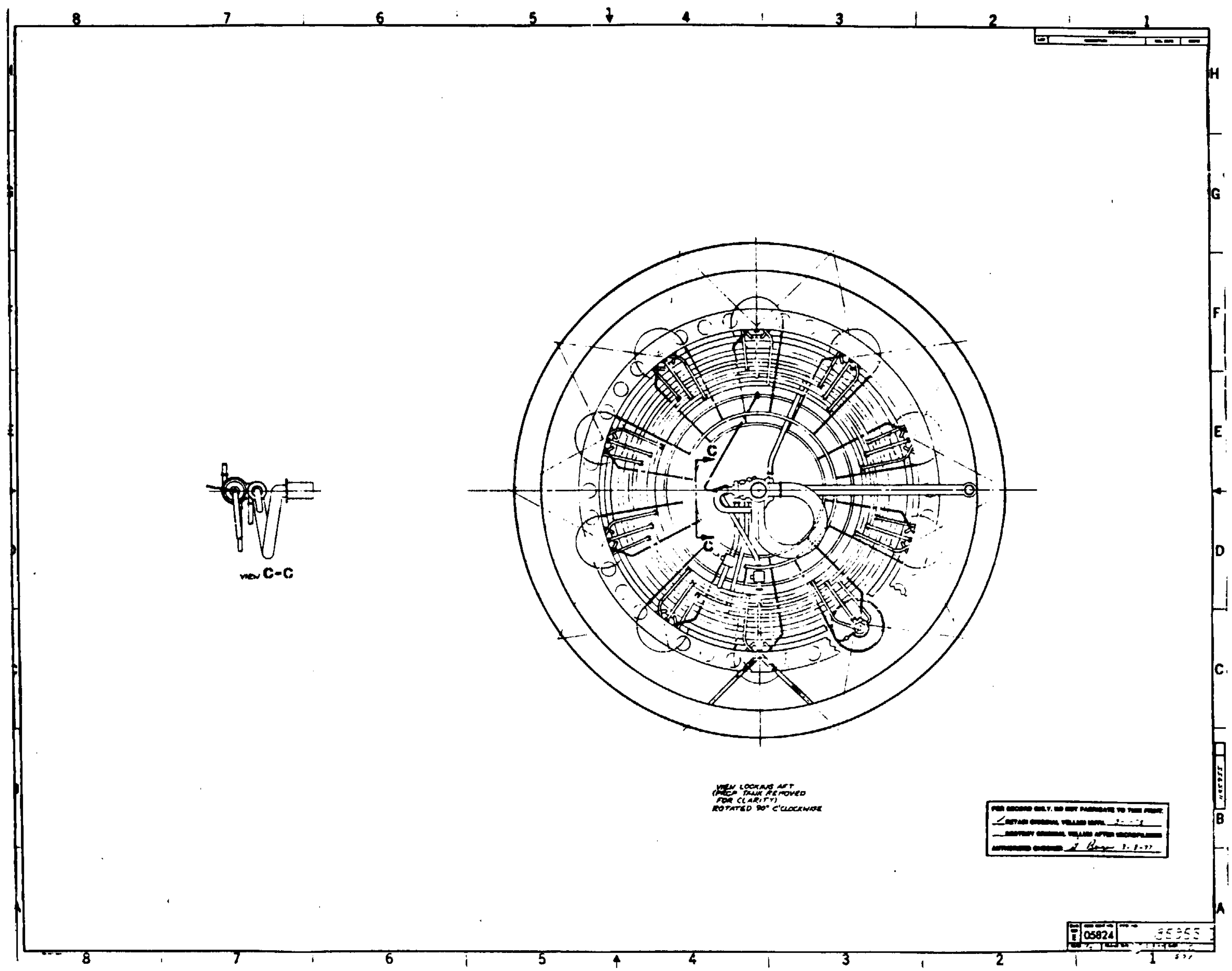

Figure 105. Regen-Cooled 100:1 Module Plug Cluster Engine Configuration EX02, Dwg No. 1185955 (Sheet 2 of 2)

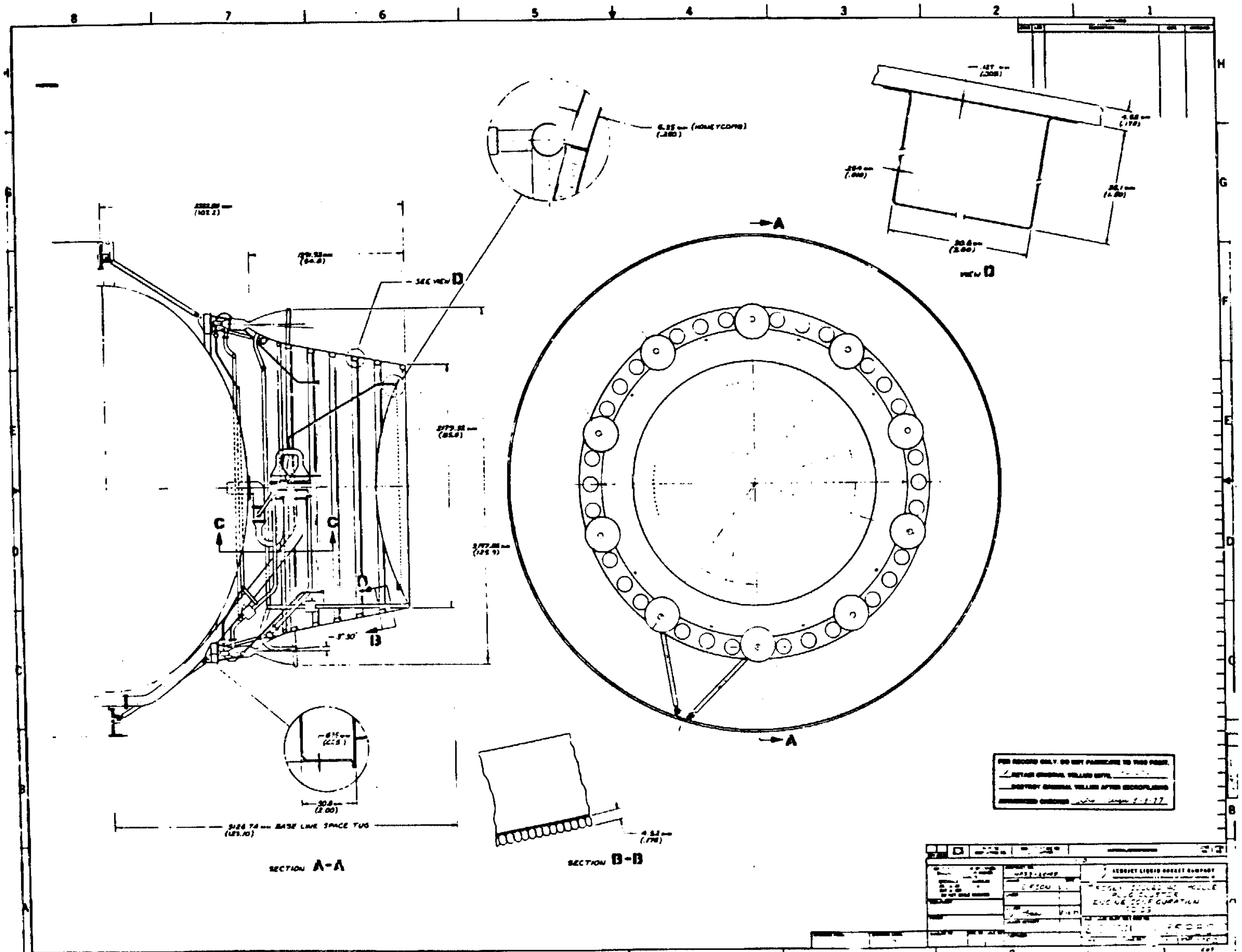

Figure 106. Regen-Cooled 40:1 Module Plug Cluster Engine Configuration GG03, Dwg No. 1185980 (Sheet 1 of 2)

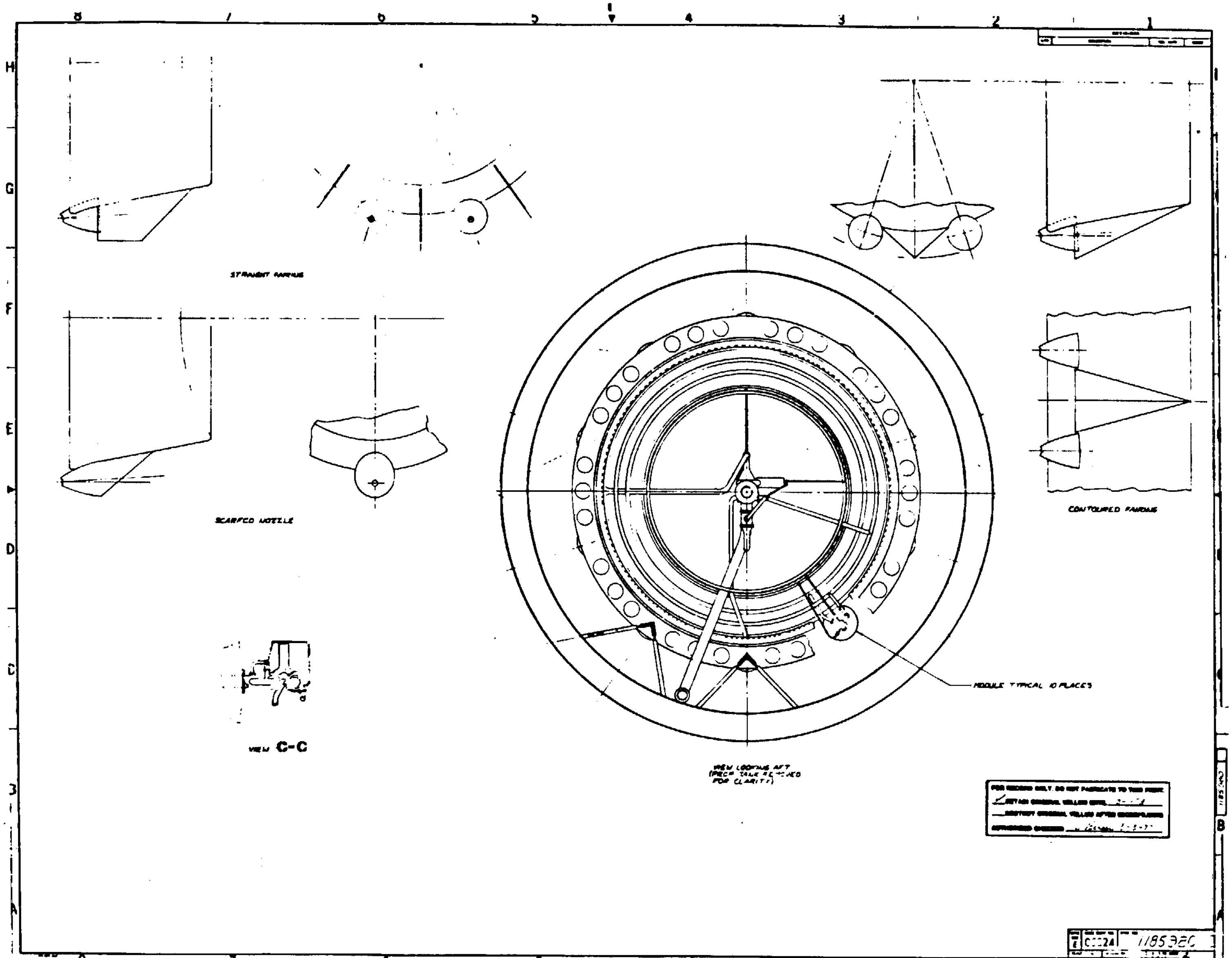

Figure 106. Regen-Cooled 40:1 Module Plug Cluster Engine Configuration GG03, Dwg No. 1185980 (Sheet 2 of 2)

Detailed discussions concerning the structure, materials and controls for the conceptual design configurations are given in the following sections.

C. STRUCTURES ANALYSIS

Stress analysis calculations were performed in support of the structural design of the plug cluster engine configurations. Results of the module design analysis are reported separately in Section VI.F. The various components were designed to provide minimum weight by comparing the known loads and stresses to stainless steel allowable strength values and critical buckling loads. Critical stress modes, such as buckling, tension, and bending were identified for each component, and the following safety factors were utilized:

Safety Factor on Yield	=	1.1 - 1.25
Safety Factor on Ultimate	=	1.4
Safety Factor on Buckling	=	1.25 - 1.4

Design criteria used in the calculations are:

Module Thrust	=	6672 N (1500 lbf)
Engine Thrust	=	68,058 N (15,300 lbf)
Acceleration	=	0.2 g
Plug Nozzle Temperature	=	533°K (500°F)
Life	=	1200 cycles
Pressure Profile	=	(given in Figure 107)

The configuration with labeled structural components is illustrated in Figure 108.

An arrangement of brazed tubes and circumferential stiffeners was found to be the lightest weight structure for the regeneratively cooled plug nozzle. This arrangement, shown in the sketches of Figure 109, utilizes five equally spaced stiffeners for an assumed uniform external pressure load of 0.04 atm (0.6 psi). If it is assumed that all of the radial load is carried by the stiffeners, the total radial load per stiffener is 7784 N (1750 lb), and the load per unit length is 947 N/m (5.4 lb/in). For a stiffener of cross section 3.81 cm x 5.08 cm (1.5 in x 2 in), the required thickness for buckling stability is 0.025 cm (0.01 in). The bending stress in the tube with a 0.23 m (9 in) span between support is 592 atm (8690 psi). The buckling margin of safety is 0.2 for the plug wall, where the margin of safety is defined as

$$M.S. = \frac{\text{allowable stress}}{\text{applied stress x safety factor}} - 1$$

The lightweight module mount ring shown in Figure 110 was designed based on a required buckling load of 5940 N/m (33.9 lb/in). The buckling margin of safety of 0.5 and the bending margin of safety of 1.8 are obtained for this structure.

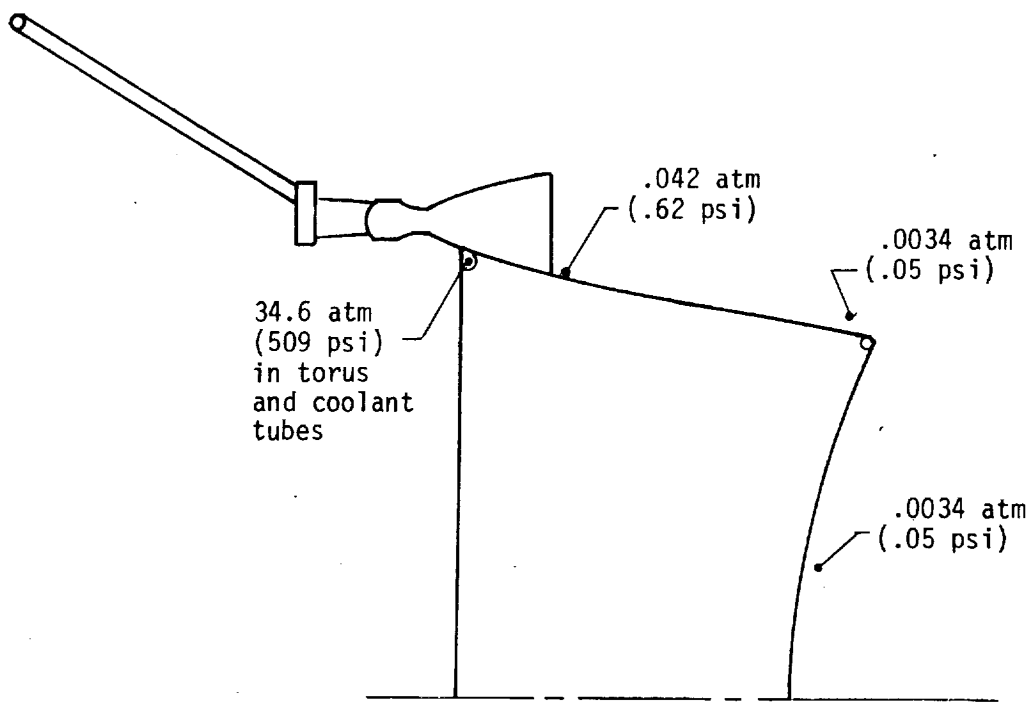

Figure 107. Plug Pressure Distribution.

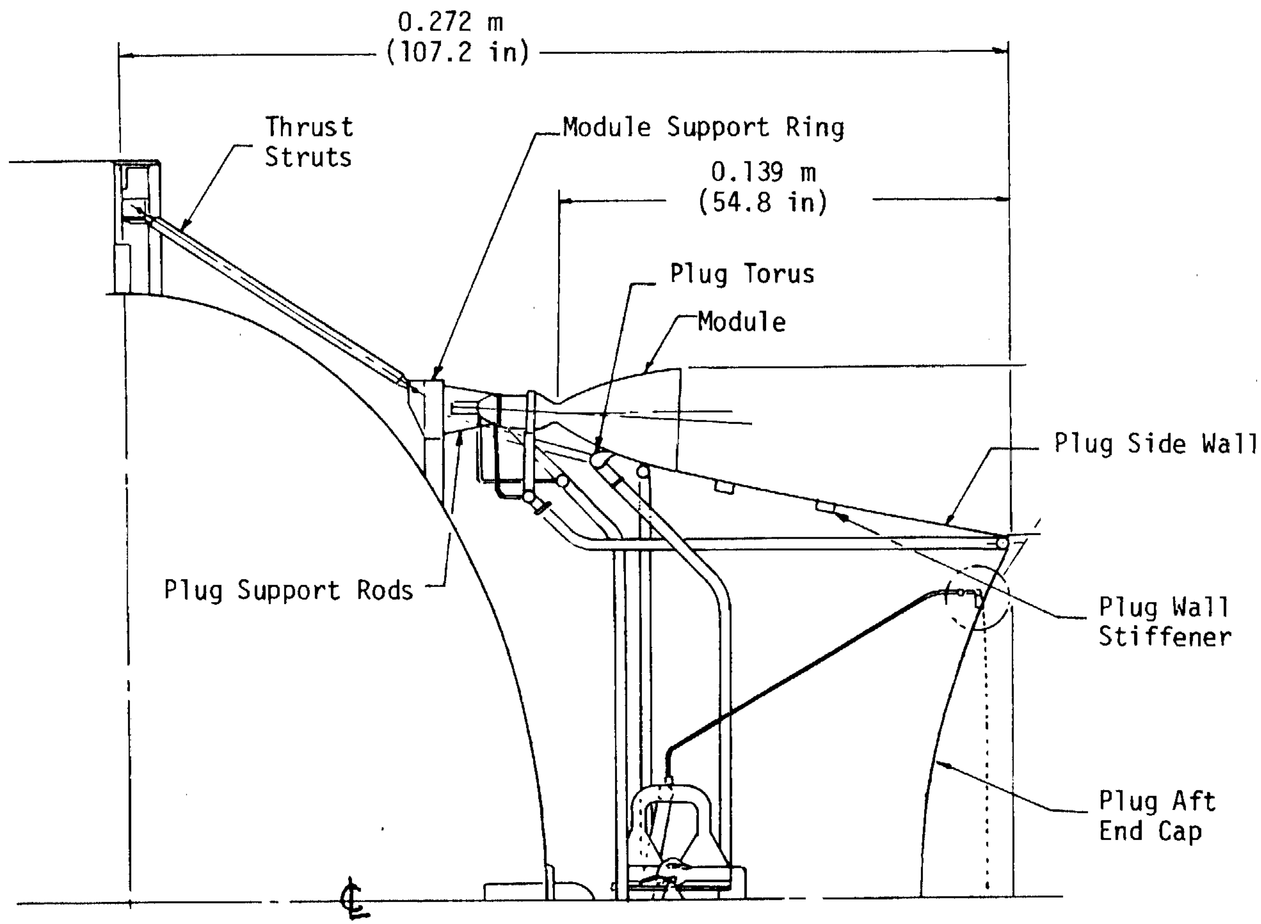

Figure 108. Plug Cluster Nozzle and Thrust Structure.

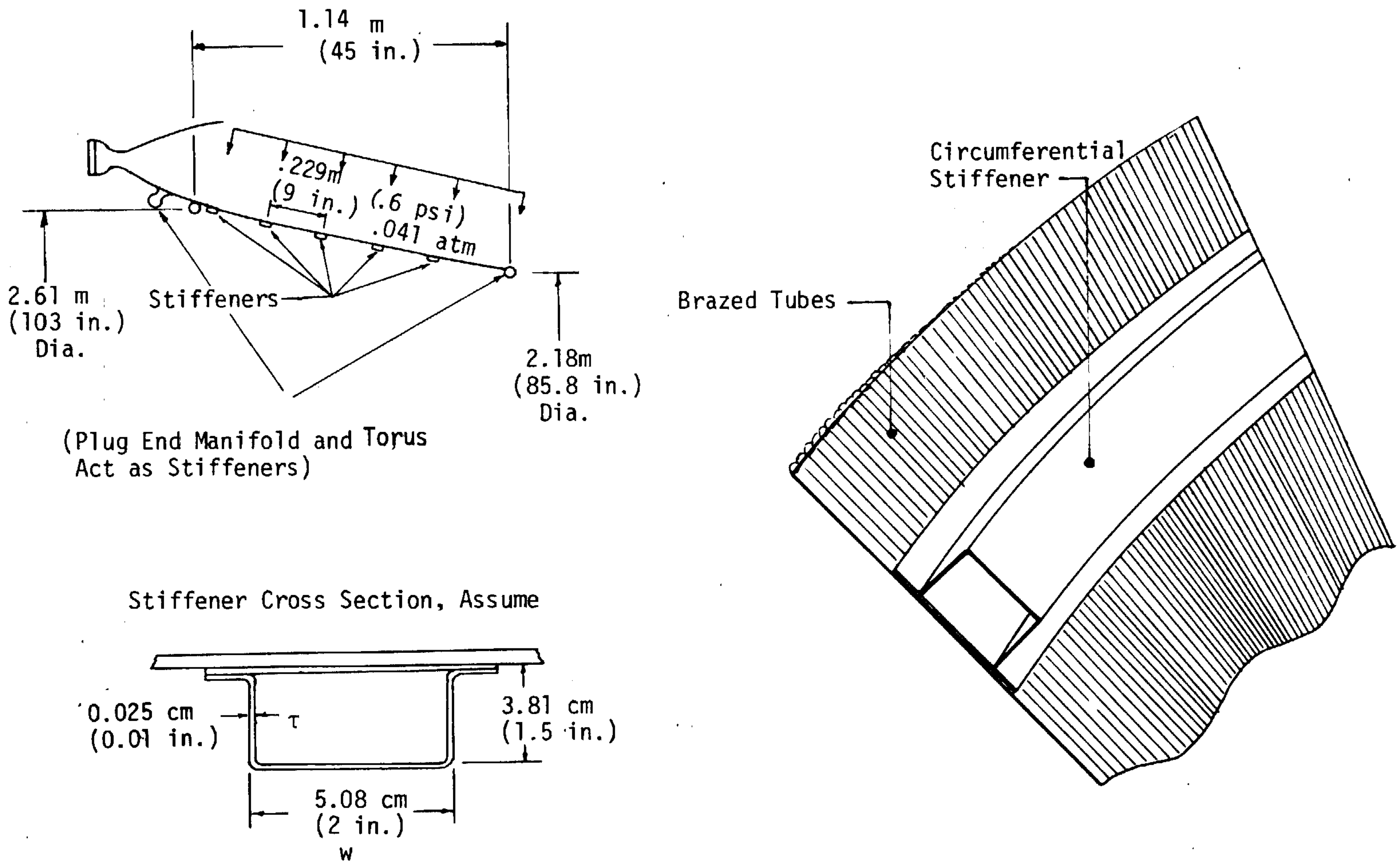

Figure 109. Plug Nozzle Structure.

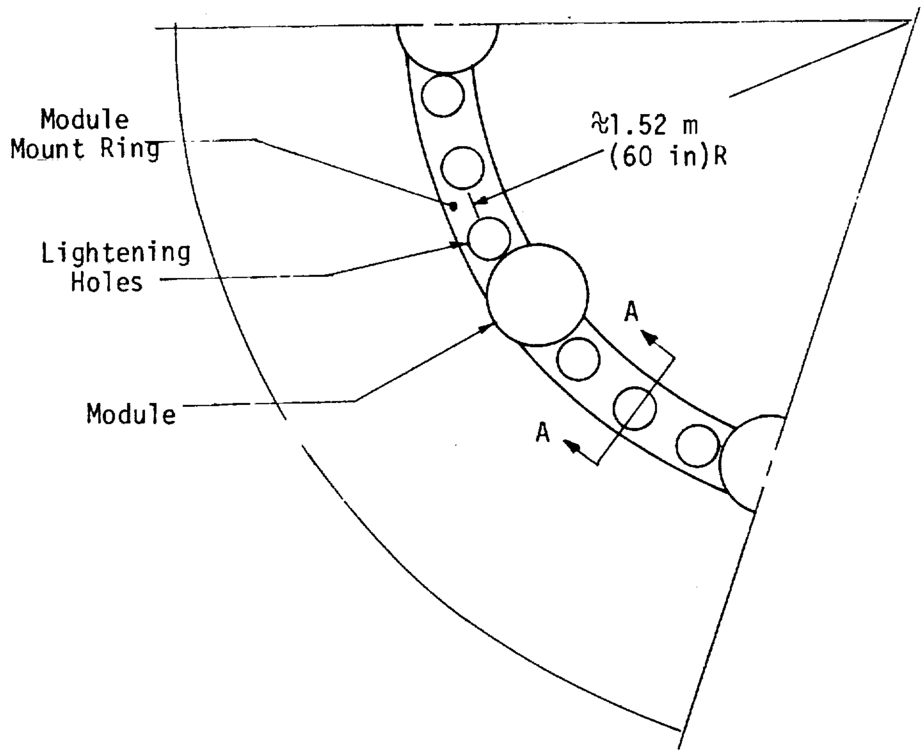

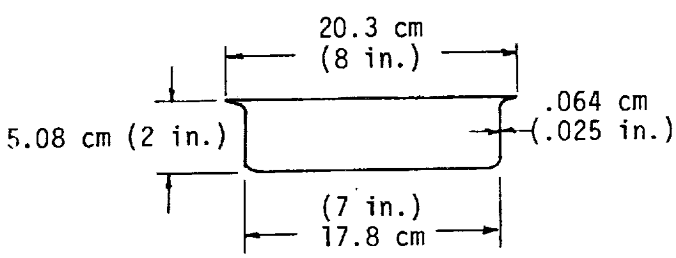

Section A-A

Figure 110. Lightweight Module Mount Ring.

The plug torus was designed to serve two functions: (1) distribute coolant to the plug wall, and (2) serve as the structural member of attaching the plug to the thrust structure. The minimum wall thickness for a margin of safety of zero is 0.058 cm. A wall thickness of 0.064 cm (0.025 in) was selected.

The thrust struts (rod braces) were sized for 950 lb_f compression in each 1.46 m (57.6 in) long strut. The strut wall thickness was selected as 0.064 cm (0.25 in) for a zero margin of safety.

Both aluminum and phenolic impregnated fiberglass cloth honeycomb structures were analyzed for the base closure structure. The margin of safety proved to be large, allowing the use of commercially available thicknesses.

D. MATERIALS ANALYSIS

The selection of materials for the plug cluster engine conceptual design (Figures 2 and 104 are typical) was based on propellant compatibility, required mechanical properties, and fabricability, with the primary emphasis being placed on compatibility. A listing of the material selected for each engine component is given in Table XXXVI.

The requirements of long life, low maintenance, postfire condensation and storage in coastal environments dictate the selection of materials with high resistance to pitting, crevice and stress corrosion. Design effects such as galvanic couples and the influence of fabrication, particularly on stress corrosion cracking susceptibility must be considered.

Hydrogen incompatibility is manifested in metals by a loss of toughness both with decreasing temperature and hydrogen absorption. The low operating temperatures and pressures of the engine allow the use of austenitic stainless steels which are both highly resistant to embrittlement by hydrogen absorption and possess excellent toughness over the range of service temperatures. The use of the susceptible nickel base alloys will be limited to the possible use of an electroformed nickel close-out of the module zirconium copper chamber liner. Limited data indicate that as-deposited electroformed nickel is susceptible to hydrogen embrittlement; however, sufficient ductility is retained in the weaker, annealed condition to allow its use. The remaining selected materials, i.e., copper and copper alloys, aluminum alloys and titanium alloys (under 100°F) are highly resistant to hydrogen embrittlement.

Oxygen incompatibility is manifested in metal either by loss of toughness at lower temperatures, reduction of fatigue life or catastrophic oxidation. With the exception of titanium alloys, the alloys anticipated for hydrogen service will also be used in oxygen. These materials possess excellent cryogenic toughness, and their ignition temperatures in oxygen are well above their respective service temperatures. Ignition is not a problem except where aluminum alloys would be subjected to high energy inputs or where organic

TABLE XXXVI - MATERIAL SELECTION FOR THE PLUG CLUSTER ENGINE CONCEPTUAL DESIGN

Component	Material
Module Chamber/Regenerative	Zirconium Copper Liner EF Nickel Close-out
Plug Nozzle	CRES 347 or Carbon-Carbon Composite
Plug Aft End Closure	Aluminum or Fiberglass Phenolic Honeycomb
Plug Wall Stiffener	CRES 347
Plug Support Rods	CRES 347
Engine Support Ring	CRES 347
Thrust Struts	CRES 347
LOX Boost Pump and LH_2 Low Speed Pump	
Housings	A356 Aluminum
Turbine Nozzles	6061 T-6 Aluminum
Impeller and Turbine Rotors	7075 T-73 Aluminum
Bearings	CRES 440
Shaft	CRES A-286
LH_2 High Speed Pump	
Turbine Housing	CRES 347 Cast
Turbine Rotors	A-286
Turbine Nozzles	CRES 347 Cast
Pump Housing	5Al-2.5Sn ELI Titanium
Impeller	5Al-2.5Sn ELI Titanium
Bearings	CRES 440C
Shaft	A-286
LOX Pump	
Turbine Housing	CRES 347 Cast
Turbine Rotors	A-286
Turbine Nozzles	CRES 347 Cast
Pump Housing	A356 Aluminum
Impeller	7075 T-73 Aluminum
Bearings	CRES 440C
Shaft	CRES-A-286

contaminants could ignite and provide a secondary source of energy to ignite the metals.

All selected non-metallic materials will be limited to those which are acceptable in accordance with MSFC-SPEC-101 and 106.

A fiber reinforced graphite composite is a candidate material for the plug nozzle. This material's chemical compatibility with combustion gases (water vapor and hydrogen) is excellent. Its calculated regression rate, due to reaction with water vapor, approaches zero at temperatures below 2500°F and is less than 2 mils/hr at 3000°F. Material regression due to reaction with hydrogen was measured at 4 mils for a ten hour test period at 3000°F and 4 psia.

E. CONTROLS ANALYSIS

The controls analysis was conducted in two parts: (1) for the fully regeneratively cooled (modules and plug nozzle) engine and (2) for the engine utilizing an uncooled plug nozzle. The analysis of the regeneratively cooled engine (Figure 104) is summarized in the first section. The second section outlines the results of the study of the engine with an uncooled plug nozzle (Figure 2) where a minimum weight control system was devised.

1. Control System for Regeneratively Cooled Engine

Engine cycle schematics were prepared to correspond to the regeneratively cooled conceptual design configurations. The schematics shown in Figures 111 and 112 are expander and gas generator (GG) cycles. Minor differences occur in the cooling circuits for different modules (e.g., ITA and minimum modification ITA).

A preliminary evaluation of the valves and controls required for the two engine cycle concepts shown in Figures 111 and 112 was performed to provide a degree of confidence that the defined system schematics could control the engine. This evaluation was performed in a very broad manner and did not include any formal analysis of system transients. The basic approach used was to examine the original schematics for both the expander and GG cycles, identify potential problem areas, attempt to minimize the control problems by adding, deleting or relocating controls and then to examine the revised system with regard to preliminary definition of controls and control modes. With this approach, the resultant schematics should be representative of what will be required; however, final definition will require programmed analyses to evaluate the varied transient conditions that may be encountered.

For both concepts, the engine start would begin with tank head operation through a cooldown phase followed by a pumped idle mode and then full thrust operation. Although the basic approach is quite simple and has been used successfully for other cryogenic, pump fed engines, the use of 10 engine modules presents some additional considerations regarding location and sequencing of controls.

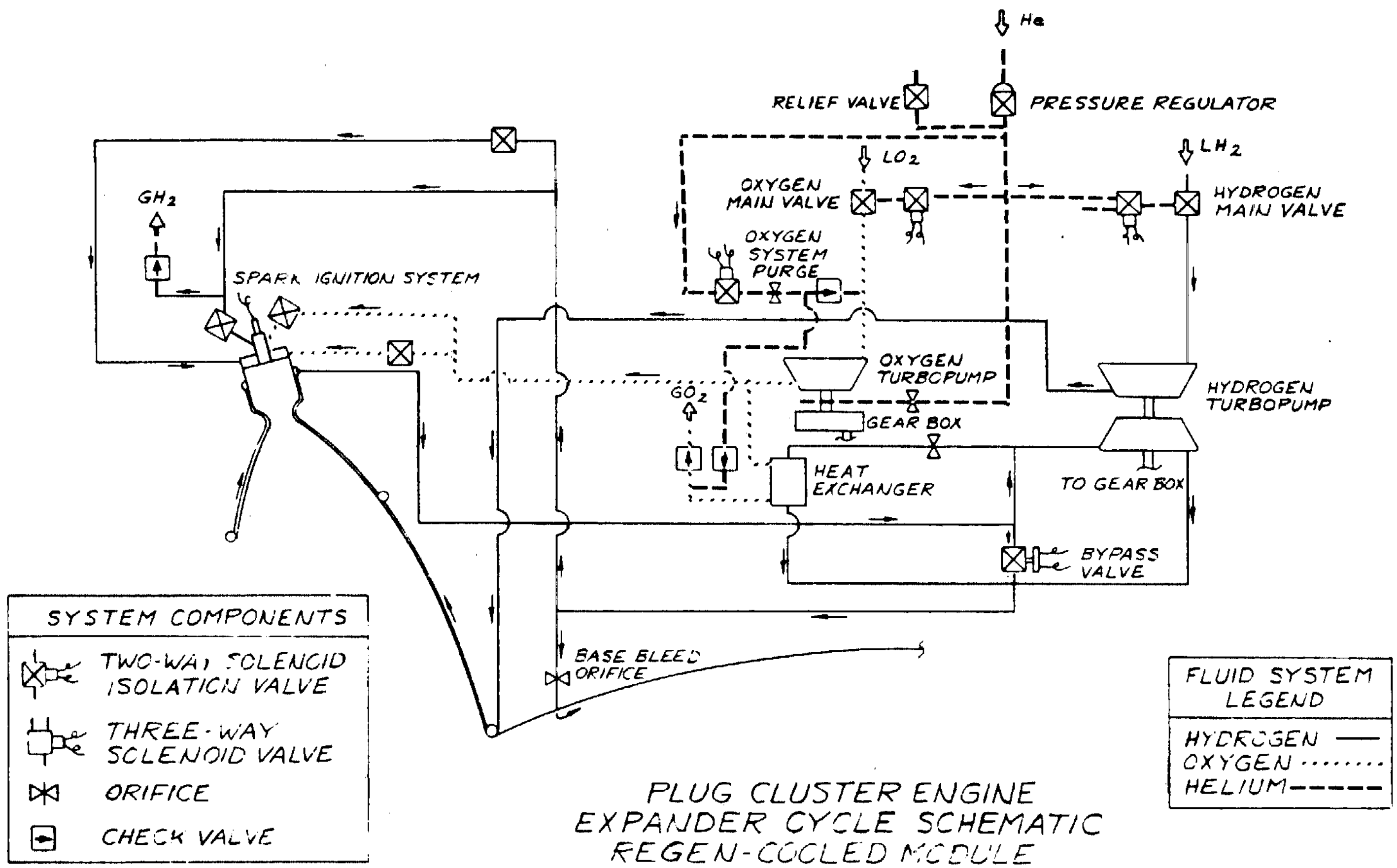

Figure 111. Plug Cluster Engine Expander Cycle Schematic-Regen-Cooled Module and Plug.

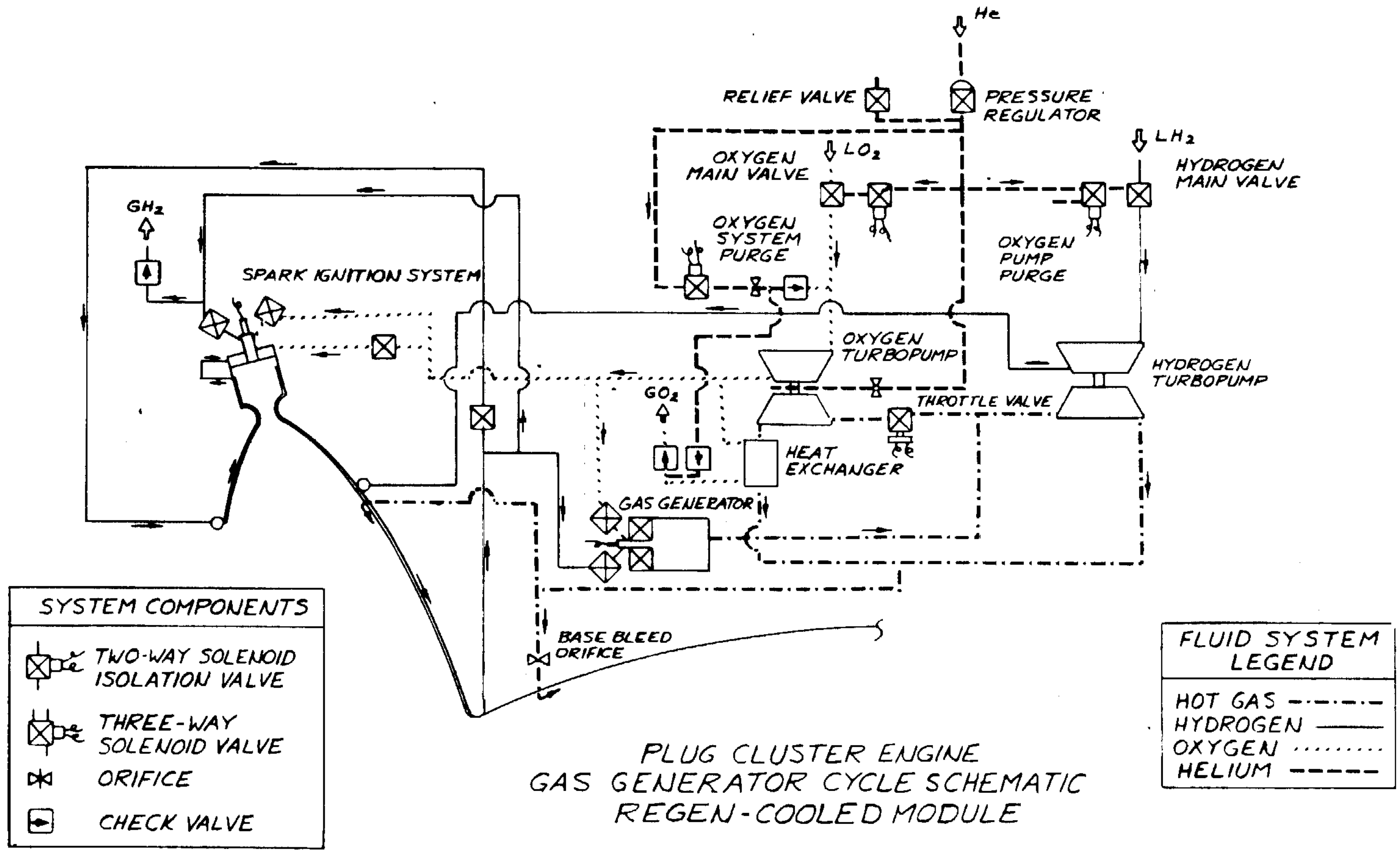

Figure 112. Plug Cluster Engine Gas Generator Cycle Schematic-Regen-Cooled Module and Plug.

The expander cycle, shown in Figure 111, uses GH_2 to drive a turbine which is coupled to both pumps by a gearbox. The oxidizer circuit has a tank shutoff valve, a single main oxidizer shutoff valve, a check valve (to control oxidizer tank pressurization gas), and small shutoff valves located at each module to control igniter flow. The fuel circuit has valves comparable in function to those in the oxidizer circuit plus a bypass valve that serves to control the flow through the turbine after the H_2 has passed through the coolant passages. Auxiliary sensing devices and an electronic controller will be required to properly accommodate the various conditions under which the engine must start and shutdown.

The GG cycle shown in Figure 112 uses hot gas to drive parallel turbines, each of which is coupled to a pump. The valves in both the fuel and oxidizer circuits are comparable to those defined for the expander cycle. In addition to the common valves, a fuel and oxidizer GG valve are required. Also, the bypass valve is relocated and functions as a throttle valve to control hot gas flow to the oxidizer turbine.

Based upon the examination of the systems, Table XXXVII was prepared to show a preliminary definition of the required valves.

For each valve defined, viable options exist dependent upon more definitive performance requirements. One major variable is the allowable pressure drop for the valve. The pressure drop could be a driver in selection of the type of valve, particularly if system weight were critical. The curves of Figure 113 show the effect of pressure drop on equivalent orifice diameter for a valve flowing liquid oxygen and a valve flowing GH_2 with flow conditions typical of those required for the main propellant shutoff valves. As is shown, the change in orifice diameter is very significant below about 20 psi. Since weight is a function of valve size, the final system pressure schedule could have a very definitive effect on the weight of the required controls. This also affects the type of valve since valves with different shutoff elements have different size requirements to provide the same equivalent orifice flow.

Although the basic system schematics are thought to be practical as depicted, there are questions that cannot be completely resolved by the limited analysis performed to date. Several of these questions are analyzed with regard to potential problems and possible options to resolve the problems.

Start Transient

With various sensing elements, signals and an electronic controller, a desired engine start should be attainable for a given set of conditions; however, there is some concern as to whether the same logic can be applied for all conditions. The effects of variations such as full vs empty lines, hot vs cold regenerative cooling section, single phase vs two phase propellants and temperature soakback into valves and turbopumps

TABLE XXXVII - PRELIMINARY VALVE SELECTIONS

NAME	FUNCTION	APPLICABILITY TO EXPANDER	APPLICABILITY TO GG	VALVE TYPE	METHOD OF ACTUATION	MODE OF OPERATION	MATERIALS OF CONSTRUCTION	ESTIMATED WEIGHT, LBS.
Fuel Tank Shutoff	Isolate fuel in propellant tank	Yes	Yes	Ball	Pneumatic	On-Off	Al & CRES	6.6
Ox Tank Shutoff	Isolate ox in propellant tank	Yes	Yes	Ball	Pneumatic	On-Off	Al & CRES	6.6
Fuel Igniter	Control fuel flow at igniter	Yes	Yes	Poppet	Solenoid	On-Off	CRES	*1.0
Ox Igniter	Control ox flow at igniter	Yes	Yes	Poppet	Solenoid	On-Off	CRES	*0.8
Main Fuel Shutoff	Control fuel flow to module injectors	Yes	Yes	Coaxial Poppet	Pneumatic	On-Off or multiple position	Al & CRES	4.5
Main Ox Shutoff	Control ox flow to module injectors	Yes	Yes	Coaxial Poppet	Pneumatic	On-Off or multiple position	Al & CRES	4.2
Turbine Bypass	Control fuel flow passing thru the turbine	Yes	No	Butterfly or Sleeve	Electrical Motor	Modulating or 3 Position	Al & CRES	4.7-5.1 or 5.9
Throttle	Control hot gas flow to ox turbine	No	Yes	Butterfly or Poppet	Electrical Motor	Modulating	High temp. steel	10.0 or 4.9
Fuel GG	Control fuel flow to GG	No	Yes	Poppet Biprop.	Pneumatic	On-Off	CRES	3.2
Ox GG	Control ox flow to GG	No	Yes	Poppet Biprop.	Pneumatic	On-Off	CRES	3.2

*Denotes 10 of these are required.

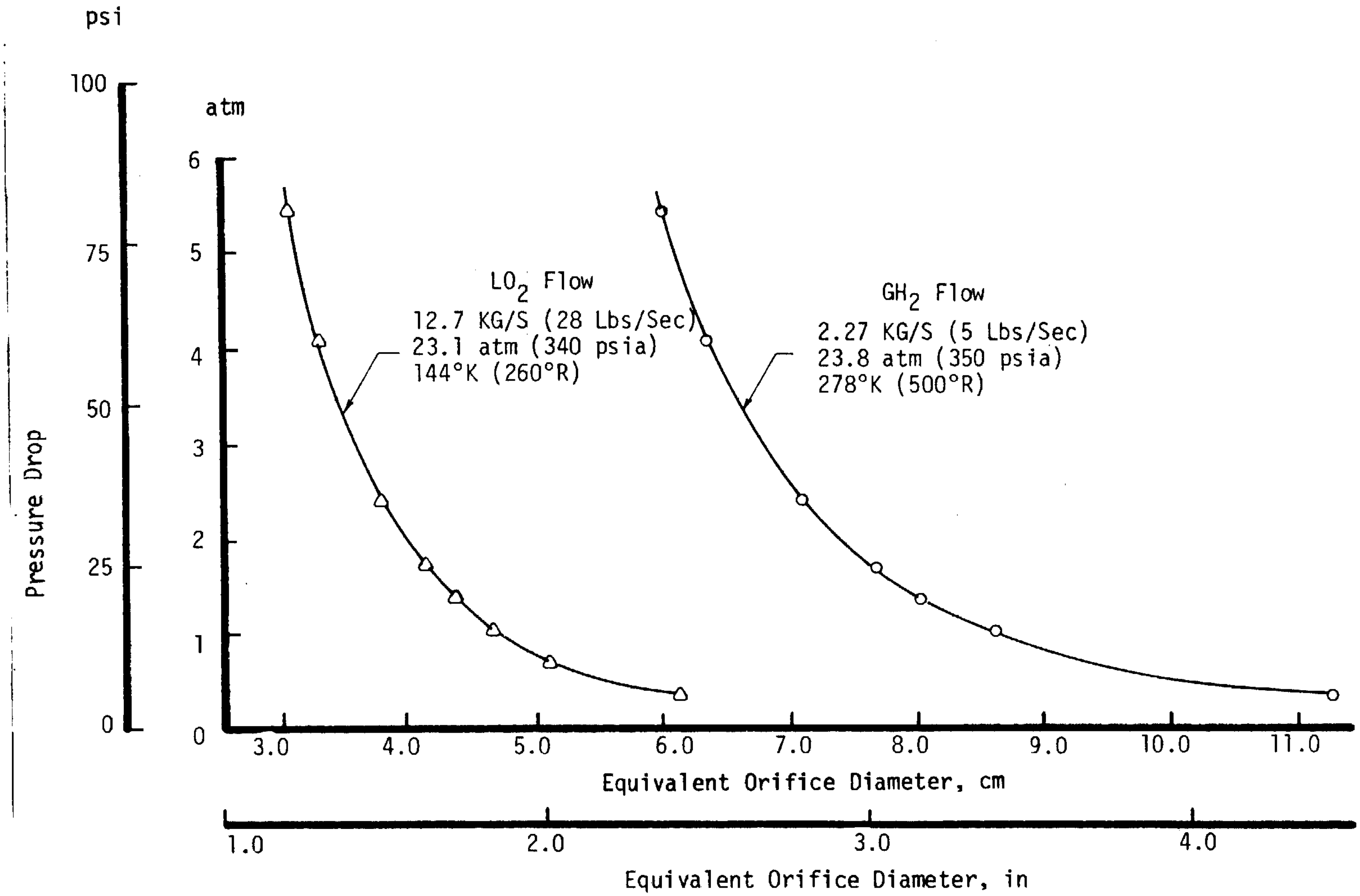

Figure 113. Effect of Pressure Drop on Equivalent Orifice Diameter.

are aspects requiring additional consideration. A more complex control approach may be required to assure a smooth start under the varying conditions that could exist on restarts. Changes that may be required are use of more modulating or step position controls and start sequence variations that would be selected as a function of several monitored parameters.

Mixture Ratio Control

The concern about mixture ratio (MR) control is related primarily to the start and shutdown transients. It is a concern because only one valve controls flow to all the modules. The need for a flow balanced distribution system to the modules is apparent.

Even with valves at each module, as is done for the igniter circuits, MR excursions during the transients could be rather severe. The MR range would be influenced by propellant conditions, driving pressure and the sizing of the igniter valves or flow orifices. It seems reasonable to assume that with a more detailed analysis, this potential problem could be accommodated by proper orificing or a modulating control in one circuit.

Module Interaction Effects

With the modules clustered around the nozzle, start timing and interaction effects are a concern. The thrust generated by a module with just the igniter portion operating would be so low that no problem would result from a start variation. As main module thrust comes up through idle mode, a variation from side to side could induce a turning moment to the vehicle. Any moments could be corrected by an attitude control system or gimbal capability; however, here again the need for a balanced flow and distribution network is emphasized to minimize the potential effect.

Another aspect of interaction relates to the common main control valve and multiple feed lines. Any significant pressure perturbation in a module chamber could reflect back into the feed system. The fluctuations at one module could then effect other modules with various time lags. Dependent upon line lengths and propellant properties, any pressure disturbances may be either amplified or attenuated. The potential for this effect could be reduced by making the system stiffer, i.e., having higher injector pressure drops, and controlling starts to limit Pc spikes.

Line Cooldown

Under the tank head and pumped idle mode start the lines will be chilled. Multi-position main shutoff valves and bypass bleed orifices are required for this operation.

Propellant Utilization

Propellant utilization in the GG cycle could be achieved quite readily by a special control signal to the throttle valve. On the expander cycle, precise control could not be readily achieved with the valves depicted on the schematic. Some degree of compensation in one direction only could be accomplished by the turbine bypass valve; however, the control and sensing logic required is believed to be complex. A simpler approach may be to make one of the main propellant shutoff valves capable of mudulation.

Tank Pressurization

The schematics show simple check valves to control the propellant flow back to the tanks for autogenous pressurization. The feasibility of this approach is somewhat questionable considering possible pump discharge pressure variations, check valve crack and reseat accuracy, desired range of tank pressure and the early mission conditions where ullage will be small. An acceptable alternative would be to make these valves a pressure differential sensing unbalanced poppet arrangement. This approach could be used with the valve size being comparable to a conventional spring loaded check valve.

Thrust Throttling

Although a throttling requirement is not currently imposed, a throttling capability could offer an attractive option to some other vehicle control requirements. The GG cycle could readily accommodate throttling by making the GG valves modulating rather than on-off. The expander cycle would probably require the main shutoff valves to have a modulating capability. This would impose a larger penalty than the GG cycle since the valves involved are much larger

Other options could be used for a stepped thrust capability rather than true throttling over a specified range. In addition to control, as described above using multiposition valves instead of full modulating valves, an approach of module control would be feasible. By adding main propellant control valves to groups of modules, groups of 2, 3, or 4 modules could be shutoff or started to change thrust. A similar approach might be used, with different module groupings, to provide maneuvering moments without requiring engine gimbaling or use of auxiliary control thrusters.

None of these areas of concern appear to be overwhelming. However, rather extensive system analyses would be required to assure that the proper control parameters and control logic are used to provide the desired performance characteristics over the full range of operating and restart conditions.

1. Control System for Engine With Uncooled Plug

Minimum weight control system schematics were formulated for both expander cycle and gas generator cycle engines with an uncooled plug nozzle (Figure 2) These are given in Figures 114 and 115.

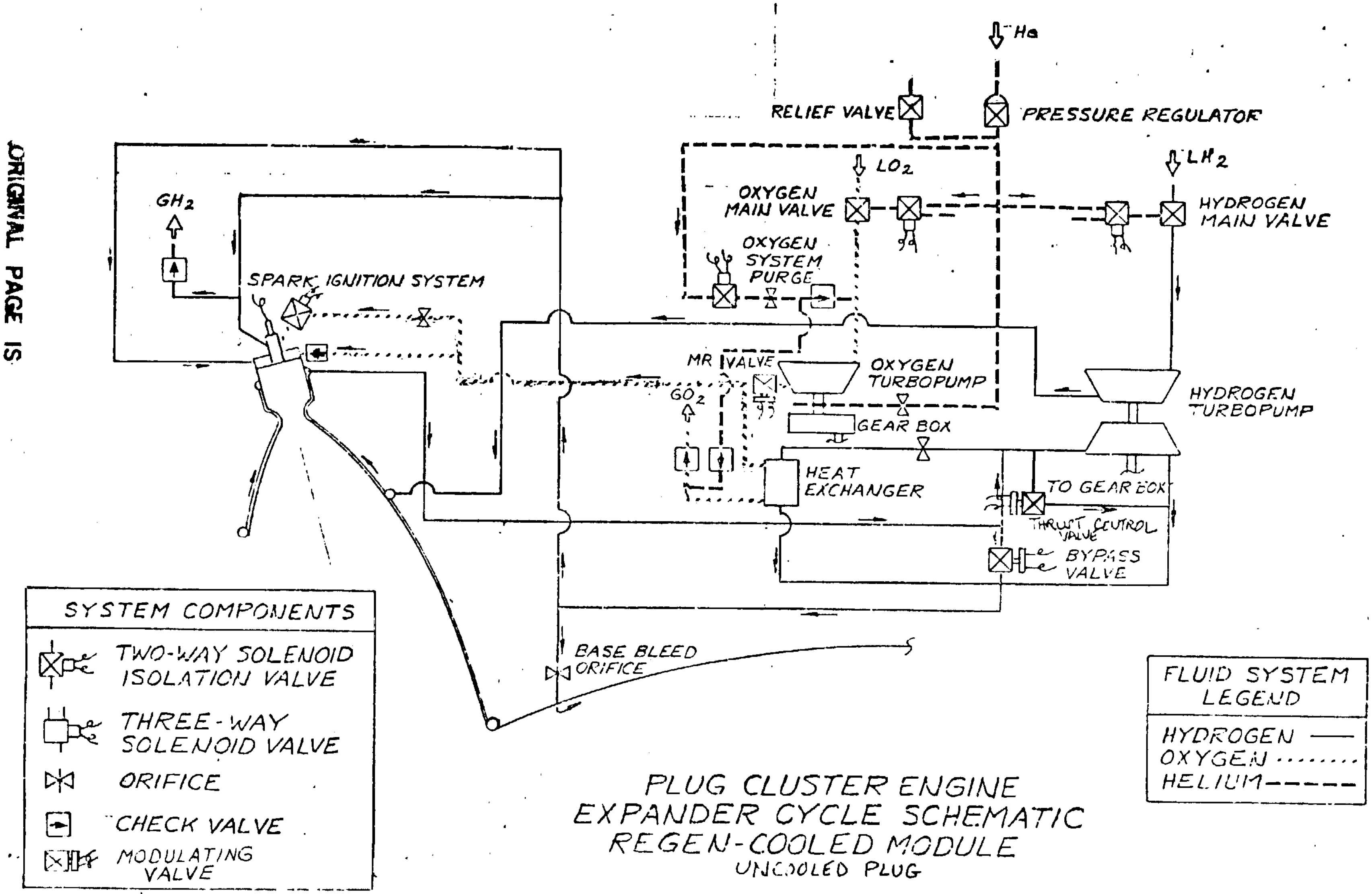

Figure 114. Plug Cluster Engine Expander Cycle - Uncooled Plug

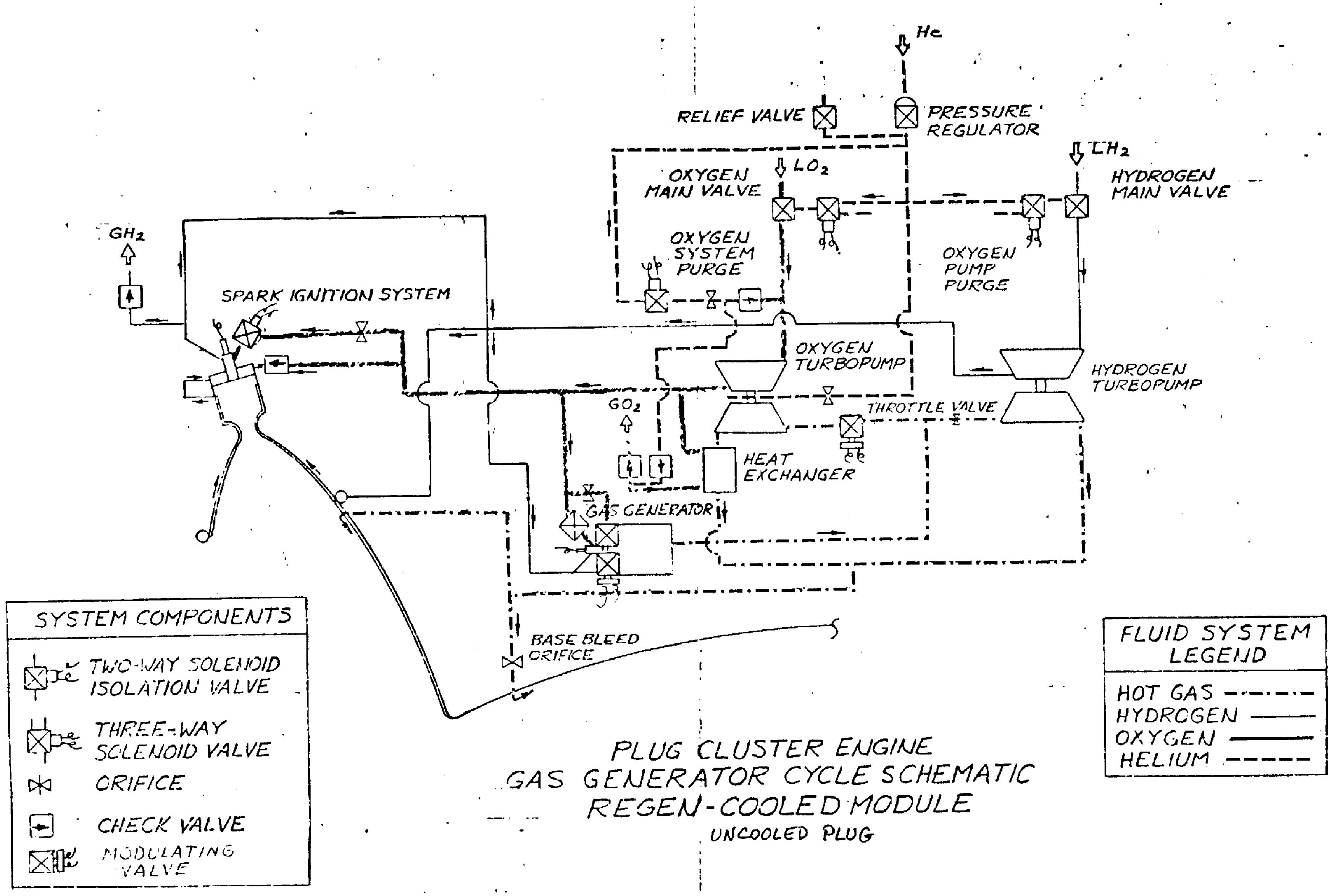

Figure 115. Plug Cluster Engine Gas Generator Cycle - Uncooled Plug

Primary control of the expander cycle (Figure 114) is attained by use of modulating or multi-position valves in the GH_2 turbine drive circuit. Secondary control, for mixture ratio (MR) and propellant utilization (PU) is achieved by a modulating valve in the oxidizer circuit downstream of the pump.

A preliminary definition of a start and shutdown sequence of operations for this expander cycle is given in Table XXXVIII. The sequence requires use of a controller having computational and logic capabilities (i.e., microprocessor) rather than a controller having only timers and signal sequencing capabilities.

Primary control of the gas generator cycle (Figure 115) is achieved by modulating GG valves. Secondary control for MR and PU is obtained by the throttle valve which controls hot gas flow to the oxidizer pump turbine.

A sequence of operations for start and shutdown of the GG cycle is shown in Table XXXIX. The comments relative to the required controller as discussed for the expander cycle also apply to the GG cycle.

Component weight estimates for the major control components are listed in Table XL. The total weight for the minimum valve expander cycle is 23.8 Kg (52.5 lbs), while the corresponding weight for the GG cycle is 20.6 Kg (45.5 lbs).

F. MODULE DESIGN

Four different modules are utilized in the conceptual designs: (1) Integrated Thrust Assembly (ITA) shown in Figure 116 and described in Section III.D.1, (2) Minimum Modification ITA, and (3) Regeneratively Cooled ITA shown in Figure 117 for both a 40:1 and a 100:1 module area ratio.

The minimum modification ITA utilized a regen cooled nozzle extension downstream of the regen-film cooled throat section. The fully regen module, Figure 117, requires no film cooling, and therefore, represents a major departure from the basic ITA design.

The ITA design has been shown to possess the capability of over 1200 cycles operation at a mixture ratio of 5.5 (Reference 45) Analysis to estimate the life cycle capability of the regeneratively cooled module design is as follows:

Design criteria for the structures analysis are:

Coolant Channel Pressure = 38.1 and 66.7 atm (560 and 980 psia).
Chamber Pressure = 20.4 and 34.0 atm (300 and 500 psia).
Coolant Channel Temperatures (given in Figures 87, 88, and 91)
Design goal = 1200 thermal cycles for a 10 hour duration.
Safety Factor on Yield = 1.1.
Safety Factor on Ultimate = 1.4.
Chamber Material = Zirconium Copper.

TABLE XXXVIII - UNCOOLED PLUG EXPANDER CYCLE OPERATIONS SEQUENCE

Command Element	Response Element	Action
Start signal	Tank shutoff valves	Both shutoff valves open; fuel and oxidizer start flowing.
Differential pressure switch	Spark exciter and oxidizer igniter solenoid valve	Spark exciter energized; solenoid valve opens; fuel and oxidizer flow in igniter is ignited.
Ignition monitor	Controller	Controller samples all modules to confirm burning in each igniter.
Controller	Spark exciter	Spark exciter is de-energized; igniter burn continues; GH_2 flows into chamber thru main injector and combusts; system cooldown continues.
Temperature sensor	Bypass valve	Pump housing temperature sensors reach the set temperature; controller energizes bypass valve to move from full open to intermediate open position; controller maintains lock-out on MR and thrust control loops; turbine rotates; pumps start pumping fuel and oxidizer.
Oxidizer line pressure	Checkvalve	Pump discharge pressure increases to open oxidizer line checkvalve; oxidizer flows into main chamber and ignites with fuel.
Pc transducer	Controller	Controller samples all chamber pressures and confirms all have achieved pre-determined pressure.
Controller	Bypass valve, thrust control valve	Controller commands bypass valve to move to steady state position and activates the thrust control loop.
Pc transducer	Thrust control valve	With thrust control loop activated, the low Pc signal causes the thrust control valve to move toward the closed position; valve closing forces rated flow thru the turbine; Pc overshoot controlled by pre-programmed valve travel rate.

TABLE XXXVIII (cont.)

Command Element	Response Element	Action
Pc transducer	Controller	Controller samples all thrusters to confirm full thrust.
Controller	MR valve, oxidizer igniter valve	Upon confirmation of proper Pc the controller de-energizes the oxidizer igniter valves and activates the MR control loop; steady state operation established; thrust controlled by Pc transducer acting on the thrust control valve; MR controlled by PU tank signal acting on MR valve.

Shutdown involves simultaneous programmed functions, which are executed by the controller. The shutdown signal results in deactivation of control loops, bypass and thrust control valves open, tank shutoff valves close and the MR valve goes to the nominal position. Upon confirmation of PC decay, the purge valves are opened to clear oxidizer and fuel bleeds out the injector and base bleed port.

TABLE XXXIX - UNCOOLED PLUG GAS GENERATOR CYCLE OPERATIONAL SEQUENCE

Command Element	Response Element	Action
Start signal	Tank shutoff valves, throttle valve	Shutoff valves open; throttle valve goes to nominal position; fuel and oxidizer start flowing.
Differential pressure switch	Spark exciters, ox. igniter valves	Spark exciter energized; solenoid valve opens; fuel and oxidizer flow and are ignited at thrusters and GG.
Ignition monitor	Controller	Controller samples all modules & GG to confirm burning in each igniter.
Controller	Spark exciter	Spark exciter is de-energized; igniter burn continues; GH_2 flows thru main injector and combusts; system chilldown continues.
Temperature sensor	GG valves	Pump housing temperature sensors reach the set temperature; controller commands GG valves to about 50% open position while maintaining control loop lock-out; turbine and pumps rotate; fuel and oxidizer pressure rise.
Ox line pressure	Ox checkvalves	Pump discharge pressure increases to open the oxidizer line checkvalves; oxidizer flows into the main chambers and ignites with the fuel.
Pc transducer	Controller	Controller samples all chamber pressures and confirms all have achieved pre-determined pressure.
Controller	GG valves	Controller removes thrust control loop lock-out; MR control loop remains locked out.
Pc transducer	GG valves	Low Pc signal causes GG valves to move to the full open position; flow thru turbines goes to rated flow and thrust rises to full thrust level.
Pc transducer	Controller	Controller samples all thrusters to confirm full thrust.
Controller	Throttle valve, Ox igniter valves	Controller activates the MR control loop which lets the throttle valve respond to tank PU signals; oxidizer igniter valves are de-energized; steady state thrust established and controlled by Pc signals to GG valves.

Shutdown involves simultaneous pre-programmed functions which are executed by the controller. The shutdown signal results in deactivation of control loops, the throttle valve is commanded to a pre-determined position, the GG valves are closed at a controlled rate and the tank shutoff valves close in response to a timer signal. The controller samples Pc decay and initiates an oxidizer purge to clear oxidizer lines. Fuel bleeds out thru the main chamber and the hot gas out the base bleed and plug wall ports.

TABLE XL - PRELIMINARY VALVE SELECTION FOR UNCOOLED PLUG SYSTEM

NAME	FUNCTION	APPLICABILITY TO EXPANDER	APPLICABILITY TO GG	VALVE TYPE	METHOD OF ACTUATION	MODE OF OPERATION	MATERIALS OF CONSTRUCTION	ESTIMATED WEIGHT, Kg (LBS)
Fuel Tank Shutoff	Isolate fuel in propellant tank	Yes	Yes	ball	pneumatic	on-off	Al & Cres	3.9 (8.5)
Ox Tank Shutoff	Isolate ox. in propellant tank	Yes	Yes	ball	pneumatic	on-off	Al & Cres	3.9 (8.5)
Ox Igniter	Control ox. flow at thruster igniter	Yes	Yes	poppet	solenoid	on-off	Cres	0.4 (*0.8 each)
Ox Checkvalve	Control ox. flow to injector	Yes	Yes	poppet	line pressure	on-off	Al & Cres	0.4 (*0.9 each)
Turbine Bypass	Control fuel flow passing thru the turbine loop	Yes	No	sleeve	electrical motor	3 position	Al & Cres	2.7 (5.9)
Thrust Control	Control fuel flow thru turbine	Yes	No	poppet	electrical motor	modulating	Al & Cres	2.1 (4.6)
Ox Control	Control MR and PU	Yes	No	sleeve	electrical motor	modulating	Al & Cres	3.6 (8.0)
Ox GG Igniter	Control ox. flow at GG igniter	No	Yes	poppet	solenoid	on-off	Cres	0.2 (0.5)
GG Biprop.	Control fuel and ox. flow to GG	No	Yes	poppet	electrical motor	modulating	Al & Cres	2.8 (6.1)
Throttle	Control hot gas flow to ox. turbine	No	Yes	poppet	electrical motor	modulating	Inconel	2.2 (4.9)

*Denotes 10 of these valves are required.

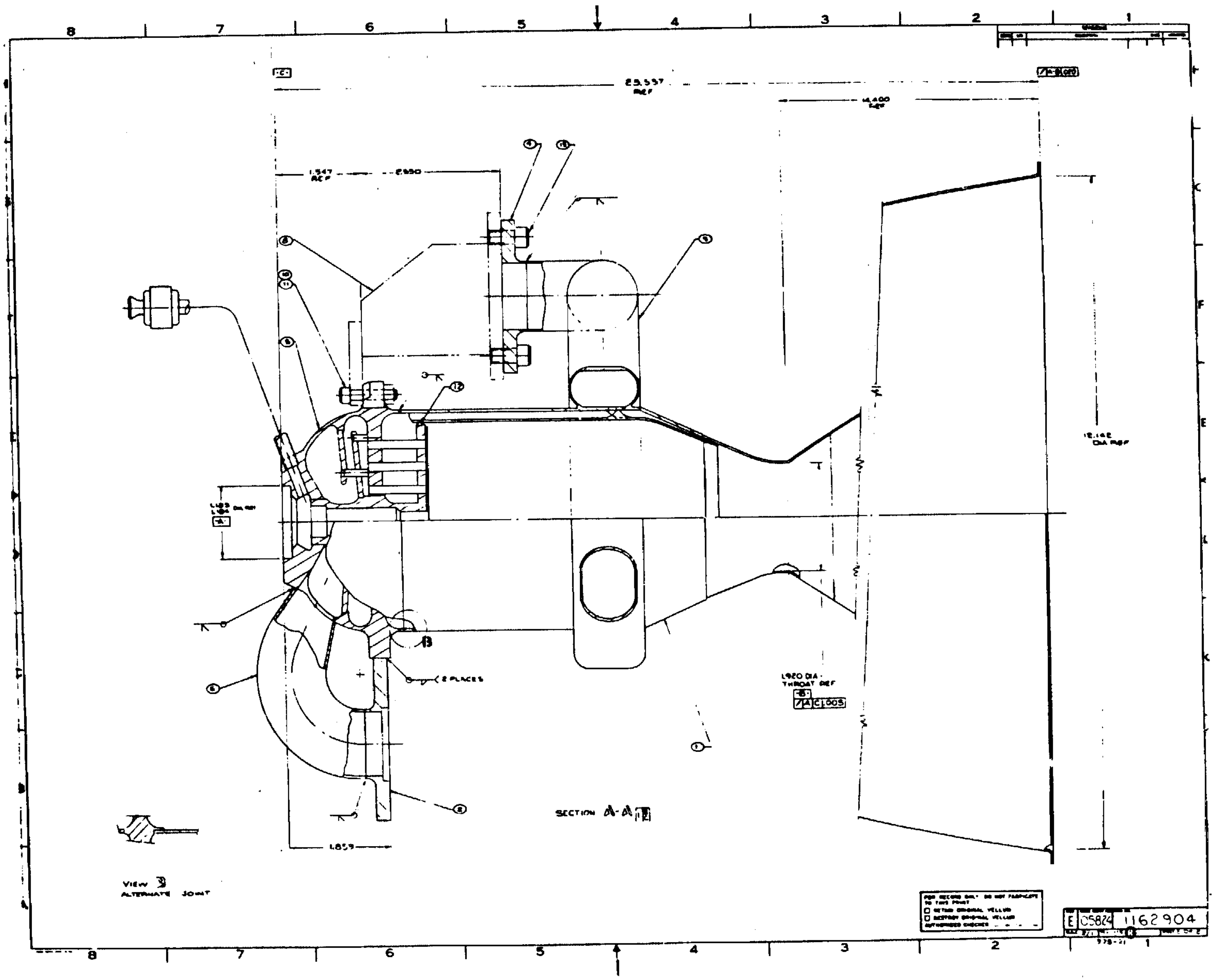

Figure 116. Integrated Thruster Assembly (ITA), Dwg. No. 1162904.

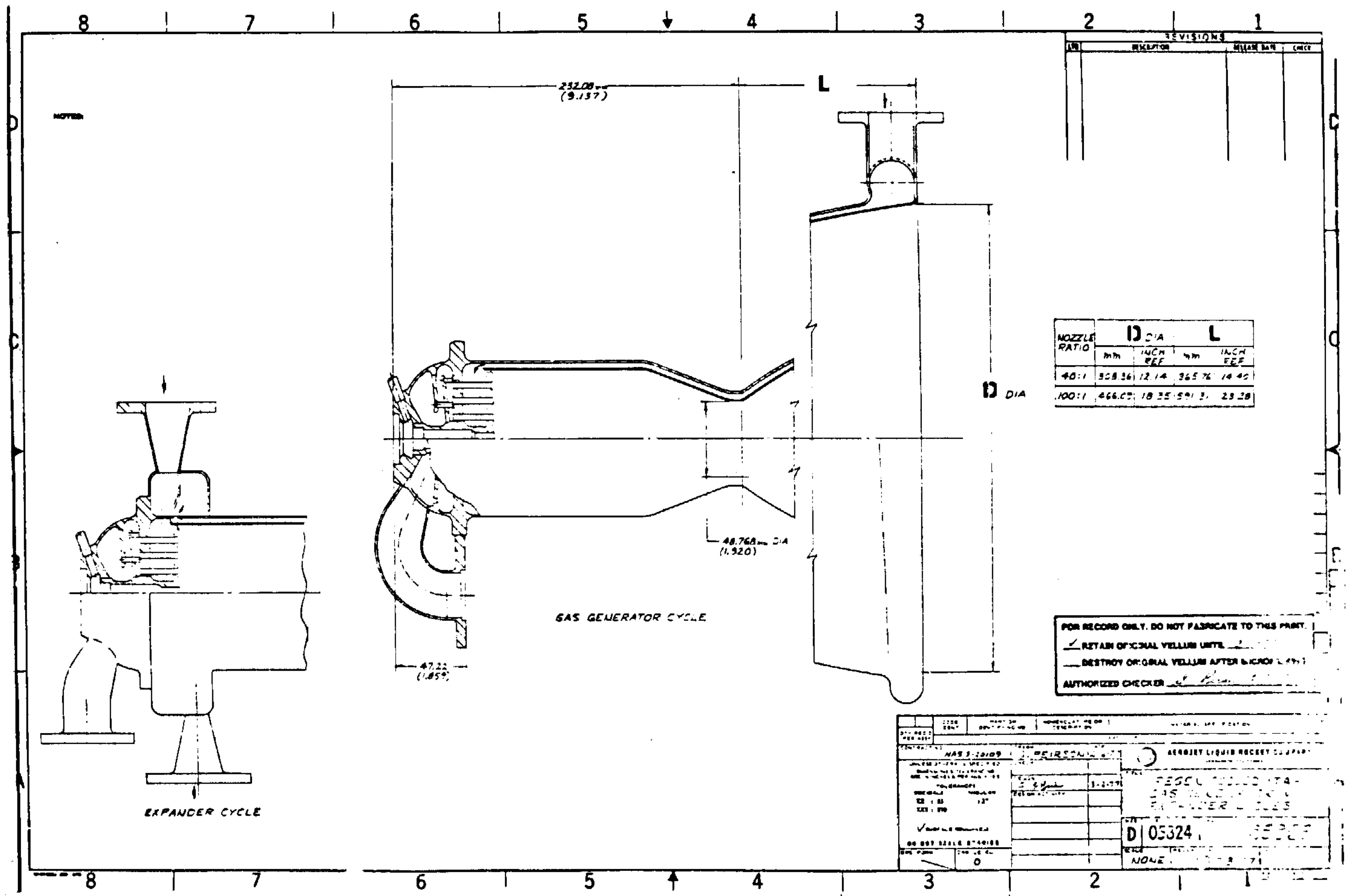

Figure 117. Regen-Cooled ITA, Dwg. No. 1185963.

The estimate of thermal strain in the coolant channel was made using the equation:

$$\varepsilon_T = K \cdot \alpha \cdot \Delta T$$

where K = 2 is a factor based on detailed finite element analyses of similar structures, α = coefficient of expansion at the average wall temperature, T_{ave}, and ΔT = gas side temperature T_{wg_3} minus cold side temperature T_{int}.

The total strain in the coolant channel is given by the sum of the thermal and pressure (bending stress) strains. Since the pressure strain in this case is negligible, the allowable cycles can be read directly from Figure 118. The calculations for life determination are summarized in Table XLI. It is seen that in all cases the cycle life for the regeneratively cooled module is greater than the required 1200 cycles.

TABLE XLI. REGEN COOLED MODULE LIFE CYCLE DETERMINATION

Chamber Pressure atm(psia)	Channel Depth cm (in)	T_{wg_3} °K (°F)	ΔT °K (°F)	ε_T	Flow	Life Cycles
20.4(300)	.38 (.15)	701 (802)	536 (504)	.011	Coflow	3400
"	.64 (.25)	761 (910)	625 (665)	.014	"	2000
20.4(300)	.38 (.15)	678 (760)	541 (514)	.010	Counterflow	3700
"	.51 (.20)	713 (824)	587 (596)	.012	"	2700
"	.64 (.25)	739 (870)	628 (671)	.014	"	1900
34.0(500)	.51 (.20)	794 (970)	661 (729)	.015	"	1700

Although creep life determination was not included in this study, it is apparent that there is adequate life for the low magnitude stress conditions that exist (cf. Reference 45).

G. UNCOOLED PLUG NOZZLE

Preliminary calculations were made for an uncooled plug nozzle configuration using graphite and carbon technology for materials of construction. AGCarb 101K, a low modulus graphite composite which can be fabricated in free standing structures, was chosen as a typical candidate material. It has been used to launch communication satellites. (SVM-7 is the Aerojet Solid Propulsion Company designation for Apogee Kick Motor used to orbit the RCA SATCOM, U. S. Domestic Communications Satellite.) This material is fully characterized and its properties are well understood. AGCarb 5451, another candidate, is made from a higher modulus, higher density version of AGCarb 101 which provides improved erosion resistance.

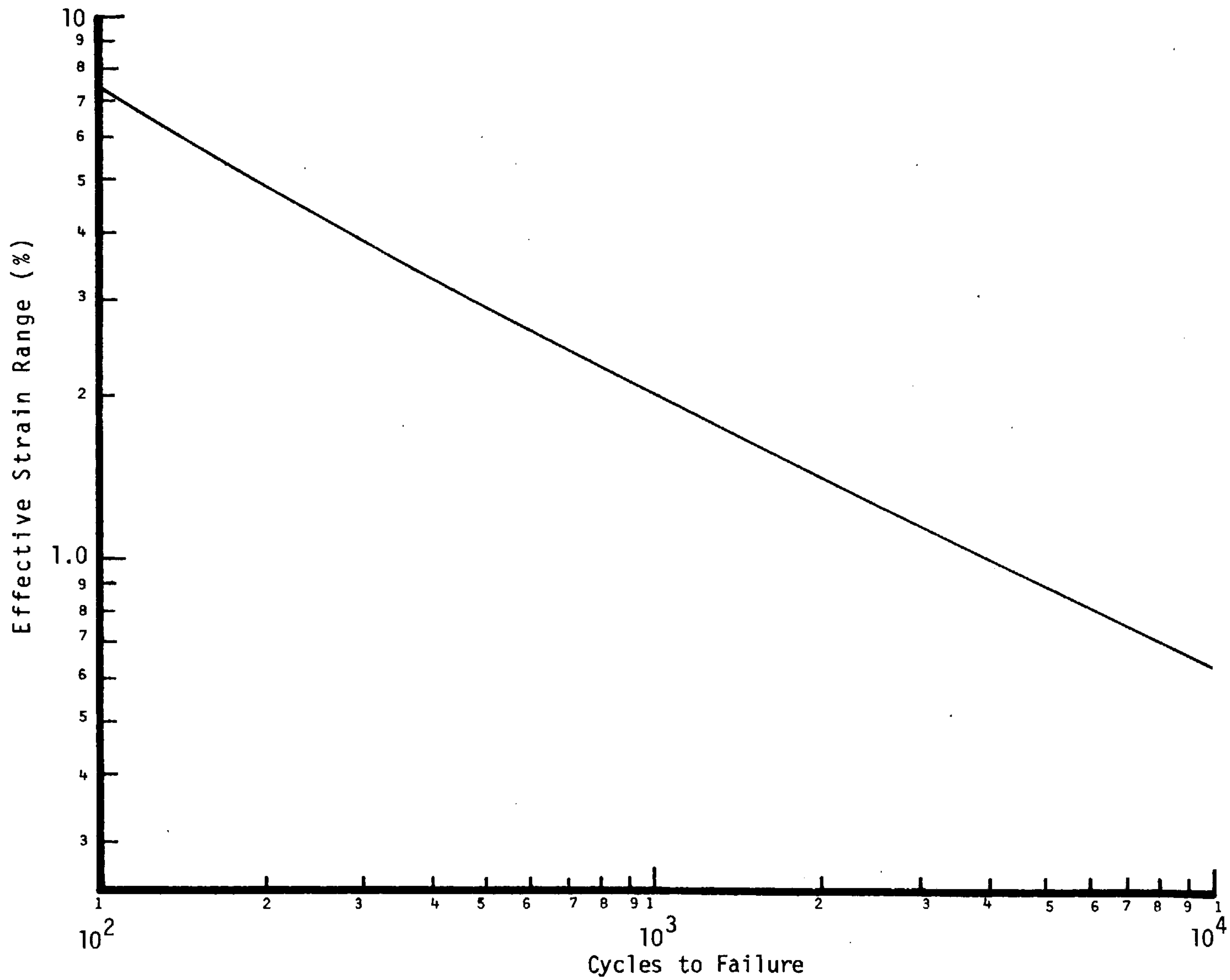

Figure 118. Isothermal Cycle Test Data - Zirconium-Copper.

Demonstrated experience with AGCarb is noted in Table XLII. Summary of selected AGCarb material properties is given in Table XLIII and a typical density of graphite composite structures varies from 1.45 to 2.20 g/cc, the higher value being for pyrolytic graphite.

Plug dimensions assumed for the nozzle calculations are 2.84 m (112 in) diameter by 2.16 m (85 in) diameter by 1.28 m (50 in) length with the geometry being approximated by a frustum of a cone. If the density of the AGCarb is taken as 1.45 g/cc, then the nozzle weight is given as 18 Kg (40 lb) for a wall thickness 0.14 cm (0.055 in), which corresponds to the weight of 45 Kg (99 lb) of the regeneratively cooled tubular structure described in Section VI.C. (and Table XLVI).

A structural analysis was performed to determine the required wall thickness for a plug nozzle with the pressure distribution shown in Figure 107. A wall thickness of 0.130 cm (0.051 in.) is acceptable for the plug from a fabrication point of view and this thickness was selected for analysis. Buckling is the critical failure mode, and was, therefore, utilized for determining the number and placement of required circumferential ring stiffeners. Four stiffeners are required with K-408 AGCarb and three with K-550D AGCarb. The circumferential ring stiffeners have square cross sections with dimensions of 2.54, 2.29, 2.03 and 1.91 cm (1, 0.9, 0.8 and 0.75 in), respectively.

A tapered panel section with the thickness varying from 1.02 to 0.25 cm (0.4 to 0.1 in) was found to be structurally suitable for the nozzle fairing. Carbon-carbon bonding techniques ensure adequate bonding strength at the fairing-nozzle interface.

1. AGCarb Nozzle Cycle Life

The life of the carbon-carbon cloth (AGCarb) plug nozzle was evaluated using an erosion rate expression of Heddon and Loewe (Reference 43). It is a Hinshelwood-type equation and is based on experimental work with a nuclear reactor grade graphite (density = 1.76 g/cc, surface area = 7.8 m^2/g at temperatures of 1213 - 1330°K (1724 - 1886°F) and H_2O partial pressures of 3.4×10^{-4} to 1.02×10^{-3} atm (0.005 to 0.015 psia). The equation is:

TABLE - XLII - DEMONSTRATED EXPERIENCE WITH AGCarb

PROGRAM	THRUST*	P_c**	PROPELLANTS	REMARKS
AF 04(611)-10918	100 5000	100 and 200	LF_2/BA1014 LF_2/BA1014	FREE STANDING FIBROUS GRAPHITE AND ABLATIVE
F04611-67-C-0003	7000	100	LF_2/BA1014	ABLATIVE WITH FIBROUS GRAPHITE THROAT INSERTS
F04611-67-C-0053	3750	200 and 300	ClF_3/MMH & LF_2/BA 1014	FREE STANDING FIBROUS GRAPHITE AND ABLATIVE
F04611-68-C-0034	3750	300 and 500	ClF_3/MMH	FREE STANDING FIBROUS GRAPHITE AND ABLATIVE
COMPANY SPONSORED	4000	[illegible]	ClF_3/BA1014	FREE STANDING FIBROUS GRAPHITE
NAS 7-100	200	100	OF_2/B_2H_6	FREE STANDING FIBROUS GRAPHITE
PROJECT 398 SNPO	75000	400	H_2, NUCLEAR	AGCarb
SVM7 APOGEE KICK MOTOR - RCA SATCOM (FLIGHT TESTED	10000	600	ANB-3066	FREE STANDING AGCarb 101K
UPPER STAGE MX SUBSCALE	-	1225	FEFO	AGCarb 5451

*lb_f **psia

TABLE XLIII - SUMMARY OF SELECTED AGCarb MATERIAL PROPERTIES

	Orientation	Temp, °F	Typical High Density Chamber Shell Material K-550D	K-408
1. TENSILE				
Strength, psi	Warp	RT	38,500	11,000
		3000	47,000	13,000
	Fill	RT	14,000	6,750
		3000	14,000	-
Modulus, 10^6 psi	Warp	RT	22.0	2.25
		3000	-	-
	Fill	RT	-	1.58
		3000	4.0	-
2. COMPRESSION				
Strength, psi	Warp	RT	30,000	12,000
		3000	39,000	-
		4000	40,000	-
		5000	26,000	-
	Fill	RT	12,000	7,000
		5000	13,000	-
Modulus, 10^6 psi	Warp	RT	23.0	2.2
		3000	16.9	-
		4000	18.0	-
		5000	4.0	-
	Fill	RT	7.0	1.5
		5000	2.0	-
3. SHEAR				
Interlaminar	Warp	RT	1,370	1,570
		5000	2,110	-
	Fill	RT	610	1,780
		3000	1,460	-
3. Shear (cont.)				
Cross Ply	Warp	RT	7,250	3,500
		3000	16,800	-
	Fill	RT	3,480	-
4. THERMAL CONDUCTIVITY BTU Hr^{-1} Ft^{-1} $°F^{-1}$	Warp	RT	75.3	35.0
		3000	47.6	19.8
		4000	43.1	19.4
	Fill	RT	28.0	35.1
		3000	17.1	17.5
		4000	16.8	16.2
Cross Ply		RT	9.46	19.0
		3000	6.63	9.88
		4000	7.02	9.63
5. CTE - in./in. - °F x 10^{-6}	Warp	RT-1000	-0.140	+0.803
		RT-3000	+0.429	+1.37
		RT-5000	+0.791	+1.70
	Fill	RT-1000	-0.126	+0.732
		RT-3000	+0.529	+1.48
		RT-5000	+0.750	+1.74
Cross Ply		RT-1000	+4.48	+2.55
		RT-3000	+4.74	+3.16
		RT-5000	+5.32	+3.56

(1) All of the elevated temperature properties are not shown; however, both materials show increasing strengths up to 4000°F with little decrease at 5000°F.

TABLE XLIV - MATERIALS AND FABRICATION TECHNIQUE TRADE STUDY

Candidate	Selected	Rejected	Comments
Material			
AGCarb	X		Good thermal stability, low erosion, gas compatible, flight tested, free standing.
Ablative		X	Too heavy; duration limited
Bulk Graphite		X	Thermal shock resistance not demonstrated.
Pyrolytic Graphite (throat insert only)		X	Can be used if necessary with AGCarb chamber shell. PG washer packs are used on MX and C-4 high pressure solid rocket.
Reinforcement			
Precursor			
Rayon, Continuous	X		Selected for graphite yarn. Demonstrated on SVM6 and SVM7.
Pan		X	Higher cost, not demonstrated, lower interlaminar shear, fabrication loss greater.
Pitch		X	New precursor, not demonstrated, fab. technicques not proven low reliability.
Fabric Weave			
Plain (square)	X		Demonstrated, flexible fabric, intermediate strength, best interlaminar shear.
Harness Satin		X	Tends to delaminate.
Fabrication - Reinforcement Orientation			
2D			
Rosette	X		Demonstrated low cost fabrication techniques.
Shingle		X	More costly, not demonstrated, primary 2D alternate.
Tape Wrap		X	Low axial compression and tensile, not demonstrated as free standing, low cost fabrication.
Angle Layup	(Throat insert)		Low cost, method to achieve high density.
3D			
Orthogonal		X	Costly, structural advantages not needed, demonstrated on reentry systems.
Cylindrical		X	Free standing, excellent mechanical properties; not demonstrated, costly, long process time.
Matrix			
Resin Pitch			
Low Pressure	X		Demonstrated, low cost, most fabrication experience.
High Pressure		X	Costly, high density not needed in chamber.
Chemical Vapor Deposition Carbon		X	Not demonstrated, costly, best 2D interlaminar shear, lower fiber content.
CVD Resin Pitch		X	More costly than resin/pitch, not demonstrated in flight, some improvement in shear over straight resin pitch, primary alternate.
Coatings			
PG or SIC/PG		X	Firing time too long for developed and demonstrated coating technology. Multiple starts requirement not demonstrated.

$$r_m = \frac{K_1 \cdot C_{H20}}{1 + K_2 \cdot C_{H2}} \qquad (\frac{\text{Mole}}{\text{g-s}})$$

where $K_1 = 5 \times 10^{12}\ e^{-68,000/RT}$ cc/g-s

$K_2 = 6.7 \times 10^{-5}\ e^{14,500/RT}$ cc/Mole

C_{H20} = H_2O concentration g/cc

C_{H2} = H_2 concentration Mole/cc

T = temperature °K

R = gas constant 1.9872 cal/Mole - °K

This equation was checked with data from Lewis, Floyd and Cowlard (Reference 44), who investigated various carbons (pyrolytic graphite, vitreous carbon and erosion- resistant synthetic graphite) at pressures of 1 to 3 atmospheres and surface temperatures of 1500 to 3000°K. The erosion rate calculated for plug cluster conditions (P_c = 20.4 atm [300 psia] and T = 1067-1875°K [1460 - 2915°F] - see Table XXIX)

Area Ratio on Plug	Erosion Rate cm/10 hr (mil/10 hr) Synthetic Graphite	Pyrolytic Graphite
40	0.16 (63)	.005 (2)
458	3×10^{-5} (.010)	8×10^{-7} (0.0003)

Examination of the table indicates that pyrolyzed graphite nozzles are capable of meeting the 10-hour life requirement with ease, while synthetic graphite nozzles would erode somewhat at the module-plug interface (εM = 40). The AGCarb nozzle will exhibit properties between those for synthetic graphite and pyrolytic graphite shown in the table. Should erosion be a problem at the module interface, a coating of pyrolytic graphite or metal carbide could be applied.

H. UNCOOLED BELL NOZZLE EXTENSION

The successful application of AGCarb carbon-carbon cloth composite materials for the plug nozzle structure prompted the investigation of these materials for uncooled nozzle extensions for the modules.

The basic module is regeneratively cooled to an area ratio of ε = 40. The AGCarb nozzle extension is attached at this point to extend the area ratio to ε = 500. The surface temperature at the attach point is 1867° (2900°F) As indicated previously for the plug, the cycle life of the AGCarb is greater than 10 hours for the environemntal conditions of this study.

Fabrication of the full or scarfed bell nozzle extension is within the state-of-the-art for this size nozzle (79 to 102 cm [31 to 40 in] exit diameter). Assembly of the cluster and installation of the base closure is also readily accomplished. The scarfed bell nozzle assembly forms a fluted plug with ideal aerodynamic contour, as opposed to the assembly of the same number of ε = 40 modules on an annular plug.

I. WEIGHT ANALYSIS

The baseline plug cluster weights for the expander and gas generator cycles were established by careful analysis of existing component weights, scaling equations, and layout drawings (Figures 104 and 106). Revisions to the component weights were made to incorporate materials and design changes.

1. Module Weight

The existing ITA module weight breakdown (cf. Tables V and XXXIV) was examined and a 15 percent weight reduction was realized by assuming that a welded joint would replace line flanges. Elimination of the oxidizer flange (PN1162901-1), the fuel flange (PN1162901-2), the fuel inlet line (PN1162906-1), and the oxidizer inlet line (PN1162885-1) resulted in a weight savings of 0.52 kg (1.14 lb) chargeable to the module. The heavy injector head and flange were modified to reduce the weight by 0.23 kg (0.5 lb), and solid state circuitry was utilized to reduce the ignition system weight from 0.99 kg (2.19 lb) to 0.77 kg (1.69 lb). This weight reduction is reflected in the plug cluster engine baseline module weight given in Table XLV.

The nozzle extension weight for the regeneratively cooled module was estimated utilizing the design data from Ref. 35 (p. 705).

TABLE XLV. MODULE WEIGHT ANALYSIS

	Module		
Component	ITA(9) Kg (lb)	Baseline ITA Module Kg (lb)	Baseline Regen Module Kg (lb)
Igniter	0.99 (2.19)	0.77 (1.69)	0.77 (1.69)
Nozzle Extension	1.64 (3.61)	1.64 (3.61)	3.18 (7.00)
Chamber	1.56 (3.43)	1.56 (3.43)	1.56 (3.43)
Chamber Line/Torus/Flange	0.56 (1.24)	0.05 (0.10)	0.05 (0.10)
Injector Assembly	1.88 (4.14)	1.65 (3.64)	1.65 (3.64)
	6.63 (14.61)	5.66 (12.47)	7.20 (15.86)

2. Plug Nozzle/Thrust Structure Weight

The weight of the plug nozzle plus fairings and thrust mount is given in Table XLVI.

A similar weight analysis was performed for the uncooled AGCarb plug nozzle and associated thrust structure. The weights are also summarized in Table XLVI.

Differences in the weights of the common components for the regen and uncooled plugs are found in the table. The major difference lies in the thrust structure assumed for the uncooled plug which is 31.4 kg (16.4 + 15.0) comparied to 22.1 kg (10.2 + 11.9) for the cooled plug nozzle. This difference indicates the uncertainty in the selection of structure for the two preliminary designs.

3. Module AGCarb Nozzle Extension and Base Closure Weight

The AGCarb nozzle extension (ε = 40 to ε = 500) weight was calculated for modules operating at both 20.4 and 34.0 atm (300 and 500 psia) chamber pressures. Geometry data for the individual module and the cluster configuration are given in Figures 119 and 120.

The procedure for computing the weights was to: (1) calculate surface area (As), (2) assume a wall thickness (t = 0.127 [0.050 in]) and density (ρ = 1.45 g/cc [0.052 lb/in^3]), and (3) calculate the weight from W = AS tρ. Tapered (0.127 to 0.064 cm thickness) nozzle weights were also calculated.

For the case of scarfed nozzles the surface area reduction due to scarfing was assemed to be 40% the corresponding surface area reduction for a 15° conical nozzle.

The resultant nozzle and base closure weights for the cluster engines formed by high area ratio bell nozzles are given in Table XLVII.

4. Turbopump Weight

The RL10 turbopump weight (35.9 Kg or 79.1 lb) from Reference 14 was utilized in determining the baseline weight of 31.8 Kg (70 lb) for the plug cluster engine. A redesign of this pump according to 1977 state-of-the-art would show a marked reduction in weight.

A parallel turbine turbopump assembly based on current state-of-the-art (Figures 78, 81 and 82) is expected to weigh only 21.3 kilograms (47 pounds).

TABLE XLVI - PLUG NOZZLE/THRUST STRUCTURE WEIGHT ANALYSIS

Component	Regeneratively Cooled Plug Nozzle	Uncooled AGCarb Plug Nozzle
	kg (lb)	kg (lb)
Thrust Ring	10.2 (22.5)	16.4 (36.2)
Plug Wall	44.9 (99.0)	18.6 (41.1)
Base Closure	4.6 (10.1)	5.6 (12.3)
Struts/Plates	11.9 (26.2)	15.0 (33.0)
Fairings	14.7 (32.4)	16.1 (35.5)
Total	86.3 (190.2)	71.7 (158.1)

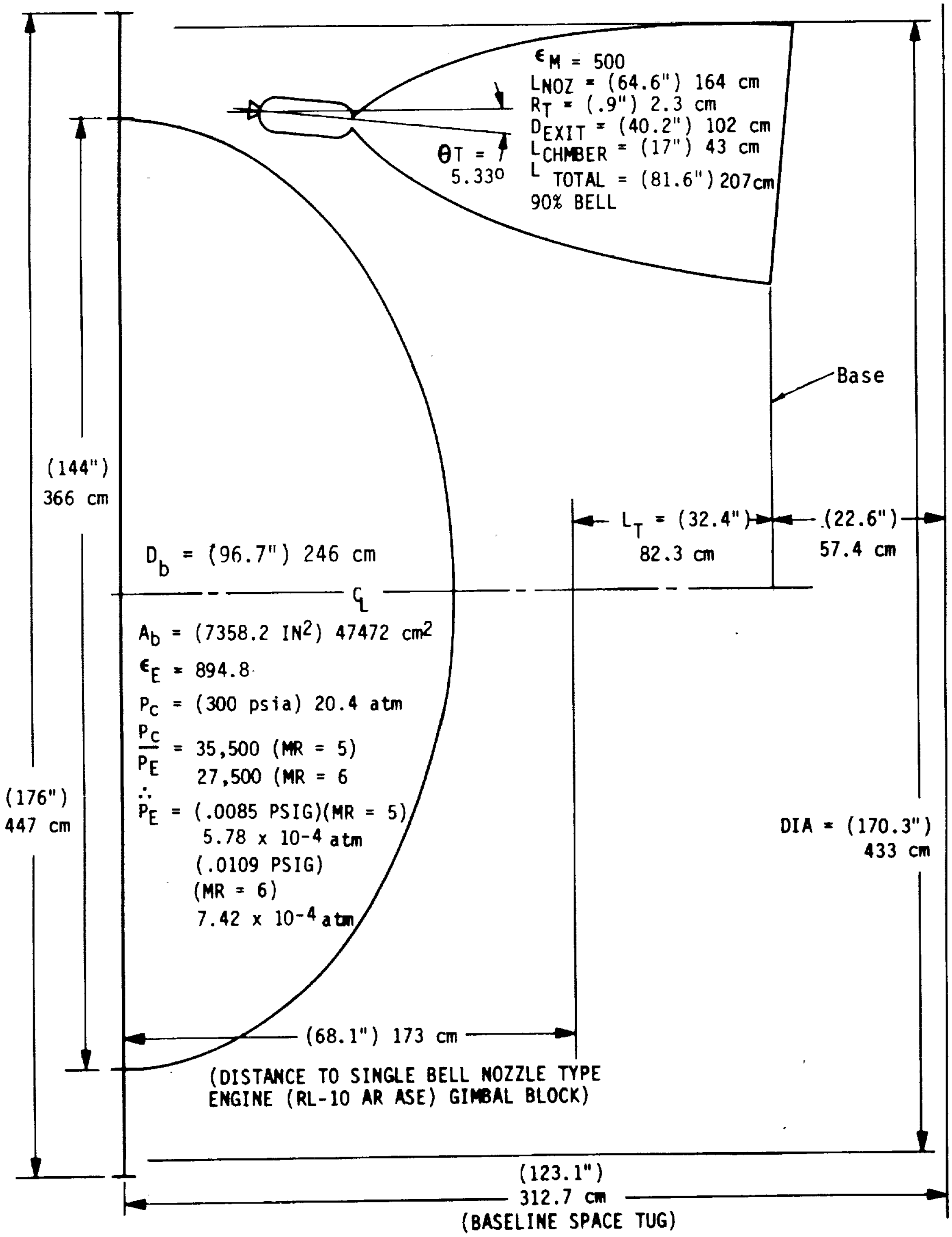

Figure 119. Plug Cluster Engine Geometry (Pc = 20.4)

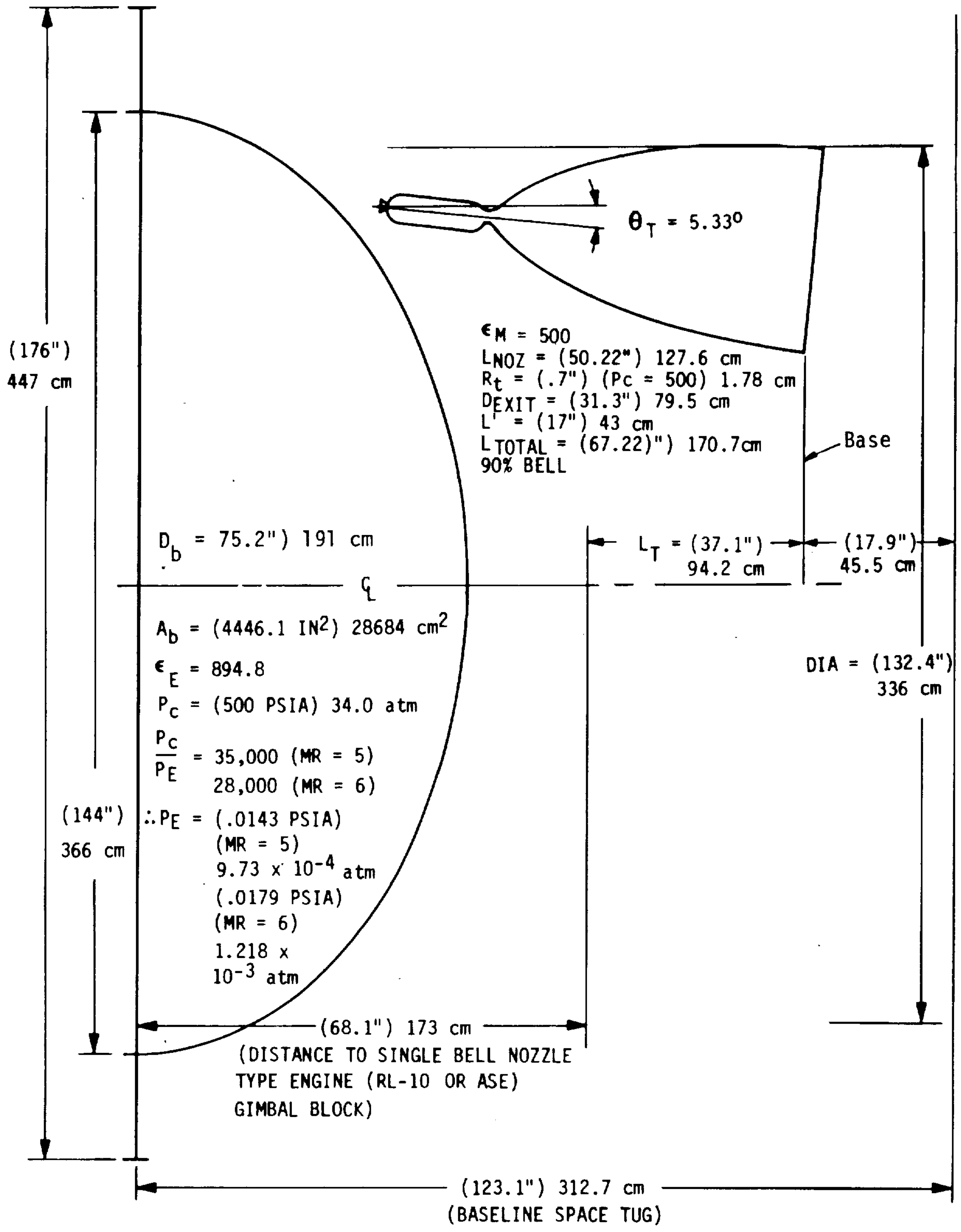

Figure 120. Plug Cluster Engine Geometry (Pc = 34.0)

TABLE XLVII - AGCarb NOZZLE EXTENSION AND BASE CLOSURE WEIGHT FOR PCE FORMED FROM BELL NOZZLES

COMPONENT	BASELINE WEIGHT Kg (lb)	
	P_c = 20.4 atm	P_c = 34.0 atm
Nozzle Extension* (10 Modules) ε = 40 to ε = 500	67.1 (148)	40.9 (90.1)
Scarfed Nozzle ** (ε 40 to ε = 500)	40.0 (88.1)	24.4 (53.9)
Base Closure	8.7 (19.1)	5.3 (11.6)
Weight Effective Plug (Unscarfed)	75.8 (167.1)	46.1 (101.7)
Weight Effective Plug (Scarfed)	48.6 (107.2)	29.7 (65.5)

*Tapered Nozzle 75% of Weight Shown
**Tapered Nozzle 80% of Weight Shown

5. Valve Weight

The baseline valve weight of 24.1 kilograms (53.2 pounds) was established for the selected cycle (Figure 111) and its required number of valves by comparison with the weights of corresponding valves of the candidate Tug engines given in Table XLVIII.

A revised valve weight statement was prepared (see Section VI.E., Table XL) for the uncooled plug and clustered bell systems. The valve listing is included in Table XLIX.

6. Line Weight

The line weights were determined from the engine layout drawings (Figures 104 and 106). Minimum wall thicknesses calculated using a safety factor of 1.5 were a factor of two to ten lower than the wall thickness values utilized.

The total line weight for the baseline expander cycle engine is 16.15 kilograms (35.6 pounds).

Line weights were reevaluated for the uncooled plug and clustered bell systems. The expander cycle and gas generator line weights amounted to 12.7 and 12.3 Kg (28.0 and 27.2 lb), respectively, showing a 20% reduction in weight. The revised line weight breakdown is given in Table XLIX.

7. Weight Summary

The baseline plug cluster engine weight, corresponding to the regeneratively cooled plug nozzle designs, in Figures 104 and 106 are summarized by component in Table XLVIII. Controls, connecting and miscellaneous hardware weight, consistent with that for the candidate Space Tug engines, are included in the table.

A similar weight breakdown is given in Table XLIX for the uncooled plug cluster engine, the clustered bell engine, the scarfed bell/fluted plug cluster engine at two chamber pressures, and the scarfed bell/fluted plug engine utilizing a gas generator cycle. Note that the GG cycle reduces engine weight by about 11.3 Kg (25 lb), and that operation at the higher chamber pressure (34.0 atm [500 psia]) reduces engine weight by 24.5 Kg (54 lb).

The minimum plug cluster engine weight appears to be about 181 Kg (400 lb) for the higher pressure engine utilizing a GG cycle. In general, however, the plug cluster engines weigh more than the candidate Space Tug engines listed in Table XLVIII. This might be expected due to the geometrical configuration of the plug cluster. Every effort has been made

TABLE XLVIII - TYPICAL WEIGHT BREAKDOWN CHART BY COMPONENT FOR CANDIDATE SPACE TUG ENGINES

ENGINE:	RL-10-IIB (Retractable Nozzle)	AMPS AEROSPIKE (Single Panel)	AMPS AEROSPIKE (Double Panel)	ASE (Retractable Nozzle)	PLUG CLUSTER (Expander Cycle; 0% FFC; ℓ/D_E = 2) MODEL I	PLUG CLUSTER (Gas Generator Cycle; 0% FFC; ℓ/D_E = 2) MODEL I
Thrust (lbf)	15,000.	25,000.	25,000.	20,000.	16,302.	16,430.
Chamber Pressure (psia)	400.	750.	1,000.	2,233.	300.	300.
Mixture Ratio	6.0	5.5	5.5	6.0	5.5	5.5
Engine Area Ratio	66.3/205. Nozzle: unextended/extended	110.	200.	100./400. Nozzle: unextended/extended	458.4 (ϵ_m = 40)	458.4 (ϵ_m = 40)
Engine Diameter (in.)	39.7/70.6 Nozzle: unextended/extended	61.1	66.9	24 2/48.5 Nozzle: unextended/extended	125.9	125.9
Engine Length (in.)	55./110. Nozzle: unextended/extended	24.1	27.0	50.5/94.0 Nozzle: unextended/extended	37.8	37.8
Nozzle (or Plug)	63.	20.	20.	30.	15.	15.
	95.6	97.6	98.5	97.5	**96.2**	**96.1**
I_{sv} (seconds)	456.5	458.0	470.4	473.4	**467.4**	**466.8**
ENGINE WEIGHT (lbm)	443.0	360.0	398.0	337.3	527.2	528.6
Injector Assembly	14.9			18.0	36.4	36.4
Thruster Chamber & Primary Nozzle	83.0	119.0	114.0	101.0	105.4	105.4
Support Ring & Seal	12.0					
Thrust Mount & Gimbal Assy.	3.0	16.0	15.0	6.0	44.6*	44.6*
Extendable Nozzle	73.0					
Extendable Nozzle Actuator	43.0					
Plug Nozzle & Fairings		33.0	45.0		135.5	135.5
Base Closure		6.0	3.0		10.1	10.1
Turbopumps & Mounts	79.1	63.0	85.0	37.9	73.0	47.0
Gas Generator or Preburner				5.6		5.6
Heat Exchanger	13.0			1.6		
Ignition System	15.0	7.0	7.0	6.0	15.9	20.3
Instrumentation	9.8			3.5		
Ox Lines	4.5	14.0	80.0	1.3	6.4	5.5
Fuel Lines	20.7			9.4	23.4	19.0
Hot Gas Lines						8.0
Misc. (small) Lines	2.2				5.8	7.7
Oxidizer Inlet Shutoff Valve	5.6			12.5	5.5	5.6
Fuel Inlet Shutoff Valve	5.8			12.5	5.3	5.3
Oxidizer Flow Control Valve	9.0			38.0	4.2	4.2
Gaseous Oxidizer Valve	2.0					
Fuel Vent Valve	6.3					
Turbine Bypass Valve	4.2				4.2	
Thrust Control Valve	3.3					10.0
Nozzle Coolant Valve	2.0					
Main Fuel Shutoff Valve	3.4				3.4	3.4
Tank Pressurizing Valves	4.0				1.0	[illegible]
Solenoid Valves	10.0				7.5	7.5
Igniter Valves					20.0	20.0
Purge System Check Valves					1.5	1.5
GG Fuel Control Valve						3.2
GG Ox Control Valve						3.2
GG Igniter Valves						1.0
Miscellaneous Valves				2.7		
Controls, Connecting & Misc Hdwr	8.2	49.0	39.0	30.2	19.5	19.5
TOTAL ENGINE WEIGHT	443.0	360.0	398.0	337.3	507.2	509.0

*20.0 lbm of thrust mount weight listed is normally included as vehicle weight

TABLE XLVIII (cont.)

ENGINE	RL-10-IIB (Retractable Nozzle)	AMPS AEROSPIKE (Single Panel)	AMPS AEROSPIKE (Double Panel)	ASE (Retractable Nozzle)	PLUG CLUSTER (Expander Cycle; 0% FFC; ℓ/D_E = 2) MODEL I	PLUG CLUSTER (Gas Generator Cycle, 0% FFC; ℓ/D_E = 2) MODEL I
Thrust (N)	66,723.3	111,205.5	111,205.5	88,964.4	72,514.9	73,384.3
Chamber Pressure (atm.)	27.2	51.0	68.1	152.0	20.4	20.4
Mixture Ratio	6.0	5.5	5.5	6.0	5.5	5.5
Engine Area Ratio	66.3/205.0 Nozzle: unextended/extended	110.0	200.0	100./400. Nozzle: unextended/extended	458.4 (ϵ_m = 40)	458.4 (ϵ_m = 40)
Engine Diameter (m)	1.01/1.79 Nozzle: unextended/extended	1.55	1.70	0.61/1.23 Nozzle: unextended/extended	3.20	3.20
Engine Length (m)	1.40/2.79 Nozzle: unextended/extended	0.61	0.69	1.28/2.39 Nozzle: unextended/extended	0.96	0.96
Nozzle (or Plug)	63	20	20	90	15	15
[illegible]	95.6	97.6	98.5	97.5	96.2	96.1
I_{sv} (seconds)	456.5	452.0	470.4	473.4	467.4	466.8
ENGINE WEIGHT (kg_m)	200.9	163.3	180.5	153.0	239.1	[illegible]
Injector Assembly	6.76			8.16	16.5	16.5
Thrust Chamber & Primary Nozzle	37.6	53.53	51.69	45.81	47.82	47.82
Support Ring & Seal	5.44					
Thrust Mount & Gimbal Assy.	3.6	7.27	8.61	2.72	20.2*	20.2*
Extendable Nozzle	33.[illegible]					
Extendable Nozzle Actuator	19.5					
Plug Nozzle & Fairings		13.6	20.4		61.5	61.5
Base Closure		[illegible]	4.1		4.6	4.6
Turbopumps & Mounts	35.9	27.2	34.6	44.4	31.8	31.8
Gas Generator or Preburner				2.5		3.8
Heat Exchanger	5.90			0.73		
Ignition System	6.80	3.2	3.2	2.2	7.68	7.68
Instrumentation	4.1			1.6		
Ox Lines	2.1				2.9	[illegible]
Fuel Lines	9.40				10.6	[illegible]
Hot Gas Lines						3.6
Misc. (Small) Lines	1.0				2.6	[illegible]
Oxidizer Inlet Shutoff Valve	2.5			5.6	2.5	[illegible]
Fuel Inlet Shutoff Valve	2.6			6.6	2.6	[illegible]
Oxidizer Flow Control Valve	4.1			11.3	1.9	[illegible]
Gaseous Oxidizer Valve	0.9					
Fuel Vent Valve	2.0					
Turbine Bypass Valve	1.9	33.6	36.2		1.9	
Thrust Control Valve	2.4					4.8
Nozzle Coolant Valve	0.9					
Main Fuel Shutoff Valve	1.5				1.5	[illegible]
Tank Pressurizing Valves	1.8				0.5	[illegible]
Solenoid Valves	4.5				3.4	3.4
Igniter Valves					9.1	[illegible]
Purge System Check Valves					0.7	[illegible]
GG Fuel Control Valve						[illegible]
GG Ox Control Valve						[illegible]
GG Igniter Valves						[illegible]
Miscellaneous Valves				1.2		
Controls, Connecting & Misc. Hdwr.	3.7	22.2	17.7	13.7	8.8	8.8
TOTAL ENGINE WEIGHT	200.9	163.3	180.5	153.0	239.1	[illegible]

*9.1 kgm of thrust mount weight listed is normally included as vehicle weight.

TABLE XLIX - WEIGHT BREAKDOWN FOR LIGHTWEIGHT PLUG CLUSTER ENGINES

ENGINE:	MODEL II PLUG CLUSTER UNCOOLED PLUG (EXPANDER CYCLE)	MODEL III CLUSTERED BELL (ϵ_M=500) (EXPANDER CYCLE)	MODEL III PLUG CLUSTER (SCARFED BELL) (EXPANDER CYCLE)	MODEL III PLUG CLUSTER (SCARFED BELL) (GAS GENERATOR CYCLE)	MODEL III PLUG CLUSTER (SCARFED BELL) (EXPANDER CYCLE)
Thrust (N)	68,950	67,230	67,230	67,141	67,230
Chamber Pressure (atm)	20.4	20.4	20.4	20.4	34.0
Mixture Ratio	5.5	5.5	5.5	5.5	5.5
Engine Area Ratio	458	895	895	895	895
Engine Diameter (cm)	320	433	433	433	336
Equivalent Engine Length (cm)	85.9	82.3	82.3	82.3	94.2
% Plug Nozzle	15	0	-	-	-
η	0.914	0.946	0.946	0.944	0.950
I_{sv} (seconds)	443.8	463.9	463.9	463.3	465.9
Injector Assembly	16.5	16.5	16.5	16.5	12.8
Thruster Chamber & Primary Nozzle	47.8	47.8	47.8	47.8	43.0
Thrust Mount & Gimbal Assy.	31.4	16.4	16.4	16.4	16.4
Nozzle Extension	0	67.1	40.0	40.0	24.4
Plug Nozzle & Fairings	34.7	0	0	0	0
Base Closure	5.6	8.7	8.7	8.7	5.3
Turbopumps & Mounts	31.8	31.8	31.8	21.3	24.2
Gas Generator or Preburner	0	0	0	2.5	3.4
Ignition System	7.7	7.7	7.7	7.7	7.7
Lines: Total Weight	12.7	12.7	1.27	12.3	11.1
Ox Lines	4.9	4.9	4.9	4.9	4.4
Fuel Lines	5.6	5.6	5.6	2.0	2.8
Hot Gas Lines	0	0	0	2.0	1.9
Line Supports	2.3	2.3	2.3	2.3	2.0
Valves: Total Weight	28.3	28.3	28.3	25.2	37.8
Oxidizer Inlet Shutoff Valve	3.9	3.9	3.9	3.9	5.1
Fuel Inlet Shutoff Valve	3.9	3.9	3.9	3.9	5.1
Oxidizer MR & PU Control Valve	3.6	3.6	3.6	-	4.9
Oxidizer Injector Check Valve (10)	4.1	4.1	4.1	4.1	5.4
Turbine Bypass Valve	2.7	2.7	2.7	-	3.6
Thrust Control Valve	2.1	2.1	2.1	-	2.8
Tank Pressurizing Valves	0.5	0.5	0.5	0.5	0.6
Solenoid Valves (3)	3.4	3.4	3.4	3.4	4.5
Igniter Valves (Oxidizer)	3.6	3.6	3.6	3.6	4.9
Purge System Check Valves	0.7	0.7	0.7	0.7	0.9
GG Inlet Control Valve (Bipropellant)	-	-	-	2.8	-
GG Ox Throttle Valve	-	-	-	2.2	-
GG Igniter Valve (Oxidizer)	-	-	-	0.2	-
Controls, Connecting & Misc Hdwr	8.8	8.8	8.8	8.8	8.0
TOTAL ENGINE WIEGHT (Kg)	225.3	245.8	218.7	207.2	194.1

TABLE XLIX (cont.)

ENGINES:	MODEL II PLUG CLUSTER UNCOOLED PLUG (EXPANDER CYCLE)	MODEL III CLUSTERED BELL (ϵ_M=500) (EXPANDER CYCLE)	MODEL III PLUG CLUSTER (SCARFED BELL) (EXPANDER CYCLE)	MODEL III PLUG CLUSTER (SCARFED BELL) (GAS GENERATOR CYCLE)	MODEL III PLUG CLUSTER (SCARFED BELL) (EXPANDER CYCLE)
Thrust (lbf)	15,500	15,114	15,114	15,094	15,114
Chamber Pressure (psia)	300	300	300	300	500
Mixture Ratio	5.5	5.5	5.5	5.5	5.5
Engine Area Ratio	458	895	895	895	895
Engine Diameter (in.)	125.9	170.3	170.3	170.3	132.4
Equivalent Engine Length (in.)	33.8	32.4	32.4	32.4	37.1
% Plug Nozzle	15	0	-	-	-
η	0.914	0.946	0.946	0.944	0.950
I_{SV} (seconds)	443.8	463.9	463.9	463.3	465.9
Injector Assembly	36.4	36.4	36.4	36.4	28.2
Thruster Chamber & Primary Nozzle	105.4	105.4	105.4	105.4	94.8
Thrust Mount & Gimbal Assy.	69.2	36.2	36.2	36.2	36.2
Nozzle Extension	0	148.	88.1	88.1	53.9
Plug Nozzle & Fairings	76.6	0	0	0	0
Base Closure	12.3	19.1	19.1	19.1	11.6
Turbopumps & Mounts	70.	70.	70.	47.	53.4
Gas Generator or Preburner	0	0	0	5.6	7.5
Ignition System	16.9	16.9	16.9	16.9	16.9
Lines: Total Weight	28.0	28.0	28.0	27.2	24.6
Ox Lines	10.7	10.7	10.7	10.8	9.8
Fuel Lines	12.3	12.3	12.3	6.9	6.2
Hot Gas Lines	0	0	0	4.5	4.1
Line Supports	5.	5.	5.	5.0	4.5
Valves: Total Weight	62.5	62.5	62.5	55.5	23.3
Oxidizer Inlet Shutoff Valve	8.5	8.5	8.5	8.5	11.3
Fuel Inlet Shutoff Valve	8.5	8.5	8.5	8.5	11.3
Oxidizer Injector Check Valve (10)	9.0	9.0	9.0	9.0	12.0
Turbine Bypass Valve	5.9	5.9	5.9	-	7.9
Thrust Control Valve	4.6	4.6	4.6	-	6.1
Tank Pressurizing Valves	1.0	1.0	1.0	1.0	1.3
Solenoid Valves (3)	7.5	7.5	7.5	7.5	10.0
Igniter Valves (Oxidizer)	8.0	8.0	8.0	8.0	10.7
Purge System Check Valves	1.5	1.5	1.5	1.5	2.0
GG Inlet Control Valve (Bipropellant)	-	-	-	6.1	-
GG Ox Throttle Valve	-	-	-	4.9	-
GG Igniter Valves (Oxidizer)	-	-	-	0.5	-
Controls, Connecting & Misc Hdwr	19.5	19.5	19.5	19.5	17.6
TOTAL ENGINE WEIGHT (lbm)	496.8	542.	482.1	456.9	428.

in this study to use similar engine state-of-the-art technology (turbopumps, injectors, combustion chamber, etc.) to provide an equivalent comparison of engines. Advantage was taken of the unique configuration of the plug cluster to evaluate the effect of lightweight uncooled nozzles.

SECTION VII

PLUG CLUSTER ENGINE OPTIMIZATION

A. OBJECTIVES AND GUIDELINES

Parametric system analyses were conducted to optimize the plug cluster engine concept for a Space Tug round trip to geosynchronous orbit mission. The engine design point for the optimization was the baseline design established in the preliminary design effort. It is consistent with the guidelines listed in Table I.

The payload capability is included using the exchange factors available from Space Tug system studies. Subsystem limitations imposed on the engine design or operation were evaluated.

Points of the study where additional technology will improve the feasibility of the plug cluster concept as a building block approach for future applications to advanced space vehicles were summarized.

B. ENGINE DESIGN SPECIFICATION

Specifications for the conventional engine design configurations are given in Appendix A Tables LXIV through LXX. The specifications are for engines utilizing expander and gas generator cycles, regeneratively-cooled and film-cooled modules, module area ratios of 40, and engine operating pressures of 20.4 and 34 atm. Geometric and performance data given in the tables were derived from the performance Model I presented in Section IV, and the performance was revised to reflect the Model II results.

In addition to these specifications, similar data are given in the Appendix Tables LXXI through LXXIV for the uncooled plug configurations.

Specifications for the recommended (optimized) engine configurations, the plug cluster/scarfed bell engines, are given in Tables L through LIII. Performance model III was utilized to generate these data.

Some of the effects that can be noticed by examination of the tables are: (1) an increase in chamber pressure leads to an increase in engine performance, and a decrease in engine diameter; (2) the gas generator cycle shows a small (about 0.1%) decrease in engine performance at Pc of 20.4 atm, a lower pump discharge pressure and a higher turbine operating temperature than a corresponding expander cycle; (3) the fuel film cooled ITA module leads to a significant decrease in specific impulse compared to a corresponding regeneratively cooled module; (4) the conventional plug cluster engine design (Tables LXIV through LXX) does not realize the high area ratio performance potential; (5) the plug cluster/scarfed bell, Tables L through LIII (PCE) engine design achieves the high area ratio performance potential through optimization of the aerodynamic flow contour of the plug nozzle.

TABLE L - PLUG CLUSTER/SCARFED BELL ENGINE OPERATING SPECIFICATION
EXPANDER CYCLE: REGEN-MODULE

MODEL III
$P_c = 20.4$

PARAMETER	SI UNITS	ALTERNATE UNITS	
ENGINE			
Vacuum Thrust	71.97 kN	16,180 lbf	
Chamber Pressure	20.41 atm	300 psia	
Vacuum Specific Impulse	463.9 s		
Mixture Ratio (O/F)	5.44		(5.50 TCA)
Total Flow Rate	15.82 kg/s	34.88 lbm/s	(34.82 TCA)
Oxidizer Flow Rate	13.36 kg/s	29.46 lbm/s	
Fuel Flow Rate	2.46 kg/s	5.42 lbm/s	
Engine Area Ratio (A_E/A_T)	895		
Module Area Ratio (A_e/A_t)	500		
Number of Modules	10		
Module Gap (δ/D_e)	0		
Engine Diameter	433 cm	170 in	
Plug Base Diameter	246 cm	96.7 in	
Engine Length	82.3 cm	32.4 in	
Module Chamber Diameter	8.59 cm	3.38 in	
Module Throat Diameter	4.72 cm	1.86 in	
Module Eixt Diameter	102 cm	40.2 in	
Module Chamber Length	16.51 cm	6.5 in	
Module Nozzle Length	164 cm	64.6 in	
Module Length	207 cm	81.6 in	
Coolant Jacket Flow Rate	2.46 kg/s	5.42 lbm/s	
Coolant Jacket ΔP	2.04 atm	30 psia	
Coolant Inlet Temperature	22 K	40 R	
Coolant Exit Temperature	246 K	442 R	
TURBINES			
Inlet Pressure	32.7 atm	480 psia	
Inlet Temperature	246 K	442	
Gas Flow Rate	1.38 kg/s	3.06 lbm/s	
Specific Heat Ratio	1.40		
Molecular Weight	2.02 g/mol		
Shaft Horsepower	290 kW	390 hp	
Percent Bypass	44		
MAIN PUMPS			
Oxidizer Pump Flow Rate	13.36 kg/s	29.46 lbm/s	
Oxidizer Pump Discharge Pressure	27.2 atm	400 psia	
Fuel Pump Flow Rate	2.46 kg/s	5.42 lbm/s	
Fuel Pump Discharge Pressure	36.7 atm	540 psia	

TABLE LI - PLUG CLUSTER/SCARFED BELL ENGINE OPERATING SPECIFICATIONS
EXPANDER CYCLE: REGEN-MODULE

MODEL III
$P_c = 34.0$

PARAMETER	SI UNITS	ALTERNATE UNITS	
ENGINE			
Vacuum Thrust	71.63 kN	16,100 lbf	
Chamber Pressure	34.02 atm	500 psia	
Vacuum Specific Impulse	465.9 s		
Mixture Ratio (O/F)	5.44		(5.50 TCA)
Total Flow Rate	15.68 kg/s	34.56 lbm/s	(34.50 TCA)
Oxidizer Flow Rate	13.24 kg/s	29.19 lbm/s	
Fuel Flow Rate	2.44 kg/s	5.37 lbm/s	
Engine Area Ratio (A_E/A_T)	894		
Module Area Ratio (A_e/A_t)	500		
Number of Modules	10		
Module Gap (δ/D_e)	0		
Engine Diameter	336 cm	132.4 in	
Plug Base Diameter	191 cm	75.2 in	
Engine Length	94.2 cm	37.1 in	
Module Chamber Diameter	6.63 cm	2.61 in	
Module Throat Diameter	3.66 cm	1.44 in	
Module Eixt Diameter	79.5 cm	31.3 in	
Module Chamber Length	16.51 cm	6.5 in	
Module Nozzle Length	127.6 cm	50.2 in	
Module Length	171 cm	67.2 in	
Coolant Jacket Flow Rate	2.44 kg/s	5.37 lbm/s	
Coolant Jacket ΔP	5.58 atm	82 psia	
Coolant Inlet Temperature	23 K	42 R	
Coolant Exit Temperature	218 K	392 R	
TURBINES			
Inlet Pressure	55.0 atm	808 psia	
Inlet Temperature	218 K	392 R	
Gas Flow Rate	2.23 Kg/s	4.92 lbm/s	
Specific Heat Ratio	1.40		
Molecular Weight	2.02 g/mol		
Shaft Horsepower	506 kW	679 hp	
Percent Bypass	8		
MAIN PUMPS			
Oxidizer Pump Flow Rate	13.24 kg/s	29.19 lbm/s	
Oxidizer Pump Discharge Pressure	43.5 atm	640 psia	
Fuel Pump Discharge Pressure	66.8 atm	982 psia	

TABLE LII - PLUG CLUSTER/SCARFED BELL ENGINE OPERATING SPECIFICATION
GAS GENERATOR CYCLE: REGEN-MODULE
MODEL III
$P_c = 20.4$

PARAMETER	SI UNITS	ALTERNATE UNITS	
ENGINE			
Vacuum Thrust	72.54	16,310 lbf	
Chamber Pressure	20.41 atm	300 psia	
Vacuum Specific Impulse	463.3		
Mixture Ratio (O/F)	5.33		(5.50 TCA)
Total Flow Rate	15.97 kg/s	34.20 lbm/s	(34.82 TCA)
Oxidizer Flow Rate	13.44 kg/s	29.64 lbm/s	(29.46 TCA)
Fuel Flow Rate	2.52 kg/s	5.56 lbm/s	(5.36 TCA)
Engine Area Ratio (A_E/A_T)	895		
Module Area Ratio (A_e/A_t)	500		
Number of Modules	10		
Module Gap (δ/De)	0		
Engine Diameter	433 cm	170 in	
Plug Base Diameter	246 cm	96.7	
Engine Length	82.3 cm	32.4	
Module Chamber Diameter	8.59 cm	3.38 in	
Module Throat Diameter	4.72 cm	1.86 in	
Module Exit Diameter	102 cm	40.2	
Module Chamber Length	16.51 cm	6.5 in	
Module Nozzle Length	164 cm	64.6	
Module Length	207 cm	81.6	
Coolant Jacket Flow Rate	2.43 kg/s	5.36 lbm/s	
Coolant Jacket ΔP	2.04 atm	30 psia	
Coolant Inlet Temperature	22 K	40 R	
Coolant Exit Temperature	246 K	442 R	
TURBINES			
Inlet Pressure	6.53 atm	96 psia	
Inlet Temperature	922 K	1,660 R	
Gas Flow Rate	0.17 kg/s	0.38 lbm/s	
Specific Heat Ratio	1.36		
Molecular Weight	3.8 g/mol		
Shaft Horsepower	189 kW	254 hp	
Percent Bypass	0		
MAIN PUMPS			
Oxidizer Pump Flow Rate	13.44 kg/s	29.64 lbm/s	
Oxidizer Pump Discharge Pressure	27.22 atm	400 psia	
Fuel Pump Flow Rate	2.52 kg/s	5.56 lbm/s	
Fuel Pump Discharge Pressure	27.2 atm	400 psia	
GAS GENERATOR			
Chamber Pressure	6.80 atm	100 psia	
Combustion Temperature	922 K	1,660 R	
Mixture Ratio (O/F)	0.9		
Total Flow Rate	0.17 kg/s	0.38 lbm/s	
Oxidizer Flow Rate	0.08 kg/s	0.18 lbm/s	
Fuel Flow Rate	0.09 kg/s	0.20 lbm/s	

TABLE LIII - PLUG CLUSTER/SCARFED BELL ENGINE OPERATING SPECIFICATION
GAS GENERATOR CYCLE: REGEN-MODULE

MODEL III
$P_c = 34.0$

PARAMETER	SI UNITS	ALTERNATE UNITS
ENGINE		
Vacuum Thrust	72.54 kN	16,310 lbf
Chamber Pressure	34.02 atm	500 psia
Vacuum Specific Impulse	465.0	
Mixture Ratio (O/F)	5.25	(5.50)
Total Flow Rate	15.91 kg/s	35.07 lbm/s (34.50 TCA)
Oxidizer Flow Rate	13.36 kg/s	29.46 lbm/s (29.19 TCA)
Fuel Flow Rate	2.54 kg/s	5.61 lbm/s (5.31 TCA)
Engine Area Ratio (A_E/A_T)	894	
Module Area Ratio (A_e/A_t)	500	
Number of Modules	10	
Module Gap (δ/D_e)	0	
Engine Diameter	336 cm	132.4 in
Plug Base Diameter	191 cm	75.2 in
Engine Length	94.2 cm	37.1 in
Module Chamber Diameter	6.63 cm	2.61 in
Module Throat Diameter	3.66 cm	1.44 in
Module Exit Diameter	79.5 cm	31.3 in
Module Chamber Length	16.51	6.5 in
Module Nozzle Length	127.6 cm	50.2 in
Module Length	171 cm	67.2 in
Coolant Jacket Flow Rate	2.41 kg/s	5.31 lbm/s
Coolant Jacket ΔP	5.58 atm	82 psia
Coolant Inlet Temperature	23 K	42 R
Coolant Exit Temperature	218 K	392 R
TURBINES		
Inlet Pressure	6.46 atm	95 psia
Inlet Temperature	922 K	1,660 K
Gas Flow Rate	0.26 kg/s	0.57 lbm/s
Specific Heat Ratio	1.36	
Molecular Weight	3.8 g/mol	
Shaft Horsepower	316 kW	424 hp
Percent Bypass	0	
MAIN PUMPS		
Oxidizer Pump Flow Rate	13.36 kg/s	29.46 lbm/s
Oxidizer Pump Discharge Pressure	43.55 atm	640 psia
Fuel Pump Flow Rate	2.54 kg/s	5.61 lbm/s
Fuel Pump Discharge Pressure	47.6 atm	700 psia
GAS GENERATOR		
Chamber Pressure	6.80 atm	100 psia
Combustion Temperature	922 K	1,660 R
Mixture Ratio (O/F)	0.9	
Total Flow Rate	0.26 kg/s	0.57 lbm/s
Oxidizer Flow Rate	0.12 kg/s	0.27 lbm/s
Fuel Flow Rate	0.14 kg/s	0.30 lbm/s

The engine length given in the tables is equivalent to the engine length reported for the baseline Space Tug candidate engines, which is measured from the gimbal point at the aft end of the LOX tank. Since the modules of the plug cluster engine are clustered around the LOX tank forward of its aft end (Figures 119 and 120), the actual engine length has no constant reference point, but varies with the engine area ratio, module area ratio and chamber pressure. In order that a direct comparison could be made between the various types of propulsion systems, the engine length was determined from the centerline of the LOX tank, and its equivalent length from the gimbal point of the baseline Tug was determined.

The longer engines shown for the higher pressure (34 atm) systems are the result of selecting the higher performing (20% L_I) plug. At an equal percent plug (15% L_I), the higher pressure engine is shorter.

C. ROUND TRIP GEOSYNCHRONOUS ORBIT MISSION

The baseline Space Tug round trip payload (W_{PL}) to geosynchronous orbit is given in Reference 36 as 939 Kg (2070 lb), with a velocity increment (Δv) budget of 8,680 m/s (28,478 ft/sec). The useable main engine propellants amount to 22,629 Kg (49,889 lb), and the burnout weight (W_{BO}) is 2617 Kg (5770 lb) when the APS propellant is ignored. The volume of the LH_2 and LOX tanks is 52.39 m^3 (1850 ft^3) and 18.12m^3 (640 ft^3), respectively. For engine mixture ratios other than 6, propellant off-loading must take place as given in Table LIV.

TABLE LIV. PROPELLANTS AVAILABLE FOR ROUND TRIP MISSION TO GEOSYNCHRONOUS ORBIT

Mixture Ratio	LH_2 Kg (lb)	LO_2 Kg (lb)	Propellant Offloaded Kg (lb)
4.0	3,233 (7,127)	12,931 (28,508)	6,465 (14,254) LO_2
5.0	3,233 (7,127)	16,164 (35,635)	3,232 (7,127) LO_2
5.5	3,233 (7,127)	17,780 (39,199)	1,616 (3,563) LO_2
6.0	3,233 (7,127)	19,396 (42,762)	0 (0)
7.0	2,771 (6,109)	19,396 (42,762)	462 (1,018) LH_2

Solution of Equation 24 gives W_I, the ignition weight (24,720 Kg or 54,499 lb_m), where

$$\Delta v = g \text{ Is } \ln \frac{W_I}{W_{PL} + W_{BO}} \qquad \text{(Eq. 24)}$$

g is the constant (9.807 m/s^2 or 32.2 ft/sec^2), Is is the RL10 specific impulse (456.5 sec), and Δv, W_{PL} and W_{BO} are as given above. The equation can be rearranged and then solved for the payload capability of other engines when the off-loaded propellant (W_{POL}) is accounted for and the appropriate specific impulse and engine weight (W_E) are utilized.

$$W_{PL} = \frac{W_I - W_{POL}}{e^{\Delta v/gIs}} - (W_{BO} - W_E\ [RL10] + W_E) \qquad \text{(Eq. 25)}$$

The RL10 engine weight (W_E [RL10]) shown in Eq. 25 is 201 Kg (443 lb_m).

The round trip payload to geosynchronous orbit for the optimized plug cluster engine (εM = 500) is given in Table LV. It is seen that off-loading propellant from the baseline mixture ratio (MR=6) Space Tug design point reduces the capability of the plug cluster engine. Therefore, the maximum payload is achieved at an MR of 6.

TABLE LV. ROUND TRIP PLUG CLUSTER (PCE) PAYLOADS TO GEOSYNCHRONOUS ORBIT

PC atm (psia)	MR	Is	W_E Kg (lb_m)	W_{PL} Kg (lb_m)	$\partial W_{PL}/\partial Is$ Kg/s (lb_m/sec)
20.4 (300)	5	463.4	219 (482)	547 (1205)	13 (29)
"	5.5	463.9	219 (482)	793 (1749)	14 (31)
"	6	464.4	219 (482)	1041 (2294)	15 (33)
34.0 (500)	5	465.2	194 (428)	595 (1311)	13 (29)
"	5.5	465.9	194 (428)	846 (1865)	14 (31)
"	6	466.6	194 (428)	1098 (2421)	15 (33)

D. TECHNOLOGY REQUIREMENTS

The plug cluster concept appears to offer a unique building block approach for advanced space vehicles. The status of technology to develop such an engine is very favorable. The ITA-type modules have been demonstrated to deliver long life (greater than 1200 cycles at a mixture ratio of 5.5). An existing RL10 turbopump could be used with a 5-hour life, or developed turbopump technology could be applied to a new design. Existing AGCarb carbon-carbon cloth nozzle technology is available for the high area ratio bell nozzle extensions. There is an inherent low cost associated with the utilization of off-the-shelf technology in the development of a plug cluster engine.

The feasibility of the plug cluster concept is based upon certain assumptions and preliminary conceptual designs. Points of the study where additional technology will improve the feasibility of the concept are summarized in Table LVI. Thrust vector control considerations are listed in greater detail in Table LVII.

TABLE LVI - PLUG CLUSTER ENGINE TECHNOLOGY REQUIREMENTS

Technology	Justification	Approach
1. Plug Cluster Analytical Design and Performance	No present means for accurately predicting plug cluster performance and for determining optimum design.	Utilize an existing Eulerian three-dimensional explicit finite difference computer code to compute plug cluster performance in terms of the behavior of the exhaust plumes and the effective thrust imparted to the vehicle.
2. Plug Cluster TVC	Gimbaling of entire engine not practical due to geometric considerations. Large angle ($\leq 90°$) gimbaling of module(s) most practical, as module-throttling or out condition requires additional valves.	Determine mission TVC requirements and examine most practical plug cluster TVC approach through design analysis.
3. Controls	Simultaneous ignition & operation of multiple numbers of modules requires an excessive number of valves or a control & start sequence specifically designed for this system.	An idle mode start sequence utilizing a minimum of control elements, for example, will be evaluated. System transients will be modeled for both expander & gas generator cycles.
4. Plug Cluster Cold Flow Demonstration	Experimental data for high area ratio plug nozzles with discrete modules was obtained from contract NAS3-20104 for tilt angles of 15-33¼. Analyses indicate that the configurations tested do not provide optimum performance.	Conduct an experimental program using hydrogen gas as the working fluid. Test high area ratio clustered scarfed bell geometries with tilt angle variation from 0-33 1/4 (overlapping NAS3-20104 data). Present data in parametric form including variables such as base pressurization.

TABLE LVI (cont.)

	Technology	Justification	Approach
5.	Lightweight Plug Cluster Engine	Lightweight structures are state-of-the-art due to advances in fabrication techniques and the development of new materials such as carbon-carbon cloth. Application of these structures to the design of a plug cluster engine could significantly reduce the engine weight.	Conduct a design analysis of the plug cluster engine evaluating both materials and fabrication techniques. Consider structural materials such as carbon-carbon cloth.
6.	Plug Cluster Engine Turbopump Design	Turbopumps for LO_2, LH_2, and hydrocarbon are considered state-of-the-art at the pressure levels required by the plug cluster engine. A TPA with 10-hour life, however, will require detailed design analysis as well as life testing.	Conduct a design analysis of LO_2, LH_2 and hydrocarbon turbopumps, and prepare design layouts. The layouts should be in sufficient detail to be used as a starting point for fabrication drawings.

TABLE LVII - TVC CONSIDERATIONS AND OPTIONS

TVC Concept	Considerations	Options
Gimbal	Effective turning moment as a function of gimbaling direction and angle. Interaction effects between gimbaled and stationary modules. Wall temperature effects. Number of flex lines required and gimbal direction. Stroke, load and response interactions. Weight vs performance trades.	Number of gimbaled modules. Number of gimbal axes. Variation in gimbal axes among gimbaled modules. Methods of gimbal actuation.
Throttling or Engine Out	Comparison of on-off operation effects on other modules vs throttling effect. Number of modules required to achieve desired TVC performance by on-off vs throttling. Response time needed for on-off vs added complexity of throttling. Potential advantage of variable thrust vs step thrust for vehicle. Effects of either method on flow, pressure, and temperature of other passive modules. Anticipated duty cycle for TVC. Control weight penalty with more module valves.	Number of active modules. Module grouping arrangement. Analog vs digital control. Range of throttling. Valve Types. Method of actuation.

E. OPTIMUM PLUG CLUSTER ENGINE

Two plug cluster/scarfed bell engines were selected for comparison with the Space Tug candidate engines. Both engines utilized regeneratively cooled modules (ε_M = 500) and the expander cycle. The plug cluster engine operating at a chamber pressure of 20.4 atm (300 psia) is designated PCE 300 and its counterpart at higher chamber pressure is PCE 500 and is described in Table XLIX.

SECTION VIII

PLUG CLUSTER ENGINE ASSESSMENT

A. OBJECTIVES AND GUIDELINES

The results of the plug cluster engine study were compared with results from previous Space Tug and Orbit-to-Orbit engine studies involving high pressure engines using bell nozzles and engines using annular plug (Aerospike) nozzles. The comparison was directed toward making a common ground of reference between the studies with regard to the assumptions and completeness. An assessment of the plug cluster concept was made as a result of these comparisons.

Specific missions that were considered for the comparison are:

(1) Round trip to geosynchronous orbit.
(2) Placement of payload into geosynchronous orbit.
(3) Retrieval of payload from geosynchronous orbit.
(4) Placement of payload into planetary or escape trajectory.

B. MISSION EXCHANGE FACTORS

Payloads and payload sensitivities for Space Tug missions are given in References 1, 2 and 37. These data, however, were derived from vehicle designs during various stages of the Space Tug studies, and therefore, are not entirely consistent. For example, studies to determine the optimum mixture ratio for the various engine candidates included vehicle redesign to accommodate the different propellant tank volumes required.

In order to provide a common ground of reference for the engine comparison, the ideal velocity (Δv) budget (Reference 36) for each mission was utilized, and the payload calculated for the baseline Space Tug in the manner previously described for the round trip mission (cf. Section VII.C.) The mission data are summarized in Table LVIII.

To simplify the analysis, the APS (auxiliary propulsion system) contribution to the ideal velocity was ignored, and ignition weights were computed using the appropriate form of Equation 24 (Section VII.C.) The resultant data are given in Table LIX. Equations were developed for each mission as shown in Table LX. The nomenclature for the equations is given in Section VII.C and the baseline Space Tug data in that section and in Tables LVIII, LIX and LX.

Results of the calculations are given in Appendix A (Table LXXV) for model I plug cluster engines compared to early estimates for the candidate Space Tug engines. Mission exchange factors ($\partial PL/\partial Is$ and $\partial PL/\partial WE$) are also included in the table.

TABLE LVIII - BASELINE SPACE TUG MISSION DATA FOR ENGINE COMPARISON (Ref. 36)

Mission	Ideal Velocity Increment: Total m/s (ft/sec) APS	Ideal Velocity Increment: Total m/s (ft/sec) Main Engine	Ideal Velocity Increment: Out m/s (ft/sec)	Ideal Velocity Increment: In m/s (ft/sec)	Payload Kg (lb_m)
Geosynchronous Delivery and Retrieval (Round Trip)	30 (98)	8,680 (28,478)	4,280 (14,044)	4,389 (14,399)	939 (2,070)
Geosynchronous Delivery (Deploy)	18 (60)	8,520 (27,953)	4,280 (14,044)	4,239 (13,909)	3,595 (7,926)
Geosynchronous Retrieval	27 (89)	8,520 (27,953)	4,280 (14,044)	4,239 (13,909)	1,540 (3,396)
Interplanetary	30 (98)	6,038 (19,811)	2,985 (9,792)	3,054 (10,019)	4,826 (10,640)

W_I = 25,754 Kg (56,779 lb_m)

W_{BO} = 2,610 Kg (5,755 lb_m)

Usable Propellant: W_{main} = 22,629 Kg (49,889 lb_m)

W_{APS} = 186 Kg (409 lb_m)

TABLE LIX - MISSION DATA FOR ENGINE COMPARISON

Mission	Ideal Velocity Increment m/s (ft/sec)	Payload Kg (lb_m)	Ignition Weight Kg (lb_m)	Burnout Weight Kg (lb_m)
Geosynchronous Delivery and Retrieval (Round Trip)	8,680 (28,478)	939 (2,070)	24,720 (54,499)	2,617 (5,770)
Geosynchronous Delivery (Deploy)	8,520 (27,953)	3,595 (7,926)	26,862 (59,221)	2,610 (5,755)
Geosynchronous Retrieval	8,520 (27,953)	1,540 (3,396)	23,848 (52,577)	2,613 (5,760)
Interplanetary	6,038 (19,811)	4,826 (10,640)	27,868 (61,439)	2,779 (6,127)

Since the compilation of the data in Appendix A (Table LXXV), additional data have become available on each of the listed engines: (1) further development of the ASE has led to more realistic weight estimates for the engine, (2) high area ratio tests have been conducted using the RL10, (3) test data have shown that the conventional configuration for the plug cluster engine (model I) does not achieve the high performance predicted, and (4) a redesign of the plug cluster concept indicates that the high area ratio performance potential of this system can be achieved.

An attempt was made to compare the Model III candidate engines using the latest empirical data, and also to compare them on the same analytical basis (i.e., JANNAF Simplified Methodology). A summary of the engine comparison using the JANNAF simplified methodology for each engine is given in Table LXI, and the overall summary depicted in Figure 121.

The results of this comparison show that the plug cluster engine concept derived from a cluster of scarfed bell nozzles offers a competitive payload when compared to the previously studied Space Tug engines. By adopting a zero gap configuration and by utilizing the available vehicle diameter, the tradeoff in engine weight with performance becomes favorable, as shown in Figure 122.

TABLE LX. PAYLOAD EQUATIONS FOR ENGINE COMPARISON

<u>Mission</u>

Round Trip
$$W_{PL} = \frac{W_I - W_{POL}}{e^{\Delta v/gIs}} - (W_{BO} + \Delta W_E) \qquad \text{(Eq. 25)}$$

Deploy
$$W_{PL} = \frac{W_I - W_{POL}}{e^{\Delta v_{out}/gIs}} - e^{\Delta v_{in}/gIs} (W_{BO} + \Delta W_E) \qquad \text{(Eq. 26)}$$

Retrieve
$$W_{PL} = \frac{e^{\Delta v_{in}/gIs} (W_{BO}+\Delta W_E) - \dfrac{W_I - W_{POL}}{e^{\Delta v_{out}/gIs}}}{1 - e^{\Delta v_{in}/gIs}} \qquad \text{(Eq. 27)}$$

Interplanetary
$$W_{PL} = \frac{W_I - W_{POL}}{e^{\Delta v_{out}/gIs}} - W_{KS} - e^{\Delta v_{in}/gIs} (W_{BO}+\Delta W_E) \qquad \text{(Eq. 28)}$$

Where: $\Delta W_E = W_E - W_E(RL10)$, W_{KS} = Kick Stage Weight + etc. (3984 Kg or 8783 lb_m)

TABLE LXI - SPACE TUG ENGINE COMPARISON (REVISED)

NOMINAL THRUST 66,723 N

ENGINE	RL10 IIB			PCB 300			PCB 500			ASE**		
MR	5	5.5	6	5	5.5	6	5	5.5	6	5	5.5	6
Pc (atm)	27.2	27.2	27.2	20.4	20.4	20.4	34.0	34.0	34.0	136	136	136
ϵ_E	205	205	205	895	895	895	894	894	894	400	400	400
W_E (Kg)	193	196	201	219	219	219	194	194	194	190	185	183
L_E (m)	1.40	1.40	1.40	0.81	0.81	0.81	0.94	0.94	0.94	1.28	1.28	1.28
I_s (s)	462.5	461.6	460.6	463.4	463.9	464.4	465.2	465.9	466.6	467.6	468.5	469.3
η_E (I_s/I_s ODE)	0.969	0.967	0.965	0.948	0.947	0.945	0.951	0.950	0.959	0.966	0.966	0.966
PAYLOAD (Kg)												
• Deploy	2568	3158	3740	2531	3178	3827	2651	3307	3964	2737	3414	4084
• Retrieve	898	1278	1649	877	1298	1721	958	1388	1820	1017	1465	1911
• Round Trip	560	783	1001	547	793	1041	595	845	1098	630	891	1150
• Planetary	3340	4146	4945	3314	4166	5019	3409	4268	5129	3477	4354	5224

*Performance based on JANNAF simplified methodology

**Thrust/Weight ratio assumed same as for 88,964 N engine (Ref. 41)

TABLE LXI (Cont.)

NOMINAL THRUST 15,000 lb_f

ENGINE	RL10 IIB			PCB 300			PCB 500			ASE**		
MR	5	5.5	6	5	5.5	6	5	5.5	6	5	5.5	6
P_c (psia)	400	400	400	300	300	300	500	500	500	2000	2000	2000
ϵ_E	205	205	205	895	895	895	894	894	894	400	400	400
W_E (lbm)	426	433	443	482	482	482	428	428	428	420	409	404
L_E (in.)	55	55	55	32	32	32	37	37	37	50.5	50.5	50.5
I_s (s)	462.5	461.6	460.6	463.4	463.9	464.4	465.2	465.9	466.6	467.6	468.5	469.3
η_E (I_s/I_s ODE)	0.969	0.967	0.965	0.948	0.947	0.945	0.951	0.950	0.949	0.966	0.966	0.966
PAYLOAD (lbm)												
• Deploy	5661	6963	8245	5581	7007	8436	5845	7290	8740	6034	7527	9003
• Retrieve	1980	2817	3135	1934	2862	3794	2111	3059	4013	2242	3230	4212
• Round Trip	1235	1726	2207	1205	1749	2294	1311	1865	2421	1389	1964	2535
• Planetary	7363	9141	10901	7307	9184	11065	7515	9409	11307	7665	9598	11518

*Performance based on JANNAF simplified methodology

**Thtust/Weight ratio assumed same as for 20,000 lb_f engine (Ref. 41)

S.I. UNITS

	RL10 IIB	PCE 300	PCE 500	ASE
MR	6	6	6	6
P_C (atm)	27.2	20.4	34.0	136
ϵ_E	205	895	894	400
W_E (Kg)	201	219	194	183**
D_E (m)	1.80	4.32	3.35	1.07
L_E (m)	1.40***	0.81	0.94	1.28***
*I_S (s)	460.6	464.4	466.6	469.3
η_E (I_S/I_S ODE)	0.965	0.945	0.949	0.966
PAYLOAD (Kg)				
Deploy	3740	3827	3964	4084
Retrieve	1649	1721	1820	1911
Round Trip	1001	1041	1098	1150
Planetary	4945	5019	5129	5224

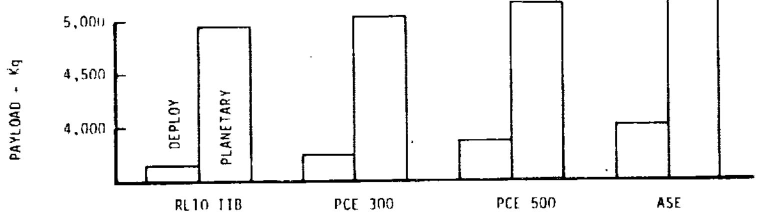

* Performance based on JANNAF simplified methodology
** Thrust/Weight ratio assumed same as for 66,723 N engine (Ref. 27)
***Stowed length of deployable nozzle

ENGLISH UNITS

	RL10 IIB	PCE 300	PCE 500	ASE
MR	6	6	6	6
P_C (psia)	400	300	500	2000
ϵ_E	205	895	894	400
W_E (lbm)	443	482	428	404**
D_E (in.)	71	170	132	42
L_E (in.)	55***	32	37	44***
*I_S (s)	460.6	464.4	466.6	469.3
η_E (I_S/I_S ODE)	0.965	0.945	0.949	0.966
PAYLOAD (lbm)				
Deploy	8245	8436	8740	9003
Retrieve	3135	3794	4013	4212
Round Trip	2207	2294	2421	2535
Planetary	10901	11065	11307	11518

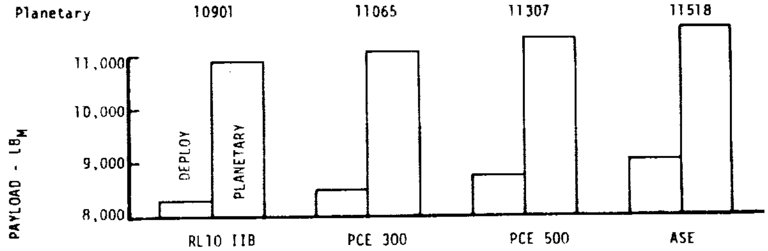

* Performance based on JANNAF simplified methodology
** Thrust/Weight ratio assumed same as for 20,000 lb_f engine (Ref. 27)
***Stowed length of deployable nozzle

Figure 121. Space Tug Engine Evaluation

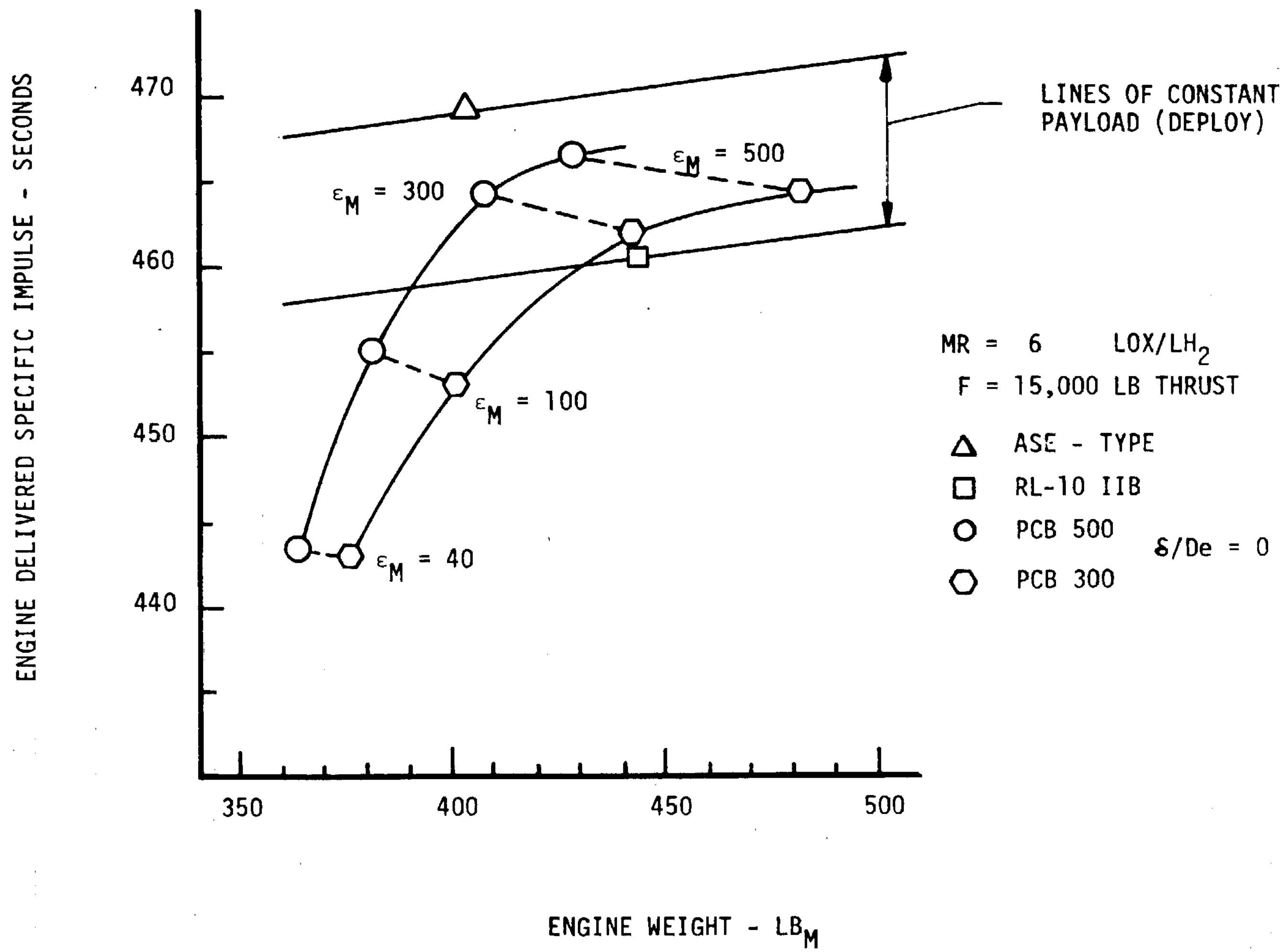

Figure 122. Plug Cluster Engine Sensitivity Summary

C. COST ANALYSIS

Engine development cost has been a major selection criteria in discussions concerning candidate Space Tug and Orbit Transfer Vehicles (OTV). In fact, the RL10 uprated engines were recommended by both MDAC and Convair (References 2 and 37) in their Space Tug studies primarily on the basis of DDT&E.

Cost data for the RL10 versions, the Aerospike, and the Advanced Space Engine are given in Table LXII. The estimates were taken from the Space Tug studies (References 2 and 37). The cost data for the plug cluster engines given in the table were estimated in several ways summarized in the following. The initial cost estimate of $0.4M to $0.7M for a plug cluster engine was made based upon conceptual design layouts. The DDT&E cost estimate for a 5-year development program was obtained by plotting the DDT&E costs shown in the table versus chamber pressure. While this plot showed some scatter due to the widely divergent engine designs, it did reflect a trend in development cost with chamber pressure, giving some credence to the selected PCE cost.

TABLE LXII. SPACE TUG ENGINE COST COMPARISON

	(1973 Dollars)		
Engine	DDT&E $M	Engine $M	Engine Maintenance $M/Year
RL10 IIA	13	0.7	0.22
RL10 IIB	50	0.8	0.22
RL10 IV	119	0.9	0.23
A/S	140	1.1	0.17
ASE	154	1.0	0.15
PCE300	52	0.4	0.16
PCE500	60	0.4	0.16

A determination was made of the number of equivalent engines required during the development program. Comparison with the Space Tug Storable Engine Study (Reference 16) showed that from 17 to 22 equivalent engines were required, and that the DDT&E cost was between $41.5M to $70M, depending upon the cycle chosen. Based on the previously cited costs per PCE300 fabrication, the manufacturing (plus procurement)

Cost of the DDT&E effort is between $6.8M and $15.4M or from 13 to 30 percent of the total cost. Comparison of these percentages with the 44 percent obtained from the on going OME program indicates that the manufacturing/procurement cost is low for this size program. A single engine cost of $1M would bring the plug cluster development cost percentage in line with that for OME. This higher figure, however, does not seem reasonable when the module high technology status is considered.

The DDT&E cost of $52M to $60M is, therefore, seen to represent a reasonable value when compared with values generated for the other OTV candidate engines. The figure also appears to be consistent with previous ALRC estimates for the development of similar space engines.

D. LIFE ANALYSIS

Typical engine life projections given for the Space Tug candidate engines are listed in Table LXIII. All of the engines except the RL10 IIB have identical life requirements if it is assumed that the Aerospike and the ASE cycle life is 300 times a safety factor of four (1200 cycles). The Aerospike, however, is also projected to have some scheduled maintenance and refurbishment after 60 cycles or 2 hours of operation, with a total engine service life of 50 hours or 1500 cycles (Reference 6).

TABLE LXIII. SPACE TUG ENGINE LIFE COMPARISON

Life	Baseline Tug RL10 IIB (Ref. 1)	Aerospike (Ref. 6)	ASE (Ref. 39)	PCE300/500
Hours	5	10	10	5*-10
Cycles	190	300	300	1200

*RL10 Turbopump

Critical components that dictate the minimum life between overhauls are the injector, thrust chamber, bearings, seals, and the igniter. Initial analysis of the low pressure plug cluster engine components indicate that lifetimes greater than those listed in Table LXIII are state-of-the-art. The plug cluster engine, therefore, should surpass the life capability of the high pressure engines and will be superior to the RL10 IIB, which utilizes fifteen-year-old technology.

SECTION IX

CONCLUSIONS

The major conclusions (Figure 123) resulting from the Unconventional Nozzle Tradeoff Study are:

PLUG CLUSTER FEATURES

- COMPETITIVE PAYLOAD
- INCREASED PAYLOAD LENGTH
- DESIGN FLEXIBILITY
- LONG LIFE
- EXISTING TURBOMACHINERY
- DEMONSTRATED MODULES
- EXISTING NOZZLE TECHNOLOGY
- LOW COST
- LOW PC ENGINE SYSTEM

The major feature of the PCE is that it is capable of delivering a competitive payload. While verification of the performance is needed, the performance methodology developed in this program indicates only a small uncertainty.

Another feature of the PCE is the allowance of increased payload length due to the shorter engine length.

The PCE offers considerable design flexibility, since the capability to increase or decrease the number of modules (and thrust) is inherent in the cluster concept. Fail operation features can be provided by the cluster configuration that are not possible with single engine configurations.

Long life has been demonstrated for the ITA modules. While life verification of the fully regeneratively cooled module is required, sufficient data have been accumulated to indicate the soundness of the approach.

Another feature of the PCE is that an existing turbopump assembly could be utilized. Likewise, well developed turbopump technology could be applied.

Existing AGCarb carbon-carbon cloth nozzle technology is available. Verification of the greater than 1-hour predicted life for this nozzle is needed.

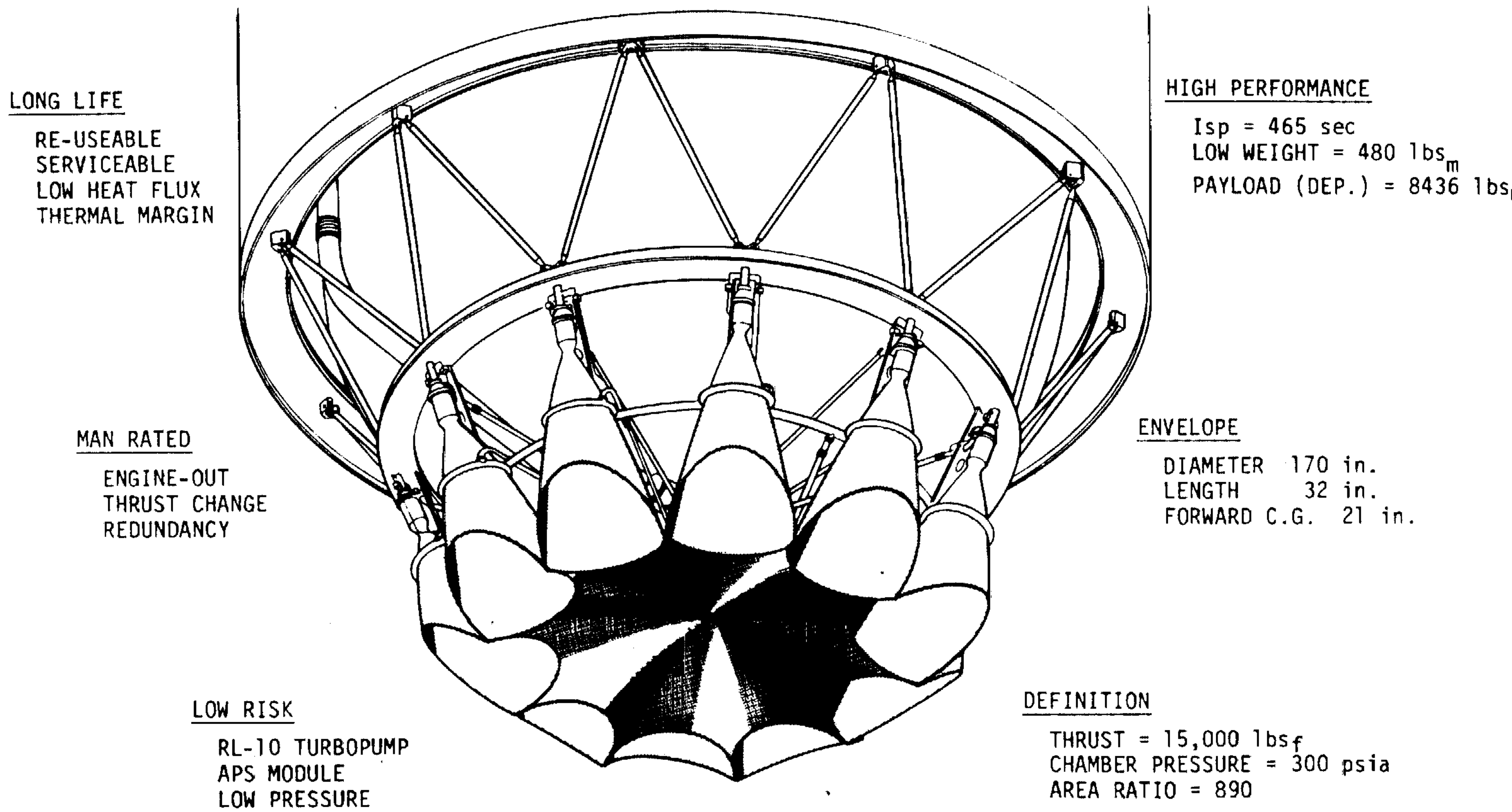

Figure 123. Plug Cluster Engine Concept Offers Many Features

An important feature of the PCE is the inherent low cost associated with utilizing off-the-shelf technology. Low cost is also inherent in the operation of low pressure systems which comprise the PCE. While a cost analysis should be conducted to verify this favorable feature of the PCE, there is little uncertainty involved in predicting low cost operation for such a Space Tug system.

This study indicates that the performance of the PCE is competitive to other Space Tug candidate engines.

SECTION X

APPENDIXES

A. CONVENTIONAL ENGINE OPERATING SPECIFICATION

These Engine Operating Specifications are Shown on Tables LXIV Through LXXV

TABLE LXIV - PLUG CLUSTER ENGINE OPERATING SPECIFICATION
EXPANDER CYCLE: REGEN-MODULE

MODEL II PERFORMANCE
$P_c = 20.4$

PARAMETER	SI UNITS	ALTERNATE UNITS	
ENGINE			
Vacuum Thrust	68.72 kN	15,451 lbf	
Chamber Pressure	20.41 atm	300 psia	
Vacuum Specific Impulse	443.8		
Mixture Ratio (O/F)	5.44		(5.50 TCA)
Total Flow Rate	15.82 kg/s	34.88 lbm/s	(34.82 TCA)
Oxidizer Flow Rate	13.36 kg/s	29.46 lbm/s	
Fuel Flow Rate	2.46 kg/s	5.42 lbm/s	
Engine Area Ratio (A_E/A_T)	458		
Module Area Ratio (A_e/A_t)	40		
Number of Modules	10		
Module Gap (δ/D_e)	2		
Engine Diameter	319.8 cm	125.9 in	
Plug Base Diameter	217.9 cm	85.8 in	
Engine Length	85.9 cm	33.8 in	
Module Chamber Diameter	8.59 cm	3.38 in	
Module Throat Diameter	4.72 cm	1.86 in	
Module Exit Diameter	29.87 cm	11.76 in	
Module Chamber Length	16.51 cm	6.5 in	
Module Nozzle Length	35.46 cm	13.96 in	
Module Length	60.33 cm	23.75 in	
Coolant Jacket Flow Rate	2.46 kg/s	5.42 lbm/s	
Coolant Jacket ΔP	4.42 atm	65 psia	
Coolant Inlet Temperature	22 K	40 R	
Coolant Exit Temperature	376 K	677 R	
TURBINES			
Inlet Pressure	31.6 atm	464 psia	
Inlet Temperature	376 K	677 R	
Gas Flow Rate	1.05 kg/s	2.32 lbm/s	
Specific Heat Ratio	1.40		
Molecular Weight	2.02 g/mol		
Shaft Horsepower	290 kW	390 hp	
Percent Bypass	57		
MAIN PUMPS			
Oxidizer Pump Flow Rate	13.36 kg/s	29.46 lbm/s	
Oxidizer Pump Discharge Pressure	27.2 atm	400 psia	
Fuel Pump Flow Rate	2.46 kg/s	5.42 lbm/s	
Fuel Pump Discharge Pressure	36.7 atm	540 psia	

TABLE LXV - PLUG CLUSTER ENGINE OPERATING SPECIFICATION
EXPANDER CYCLE: REGEN-MODULE

MODEL II PERFORMANCE
P_c = 34.0

PARAMETER	SI UNITS	ALTERNATE UNITS	
ENGINE			
Vacuum Thrust	68.77	15,460 lbf	
Chamber Pressure	34.02 atm	500 psia	
Vacuum Specific Impulse	447.3 s		
Mixture Ratio (O/F)	5.44		(5.50 TCA)
Total Flow Rate	15.68 kg/s	34.56 lbm/s	(34.50 TCA)
Oxidizer Flow Rate	13.24 kg/s	29.19 lbm/s	
Fuel Flow Rate	2.44 kg/s	5.37 lbm/s	
Engine Area Ratio (A_E/A_T)	458		
Module Area Ratio (A_e/A_t)	40		
Number of Modules	10		
Module Gap (δ/D_e)	2		
Engine Diameter	247.4 cm	97.4 in	
Plug Base Diameter	168.1 cm	66.2 in	
Engine Length	106.2 cm	41.8 in	
Module Chamber Diameter	6.63 cm	2.61 in	
Module Throat Diameter	3.66 cm	1.44 in	
Module Exit Diameter	23.11 cm	9.10 in	
Module Chamber Length	16.51 cm	6.5 in	
Module Nozzle Length	27.41 cm	10.79 in	
Module Length	52.27 cm	20.58 in	
Coolant Jacket Flow Rate	2.44 kg/s	5.37 lbm/s	
Coolant Jacket ΔP	10.3 atm	152 psia	
Coolant Inlet Temperature	23 K	42 R	
Coolant Exit Temperature	269 K	485 R	
TURBINES			
Inlet Pressure	55.3 atm	812 psia	
Inlet Temperature	269 K	485 R	
Gas Flow Rate	2.24 Kg/s	4.94 lbm/s	
Specific Heat Ratio	1.40		
Molecular Weight	2.02 g/mol		
Shaft Horsepower	520 kW	697 hp	
Percent Bypass	8		
MAIN PUMPS			
Oxidizer Pump Flow Rate	13.24 kg/s	29.19 lbm/s	
Oxidizer Pump Discharge Pressure	43.5 atm	640 psia	
Fuel Pump Flow Rate	2.44 kg/s	5.37 lbm/s	
Fuel Pump Discharge Pressure	66.8 atm	982 psia	

TABLE LXVI - PLUG CLUSTER ENGINE OPERATING SPECIFICATION
GAS GENERATOR CYCLE: REGEN-MODULE

MODEL II PERFORMANCE
$P_c = 20.4$

PARAMETER	SI UNITS	ALTERNATE UNITS	
ENGINE			
Vacuum Thrust	69.27 kN	15,573 lbf	
Chamber Pressure	20.41 atm	300 psia	
Vacuum Specific Impulse	443.2		
Mixture Ratio (O/F)	5.33		(5.50 TCA)
Total Flow Rate	15.97 kg/s	35.20 lbm/s	(34.82 TCA)
Oxidizer Flow Rate	13.44 kg/s	29.64 lbm/s	(29.46 TCA)
Fuel Flow Rate	2.52 kg/s	5.56 lbm/s	(5.36 TCA)
Engine Area Ratio (A_E/A_T)	458		
Module Area Ratio (A_e/A_t)	40		
Number of Modules	10		
Module Gap (δ/D_e)	2		
Engine Diameter	319.8 cm	125.9 in	
Plug Base Diameter	217.9 cm	85.8 in	
Engine Length	85.9 cm	33.8 in	
Module Chamber Diameter	8.59 cm	3.38 in	
Module Throat Diameter	4.72 cm	1.86 in	
Module Exit Diameter	29.87 cm	11.76 in	
Module Chamber Length	16.51 cm	6.5 in	
Module Nozzle Length	35.46 cm	13.96 in	
Module Length	60.33 cm	23.75 in	
Coolant Jacket Flow Rate	2.43 kg/s	5.36 lbm/s	
Coolant Jacket ΔP	4.42 atm	65 psia	
Coolant Inlet Temperature	22 K	40 R	
Coolant Exit Temperature	376 K	677 R	
TURBINES			
Inlet Pressure	6.53 atm	96 psia	
Inlet Temperature	922 K	1,660 R	
Gas Flow Rate	0.17 kg/s	0.38 lbm/s	
Specific Heat Ratio	1.36		
Molecular Weight	3.8 g/mol		
Shaft Horsepower	189 kW	254 hp	
Percent Bypass	0		
MAIN PUMPS			
Oxidizer Pump Flow Rate	13.44 kg/s	29.64 lbm/s	
Oxidizer Pump Discharge Pressure	27.22 atm	400 psia	
Fuel Pump Flow Rate	2.52 kg/s	5.56 lbm/s	
Fuel Pump Discharge Pressure	27.90 atm	410 psia	
GAS GENERATOR			
Chamber Pressure	6.80 atm	100 psia	
Combustion Temperature	922 K	1,660 R	
Mixture Ratio (O/F)	0.9		
Total Flow Rate	0.17 kg/s	0.38 lbm/s	
Oxidizer Flow Rate	0.08 kg/s	0.18 lbm/s	
Fuel Flow Rate	0.09 kg/s	0.20 lbm/s	

TABLE LXVII - PLUG CLUSTER ENGINE OPERATING SPECIFICATION
GAS GENERATOR CYCLE: REGEN-MODULE

MODEL II PERFORMANCE
P_c = 34.0

PARAMETER	SI UNITS	ALTERNATE UNITS	
ENGINE			
Vacuum Thrust	69.63 kN	15,650 psia	
Chamber Pressure	34.02 atm	500 psia	
Vacuum Specific Impulse	446.4		
Mixture Ratio (O/F)	5.25		(5.50 TCA)
Total Flow Rate	15.91 kg/s	35.07 lbm/s	(34.50 TCA)
Oxidizer Flow Rate	13.36 kg/s	29.46 lbm/s	(29.19 TCA)
Fuel Flow Rate	2.54 kg/s	5.61 lbm/s	(5.31 TCA)
Engine Area Ratio (A_E/A_T)	458		
Module Area Ratio (A_e/A_t)	40		
Number of Modules	10		
Module Gap (δ/D_e)	2		
Engine Diameter	247.4 cm	97.4 in	
Plug Base Diameter	168.1 cm	66.2 in	
Engine Length	106.2 cm	41.8 in	
Module Chamber Diameter	6.63 cm	2.61 in	
Module Throat Diameter	3.66 cm	1.44 in	
Module Exit Diameter	23.11 cm	9.10 in	
Module Chamber Length	16.51	6.5 in	
Module Nozzle Length	27.41 cm	10.79 in	
Module Length	52.27 cm	20.58 in	
Coolant Jacket Flow Rate	2.41 kg/s	5.31 lbm/s	
Coolant Jacket ΔP	10.3 atm	152 psia	
Coolant Inlet Temperature	23 K	42 R	
Coolant Exit Temperature	269 K	485 R	
TURBINES			
Inlet Pressure	6.46 atm	95 psia	
Inlet Temperature	922 K	1,660 K	
Gas Flow Rate	0.26 kg/s	0.57 lbm/s	
Specific Heat Ratio	1.36		
Molecular Weight	3.8 g/mol		
Shaft Horsepower	316 kW	424 hp	
Percent Bypass	0		
MAIN PUMPS			
Oxidizer Pump Flow Rate	13.36 kg/s	29.46 lbm/s	
Oxidizer Pump Discharge Pressure	43.55 atm	640 psia	
Fuel Pump Flow Rate	2.54 kg/s	5.61 lbm/s	
Fuel Pump Discharge Pressure	49.47 atm	727 psia	
GAS GENERATOR			
Chamber Pressure	6.80 atm	100 psia	
Combustion Temperature	922 K	1,660 R	
Mixture Ratio (O/F)	0.9		
Total Flow Rate	0.26 kg/s	0.57 lbm/s	
Oxidizer Flow Rate	0.12 kg/s	0.27 lbm/s	
Fuel Flow Rate	0.14 kg/s	0.30 lbm/s	

TABLE LXVIII - PLUG CLUSTER ENGINE OPERATING SPECIFICATION
EXPANDER CYCLE: ITA MODULE 16% FFC
MODEL II PERFORMANCE
$P_c = 20.4$

PARAMETER	SI UNITS	ALTERNATE UNITS	
ENGINE			
Vacuum Thrust	68.88 kN	15.480 lbf	
Chamber Pressure	20.41 atm	300 psia	
Vacuum Specific Impulse	431.9 s		
Mixture Ratio (O/F)	5.44		(5.50 TCA)
Total Flow Rate	16.26 kg/s	35.85 lbm/s	(35.79 TCA)
Oxidizer Flow Rate	13.73 kg/s	30.28 lbm/s	
Fuel Flow Rate	2.53 kg/s	5.57 lbm/s	(5.51 TCA)
Engine Area Ratio (A_E/A_T)	458		
Module Area Ratio (A_e/A_t)	40		
Number of Modules	10		
Module Gap (δ/D_e)	2		
Engine Diameter	319.8 cm	125.9 in	
Plug Base Diameter	217.9 cm	85.8 in	
Engine Length	85.9 cm	33.8 in	
Module Chamber Diameter	8.59 cm	3.38 in	
Module Throat Diameter	4.72 cm	1.86 in	
Module Exit Diameter	29.87 cm	11.76 in	
Module Chamber Length	16.51 cm	6.5 in	
Module Nozzle Length	35.46 cm	13.95 in	
Module Length	60.33 cm	23.75 in	
Coolant Jacket Flow Rate	2.53 kg/s	5.57 lbm/s	
Coolant Jacket ΔP	4.08 atm	60 psia	
Coolant Inlet Temperature	22 K	40 R	
Coolant Exit Temperature	104 K	188 R	
TURBINES			
Inlet Pressure	39.74 atm	584 psia	
Inlet Temperature	104 K	188 R	
Gas Flow Rate	2.53 kg/s	5.57 lbm/s	
Specific Heat Ratio	1.40		
Molecular Weight	2.02 g/mol		
Shaft Horsepower	353 kW	474 hp	
Percent Bypass	0		
MAIN PUMPS			
Oxidizer Pump Flow Rate	13.73 kg/s	30.28 lbm/s	
Oxidizer Pump Discharge Pressure	27.22 atm	400 psia	
Fuel Pump Flow Rate	2.53 kg/s	5.57 lbm/s	
Fuel Pump Discharge Pressure	44.64 atm	656 psia	

ORIGINAL PAGE IS
OF POOR QUALITY

TABLE LXIX - PLUG CLUSTER ENGINE OPERATING SPECIFICATION
GAS GENERATOR CYCLE: ITA MODULE 16% FFC

MODEL II PERFORMANCE
$P_c = 20.4$

PARAMETER	SI UNITS	ALTERNATE UNITS	
ENGINE			
Vacuum Thrust	69.38 kN	15,596 lbf	
Chamber Pressure	20.41 atm	300 psia	
Vacuum Specific Impulse	431.4		
Mixture Ratio (O/F)	5.34		(5.50 TCA)
Total Flow Rate	16.40 kg/s	36.15 lbm/s	(35.79 TCA)
Oxidizer Flow Rate	13.81 kg/s	30.45 lbm/s	(30.28 TCA)
Fuel Flow Rate	2.59 kg/s	5.70 lbm/s	(5.51 TCA)
Engine Area Ratio (A_E/A_T)	458		
Module Area Ratio (A_e/A_t)	40		
Number of Modules	10		
Module Gap (δ/D_e)	2		
Engine Diameter	319.8 cm	125.9 in	
Plug Base Diameter	217.9 cm	85.8 in	
Engine Length	85.9 cm	33.8 in	
Module Chamber Diameter	8.59 cm	3.38 in	
Module Throat Diameter	4.72 cm	1.86 in	
Module Exit Diameter	29.87 cm	11.76 in	
Module Chamber Length	16.51 cm	6.50 in	
Module Nozzle Length	35.46 cm	13.95 in	
Module Length	60.33 cm	23.75 in	
Coolant Jacket Flow Rate	2.50 kg/s	5.51 lbm/s	
Coolant Jacket ΔP	4.08 atm	60 psia	
Coolant Inlet Temperature	22 K	40 R	
Coolant Exit Temperature	104 K	188 R	
TURBINES			
Inlet Pressure	6.46 atm	95 psia	
Inlet Temperature	922 K	1,660 R	
Gas Flow Rate	0.16 kg/s	0.36 lbm/s	
Specific Heat Ratio	1.36		
Molecular Weight	3.8 g/mol		
Shaft Horsepower	189 kW	254 hp	
Percent Bypass	0		
MAIN PUMPS			
Oxidizer Pump Flow Rate	13.81 kg/s	30.45 lbm/s	
Oxidizer Pump Discharge Pressure	27.22 atm	400 psia	
Fuel Pump Flow Rate	2.59 kg/s	5.70 lbm/s	
Fuel Pump Discharge Pressure	27.56 atm	405 psia	
GAS GENERATOR			
Chamber Pressure	6.80 atm	100 psia	
Combustion Temperature	922 K	1,660 R	
Mixture Ratio (O/F)	0.9		
Total Flow Rate	0.16 kg/s	0.36 lbm/s	
Oxidizer Flow Rate	0.08 kg/s	0.17 lbm/s	
Fuel Flow Rate	0.09 kg/s	0.19 lbm/s	

TABLE LXX - PLUG CLUSTER ENGINE OPERATING SPECIFICATION
GAS GENERATOR CYCLE: ITA MODULE 16% FFC

MODEL II PERFORMANCE
$P_c = 34.0$

PARAMETER	SI UNITS	ALTERNATE UNITS	
ENGINE			
Vacuum Thrust	69.66 kN	15,660 lbf	
Chamber Pressure	34.02 atm	500 psia	
Vacuum Specific Impulse	434.6		
Mixture Ratio (O/F)	5.26		(5.50 TCA)
Total Flow Rate	16.34 kg/s	36.03 lbm/s	(35.46 TCA)
Oxidizer Flow Rate	13.73 kg/s	30.27 lbm/s	(30.00 TCA)
Fuel Flow Rate	2.61 kg/s	5.76 lbm/s	(5.46 TCA)
Engine Area Ratio (A_E/A_T)	458		
Module Area Ratio (A_e/A_t)	40		
Number of Modules	10		
Module Gap (δ/D_e)	2		
Engine Diameter	247.4 cm	97.4 in	
Plug Base Diameter	168.1 cm	66.2 in	
Engine Length	106.2 cm	41.8 in	
Module Chamber Diameter	6.63 cm	2.61 in	
Module Throat Diameter	3.66 cm	1.44 in	
Module Exit Diameter	23.11 cm	9.10 in	
Module Chamber Length	16.51 cm	6.5 in	
Module Nozzle Length	27.41 cm	10.79 in	
Module Length	52.27 cm	20.58 in	
Coolant Jacket Flow Rate	2.48 kg/s	5.46 lbm/s	
Coolant Jacket ΔP	9.53 atm	140 psia	
Coolant Inlet Temperature	23 K	42 R	
Coolant Exit Temperature	97 K	174 R	
TURBINES			
Inlet Pressure	6.46 atm	95 psia	
Inlet Temperature	922 K	1,660 R	
Gas Flow Rate	0.26 kg/s	0.57 lbm/s	
Specific Heat Ratio	1.36		
Molecular Weight	3.8 g/mol		
Shaft Horsepower	316 kW	424 hp	
Percent Bypass	0		
MAIN PUMPS			
Oxidizer Pump Flow Rate	13.73 kg/s	30.27 lbm/s	
Oxidizer Pump Discharge Pressure	43.55 atm	640 psia	
Fuel Pump Flow Rate	2.61 kg/s	5.76 lbm/s	
Fuel Pump Discharge Pressure	48.65 atm	715 psia	
GAS GENERATOR			
Chamber Pressure	6.80 atm	100 psia	
Combustion Temperature	922 K	1,660 R	
Mixture Ratio (O/F)	0.9		
Total Flow Rate	0.26 kg/s	0.57 lbm/s	
Oxidizer Flow Rate	0.12 kg/s	0.27 lbm/s	
Fuel Flow Rate	0.14 kg/s	0.30 lbm/s	

TABLE LXXI - PLUG CLUSTER ENGINE OPERATING SPECIFICATION
EXPANDER CYCLE: REGEN-MODULE/UNCOOLED PLUG

MODEL II PERFORMANCE
$P_c = 20.4$

PARAMETER	SI UNITS	ALTERNATE UNITS	
ENGINE			
Vacuum Thrust	68.72 kN	15,451 lbf	
Chamber Pressure	20.41 atm	300 psia	
Vacuum Specific Impulse	443.8		
Mixture Ratio (O/F)	5.44		(5.50 TCA)
Total Flow Rate	15.82 kg/s	34.88 lbm/s	(34.82 TCA)
Oxidizer Flow Rate	13.36 kg/s	29.46 lbm/s	
Fuel Flow Rate	2.46 kg/s	5.42 lbm/s	
Engine Area Ratio (A_E/A_T)	458		
Module Area Ratio (A_e/A_t)	40		
Number of Modules	10		
Module Gap (δ/D_e)	2		
Engine Diameter	319.8 cm	125.9 in	
Plug Base Diameter	217.9 cm	85.8 in	
Engine Length	85.9 cm	33.8 in	
Module Chamber Diameter	8.59 cm	3.38 in	
Module Throat Diameter	4.72 cm	1.86 in	
Module Exit Diameter	29.87 cm	11.76 in	
Module Chamber Length	16.51 cm	6.5 in	
Module Nozzle Length	35.46 cm	13.96 in	
Module Length	60.33 cm	23.75 in	
Coolant Jacket Flow Rate	2.46 kg/s	5.42 lbm/s	
Coolant Jacket ΔP	2.04 atm	30 psia	
Coolant Inlet Temperature	22 K	40 R	
Coolant Exit Temperature	246 K	442 R	
TURBINES			
Inlet Pressure	32.7 atm	480 psia	
Inlet Temperature	246 K	442 R	
Gas Flow Rate	1.38 kg/s	3.76 lbm/s	
Specific Heat Ratio	1.40		
Molecular Weight	2.02 g/mol		
Shaft Horsepower	290 kW	390 hp	
Percent Bypass	44		
MAIN PUMPS			
Oxidizer Pump Flow Rate	13.36 kg/s	29.46 lbm/s	
Oxidizer Pump Discharge Pressure	27.2 atm	400 psia	
Fuel Pump Flow Rate	2.46 kg/s	5.42 lbm/s	
Fuel Pump Discharge Pressure	36.7 atm	540 psia	

TABLE LXXII - PLUG CLUSTER ENGINE OPERATING SPECIFICATION
EXPANDER CYCLE: REGEN-MODULE/UNCOOLED PLUG
MODEL II PERFORMANCE
$P_c = 34.0$

PARAMETER	SI UNITS	ALTERNATE UNITS	
ENGINE			
Vacuum Thrust	68.77 kN	15,460 lbf	
Chamber Pressure	34.02 atm	500 psia	
Vacuum Specific Impulse	447.3		
Mixture Ratio (O/F)	5.44		(5.50 TCA)
Total Flow Rate	15.68 kg/s	34.56 lbm/s	(34.50 TCA)
Oxidizer Flow Rate	13.24 kg/s	29.19 lbm/s	
Fuel Flow Rate	2.44 kg/s	5.37 lbm/s	
Engine Area Ratio (A_E/A_T)	458		
Module Area Ratio (A_e/A_t)	40		
Number of Modules	10		
Module Gap (δ/D_e)	2		
Engine Diameter	247.4 cm	97.4 in	
Plug Base Diameter	168.1 cm	66.2 in	
Engine Length	106.2 cm	41.8 in	
Module Chamber Diameter	6.63 cm	2.61 in	
Module Throat Diameter	3.66 cm	1.44 in	
Module Exit Diameter	23.11 cm	9.10 in	
Module Chamber Length	16.51 cm	6.5 in	
Module Nozzle Length	27.41 cm	10.79 in	
Module Length	52.27 cm	20.58 in	
Coolant Jacket Flow Rate	2.44 kg/s	5.37 lbm/s	
Coolant Jacket ΔP	5.58 atm	82 psia	
Coolant Inlet Temperature	23 K	42 R	
Coolant Exit Temperature	218 K	392 R	
TURBINES			
Inlet Pressure	54.98 atm	808 psia	
Inlet Temperature	218 K	392 R	
Gas Flow Rate	2.23 Kg/s	4.92 lbm/s	
Specific Heat Ratio	1.40		
Molecular Weight	2.02 g/mol		
Shaft Horsepower	506 kW	679 hp	
Percent Bypass	15		
MAIN PUMPS			
Oxidizer Pump Flow Rate	13.24 kg/s	29.19 lbm/s	
Oxidizer Pump Discharge Pressure	43.5 atm	640 psia	
Fuel Pump Flow Rate	2.44 kg/s	5.37 lbm/s	
Fuel Pump Discharge Pressure	64.62 atm	950 psia	

TABLE LXXIII - PLUG CLUSTER ENGINE OPERATING SPECIFICATION
GAS GENERATOR CYCLE: REGEN-MODULE/UNCOOLED PLUG
MODEL II PERFORMANCE
$P_C = 20.4$

PARAMETER	SI UNITS	ALTERNATE UNITS	
ENGINE			
Vacuum Thrust	69.27 kN	15,573 lbf	
Chamber Pressure	20.41 atm	300 psia	
Vacuum Specific Impulse	443.2		
Mixture Ratio (O/F)	5.33		(5.50 TCA)
Total Flow Rate	15.97 kg/s	35.20 lbm/s	(34.82 TCA)
Oxidizer Flow Rate	13.44 kg/s	29.64 lbm/s	(29.46 TCA)
Fuel Flow Rate	2.52 kg/s	5.56 lbm/s	(5.36 TCA)
Engine Area Ratio (A_E/A_T)	458		
Module Area Ratio (A_e/A_t)	40		
Number of Modules	10		
Module Gap (δ/D_e)	2		
Engine Diameter	319.8 cm	125.9 in	
Plug Base Diameter	217.9 cm	85.8 in	
Engine Length	85.9 cm	33.8 in	
Module Chamber Diameter	8.59 cm	3.38 in	
Module Throat Diameter	4.72 cm	1.86 in	
Module Exit Diameter	29.87 cm	11.76 in	
Module Chamber Length	16.51 cm	6.5 in	
Module Nozzle Length	35.46 cm	13.96 in	
Module Length	60.33 cm	23.75 in	
Coolant Jacket Flow Rate	2.43 kg/s	5.36 lbm/s	
Coolant Jacket ΔP	2.04 atm	30 psia	
Coolant Inlet Temperature	22 K	40 R	
Coolant Exit Temperature	246 K	442 R	
TURBINES			
Inlét Pressure	6.53 atm	96 psia	
Inlet Temperature	922 K	1,660 R	
Gas Flow Rate	0.17 kg/s	0.38 lbm/s	
Specific Heat Ratio	1.36		
Molecular Weight	3.8 g/mol		
Shaft Horsepower	189 kW	254 hp	
Percent Bypass	0		
MAIN PUMPS			
Oxidizer Pump Flow Rate	13.44 kg/s	29.64 lbm/s	
Oxidizer Pump Discharge Pressure	27.22 atm	400 psia	
Fuel Pump Flow Rate	2.52 kg/s	5.56 lbm/s	
Fuel Pump Discharge Pressure	27.22 atm	400 psia	
GAS GENERATOR			
Chamber Pressure	6.80 atm	100 psia	
Combustion Temperature	922 K	1,660 R	
Mixture Ratio (O/F)	0.9		
Total Flow Rate	0.17 kg/s	0.38 lbm/s	
Oxidizer Flow Rate	0.08 kg/s	0.18 lbm/s	
Fuel Flow Rate	0.09 kg/s	0.20 lbm/s	

TABLE LXXIV - PLUG CLUSTER ENGINE OPERATING SPECIFICATION
GAS GENERATOR CYCLE: REGEN-MODULE/UNCOOLED PLUG
MODEL II PERFORMANCE
$P_c = 34.0$

PARAMETER	SI UNITS	ALTERNATE UNITS	
ENGINE			
Vacuum Thrust	69.63 kN	15,650 lbf	
Chamber Pressure	34.02 atm	500 psia	
Vacuum Specific Impulse	446.4		
Mixture Ratio (O/F)	5.25		(5.50 TCA)
Total Flow Rate	15.91 kg/s	35.07 lbm/s	(34.50 TCA)
Oxidizer Flow Rate	13.36 kg/s	29.46 lbm/s	(29.19 TCA)
Fuel Flow Rate	2.54 kg/s	5.61 lbm/s	(5.31 TCA)
Engine Area Ratio (A_E/A_T)	458		
Module Area Ratio (A_e/A_t)	40		
Number of Modules	10		
Module Gap (δ/D_e)	2		
Engine Diameter	247.4 cm	97.4 in	
Plug Base Diameter	168.1 cm	66.2 in	
Engine Length	106.2 cm	41.8 in	
Module Chamber Diameter	6.63 cm	2.61 in	
Module Throat Diameter	3.66 cm	1.44 in	
Module Exit Diameter	23.11 cm	9.10 in	
Module Chamber Length	16.51	6.5 in	
Module Nozzle Length	27.41 cm	10.79 in	
Module Length	52.27 cm	20.58 in	
Coolant Jacket Flow Rate	2.41 kg/s	5.31 lbm/s	
Coolant Jacket ΔP	5.58 atm	82 psia	
Coolant Inlet Temperature	23 K	42 R	
Coolant Exit Temperature	218 K	392 R	
TURBINES			
Inlet Pressure	6.46 atm	95 psia	
Inlet Temperature	922 K	1,660 K	
Gas Flow Rate	0.26 kg/s	0.57 lbm/s	
Specific Heat Ratio	1.36		
Molecular Weight	3.8 g/mol		
Shaft Horsepower	316 kW	424 hp	
Percent Bypass	0		
MAIN PUMPS			
Oxidizer Pump Flow Rate	13.36 kg/s	29.46 lbm/s	
Oxidizer Pump Discharge Pressure	43.55 atm	640 psia	
Fuel Pump Flow Rate	2.54 kg/s	5.61 lbm/s	
Fuel Pump Discharge Pressure	47.63 atm	700 psia	
GAS GENERATOR			
Chamber Pressure	6.80 atm	100 psia	
Combustion Temperature	922 K	1,660 R	
Mixture Ratio (O/F)	0.9		
Total Flow Rate	0.26 kg/s	0.57 lbm/s	
Oxidizer Flow Rate	0.12 kg/s	0.27 lbm/s	
Fuel Flow Rate	0.14 kg/s	0.30 lbm/s	

TABLE LXXV - BASELINE SPACE TUG ENGINE COMPARISON

Nominal Thrust 66,723 N

ENGINE	RL10 IIB*				MODEL I PCE 300 $\epsilon_M = 40$				AEROSPIKE*				MODEL I PCE 500 $\epsilon_M = 40$				ASE*			
MR	5	5.5	6	7	5	5.5	6	7	5	5.5	6	7	5	5.5	6	7	6	5.5	6	7
P_C (atm)	27.2	27.2	27.2	27.2	20.4	20.4	20.4	20.4	54.4	52.4	49.7	54.4	34.0	34.0	34.0	34.0	113.6	111.6	108.9	103.4
ϵ_E	168	185	205	257	458	458	458	458	185	165	140	100	458	453	458	458	400	400	400	400
WE (Kg)	193	196	201	215	240	239	239	238	111	108	104	95	219	219	219	218	122	119	118	122
Is (s)	462.5	461	456.5	441	468.2	467.4	465.6	458.1	468	463	459.5	443.4	471.8	471.1	470.2	463.4	469	471	470	464
LE (m)	1.40	1.40	1.40	1.40	0.86	0.86	0.86	0.86	0.51	0.48	0.43	0.38	0.71	0.71	0.71	0.71	1.28	1.28	1.28	1.28
η_E	0.973	0.967	0.956	0.925	0.966	0.962	0.958	0.947	0.982	0.974	0.971	0.957	0.973	0.959	0.967	0.957	0.969	0.972	0.970	0.959
PAYLOAD (Kg)																				
• Deploy	2558	3138	3595	2817	2631	3243	3818	3378	2949	3429	3949	3225	2797	3416	4026	3613	2952	3661	4271	3877
• Retrieve	898	1263	1540	1015	948	1349	1720	1408	1158	1502	1778	1268	1064	1475	1876	1578	1161	1637	2038	1751
• Round Trip	560	774	939	629	588	822	1039	859	714	891	1081	784	656	894	1128	958	716	992	1226	1062
• Planetary	3340	4130	4826	4101	3396	4220	5013	4561	3641	4357	5103	4417	3528	4358	5180	4751	3645	4548	5371	4955
$\partial PL/\partial Is$																				
• Deploy	32	34	35	38	32	33	34	35	31	33	34	36	31	32	34	34	31	32	33	34
• Retrieve	22	24	26	25	23	24	27	26	23	24	27	25	23	25	27	26	23	25	27	26
• Round Trip	13	14	15	15	13	14	15	15	13	14	15	15	13	14	15	15	13	14	15	15
• Planetary	26	27	29	30	25	27	28	29	25	27	29	30	25	26	28	28	25	26	27	28
$\partial PL/\partial W_E$																				
• Deploy	-2.5	-2.6	-2.6	-2.7	-2.5	-2.5	-2.5	-2.6	-2.5	-2.5	-2.6	-2.7	-2.4	-2.5	-2.5	-2.5	-2.5	-2.5	-2.5	-2.5
• Retrieve	-1.6	-1.6	-1.7	-1.6	-1.7	-1.6	-1.7	-1.6	-1.7	-1.7	-1.7	-1.6	-1.7	-1.6	-1.7	-1.7	-1.6	-1.7	-1.7	-1.6
• Round Trip	-1.0	-1.0	-1.0	-1.0	-1.0	-1.0	-1.0	-1.0	-1.0	-1.0	-1.0	-1.0	-1.0	-1.0	-1.0	-1.0	-1.0	-1.0	-1.0	-1.0
• Planetary	-2.0	-2.0	-2.0	-2.0	-1.9	-1.9	-2.0	-2.0	-1.9	-2.0	-2.0	-2.0	-1.9	-1.9	-1.9	-2.0	-1.9	-1.9	-1.9	-2.0

*Parametric Weight & Performance from MSFC Data Package (17 April 1973) and PW&A FR-6011 Vol. II (15 Dec 1973). Ref. 14 & 38

TABLE LXXV (Cont.)

Baseline Space Tug Engine Comparison (cont.)

Nominal Thrust 15,000 lb_f

ENGINE	RL10 IIB*				MODEL I PCE 300 $\epsilon_M = 40$				AEROSPIKE*				MODEL I PCE 500 $\epsilon_M = 40$				ASE*			
MR	5	5.5	6	7	5	5.5	6	7	5	5.5	6	7	5	5.5	6	7	5	5.5	6	7
P_c (psia)	400	400	400	400	300	300	300	300	800	770	730	800	500	500	500	500	1670	1640	1600	1520
ϵ_E	168	185	205	257	458	458	458	458	185	165	140	100	458	458	458	458	400	400	400	400
Wt (lbm)	426	433	443	474	529	527	526	525	245	239	230	209	483	482	482	481	270	263	260	270
Is (s)	462.5	461	456.5	441	468.2	467.4	465.6	458.1	468	463	459.5	443.4	471.8	471.1	470.2	463.4	469	471	470	464
L (in)	55	55	55	55	34	34	34	34	20	19	17	15	28	28	28	28	50.5	50.5	50.5	50.5
η_E	0.973	0.967	0.956	0.925	0.966	0.962	0.958	0.947	0.982	0.974	0.971	0.957	0.973	0.969	0.967	0.957	0.969	0.972	0.970	0.959
PAYLOAD (LBM)																				
• Deploy	5661	6918	7926	6210	5801	7150	8417	7447	6502	7560	8705	7111	6166	7531	8875	7966	6508	8072	9417	8547
• Retrieve	1980	2785	3396	2238	2091	2975	3791	3104	2552	3212	3920	2795	2346	3251	4136	3478	2560	3610	4493	3861
• Round Trip	1235	1707	2070	1386	1297	1812	2290	1894	1575	1964	2383	1729	1447	1972	2487	2111	1579	2183	2702	2342
• Planetary	7363	9104	10640	9042	7487	9303	11052	10056	8028	9605	11251	9738	7778	9608	11421	10475	8035	10027	11840	10925
∂PL/∂Is																				
• Deploy	71	74	78	83	70	73	76	77	68	72	76	80	69	71	74	76	68	70	73	74
• Retrieve	49	54	58	55	50	54	59	57	50	54	59	55	50	55	60	57	50	55	60	58
• Round Trip	29	31	33	33	29	31	33	33	29	31	33	33	29	31	33	33	29	31	33	33
• Planetary	57	60	64	67	56	59	62	63	56	59	63	66	56	58	61	62	56	58	60	61
∂PL/∂WE																				
• Deploy	-2.5	-2.6	-2.6	-2.7	-2.5	-2.5	-2.5	-2.6	-2.5	-2.5	-2.6	-2.7	-2.4	-2.5	-2.5	-2.5	-2.5	-2.5	-2.5	-2.5
• Retrieve	-1.6	-1.6	-1.7	-1.6	-1.7	-1.6	-1.7	-1.6	-1.7	-1.7	-1.7	-1.6	-1.7	-1.6	-1.7	-1.7	-1.6	-1.7	-1.7	-1.6
• Round Trip	-1.0	-1.0	-1.0	-1.0	-1.0	-1.0	-1.0	-1.0	-1.0	-1.0	-1.0	-1.0	-1.0	-1.0	-1.0	-1.0	-1.0	-1.0	-1.0	-1.0
• Planetary	-2.0	-2.0	-2.0	-2.0	-1.9	-1.9	-2.0	-2.0	-1.9	-2.0	-2.0	-2.0	-1.9	-1.9	-1.9	-2.0	-1.9	-1.9	-1.9	-2.0

*Parametric Weight & Performance from MSFC Data Package 17 April 1973 and P&WA FR-6011 Vol. II 15 December 1973. Ref. 14 & 30

B. SPACE TUG SYSTEM STUDY BIBLIOGRAPHY

1. "Space Tug Systems Study (Cryogenic)," Vol. 1: Final Overview Briefing Manual, McDonnell-Douglas Astronautics Co., Contract NAS8-29677, NASA-CR-120459, MDC G5031, Jan 1974.

2. Ibid, Vol. 2: Technical Compendium Final Report, NASA-CR-120460, MDC G5029.

3. Ibid, Vol. 3: Executive Summary Final Report NASA-CR-120461, MDC G5030.

4. Ibid, Data Dump Overview, MDC G4813, Sep 1973.

5. Ibid, September Data Dump, Vol. 1, Summary, Program Option 1, Sep 1973.

6. Ibid, September Data Dump, Vol. 2, Summary, Program Option 2.

7. Ibid, September Data Dump, Vol. 3, Summary, Program Option 3.

8. Ibid, Concept Selection Overview, MDC G4770, Jul 1973.

9. Ibid, First Review Overview, MDC G4729, May 29, 1973.

10. "Space Tug Systems Study (Cryogenic)," Final Report, Vol. I - Final Briefing, General Dynamics, Convair Aerospace Division, Contract NAS8-29676, CASD-NAS73-033, Jan 1974.

11. Ibid, Vol. II - Compendium.

12. Ibid, Vol. III - Executive Summary.

13. Ibid, First Review, May 29, 1973.

14. Ibid, Data Dump, Vol. 1 - Program 1 Summary, Sep 18, 1973.

15. Ibid, Vol. II - Program 2 Summary.

16. Ibid, Vol. III - Program 3 Summary.

17. "Space Tug Systems Study (Storable)," Final Report, Vol. 1, Overview Presentation, Martin Marietta Corp., Contract NAS8-29675, MCR-73-314, Jan 1974.

18. Ibid, Vol. 2, Compendium.

19. Ibid, Vol. 3, Executive Summary.

20. Ibid, Requirements Assessment Presentation, MCR-73-82, 11 Apr 1973

21. Ibid, First Review Presentation, Propulsion Addendum, 30 May 1973.

22. Ibid, Program Concept Evaluation, MCR 73-193, 19 Jul 1973.

23. Ibid, Propulsion Addendum, 19 Jul 1973.

24. Ibid, Vol. 1, Summary, Program Option 1, Selected Option Data Dump, MCR 73-235, Sep 1973.

25. Ibid, Vol. 2, Summary, Program Option 2

26. Ibid, Vol. 3, Summary, Program Option 3

27. "Storable Space Tug Systems Study", Final Presentation, Vol. I, Grumman Aerospace Corp., Contract NAS8-29674, 300 RP-73-013 Final Report, 31 Jan 1974

28. Ibid, Final Report, Vol. 2, 300 RP-73-015

29. Executive Summary, Vol. 3, 300 RP-73-014.

30. Ibid, Requirements Assessment Meeting B80-RP-95-73-002, 12 Apr 1973.

31. "Space Tug First Review," Propulsion Panel Meeting, Grumman Aerospace Corp., Contract NAS8-29674, 31 May 1973.

32. "Storable Space Tug Systems Study," Concept Selection Meeting, Grumman Aerospace Corp., Contract NAS8-29674, B80-RP-95-73-004, 20 July 1973.

33. Ibid, Propulsion Panel Meeting, 21 Jul 1973.

34. Ibid, Data Dump, Vol. I - Summary, Program Option I, 300 RP-73-004, 19 Sep 1973.

35. Ibid, Vol. II - Summary, Program Option II, 300 RP-73-005.

36. Ibid, Vol. III - Summary, Program Option III, 300 RP-73-006.

37. "Baseline Tug Definition Document," Rev. A, Preliminary Design Office, Program Development, NASA Marshall Space Flight Center, 26 Jun 1972.

38. "Space Tug Point Design Study," Vol. I, Management and Technical Summary, McDonnell Douglas Astronautics Co., Contract NAS7-101, MDC G2818, Feb 1972.

39. Ibid, Vol. II, Design and Analysis.

40. "Space Tug Point Design Study, Final Report, Vol. I, Summary, North American Rockwell Space Division, Contract NAS 7-200, SD72-SA-0032, 11 Feb 1972.

41. Ibid, Vol. II, Operations, Performance, and Requirements.

42. Ibid, Vol. III, Design Definition.

43. Ibid, Vol. IV, Program Requirements.

44. Ibid, Vol. V, Cost Analysis

45. "MSC In-House Storable Propellant Space Tug Study Report Draft," Payloads Engineering Office, Future Programs Division, NASA Manned Spacecraft Center, Jan 1973.

46. "Addendum 1, Space Tug System Study Data Package, Propulsion Systems Control Data," NASA/Marshall Space Flight Center, 17 April 1973.

47. "Baseline Space Tug System Requirements and Guidelines," NASA/Marshall Space Flight Center, 15 Jul 1974 MSFC 68M00039-1

48. "Baseline Space Tug Configuration Definition," NASA/Marshall Space Flight Center, MSFC 68M00039-2, 15 July 1974.

49. "Baseline Space Tug Flight Operations," NASA/Marshall Space Flight Center, MSFC 68M000039-3, 15 Jul 1974.

50. "Baseline Space Tug Ground Operations, Verification, Analysis and Processing," NASA/Marshall Space Flight Center, MSFC 68M00039-4, 15 July 1974.

51. "Baseline Space Tug Executive Summary," NASA/Marshall Space Flight Center, MSFC 68M00039-5, 11 Oct 1974.

52. "Orbit-To-Orbit Shuttle (Chemical) Feasibility Study," Vol. 1 - Management Summary, McDonnel Douglas Astronautics Co., Contract F04701-71-C-0173, SAMSO-TR-71-221-1, Oct 1971.

53. Ibid, Vol. 2 - Technical Summary, SAMSO-TR-71-221-2.

54. Ibid, Vol. 3, Book 1 - Missions, Operations and Requirements, SAMSO-TR-71-221-3, Book 1

55. Ibid, Vol. 3, Book 2 - Missions, Operations & Requirements, Appendix, SAMSO-TR-71-221-3, Book 2.

56. Ibid, Vol. 4, Book 1 - Design and Integration, SAMSO-TR-71-221-4, Book 1.

57. Ibid, Vol. 4, Book 2 - Design and Integration - Appendices, SAMSO-TR-71-221-4, Book 2.

58. Ibid, Vol. 5, Book 1 - Subsystems: Structures and Propulsion, SAMSO-TR-71-221-5, Book 1.

59. Ibid, Vol. 5, Book 2 - Subsystems: Avionics, SAMSO-TR-71-221-5, Book 2.

60. Ibid, Vol. 5, Book 3 - Avionics, Appendix, SAMSO-TR-71-221-5, Book 3.

61. Ibid, Vol. 6 - Program Plans and Costs, SAMSO-TR-71-221-6.

62. "Extended Applications Study of AMOOS Aeromaneuvering Orbit to Orbit Shuttle and AMRS Aeromaneuvering Reentry System, Orientation and Study Plan Review, Lockheed Missiles & Space Co., Huntsville, Contract NAS8-31997, LMSC-HREC SD D496798, Apr 1976.

63. "Space Tug Storable Engine Study," Vol. I: Executive Summary, Aerojet Liquid Rocket Co., Contract NAS 8-29806, DPD 396; DR-MA-04, 31 Jan 1974.

64. Ibid, Vol. II: Engine Design and Performance Characteristics, DPD 396; DR-MA-03.

65. Ibid, Vol. III: Engine/Tug Interface and Operational Requirements, DPD 396; DR-MA-03.

66. Ibid, Vol. IV: Project Planning Data, DPD 396; DR-MA-03.

67. Ibid, Final Program Review, DPD 396; DR-MA-02-9, 22 Jan 1974.

68. "Advanced Space Engine Preliminary Design Final Report," Pratt & Whitney Aircraft Div., Contract NAS3-16750, NASA CR-121237, FR-5654, Dec 1973.

69. "Advanced Space Engine Preliminary Design, Rocketdyne Div. Rockwell Intl., Contract NAS3-16751, NASA CR-121236, R-9269, Oct 1973.

70. "O_2/H_2 Advanced Maneuvering Propulsion Technology Program Engine System Studies Final Report," Vol. I: Aerospike Engine Configuration Design and Analysis, Rocketdyne Div., No. American Rockwell Corp., Contract F04611-67-C-0116, AFRPL-TR-72-4, Dec 1971.

71. Ibid, Vol. II: 25,000-Pound-Thrust Bell Engine Configuration Design and Analysis.

72. Ibid, Vol. III: 10,000-Pound-Thrust Bell Engine Configuration Design and Analysis, Jan 1972.

73. "Design Study of RL10 Derivatives," Final Report Vol. I Program Summary, Pratt & Whitney Aircraft Div., Contract NAS8-28989, FR-6011 Vol. I, 15 Dec 1973.

74. Ibid, Vol. II Engine Design Characteristics.

75. Ibid, Vol. II Appendices.

76. Ibid, Vol. III, Part 1 Preliminary Interface Control Document.

77. Ibid, Vol. III, Part 2 Operational and Flight Support Plan.

78. Ibid, Vol. IV, Development Plans and Program Costs.

79. "Application of Bell 8096 Engine for Space Tug Propulsion," Final Report, Volume I - Executive Summary, Bell Aerospace Div., Contract NAS8-29765, DPD 394; DR-MA03, Report 8096-910513, Feb 1974.

80. Ibid, Vol. II - Engine Design and Performance Analysis.

81. Ibid, Vol. III - Engine/Tug Interface and Operational Requirements.

82. Ibid, Vol. IV - Project Planning Data.

83. Ibid, Vol. V - Costs.

84. "Pre-Phase A Study for an Analysis of a Reusable Space Tug," Vol. I - Management Summary, North American Rockwell Corp., Contract NAS9-10925, NASA-CR-114937, SD-71-292-1-Vol. I, 22 Mar 1971.

85. Ibid, Vol. II - Technical Summary, NASA-CR-114936, SD-71-292-2-Vol. II.

86. Ibid, Vol. III - Mission and Operations Analysis, NASA-CR-114935, SD-71-292-3-Vol. III.

87. Ibid, Vol. IV - Spacecraft Concepts and Systems Design, NASA-CR-114938, SD-71-292-4-Vol. IV.

88. Ibid, Vol. V - Subsystems, NASA-CR-114939, SD-71-292-5- Vol. V.

89. Ibid, Vol. VI - Planning Documents, NASA-CR-114940, SD-71-292-6-Vol. VI.

90. "Performance of Recoverable Single and Multiple Space Tugs for Missions Beyond Earth Escape," NASA/LeRC, NASA-TM-X-68136, Nov 1972. (Zimmerman, A.V.)

91. "European Space Tug Pre-Phase A Study," Appendix 3 Propellant Control and Propulsion, Hawker Siddeley Dynamics Ltd., ELDO-CTR-17/7/44, HSD-TP-7227-APP-3, Jan 1971.

92. "IUS/Tug Operations and Mission Support Study," Vol. III Space Tug Operations, International Business Machines Corp., Contract NAS8-31009, NASA-CR-143855, IBM-75W-00072-Vol. III, May 1975.

93. "DOD Upper Stage/Shuttle System Preliminary Requirements Study," Vol. I Summary, North American Rockwell Corp., Contract F04701-72-C-0305, SAMSO-TR-72-195-Vol. I, SD-72-SA-0115-1-Vol. I, Aug 1972.

94. Ibid, Vol. II OOS Vehicle and Shuttle Interface Analysis, SD-72-SA-0115-2.

95. Ibid, Vol. II, Appendix I DOD Upper Stage Functional Analysis and System Requirements, SD-72-SA-0115-3.

96. Ibid, Vol. II, Appendix II Reference Shuttle Definition, SD-72-SA-0115-4.

97. "A Study of Compatibility of a Cryogenic Upper Stage with Space Shuttle," General Dynamics/Convair, Contract NAS3-14389, NASA-CR-120897, GDCA-BNZ71-020-7, Apr 1972.

98. "Orbit-To-Orbit Shuttle Engine Design Study," Final Report Book 1 Parametric Cycle Study, Aerojet Liquid Rocket Co., Contract F04611-71-C-0040, AFRPL TR-72-45 Book 1, May 1972.

99. Ibid, Book 2 25K LB Engine Design.

100. Ibid, Book 3 25K LB Engine Maintenance, Development Plans, Cost Estimates and 10K LB Engine Design.

101. Ibid, Book 4 Appendices.

102. "Study of Liquid Oxygen/Liquid Hydrogen Auxiliary Propulsion Systems for the Space Tug," Final Report, Space Div., Rockwell International Corp., Contract NAS3-18913. NASA CR-134790, SD 75-SA-0043, 15 Jun 1975.

C. PLUG AND PLUG-CLUSTER ROCKET NOZZLE BIBLIOGRAPHY

1. "Results of a Program for Theoretical and Experimental Evaluation of the Plug Nozzle Concept", Aerojet-General Corporation (V. H. Ransom, S. A. Lorenc, J. J. Williams, T. L. DeYoung), Technical Memorandum No. 159 SRP, 8 Mar. 1961.

2. "Results of Plug-Nozzle Cold-Flow Experiments", Aerojet-General Corporation (J. J. Williams), Technical Memorandum 160 SRP, 20 Apr. 1961.

3. "Model Tests of Several Rocket Exhaust Nozzle Configurations Including Thrust Vector Control Devices", Fluidyne Engineering Corporation (R. G. Brasket and C. W. Landgraf), Report on F.E.C. Project 0160, Nov. 1960.

4. "A Second-Order Numerical Method of Characteristics for Three-Dimensional Supersonic Flow", Volume I. Theoretical Development and Results, Jet Propulsion Center, Purdue University (V. H. Ransom, J. E. Hoffman, and H. D. Thompson), Lafayette, Indiana 47907, Technical Report AFAPL-TR-69-98, Oct. 1969.

5. "Performance of Annular Plug and Expansion-Deflection Nozzles Including External Flow Effects at Transonic Mach Numbers", Lewis Research Center (R. A. Wasko), Cleveland, Ohio, NASA TN D-4462, Apr. 1968.

6. "Design and Analysis of Altitude-Compensating Rocket Nozzles", Aerojet-General Corporation (C. A. Bryce, T. L. DeYoung, J. C. Eschweiler, and R. L. Strickler), Report No. 8548-SR-1, Dec. 1964.

7. "Study of High Effective Area Ratio Nozzles for Space Craft Engines", Aerojet-General Corporation Report No. NAS7-136-F, Vol. 1 and 2, Contract NAS7-136, Jun. 1964.

8. "J-2T Aerodynamic Spike Thrust Chamber Study, Phase Zero Final Report", Advanced Projects Department Rocketdyne Engineering, Report No. R-5905, Contract No. NAS8-19, 15 May 1965.

9. "Multichamber Plug-Nozzle Systems Analysis", Rocketdyne (M. S. Bensky), Report No. R-6494, Contract No. NAS8-20237, May 1966.

10. "Advanced Engine Aerospike Experimental Program Thrust Chamber Performance" (Volume 2, Final Report), Rocketdyne Engineering, Report No. R-7760, Contract NAS8-20237, May 1966.

11. "Plug Nozzle Study" - Final Report, Pratt and Whitney Aircraft, Report No. FR-1013, Contract NAS8-11023, 8 Sep. 1964.

12. "An Experimental Hot Rocket Model Investigation of a Plug Cluster Nozzle Propulsion System. Part 1: Base Thermal and Pressure Environment for a Module Chamber Pressure of 300 psia and Simulated Altitudes to 150,000 Feet", Cornell Aeronautical Lab. (R. J. Sergeant), Cal No. HM-2024-Y-5 (1), Contract No. NAS8-20027, Sep. 1967.

13. "Trade-Off Between Different Possible Engine Concepts Using LOX/LH_2 -- Low Thrust High Pressure Engines for European Launch Vehicle With Conventional Bell Nozzles or Aerospike Nozzles, Europa 3, Stage 2," Cryorocket, MBB and SEP, NASA DCAF E003091, ELDO-CTR-17/3/191, 30 Mar 1973.

14. "Space Tug Engine Study, Phase A -- Ranking of Different Engine Designs, ELDO Launch Vehicle Studies," Cryorocket, Neuilly (France), NASA DCAF E003091, ELDO-CTR-17/3/174, 21 Aug 1972.

15. "A Liquid Oxygen-Liquid Hydrogen Rocket Engine for Satellite Launching Vehicle Upper Stages -- Providing for De Havilland Third Stage of Multi-Engines Installation in Second Stage," Rolls-Royce Ltd. (England), NASA DCAF E003091, Mar 1973.

16. "Zero NPSP Pumping Tests with an Operational Hydrogen Turbopump," Aerojet-General Corp., Nuclear Rocket Operations (W. E. Campbell), in 9th Liq. Prop. Symp., Vol. II, pp. 169-81, Sep 1967.

17. "Mark III Turbopump Assembly Performance Test Results," Aerojet-General Corp., NASA-CR-79824, RN-S-0110, SNP-1, Sep 1964.

18. "Operation Handbook, Partial Model Turbopump P/N P9230792," Aerojet-General Corp. (C. J. Reynolds and S. R. Andrus), Contract DAAG05-69-0453, AGC RMR-0127, Dec 1969.

D. H/O THRUST CHAMBER BIBLIOGRAPHY

1. "Hydrogen-Oxygen Space Shuttle ACPS Thruster Technology Review," NASA/LeRC (J. W. Gregory and P. N. Herr), AIAA Paper 72-1158, 29 Nov 1972.

2. "Integrated Thruster Assembly Program," Aerojet Liquid Rocket Co., Contract NAS3-15850, NASA CR-134509, Nov 1973.

3. "Extended Temperature Range ACS Thruster Investigation," Aerojet Liquid Rocket Co. (A. L. Blubaugh and L. Schoenman), Contract NAS3-16775, NASA CR-134655, 1 Aug 1974.

4. "Hydrogen-Oxygen Auxiliary Propulsion for the Space Shuttle," Volume I: High Pressure Thrusters, Aerojet Liquid Rocket Co., Contract NAS3-14354, NASA CR-120895, 30 Jan 1973.

5. "Hydrogen-Oxygen APS Engines," Volume I: High Pressure Thruster, Rocketdyne Div. of NAR (R. D. Paster), Contract NAS3-14352, NASA CR-120805, Feb. 1973.

6. "High Pressure Reverse Flow APS Engine," Bell Aerospace Co. (J. M. Senneff), Contract NAS3-14353, NASA CR-120881, Nov 1972.

7. "Investigation of Gaseous Propellant Combustion and Associated Injector/Chamber Design Guidelines," Aerojet Liquid Rocket Co. (D. F. Calhoon, J. I. Ito, and D. L. Kors), Contract NAS3-14379, NASA CR-121234, 31 Jul 1973.

8. "Combustion Effects on Film Cooling," Aerojet Liquid Rocket Co. (D. C. Rousar and R. L. Ewen), Contract NAS3-17813, NASA CR-   , 1976.

9. "Test Results with a Regeneratively Cooled LOX/LH_2 Thrust Chamber for the Ariane 3rd Stage Propulsion System," Messerschmitt-Boelkow-Blohm GMBH (H. Dederra), AIAA Paper 75-1189, Sep 1975.

10. "Development of Pulsed Hydrogen/Oxygen Attitude-Control Engines," Messerschmitt-Boelkow-Blohm GMBH (G. Pulkert), DGLR Paper 72-077, Oct 1972.

11. "Investigation of Thrusters for Cryogenic Reaction Control Systems," TRW Systems Group (R. J. Johnson), Contract NAS3-11227, NASA-CR-72608, Mar 1970.

12. "Space Shuttle High Pressure Auxiliary Propulsion Subsystem Definition," TRW Systems Group (R. A. Benson, et al), Contract NAS9-11013, NASA-CR-115162, Mar 1971.

13. "Ignition Devices for ACPS," Aerojet Liquid Rocket Co. (S. D. Rosenberg), Contract NAS3-14348, in MSFC Proc. - Space Transportation System Propulsion Technol. Conf., Vol. 2, pp. 613-64, 28 Apr 1971.

14. "Space Shuttle ACPS Shutoff Valve," Rocketdyne (G. M. Smith), Contract NAS3-14350, in MSFC Proc. - ibid, Vol. 2, pp. 563-612, 28 Apr 1971

15. "Space Shuttle ACPS Shutoff Valve," Marquardt Corp. (H. Wichmann), Contract NAS3-14349, in MSFC Proc. - ibid, Vol. 2, pp. 501-62, 28 Apr 1971.

16. "Space Tug Engine Performance Verification Program," Vol. I, Program Summary, Pratt & Whitney Aircraft, Contract NAS8-31008, FR-7509, 14 May 1976.

17. Ibid, Vol. II, Final Report.

E. H/O TURBOPUMP ASSEMBLY BIBLIOGRAPHY

1. "Turbopumps for Cryogenic Upper-Stage Engines," Rocketdyne Div. (A. T. Zachary, A. Csomor, and L. L. Tignac), Contract NAS8-27794, R-9367, Dec 1973.

2. "Design Study of RL-10 Derivatives," Vol. II, Engine Design Characteristics, Pratt & Whitney Aircraft, Contract NAS8-28989, FR-6011, 15 Dec 1973.

3. Ibid, Vol. II Appendices.

4. "Turbopump Systems for Liquid Rocket Engines," NASA Space Vehicle Design Criteria (Chemical Propulsion), NASA SP-8107, Aug 1974.

5. "An Experimental Investigation of Two-Phase Liquid Oxygen Pumping," NASA/MSFC (L. A. Gross), NASA-TN-D-7451, Nov 1973.

6. "Study and Technological Work on Some Aspects of the U.S. Space Shuttle Auxiliary Propulsion System," Cryorocket, Neuilly (France), Rept-D-9/71-MK/DH, Aug 1971.

7. "Study on a Combined OMS/ACPS Propulsion System," Messerschmitt-Boelkow-Blohm GMBH and Cryorocket, MBB-UR-82-71, Aug 1971.

8. "Preliminary Design Study of Space Shuttle Auxiliary Propulsion System," Societe Europeenne De Propulsion and Cryorocket (France), SEP-NT-3054/71-M, Aug 1971.

9. "Experimental Findings from Zero-Tank Net Positive Suction Head Operation of the J-2 Hydrogen Pump, NASA/MSFC (H. P. Stinson and R. J. Strickland), NASA-TN-D-6824, Aug 1972.

10. "Study of Influence of the Variation of the Parameters on the Functioning of the 200KN HP Engine -- Without Considering Return of Part of Pump Flow to Tank, Europa 3, Stage 2," Societe Europeenne De Propulsion (P. Bordier), NASA DCAF E003091, SEP-TL/LH-3049/71M, 29 Jun 1971.

11. "Studies of the Parameter Variations of the 200KN HP Engine -- Considering Return of Part of Pump Flow to Tank, Europa 3, Stage 2," Societe Europeenne De Propulsion (P. Bordier), NASA DCAF E003091, SEP-TL/LH-3050/71M, 29 Jun 1971.

12. "European Space Tug Engine Study Pre-Phase A General Studies," Cryorocket and Messerschmitt-Boelkow-Blohm GMBH and Soeiete Europeenne De Propulsion, NASA DCAF E003091, ELDO-CTR-17/3/101, 29 Jan 1971.

13. "The Effects of Base Bleed on Plug Nozzles," Aeronautical Research Council, London, ARC-R&M-3466 RAE-TR-65043, 1967.

14. "A Report on the Constructive Design and on the Weight Estimation of the Skin Structure of the Plug-Nozzle of the Second Stage of the Space Transportation System, Neptun," Technische Univ., Berlin (J. Allesch), TUB-IR-3/1968, Mar. 1968.

15. "Analytical and Experimental Study of Axisymmetric Truncated Plug Nozzle Flow Fields," Notre Dame Univ. (T. J. Mueller, et al), Contract NAS8-25601, NASA-CR-123941, Sep. 1972.

16. "Comparison of Performance of a Double-Cornered Plug Nozzle with a Conventional Convergent-Divergent Rocket Nozzle," Army Missile Command, Redstone Arsenal (A. T. Stokes), RK-TR-72-17, Jun. 1972.

17. "Three Dimensional Thrust Chamber Life Prediction," Boeing Aerospace Co., Contract NAS3-19717, NASA-CR-134979, D180-19309-1, Mar. 1976.

18. "Fortran Program for Plug Nozzle Design," NASA/MSFC (C. Lee and D. Thompson), Contract NASA-TM-X-53019, Jul. 1964.

19. "Truncated Plug Nozzle Computer Program Documentation," Vol. I, Notre Dame Univ. (C. R. Hall), Contract NAS8-25601, NASA-CR-132965, UNDAS-PD-601-1-Vol-I, Jul. 1971.

20. Ibid, Vol. II, NASA-CR-132966.

21. "Plug-Nozzle Program," General Electric Co. (A. R. Graham), Contract NAS5-445, NASA-CR-135802, DM-61-154, Oct. 1961.

22. "Analytical and Experimental Investigations of High Expansion Area Ratio Nozzles," Vol. I, Analytical and Model Cold-Flow Studies, Rocketdyne (D. W. Hege), Contract AF04(611)-8509, RPL-TDR-64-3-Vol. I, Dec. 1964.

23. "An Analytical and Experimental Study of Nonuniform Plug Nozzle Flow Fields," Notre Dame Univ. (C. R. Hall and T. J. Mueller), NSR-15-004-029, AIAA Paper 71-41, Jan. 1971.

24. "Design of Maximum Thrust Plug Nozzles with Variable Inlet Geometry," Colorado State Univ. and Purdue Univ. (G. R. Johnson, H. D. Thompson, and J. D. Hoffman), Computers and Fluids, Vol. 2, pp. 173-90, Aug. 1974.

25. "The Mach Disc in Truncated Plug Nozzle Flows," ARO, Inc. and Notre Dame Univ. (T. V. Giel and T. J. Mueller), Contract NAS8-25601, AIAA Paper 75-886, Jun. 1975.

26. "The Computation of Steady Exhaust Nozzle Flows by a Time Dependent Method," AVCO Corp. (K. P. Sarathy and R. Bozzola), AIAA Paper 76-151, Jan. 1976.

27. "Fortran Program for Design of Pure External and Internal-External Expansion Plug Nozzles," Brown Engineering Co. (C. C. Lee), Contract NAS8-2485, NASA-CR-51300, R-41, Mar. 1963.

28. "Fortran Computer Program to Design Plug Nozzle By Using Rao Maximum Thrust Theory," Brown Engineering Co. (C. C. Lee), Contract NAS8-5289, NASA-CR-51301, Jul. 1963.

29. "Plug Nozzle Propulsion Efficiency," NASA/LaRC (C. E. Mercer and L. B. Salters), NASA-TN-D-1804, May 1963.

30. "NASA Plug Nozzle Handbook," General Electric Co. (A. R. Graham), NAS9-3748, NASA-CR-117018, Aug. 1965.

31. "An Experimental Model Investigation of a Plug Cluster Nozzle Propulsion System," Cornell Aeronautical Lab (K. C. Hendershot and R. J. Sergeant), Contract NAS8-823,, NAS8-20027, in APL Eighth Liq. Prop. Symp., Vol. I, pp. 293-334, Oct. 1966.

32. "Cold Flow Thrust and Pressure Investigations of a Plug Cluster Nozzle Using Short-Duration Techniques," Cornell Aeronautical Lab (R. K. Ellison and K. C. Hendershot), Contract NAS8-823, NASA-CR-68956, CAL-HM-1510-Y-13, Apr. 1965.

33. "Base Pressure and Heating of Truncated Plug Rocket Exhaust Nozzle," Martin Co. (R. C. Schmidt), in APL Bull. of the 6th Liq. Prop. Symp., Vol. I, pp. 537-53, Aug. 1964.

34. "Base Pressure Effects on the Thrust Performance of Unconventional Rocket Nozzles," Douglas Aircraft Co. (G. W. Burge and D. W. Kendle), in APL Bull. of the 5th Liq. Prop. Symp., Vol. II, pp. 730-68, Dec. 1963.

35. "Study for Evaluation of Plug Multichamber Configuration," Phase I Pratt & Whitney Aircraft, Contract NAS8-11436, FR-1415, 29 Oct 1965.

36. Ibid, Phase II, FR-2400, 31 Oct 1967.

SECTION XI

REFERENCES

1. Baseline Space Tug Executive Summary, NASA/Marshall Space Flight Center, MSFC 68M00039-5, 11 October 1974.

2. Space Tug Systems Study (Cryogenic), September Data Dump, McDonnell-Douglas Astronautics Co., Contract NAS8-29677, September 1973.

3. Wasko, R. A., Performance of Annular Plug and Expansion-Deflection Nozzles Including External Flow Effects at Transonic Mach Numbers, NASA TN D-4462, April 1968.

4. Booz, D. E. and Schilling, M.T., Plug Cluster Nozzle Study, Pratt and Whitney Aircraft, Florida, PWA FR-1013, Contract NAS 8-11023, 8 September 1964.

5. Bensky, M.S. Multichamber Plug-Nozzle Systems Analysis, Rocketdyne, Canoga Park, California, R-6494, Contract NAS 8-20237, May 1966.

6. Diem, H. G., Huang, D. H. and Wheeler, D.B., O_2/H_2 Advanced Maneuvering Propulsion Technology Program Engine System Studies Final Report, Volume 1 Aerospike Engine Configuration Design and Analysis, Rocketdyne, Canoga Park, California, AFRPL-TR-72-4, Contract F04611-67-C-0116, December 1971

7. Monteath, E. B., Advanced Engine Aerospike Experimental Program Thrust Chamber Performance, Volume 2, Final Report, Rocketdyne, Canoga Park, California, R-7760, Contract NAS 8-20349, July 1969.

8. Gregory, J. W. and Herr, P.N., Hydrogen-Oxygen Space Shuttle ACPS Thruster Technology Review, NASA/Lewis Research Center, AIAA Paper 72-1158, 29 November 1972.

9. LaBotz, R. J. and Blubaugh, A. L., Integrated Thruster Assembly Program, Aerojet Liquid Rocket Company, Sacramento, California, NASA CR-134509, Contract NAS 3-15850, November 1973.

10. Blubaugh, A. L. and Schoenman, L., Extended Temperature Rangs ACPS Thruster Investigation, Aerojet Liquid Rocket Company, Sacramento, California, NASA CR-134655, Contract NAS 3-16775, 1 August 1974.

11. Schoenman, L. and LaBotz, R. J., Hydrogen-Oxygen Auxiliary Propulsion for the Space Shuttle, Volume I: High Pressure Thrusters, Aerojet Liquid Rocket Company, Sacramento, California, NASA CR-120895, Contract NAS 3-14354, 30 January 1973.

12. Paster, R. D., Hydrogen-Oxygen APS Engines, Volume I: High Pressure Thruster, Rocketdyne, Canoga Park, California, NASA CR-120805, Contract NAS 3-14352, February 1973.

13. Zachary, A.T., Csomor, A. and Tignac, L.L., Turbopumps for Cryogenic Upper-Stage Engines, Rocketdyne, Canoga Park, California, R-9367, Contract NAS8-27794, December 1973.

14. Adams, A., Mayes, T.C. and Walter, J.D., Design Study of RL10 Derivatives, Final Report, Volume II, Engine Design Characteristics, Pratt & Whitney Aircraft, West Palm Beach, Florida, FR-6011, Contract NAS8-28989, 15 December 1973.

15. JANNAF Rocket Engine Performance Prediction and Evaluation Manual, Johns Hopkins University, Applied Physics Laboratory, Silver Spring, Maryland, CPIA Publication 246, April 1975.

16. Williams, C.W., and Mellish, J.A., Space Tug Storable Engine Study, Volume II; Engine Design and Performance Characteristics, Aerojet Liquid Rocket Company, Sacramento, California, DPD 396; DR-MA-03, Contract NAS8-29806, 31 January 1974.

17. Pieper, J. L. for ICRPG Performance Standardization Working Group, Aerojet General Corporation, Sacramento, California, CPIA Publication No. 178, 30 September 1968.

18. Calhoon, D.F., Ito, J.I. and Kors, D.L. Investigation of Gaseous Propellant Combustion and Associated Injector/Chamber Design Guidelines, Aerojet Liquid Rocket Company, Sacramento, California, NASA-CR-121234, Contract NAS 3-14379, 31 July 1973.

19. Rao, G.V.R., Spike Nozzle Contour for Optimum Thrust, AFBMD/STL Symposium on Advances in Ballistic Missile & Space Technology, 4th, Los Angeles, California, August 24-27, 1959, Planetary & Space Science, Volume 4, pp.92-101, Pergamon Press, 1961.

20. Johnson, G.R., Thompson, H.B. and Hoffman, J.D., Design of Maximum Thrust Plug Nozzles with Variable Inlet Geometry, Vol. 1, Theoretical Development and Results, Jet Propulsion Center, Purdue University, Lafayette, Indiana, AFRPL-TR-70-75, October 1970.

21. Liquid Rocket Engine Turbines, NASA Space Vehicle Design Criteria (Chemical Propulsion), NASA SP-8110, January 1974.

22. Turbopump Systems For Liquid Rocket Engines, NASA Space Vehicle Design Criteria (Chamical Propulsion), NASA SP-8107, August 1974.

23. Luscher, W.P. and Mellish, J. A., Advanced High Pressure Engine Study for Mixed-Mode Vehicle Applications, Aerojet Liquid Rocket Company, NASA CR-135141, Contract NAS 3-19727, January 1977.

24. Rousar, D.C. and Ewen, R.L., Combustion Effects on Film Cooling, Aerojet Liquid Rocket Company, NASA CR-135052, Contract NAS 3-17813. February, 1977.

25. Sergeant, R.L., An Experimental Hot Model Investigation of a Plug Cluster Nozzle Propulsion System, Part 1: Base Thermal and Pressure Environment for a Module Chamber Pressure of 300 psia and Simulated Altitudes to 150,000 Feet, Cornell Aeronautical Laboratory, Inc., CAL No. HM-2045-Y-5 (I), Figure 33, September 1967.

26. Rousar, D. and Miller, F., Cooling With Supercritical Oxygen, Aerojet Liquid Rocket Company, AIAA Paper 75-1248, 29 September 1975.

27. Van Huff, N.E. and Rousar, D.C., Ultimate Heat Flux Limits of Storable Propellants, Aerojet General Corporation, 8th Liquid Propulsion Symposium, Volume II, 7 November 1966.

28. Giarratano, P. J., and Smith, R.V., Comparative Study of Forced Convention Boiling Heat Transfer Correlations for Cryogenic Fluids, Advances in Cryogenic Engineering, Vol. 11, 492-506 (Equation 4), August 1965.

29. Tong, L.S., Boiling Heat Transfer and Two-Phase Flow, John Wiley & Sons, Inc., New York.

30. Davidson, W.F., Studies of Heat Transmission Through Boiler Tubing at Pressures from 500-3300 Pounds, Transactions ASME, 1948.

31. Mellish, J.A., Space Tug Storable Engine Study, Aerojet Liquid Rocket Company, Contract NAS 8-29806, DPD 396, 31 January 1974.

32. Luscher, W.P., Orbit-to-Orbit Shuttle Engine Design Study, Aerojet Liquid Rocket Company, Contract F04611-71-C-0040, AFRPL TR-72-45, May 1972.

33. Diem, H.G., Burry, R.V. and Evans, S.A., O_2/H_2 Advanced Maneuvering Propulsion Technology Program, Engine System Studies Final Report, Volume II 25,000-Pound-Thrust Bell Engine Configuration Design and Analysis, Rocketdyne, Canoga Park, California, AFRPL TR-72-4, Contract F04611-67-C-0116, December 1971.

34. Diem, H.G., Burry, R.V. and Evans, S.A., O_2/H_2 Advanced Maneuvering Propulsion Technology Program, Engine System Studies Final Report, Volume III 10,000-Pound-Thrust Bell Engine Configuration Design and Analysis, Rocketdyne, AFRPL TR-72-4, Contract F04611-67-C-0116, January 1972.

35. Luscher, W. P., Orbit-to-Orbit Shuttle Engine Design Study, Book 3, Aerojet Liquid Rocket Company, AFRPL TR-72-45, Contract F04611-71-C-0040, May 1972.

36. Baseline Space Tug Configuration Definition, NASA/Marshall Space Flight Center, MSFC 68M00039-2, 15 July 1974.

37. Space Tug Systems Study (Cryogenic), Final Report, General Dynamics, Convair Aerospace Division, CASD-NAS73-033, NAS8-29676, January 1974.

38. Addendum 1, Space Tug System Study Data Package, Propulsion Systems Control Data, NASA/Marshall Space Flight Center, 17 April 1973.

39. Advanced Space Engine Requirements and Operating Conditions, NASA/Lewis Research Center, 1976.

40. Shubert, W. C., Thompson, P. S. Mayes, T. C. and Brown, J. R., Space Tug Engine Performance Verification Program, Pratt & Whitney Aircraft Report FR-7509, Contract NAS 8-31008, 14 May 1976.

41. Advanced Space Engine, Rockwell International Document LC332-977D.

42. Handbook of Supersonic Aerodynamics, Section 17, Ducts, Nozzles and Diffusers, NAVWEPS Report 1488 (Volume 6), January 1964, p. 368.

43. Heddon, K. and Loewe, A., Carbon, Volume 5, No. 4, 339-53 (1967); NASA Microfiche N69-34048.

44. Lewis, J. C. A., Floyd, I. J. and Cowlard, F. C., Laboratory Investigation of Carbon-Gas Reactions of Relevance to Rocket-Nozzle Erosion, Paper No. 29, AGARD Conf. Proc. 52 (1970); NASA Microfiche N70-24576.

45. Rousar, D. C., Plug Cluster Module Demonstration, Aerojet Liquid Rocket Company, NASA CR-135385, Contract NAS 3-20107, July 1978.

46. Kirby, F. M. Plug Cluster Nozzle Flow Evaluation, Final Report, Rocketdyne Division, NASA CR-135229, Contract NAS 3-20104, to be published.

DISTRIBUTION LIST FOR CONTRACT NAS 3-20109

National Aeronautics & Space Administration
Lewis Research Center
21000 Brookpark Road
Cleveland, Ohio 44135

1 Attn: New Technology Office, MS 7-3
1 Contracting Officer, MS 500313
1 E.A. Bourke, MS 501-5
1 Technical Report Control Office, MS 5-5
1 AFSC Liaison Office, MS 501-3
2 Library, MS 60-3
10 Carl A. Aukerman, Project Manager, MS 501-7
1 Patent Counsel, MS 500-311

National Aeronautics & Space Administration
Headquarters
Washington, D.C. 20546

Attn: Office of Aeronautics & Space Technology
1 Director, Space Systems Division/RS-5
1 Director, Research & Technology Division/RT-6
1 R.A. Rudey/RTP-6
1 F.W. Stephenson/RTP-6
1 J.R. Mullin/RTS-6
1 S.R. Sadin/RS-5

Attn: Office of Space Transportation Systems
1 Director, Advanced Programs/MT-3
1 Director, Advanced Studies/MTE-3
1 Director, Advanced Development/MTG-3
1 P.N. Herr/MTE-7

1 National Aeronautics & Space Administration
Flight Research Center
P.O. Box 273
Edwards, CA 93523

National Aeronautics & Space Administration
George C. Marshall Space Flight Center
Huntsville, Alabama 35912

1 Attn: Library
1 J.L. Sanders/PD13
1 J.A. Lombardo/EP21
1 R.J. Richmond/EP24
1 F.W. Braam/EP24
1 R.D. Kramer/PD13

National Aeronautics & Space Administration
Goddard Space Flight Center
Greenbelt, MD 20771

1 Attn: Library

National Aeronautics & Space Administration
John F. Kennedy Space Center
Cocoa Beach, FL 32931

1 Attn: Library

National Aeronautics & Space Administration
Lyndon B. Johnson Space Center
Houston, TX 77001

1 Attn: Library
1 C.W. Yodzis/EP2
1 R.W. Polifka/EP2
1 H.P. Davis/ER
1 J.G. Thibadaux/EP

National Aeronautics & Space Administration
Langley Research Center
Langley Station
Hampton, VA 23365

1 Attn: Library
1 B.Z. Henry, MS 365
1 C.H. Eldred, MS 365

NASA Scientific & Technical Information Facility
P.O. Box 8757
Baltimore-Washington International Airport
Baltimore, Maryland 21240

10 Attn: Accessioning Department

Jet Propulsion Laboratory
4800 Oak Grove Drive
Pasadena, CA 91103

Attn: Library
1 D. Dipprey

Defnese Documentation Center
Cameron Station
Building 5
5010 Duke Street
Alexandria, VA 22314

1 Attn: TISIA

Defense Advanced Research Projects Agency
1400 Wilson Blvd.
Arlington, VA 22209

1 Attn: Library

Air Force Rocket Propulsion Laboratory
Edwards, CA 93523

1 Attn: Library
1 R.L. Wiswell/LKDS
1 W.W. Wells/LKDS

1 U.S. Air Force, Office of Information
Office of Sec. of Air Force
The Pentagon
Washington, D.C. 20330

Air Force Aero Propulsion Laboratory
U.S. Air Force
Wright-Patterson AFB, Ohio 45433

1 Attn: E.E. Bailey

Arnold Engineering Development Center
Air Force Systems Command
Tullahoma, Tennessee 37388

1 Attn: Library

Space & Missile Systems Organization
Worldway Postal Center
P.O. Box 92960
Los Angeles, CA 90009

1 Attn: Library (Technical Data Center)
1 Lt. Col. J. Graetch

Bureau of Naval Weapons
Department of the Navy
Washington, D.C.

1 Attn: Library

1 United Aircraft Corporation
Corporation Library
400 Main Street
East Hartford, Conn. 06108

United Technology
Chemical Systems Division
P.O. Box 358
Sunnyvale, CA 94088

1 Attn: Library

Picatinny Arsenal
Dover, NJ 07801

1 Attn: Library

U.S. Naval Research Laboratory
Washington, DC 20390

1 Attn: Library

U.S. Army Missile Command
Redstone Scientific Information Center
Redstone Arsenal, AL 35808

1 Attn: Document Section

U.S. Naval Missile Center
Point Mugu, CA 93041

1 Attn: Technical Library

U.S. Naval Weapons Center
China Lake, CA 93557

1 Attn: Library

Aerospace Corporation
2350 E. El Segundo Blvd.
Los Angeles, CA 90045

1 Attn: Library
1 R.L. Doebler
1 I. Madison

Battelle Memorial Institute
505 King Avenue
Columbus, OH 43201

1 Attn: Library

Bell Aerosystems, Inc.
Box 1
Buffalo, NY 14240

1 Attn: Library

Boeing Company
Space Division
P.O. Box 868
Seattle, WA 98124

Attn: Library

1 Chemical Propulsion Information Agency
Applied Physics Laboratory
8621 Georgia Avenue
Silver Spring, MD 20910

General Dynamics/Convair
P.O. Box 1128
San Diego, CA 92112

1 Attn: Library
1 W.J. Ketcham, MZ 21-9500

Grumman Aerospace Corp.
Bethpage, NY 11714

1 Attn: Library

Hughes Aircraft Co.
Research Laboratories
3011 Malibu Canyon Rd.

1 Attn: Library

IIT Research Institute
Technology Center
Chicago, Illinois 60616

1 Attn: Library

Lockheed Missile & Space Company
1111 Lockheed Way
Sunnyvale, CA 94088

1 Attn: Library

Marquardt Corporation
16555 Saticoy Street
Box 2013 South Annex
Van Nuys, CA 91409

1 Attn: Library

Martin-Marietta Aerospace
P.O. Box 179
Denver, CO 80201

1 Attn: Library

McDonnell Douglas Astronautics
5301 Bosa Avenue
Hungtington Beach, CA 92647

1 Attn: Library

Pratt & Whitney Aircraft Group
Government Products Division
United Technologies Corp.
West Palm Beach, FL 33402

1 Attn: Library

Purdue University
Lafayett, IN 47907

1 Attn: Library

Rocketdyne
A Division of Rockwell International
6633 Canoga Avenue
Canoga Park, CA 91304

1 Attn: Library
1 H.G. Diem
1 F.M. Kirby

Rocket Research Corporation
Willow Road at 116th Street
Redmond, WA 98052

1 Attn: Library

1 R. J. Salkeld
5921 Floris Heights Road
Malibu, CA 90265

TRW Systems Inc.
1 Space Park
Redondo Beach, CA 90278

1 Attn: Library